UNIVERSIDAD DE GRANADA

UNIVERSIDAD DE GRANADA

PROGRAMA DE DOCTORADO EN BIOQUÍMICA Y BIOLOGÍA MOLECULAR

INSTITUTO DE PARASITOLOGÍA Y BIOMEDICINA "LÓPEZ-NEYRA"

CONSEJO SUPERIOR DE INVESTIGACIONES CIENTÍFICAS (CSIC)

Mechanisms underlying endolysosomal deficits mediated by the Parkinson's disease-related kinase LRRK2

María del Pilar Rivero Ríos

Tesis doctoral

Marzo 2019

Editor: Universidad de Granada. Tesis Doctorales
Autor: María del Pilar Rivero Ríos
ISBN: 978-84-1117-274-5
URI: http://hdl.handle.net/10481/74032

AGRADECIMIENTOS

En primer lugar, quiero darle las gracias a la Dra. Sabine Hilfiker por haberme dado la oportunidad de iniciarme en el mundo de la investigación científica y por haber sido mi directora de tesis doctoral. Han pasado casi diez años desde que llegué a tu laboratorio en tercero de carrera con la beca JAE-Intro y he tenido la oportunidad de aprender mucho de ti a lo largo de estos años. Gracias por todo lo que me has enseñado de ciencia y de la carrera científica, que sin duda me será de utilidad cuando tenga mi grupo de investigación.

También estoy agradecida a los doctores Rafael Fernández Chacón y Haoxing Xu por haberme permitido realizar estancias de investigación en sus laboratorios. Ambas han sido experiencias excelentes desde un punto de vista profesional y personal.

Me gustaría agradecer a los miembros del departamento de Biología Celular de la Universidad de Granada, en especial al Dr. Ramón Carmona, que me hayan ofrecido la posibilidad de realizar la docencia asociada a la FPU en dicho departamento.

Asimismo, me gustaría mostrar mi agradecimiento a todas las personas con las que he coincidido en el laboratorio 114, a los miembros actuales y a los que ya terminaron, así como a nuestros “fichajes externos”. Me alegro mucho de haber tenido la oportunidad de trabajar con todos vosotros. Gracias a Mar y Patri, por enseñarme y guiarme en mis inicios en el laboratorio. Gracias a Ele, por esas historias que nos cuenta que sólo le pueden pasar a ella. Gracias a Belén, por estar siempre dispuesta a ayudar cuando hace falta. Gracias a Marian, por los cotilleos de todos los temas. Gracias a Jesús, por los momentos de risas que nos daba cuantificando. Gracias a Antonio, por traer la alegría (y el ruido) al laboratorio. Gracias a María, por haber “sufrido” los *referees* conmigo y su valiosa ayuda. Gracias a Mariascen por sus visitas casi diarias al 114. Gracias a Laura por los ratos compartidos en confocal y Olympus. Gracias a todos por ser tan buen equipo.

Por otra parte, quiero darle las gracias a mi familia y a todos los que han estado conmigo en esta etapa de mi vida. En especial, agradezco a mis padres Rafi y Mari el haberme apoyado en todas mis decisiones. Gracias a mi abuela Pilar, por ser un ejemplo de fortaleza, y a mis abuelos Antonio y Aurora, que aunque ya no están, hicieron mucho por mí. Gracias a Choli, por su fiel compañía. Por supuesto, un especial agradecimiento a Pepe, simplemente por ser como eres y por todos los momentos vividos desde que nos conocimos en Ann Arbor. Por último, gracias a mis amigas Raquel y Mariló, por tantas risas las tardes de domingo.

CONTENTS

LIST OF FIGURES

I. SUMMARY/RESUMEN

Mutations in the gene encoding for leucine-rich repeat kinase 2 (LRRK2) are a common cause of hereditary Parkinson´s disease (PD), and some variants also confer risk to develop sporadic PD. LRRK2 has been reported to regulate various intracellular vesicular trafficking pathways, including autophagy, retromer-mediated trafficking, synaptic vesicle dynamics and endolysosomal degradative events, although the precise molecular mechanism(s) underlying these alterations remain to be elucidated.

Recent studies have revealed that a subset of Rab proteins involved in secretory and endocytic recycling are LRRK2 kinase substrates *in vivo*. However, the effects of LRRK2-mediated phosphorylation of these substrates on membrane trafficking remain unknown. Here, by studying the well-characterized epidermal growth factor receptor (EGFR) trafficking pathway, we report that expression of active or phospho-deficient, but not phospho-mimetic, RAB8A variants rescues the G2019S LRRK2-mediated effects on endolysosomal membrane trafficking. Similarly, upregulation of the RAB11-Rabin8-RAB8A cascade, which activates RAB8A, also reverted these trafficking deficits. Strikingly, we found that the loss of RAB8A delayed EGFR degradation and decreased RAB7A activity, mimicking the previously described effect of pathogenic LRRK2 on EGFR trafficking.

Moreover, expression of pathogenic G2019S LRRK2 or loss of RAB8A resulted in mistargeting of the EGFR into a RAB4-positive endocytic compartment, which was accompanied not only by endocytic degradation defects, but also by a deficit in EGFR recycling to the plasma membrane. Both the accumulation of EGFR in the RAB4-positive compartment and the recycling deficits were rescued upon expression of active RAB7A.

Finally, we showed that dominant-negative RAB7A expression resulted in similar defects in EGF degradation, accumulation in a RAB4 compartment, and deficits in EGFR recycling, which were all rescued upon expression of active RAB8A.

Taken together, these findings suggest that LRRK2-mediated phosphorylation and subsequent impairment of RAB8A function may form the basis of how pathogenic LRRK2 deregulates endolysosomal transport and endocytic recycling events.

Mutaciones en el gen que codifica la quinasa rica en repeticiones de leucina 2 (*leucine-rich repeat kinase 2*, LRRK2) son una causa común de enfermedad de Parkinson (EP) hereditaria y algunas variantes también aumentan el riesgo de EP esporádica. LRRK2 participa en la regulación de una serie de rutas de tráfico intracelular de membranas, incluyendo autofagia, tráfico mediado por el retrómero, dinámica de las vesículas sinápticas y degradación endolisosomal, si bien no se conocen con exactitud los mecanismos moleculares responsables de estas alteraciones.

Estudios recientes han revelado que varias proteínas Rab que participan en las rutas secretora y de reciclaje endocítico son sustratos de la actividad quinasa de LRRK2 *in vivo*. Sin embargo, los efectos de su fosforilación por LRRK2 sobre las rutas de tráfico intracelular de membranas permanecen desconocidos. En esta tesis, mediante el estudio de la bien caracterizada ruta del receptor del factor de crecimiento epidérmico (*epidermal growth factor receptor*, EGFR), observamos que la expresión de una versión catalíticamente activa o de una variante fosfodeficiente, pero no así de variantes fosfomiméticas, de RAB8A rescata las alteraciones sobre el tráfico endolisosomal mediadas por G2019S, un mutante patogénico de LRRK2. De forma similar, RAB11 y Rabin8, que forman parte de una cascada de activación de RAB8A, revierten dichas alteraciones. Además, observamos que el silenciamiento de RAB8A retrasa la degradación del EGFR y provoca una disminución de la actividad de RAB7A, al igual que se había descrito anteriormente para LRRK2 patogénica.

Tanto la expresión de la variante G2019S como el silenciamiento de RAB8A resultan en la acumulación aberrante del EGFR en un compartimento endocítico positivo para RAB4, lo cual impide su eficiente degradación endolisosomal, así como su reciclaje de vuelta a la membrana plasmática. Tanto la acumulación del EGFR en el compartimento positivo para RAB4 como las alteraciones en su reciclaje son revertidas por una forma activa de RAB7A.

Finalmente, mostramos que la expresión de una mutación dominante negativa de RAB7A da como resultado defectos similares en la degradación y en el reciclaje del EGFR, provocando su acumulación en el compartimento positivo para RAB4.

En conjunto, nuestros descubrimientos sugieren que la fosforilación y consiguiente inactivación de RAB8A mediada por LRRK2 patogénica podría constituir la base de cómo esta proteína desregula las rutas de tráfico intracelular de membranas.

II. ABBREVIATIONS

α-syn: Alpha-synuclein

BAC: bacterial artificial chromosome

BBB: Blood brain barrier

CCP: clathrin-coated pit

CCV: clathrin-coated vesicle

CIE: clathrin-independent endocytosis

CMA: chaperone-mediated autophagy

CME: clathrin-mediated endocytosis

CNS: central nervous system

COR: C-terminal of ROC

DA: dopamine

EGF: epidermal growth factor

EGFR: epidermal growth factor receptor

ER: endoplasmic reticulum

ERC: early recycling compartment

GAD: G proteins activated by nucleotide-dependent dimerization

GAP: GTPase-activating protein

GBA: β-glucocerebrosidase

GDI1/2: GDP dissociation inhibitor 1/2

GDP: guanosine diphosphate

GEF: guanine nucleotide exchange factor

GGTII: geranylgeranyl transferase type II

GST: glutathione S-transferase

GTP: guanosine triphosphate

GWAS: genome wide association studies

ILV: intraluminal vesicle

In-1: inhibitor-1

iPSC: induced pluripotent stem cells

KI: knock-in

KO: Knock-out

LB: Lewy body

LE: late endosome

LECA: last eukaryotic common ancestor

LN: Lewy neurite

LRRK2: Leucine-rich repeat kinase 2

M6P: mannose 6-phosphate

M6PR: mannose 6-phosphate receptor

MAPT: Microtubule associated protein Tau

MPTP: 1-methyl-4-phenyl-1,2,3,6-tetrahydropyridine

MTOC: microtubule-organizing center

mTOR: mammalian target of rapamycin

MTs: microtubules

MVB: multivesicular body

PD: Parkinson’s disease

PM: Plasma membrane

RE: recycling endosome

REP: Rab escort proteins

RILP: Rab-interacting lysosomal protein

ROC: Ras of complex

ROS: reactive oxygen species

SE: sorting endosome

SNARE: soluble NSF (N-ethylmaleimide-sensitive factor)-attachment protein receptors

SNP: single nucleotide polymorphism

SNpc: *substancia nigra pars compacta*

Tfn: transferrin

TfnR: transferrin receptor

TGN: trans-Golgi network

WB: Western-blotting

WT: wild-type

III. INTRODUCTION

1. PARKINSON'S DISEASE

In 1817, James Parkinson (1775-1824), a British medical practitioner, published "An Essay on the Shaking Palsy", in which he described the clinical features of *paralysis agitans* (shaking palsy). His work was largely unrecognized until, some decades later, the 19th century neurologist Jean-Martin Charcot proposed the eponym of Parkinson's disease (PD) for this disorder and added new knowledge to Parkinson's observations (1). PD is a progressive neurodegenerative disorder affecting 1 % of the population above 60 years and 5 % of individuals over the age of 85 (2). With an aging population and increasing life expectancy, neurodegenerative disorders have important public health implications. Indeed, the number of people with PD is expected to rise by more than 50 % by 2030 (3).

There are two main neuropathological hallmarks in PD: neuronal loss, which mainly affects dopaminergic (DA) neurons in the substancia nigra pars compacta (SNpc), and the presence of proteinaceous inclusions known as Lewy bodies (LB) and Lewy neurites (LN) in the cytoplasm and neuritic processes, respectively, of many of the surviving neurons (4). LB and LN are a heterogeneous mixture of proteins, being composed mostly of aggregated α-synuclein (α-syn) and ubiquitin (5). The cellular consequences of their accumulation are not well understood yet. Some reports support a cytoprotective role, with misfolded proteins accumulating to block cellular damage, while others suggest a cytotoxic role, causing excessive build-up of protein aggregates which would finally lead to cell death (6). Probably a combination of both hypotheses is true, with the initial accumulation of misfolded and unfunctional proteins playing a protective role, while massive accumulation at later stages would be detrimental for survival.

The progressive loss of DA neurons in the SNpc causes an important deficiency of dopamine in the striatum, to where these neurons project, and being the nigrostriatal pathway primarily involved in the execution of movement, its degeneration is responsible for the motor symptoms which characterize the disease. Amongst them, the most prominent ones are: resting tremor (involuntary shaking), rigidity (stiffness and inflexibility of the limbs, neck or trunk), bradykinesia (slowness of movement) and postural instability (7). Motor manifestations appear after a loss of around 50 % of SNpc DA neurons, although estimates of up to 70-80 % have also been made (8).

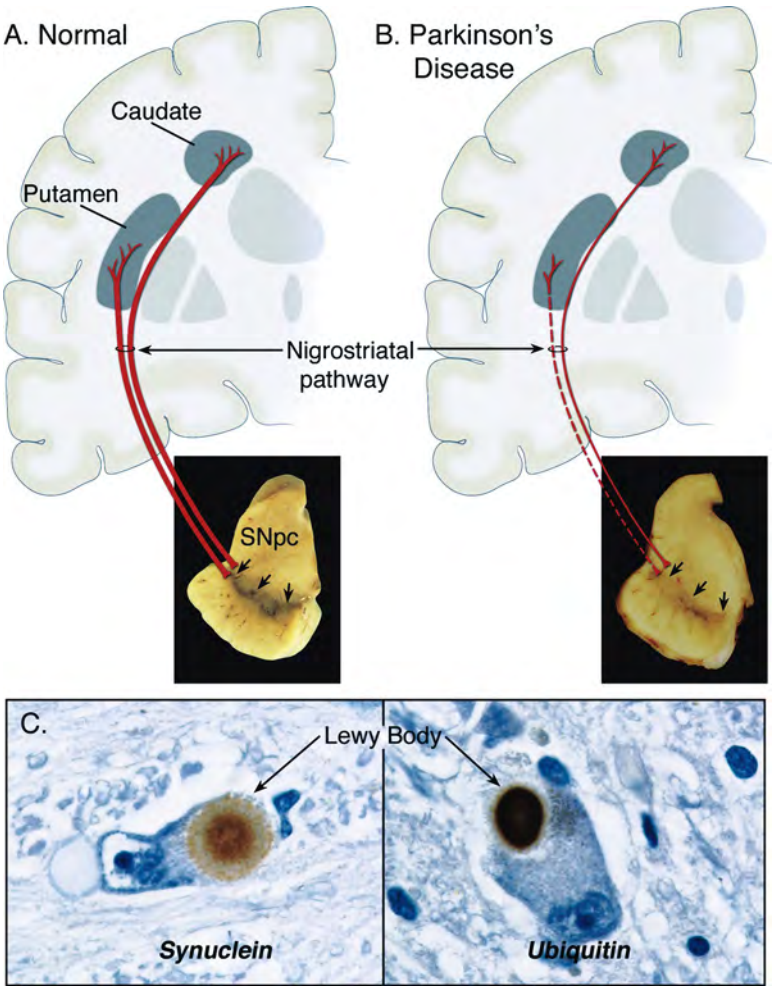

Fig. 1. Neuropathological hallmarks of PD. **(A)** Schematic representation of the nigroestriatal pathway under normal conditions (in red). It is composed of DA neurons whose cell bodies are located in the SNpc, and their projections (thick red lines) synapse in the striatum (caudate and putamen). The pigmentation of the SNpc, produced by neuromelanin within the DA neurons, is normal. **(B)** The nigroestriatal pathway in PD (in red). There is a marked loss of DA neurons projecting to the striatum (thin red lines) and a loss of pigmentation of the SNpc due to the marked loss of DA neurons **(C)** Immunohistochemistry of Lewy bodies in a SNpc DA neuron. Immunostaining with antibodies against α-syn or ubiquitin reveals the presence of these proteins within the LB (black arrow) Taken from (4).

PD patients also experience a broad range of non-motor symptoms, which are likely to be caused by the loss of non-DA neurons and altered neurotransmission in additional regions of the brain, with alterations in the pathways in which they are implicated. Cholinergic neurons in the pedunculopontine nucleus, noradrenergic neurons of the locus coeruleus, cholinergic neurons of the nucleus basalis of Meynert and of the dorsal motor nucleus of the vagus and serotonergic neurons of the raphe nuclei have been reported to be lost in PD (9). Non-motor

features include neuropsychiatric symptoms (e.g. depression, anxiety, cognitive impairment, dementia), autonomic dysfunction (e.g. bladder disturbances, sweating, erectile impotence), gastrointestinal symptoms (e.g. constipation, nausea), sensory symptoms (e.g. olfactory disturbances, pain) and sleep disturbances. They can occur throughout the disease course, but some symptoms may be evident prior to the onset of motor dysfunction (10). Indeed, the premotor or prodromal phase, which can last for 20 years or even more, is often characterized by impaired olfaction, constipation, depression and sleep disorders (11).

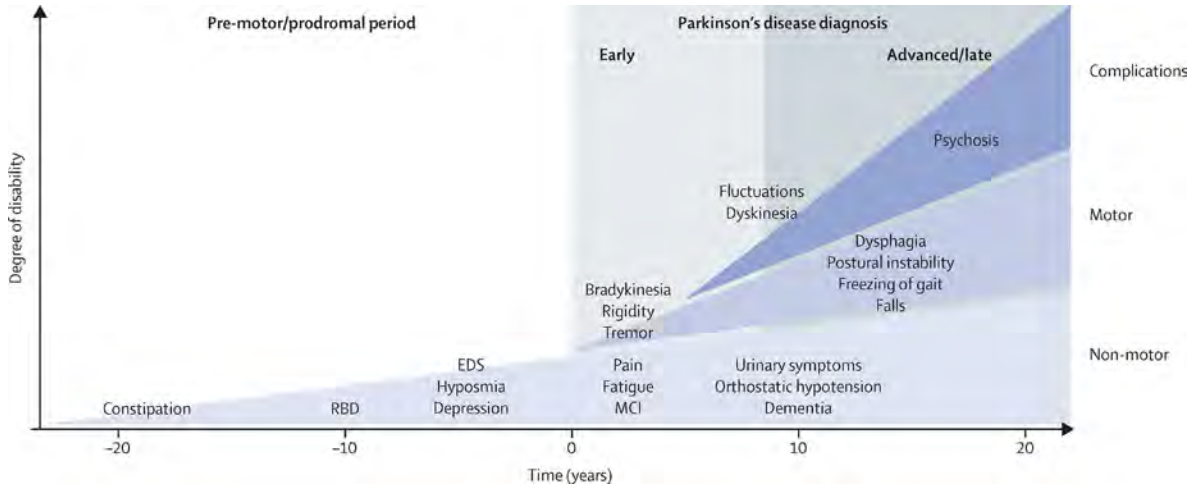

Fig. 2. Clinical manifestations of PD. A premotor or prodromal phase, which can last for more than 20 years and is characterized by specific non-motor symptoms, precedes the onset of motor symptoms (time 0 years). Diagnosis of PD typically occurs with the onset of the characteristic motor symptoms of the disease, including bradykinesia, rigidity and resting tremor. As disease progresses, additional non-motor as well as motor features develop. Long-term complications of dopamine replacement therapy, including fluctuations, dyskinesia and psychosis start appearing at late stages of the disease. Taken from (11).

Many of the neurons that die in PD exhibit common anatomical and physiological traits which could explain their selective vulnerability, including a long, highly branched axon with many neurotransmitter release sites, autonomous spiking, elevated calcium entry and basal mitochondrial oxidant stress. These characteristics place a big bioenergetics burden on these cells, leaving little margin for additional stress (12). Even though non-cell-autonomous processes, such as α-syn spread and microglial-induced degeneration, also contribute to cell

death (13), as further explained below, it is possible that the intrinsic characteristics of these neurons make them especially vulnerable to abnormalities in their microenvironment.

Although slow in most cases, the progression of the disease is irreversible. Treatment of PD is currently symptomatic, and basically involves substituting dopamine with levodopa (the precursor of dopamine) administration (14), or suppressing pathological neuronal oscillations via deep brain stimulation (15). None of the currently available treatment options are able to halt or slow down the progression of the disease. Moreover, prolonged treatment with levodopa has been associated with motor fluctuations and dyskinesia (involuntary movements), and treatment needs to be stopped after several years (16). A thorough understanding of the molecular mechanism(s) involved in neurodegeneration is clue to facilitate the development of disease-modifying therapies, which is a major goal of PD research.

1.1. Etiology

The vast majority of PD cases are designated as idiopathic or sporadic, meaning that there is no apparent underlying cause. However, approximately 5-10 % of patients suffer from familial PD, in which autosomal-dominant or autosomal-recessive mutations in certain genes cause the disease with high penetrance. The identification of such monogenic forms has been of great importance to PD research, allowing the generation of cellular and animal models carrying the mutations in order to study the mechanisms implicated in PD.

Before the discovery of the genetic contribution to PD, the exposure to environmental toxins was identified as a cause for PD, and the first evidence came in 1982, when several intravenous drugs users in San Jose (California) went to local hospitals with clear signs and symptoms of advanced PD. The toxic agent was later identified as 1-methyl-4-phenyl-1,2,3,6-tetrahydropyridine (MPTP), which had formed as a contaminant in the synthetic heroin preparations that they used (17). In fact, intravenous administration of MPTP in squirrel monkeys recapitulated the clinical manifestations observed in humans (18). Other toxic compounds causing PD such as paraquat (a herbicide) and rotenone (a pesticide) were further identified. All three compounds act through the inhibition of mitochondrial complex

I, and lead to progressive DA neuron degeneration (19), which points towards mitochondrial dysfunction and oxidative stress playing an important role in the development of PD.

The first causative gene for PD was found in 1997, when, a point mutation in the *SNCA* gene, encoding the protein α-syn, was related to the disease (20). α-Syn was then revealed to be the main component of LB (21). In the following years, genetic studies focused on rare forms of PD in large families, which were mapped to other causative mutations. Up to date, six genes have been identified in many genetic investigations to be unequivocally linked to PD, and can be classified according to their mode of inheritance. Mutations in *SNCA*, Vacuolar protein sorting-associated protein 35 *(VPS35)* and Leucine-rich repeat kinase 2 (*LRRK2)* are dominantly inherited, causing late-onset and progressive PD which closely resembles idiophatic PD, while mutations in *PARKIN*, *PINK1* and *DJ-1* are recessive and cause early-onset PD. Mutations in many other genes, such as Eukaryotic translation initiation factor 4 gamma 1 (*EIF4G1)* (22), Ubiquitin C-terminal esterase L1 (*UCHL1)* (23) or Growth-factor receptor-bound protein 10-interacting GYF protein 2 (*GIGYF2)* (24) have also been linked to PD, but await validation in further studies. The mutations in all these genes, with the exception of LRRK2, cause PD in a small subset of patients.

More recently, genome-wide association studies (GWAS), which searches the whole genome for small variations which occur more frequently in people with a particular disease than in control individuals, have added an additional layer of complexity to the genetics of PD with the identification of common genetic variations (mostly single nucleotide polymorphisms; SNPs) that modify disease risk, suggesting that genetic contribution to the disease has been greatly underestimated, as these genetic variants could be playing an important role in the common, sporadic form of the disease. Importantly, a subset of the identified variations lie within loci previously associated with familial disease, such as these containing *LRRK2* or *SNCA*, pointing towards the existence of common pathways underlying both inherited and idiopathic PD. Of particular note are the consistently strong associations for variants in the gene encoding β-glucocerebrosidase (*GBA)*, a lysosomal enzyme which cleaves glucocerebrosidase to ceramide and glucose (25). Homozygous mutations in this gene cause the autosomal recessive lysosomal storage disorder Gaucher disease, while heterozygous mutations have been shown to increase risk for PD around 5-fold (26). Variants

in the gene encoding the microtubule associated protein Tau (MAPT) have also been consistently found to increase PD risk (27). The fact that this gene is associated with Alzheimer disease suggests the existence of a common mechanistic link between these two apparently different disorders. Tau participates in the assembly and stabilization of microtubules (28), suggesting that improper microtubule organization and subsequent alterations in membrane trafficking play an important role in neurodegeneration.

During the past few years, many other genes have emerged as susceptibility genes. Of special interest are variations in RAB7L1, a retromer-linked gene recently found to interact with LRRK2, which are associated with risk for PD in different populations (29).

Importantly, studying the gene products associated with PD has provided vital clues to better understand some of the key dysfunctional processes implicated in the disease.

1.2. Molecular mechanisms

Several highly-interconnected and not mutually exclusive mechanisms have been proposed to explain neurodegeneration in PD, including α-syn-mediated toxicity, mitochondrial damage and oxidative stress, excitotoxicity, neuroinflammation, and intracellular vesicular trafficking deficits.

1.2.1. Alpha-syn- mediated toxicity and transmission

Multiple lines of evidence support that α-syn plays a central role in PD pathogenesis, with the formation of aggregating α-syn species preceding neuronal loss. This 140 amino acid protein is ubiquitously expressed in neurons (30), where it participates in neurotransmitter release by regulating the soluble NSF (N-ethylmaleimide-sensitive factor)-attachment protein receptors (SNARE) complex in the presynapse (31). As a natively unfolded protein, α-syn is prone to aggregation giving rise to oligomeric or protofibrillar structures. Importantly, at least two PD-associated mutations in the *SNCA* gene were shown to promote an increased formation of oligomers (32), and elevated levels of α-syn oligomers have been described in the cerebrospinal fluid of PD patients as compared to control subjects (33, 34), supporting their role in PD pathogenesis. Alpha-syn oligomers comprise a very heterogeneous population and not all of them are toxic to cells. However, for reasons that

have not been fully elucidated, certain oligomeric species can be highly toxic. In particular, they have been shown to increase cell permeability by promoting the formation of pores in the plasma membrane (PM), and disrupt several organelles such as mitochondria, Golgi complex, and endoplasmic reticulum (ER), as well as protein degradation pathways and synaptic transmission (35–37).

Intriguingly, α-syn has been reported to act as a "prion protein", spreading throughout the central nervous system (CNS). Indeed, different studies have found LB in fetal grafted neurons in PD patients (38, 39). Alpha-syn oligomers can be released as free floating proteins or via exosomes and infect adjacent, healthy neurons, where they would act as a seed, inducing intracellular α-syn aggregation and further contributing to the progression of the disease (40, 41). Innate-immune astrocytes and microglia, with an enhanced capacity for endocytosis and lysosomal degradation, would also uptake α-syn oligormers, as this has been related to multiple proinflammatory changes that are ultimately neurotoxic. For example, α-syn uptake by microglial cells has been shown to induce the activation of the enzyme NADPH oxidase, leading to elevated ROS production and contributing to tissue damage if maintained over time (42).

Related to the prion-like propagation hypothesis, Braak and colleagues suggested that PD pathogenesis would originate in the gut, where an unknown pathogen or toxin would trigger α-syn aggregation, and aggregated α-syn would subsequently spread to the CNS, through synaptic connections, probably via the vagus nerve, eventually arriving at the SNpc (43). This is known as Braak's hypothesis. Indeed, enteroendocrine cells possess many neuron-like properties and connect to enteric nerves forming a neural circuit between the gut and the nervous system. Misfolded α-syn have been found in enteroendocrine cells in early PD models, suggesting that it could propagate in a prion-like manner to the brain (44, 45). However, the Braak's hypothesis cannot explain PD development in all patients, as only around half of the people with PD adhere to the Braak staging system and there is more variation in the temporal pattern of LB appearance than originally proposed by Braak (12).

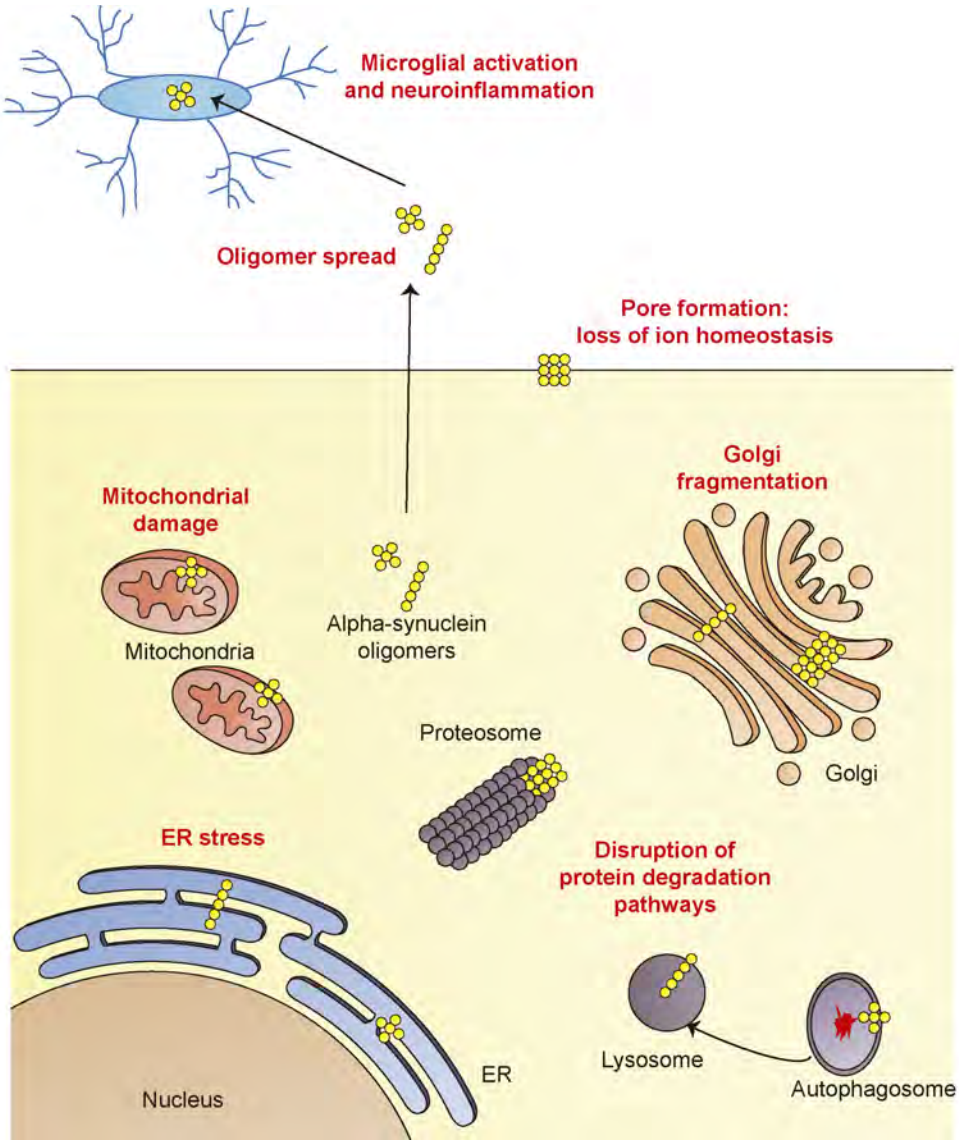

Fig. 3. Proposed targets for α-syn-mediated toxicity. Several mechanisms have been associated with α-syn-mediated toxicity, including the formation of pores in the PM, damage of several organelles such as mitochondria, ER and Golgi, as well as the impairment of various protein degradation pathways, including the proteasome and the autophagy-lysosomal pathway. Moreover, α-syn oligomers can be released by neurons and taken up by other cells, including microglia, promoting their activation and release of pro-inflammatory substances.

1.2.2. Mitochondrial dyshomeostasis and oxidative stress

Proper functioning of the mitochondrial electron transfer chain is crucial for ATP production. In the mitochondrial inner membrane, electrons are transferred via redox reactions through a series of protein complexes to the last electron acceptor, which is oxygen.

As the electrons pass, some protons are translocated by the electron carriers from the mitochondrial matrix to the intermembrane space, creating a proton gradient. The flow of protons back into the matrix, following this gradient, provides energy for the ATP synthase to phosphorylate ADP into ATP (46).

Abnormal activity of mitochondrial complex-I, which would interfere with ATP production leading to cell death, has been reported in PD patients (47–49). Additional evidence for a role of altered mitochondrial homeostasis in PD comes from the fact that some PD-causing drugs, such as MPTP, alter the mitochondrial respiratory chain (50). In addition, the gene products of some PD-associated genes, such as PINK1 and PARKIN, function in mitochondrial homeostasis (51), further supporting an important role for mitochondria in PD pathogenesis.

Mitochondrial dysfunction leads to oxidative stress, as mitochondria are one of the main reactive oxygen species (ROS) producers in the cell (52). ROS develop when electrons prematurely escape from the electron transport chain, being the major sites for such events located at respiratory chain complexes I and III (53). Although ROS are important for normal cellular physiology, because they play a role in regulating the activity of several enzymes, increased ROS levels lead to oxidative stress, with a variety of detrimental consequences due to the random oxidation of macromolecules inside the cell. Consequently, their intracellular levels need to be precisely regulated by antioxidants such as superoxide dismutase and glutathione (46). However, the balance between ROS formation and elimination seems to be disturbed in PD, and several studies have detected increased oxidation of DNA, lipids and proteins in the brain of both familial and sporadic PD patients (54, 55).

Oxidative stress is not just a result of mitochondrial dysfunction, but also a pathogenic factor *per se*, and dopamine metabolism may contribute to the selective vulnerability of DA neurons in PD. In fact, DA neurons are particularly vulnerable to oxidative stress, as dopamine can undergo oxidation in the cytosol with subsequent ROS generation. For this reason, DA is quickly sequestered into synaptic vesicles soon after its synthesis (56). Importantly, overexpression of α-syn has been shown to have an inhibitory effect on VMAT2 activity, responsible for DA uptake from the cytoplasm into synaptic vesicles, promoting an increase in the cytosolic levels of dopamine (57).

1.2.3. Excitotoxicity

Excitotoxicity is the pathological process through which neurons are damaged after excessive stimulation of glutamatergic receptors by glutamate, the main excitatory neurotransmitter in the CNS, which leads to calcium overload and bioenergetics changes (58).

Both in animal models and PD patients, DA depletion was shown to alter the balance between excitatory and inhibitory neurotransmission (59, 60). DA maintains the excitation status of the subthalamic nuclei at basal levels. However, due to the loss of DA neurons in PD, the subthalamic nuclei become over-activated, leading to excessive release of the neurotransmitter glutamate, which binds to glutamatergic receptors causing an increase in intracellular calcium levels and leading to excitotoxicity (61). Calcium overload can damage mitochondria and produce ROS, further contributing to oxidative stress (62, 63).

1.2.4. Neuroinflammation and peripheral inflammatory response

Increasing evidence supports the involvement of central and peripheral immune responses in PD pathogenesis.

Neuroinflammation is observed in classical toxin-induced PD models (64), and importantly, the activation of microglia and astrocytes (the immune cells of the brain) and an increased secretion of cytokines have been reported in the PD brain (65, 66). In addition, various gene products linked to PD such as LRRK2 or α-syn have been demonstrated to regulate microglia and T-cell functions (67, 68), and LRRK2 is highly expressed in immune cells (69). Further highlighting the relevance of the immune system, SNPs in cytokine genes (70), as well as in the HLA genetic loci (71), have been associated with increased risk for PD.

The central inflammatory process, which is characterized by activation and proliferation of microglia and astrocytes, as well as secretion of proinflammatory cytokines and free radicals, was long believed to be a secondary consequence of neuronal death. However, the realization that α-syn pathology is associated with microglial activation even in the absence of neuronal loss has challenged this view (72–74), giving rise to the “inflammation

hypothesis of neurodegeneration" in PD. This hyphotesis is also supported by clinical observations, as microglial activation has been reported in patients with REM sleep behavioral disorders, considered a prodromal form of PD (75).

A sustained neuroinflammatory response causes tissue damage and can eventually lead to cell death. In this regard, robust immune activation in mice injected in the SNpc with the bacterial membrane molecule lipopolysaccharide has been shown to cause nigral DA neuron death (76), suggesting that neuroinflammation could be the primary event triggering neurodegeneration.

Positron-emission tomography measurement of ligand uptake by P-glycoprotein, a molecular efflux pump present in the blood brain barrier (BBB), revealed increased permeability of the BBB in PD patients (77), and peripheral innate (monocytes and macrophages) immune cells have been reported to infiltrate the brain during neurodegeneration (78). Interestingly, the peripheral monocyte population is anomalous in PD patients and shows an exaggerated response to defined immune stimuli (78), which would further contribute to the propagation of the inflammatory damage.

T cell infiltration has also been demonstrated in both PD patients and animal models (79), suggesting a role for adaptive immunity in PD. In this context, DA neuron loss caused by MPTP administration is attenuated in mice lacking both B and T cells (80). Importantly, pathogenic changes in peripheral blood lymphocytes from PD patients have been described, although the pathogenic relevance of these changes remains to be elucidated (81).

1.2.5. Impaired intracellular vesicular trafficking

The impairment of intracellular trafficking is emerging as a mechanistic link between many gene products, either familial or risk factors, associated with PD. A considerable number of PD-related genes are involved, directly or indirectly, in endosome-lysosome trafficking (27, 31, 90–99, 82, 100, 83–89), as summarized in Table 1. Importantly, a recent report suggests that the number of PD-associated genes which are implicated in vesicular trafficking has been greatly underestimated (101).

Gene	Familial/Risk	Encoded protein	Trafficking steps	References
SNCA	Both	α-synuclein	Endosome-lysosome, synaptic	(31, 82)
LRRK2	Both	LRRK2	Endosome-lysosome, synaptic	(83)
GBA	Risk	Glucocerebrosidase	Lysosome, ER, Golgi	(84)
SCARB2	Risk	LIMP2	Lysosome	(85)
ATP13A2	Familial	ATPase 13A2	Lysosome	(86, 87)
ATP6AP2	Familial	ATP6AP2	Lysosome	(88)
VPS13C	Both	VPS13C	Endosomal sorting, mitophagy	(89, 90)
VPS35	Familial	VPS35	Endosome-lysosome, Golgi	(91)
DNAJC13	Familial	RME-8	Endocytosis, synaptic	(92)
DNAJC6	Familial	Auxilin	Endocytosis, synaptic	(93)
GAK	Risk	GAK	Endocytosis, synaptic	(90)
SYNJ1	Familial	Synaptojanin-1	Endocytosis, synaptic	(94, 95)
RAB39B	Familial	RAB39B	Endosome	(96)
TMEM230	Familial	Transmembrane protein 230	Endosome-lysosome, synaptic	(97)
MAPT	Risk	Tau	Axonal transport	(27, 98)
LAMP3	Risk	Lysosome-associated membrane protein 3	Lysosome	(99)
PINK1	Familial	PINK1	Mitophagy	(102)
PARKIN	Familial	Parkin	Mitophagy	(102)
RAB29	Risk	RAB29/RAB7L1	Endosome-lysosome, Golgi	(100)

Table 1. Several PD-related genes have functions in endomembrane trafficking pathways. Adapted from (103).

Altered functioning of the proteins coded by these genes would lead to defects in intracellular vesicular trafficking and synaptic dysfunction. Moreover, as α-syn oligomeric structures cannot pass through the narrow proteasome barrel and can only be degraded by autophagy/lysosome-related pathways (104, 105), lysosomal defects would result in α-syn accumulation (106). The consequences of impaired intracellular trafficking in PD will be further elaborated upon in the discussion of this thesis.

2. INTRACELLULAR VESICULAR TRAFFICKING

Intracellular vesicular trafficking defines a complex network of pathways that connects the membranous organelles of eukaryotic cells. It allows proteins and other large molecules in vesicles to be transported between different membrane compartments without ever crossing a membrane. The first step in this process is the formation of a vesicle by budding from a membrane, which implies the cooperation of specific coat and adaptor proteins. Cargo-containing vesicles are then targeted along cytoskeletal components to reach their acceptor compartment, to which they fuse with the help of SNAREs. In eukaryotic cells, membrane trafficking is divided into two major routes: exocytosis and endocytosis, with a few examples of cross-talk between both pathways, such as retromer-mediated trafficking (further explained below) (107, 108).

Intracellular vesicular trafficking allows for the interaction between cells and their environment. Moreover, membrane trafficking between distant axonal and dendritic extensions is key in neurons to maintain function, as it allows the regulation of protein and organelle compositions in dendrites and axons, synaptic transmission, and the correct distribution of cell surface receptors (109).

2.1. Transport from the Golgi apparatus to the cell exterior: Exocytosis

Exocytosis is the process by which secretory vesicles fuse with the PM to allow release of their contents and insertion of new membrane components. It is essential for cell growth and for the release of substances destined to the extracellular space (110).

Exocytosis is linked to the biosynthetic pathway. In eukaryotic cells, most membrane and soluble proteins, as well as many lipids, are synthesized in the endoplasmic reticulum (ER) and then incorporated into the ER lumen or membrane, depending on whether they are soluble or transmembrane, respectively (107, 111).. The export of newly made proteins from the ER is mediated by COP-II-coated vesicles at the ER exit sites, a process dependent on the protein SEC16 (112). These small transport vesicles, of around 50-nm-diameter, fuse then with the cis-Golgi or with one another to form the membrane stacks that constitute the cis-Golgi network. In the process called cisternal migration, a new cis-Golgi stack with its cargo moves from the cis position (nearer the ER) to the trans position (farther from the ER), being

firstly a cis-Golgi cisterna, then a medial-Golgi cisterna and finally a trans-Golgi cisterna, and as this progression happens, many proteins undergo post-translational modifications (107, 111).

At the trans-Golgi network (TGN), proteins are sorted for their final destinations, which can be the PM (exocytosis) or organelles of the endocytic pathway. However, some proteins are retrieved from the cis-Golgi to the ER and from later Golgi cisternae to earlier ones by small retrograde transport vesicles. This is the case of ER-resident proteins that need to be modified in the Golgi and then transported back to the ER (113). COP-I-coated vesicles mediate intra-Golgi transport, as well as Golgi-to-ER retrograde transport (114).

The final steps of exocytosis involve the participation of the exocyst, an octomeric complex that tethers secretory vesicles to the PM prior to SNARE-mediated fusion. In yeast, it is recruited by the Rab GTPase Sec4, present in the vesicle membrane, and it binds to $PI(4,5)P_2$ at the inner leaflet of the PM (115, 116).

All cells display constitutive exocytosis, but many also possess a pathway for regulated exocytosis, which is the process in which the membranes of cytoplasmic organelles fuse with the PM in response to an appropriate hormonal or neural stimulus. In many cases, it has a secretory function, promoting the release of specific products such as neurotransmitters or hormones to the extracellular space. Most commonly, this process occurs in endocrine glands and presynaptic terminals in response to calcium, but the dynamics of secretion are very different in both cases. In the nerve terminals, calcium stimulates exocytosis of predocked synaptic vesicles, resulting in very fast secretory events. Conversely, in endocrine glands, calcium not only triggers fusion, but also promotes the mobilization of secretory vesicles, resulting in slower and longer lasting secretion (117).

On the other hand, regulated exocytosis can function to transfer the organelle membrane and its components, such as receptors or channels, to the PM (non-secretory exocytosis). One such example is the translocation of the glucose transporter GLUT4 to the PM in response to insulin (118).

Interestingly, some cells use their lysosomes as regulated secretory organelles, termed secretory lysosomes. Exocytosis of secretory lysosomes is very similar to the release of

secretory granules. A signal results in calcium mobilization within the cell, promoting the movement of secretory lysosomes to the PM and subsequent fusion, thus releasing their contents to the extracellular space. Melanosomes, lamellar bodies of pulmonary alveolar type II cells, and lytic granules from cytotoxic lymphocytes are examples of secretory lysosomes (119). More recently, conventional lysosomes have also been shown to undergo calcium-regulated exocytosis, with this process playing a crucial role in PM repair (120).

2.2. Transport into the cell from the plasma membrane: Endocytosis

Endocytosis is the process by which extracellular molecules, including nutrients, pathogens, antigens, receptors and growth factors, are internalized at the PM to the interior of the cell. It controls the composition of the PM and, consequently, how cells respond to their environment. For example, endocytosis has functions in nutrient uptake, cell signaling, and cell shape changes. A clear example is the internalization of PM-bound receptors, a process termed receptor-mediated endocytosis, which controls the sensitivity of cells to their particular ligands (121, 122).

Endocytosis can be classified into different categories based on the particular cargo transported, and on the intracellular mechanisms involved in vesicle formation and scission from the PM. Two major categories have been traditionally established: clathrin-mediated endocytosis (CME) and clathrin-independent endocytosis (CIE).

CIE comprises a series of pathways, not all of them completely understood, including the CLIC/GEEC pathway, ARF6-dependent endocytosis, flotillin-dependent endocytosis, macropinocytosis, circular dorsal ruffles, phagocytosis, and trans-endocytosis (123, 124). Some of these pathways are constitutive, while others are triggered by specific signals (125). For instance, phagocytosis starts when the phagocytic receptors of specialized cells, referred to as phagocytes, interact with ligands on the surface of pathogens or apoptotic cells, triggering a series of signaling events which lead to actin cytoskeleton remodeling and the formation of pseudopods covering the particle (126).

CME is the most common and best studied route of endocytosis. In CME, clathrin polymerization at sites of the PM which are destined to be internalized, allows for the formation and constriction of the vesicle neck cargo giving rise to clathrin-coated pits

(CCPs), which subsequently invaginate and separate from the PM, thanks to the action of the membrane scission protein dynamin, generating clathrin-coated vesicles (CCVs) (108, 127). The ATP-dependent dissociation of clathrin from CCVs is mediated by the molecular chaperone HSC70, which requires either the neuron-specific auxilin or the ubiquitous GAK as cofactors (128). The resulting naked vesicles rapidly fuse with sorting endosomes (SEs) through SNARE-based fusion events (108, 127).

The SE is a peripherally-localized highly dynamic compartment which constantly undergoes fission and fusion (homotypic within itself or heterotypic with incoming endocytic vesicles) events (129, 130). It is composed of regions of thin tubular extensions (≈60 nm diameter) and large vesicles (≈400 nm diameter) (131). SEs are enriched in the lipid PI(3)P, as well as in the small GTPase RAB5 and its protein effectors Early Endosome Antigen 1 (EEA1) and VPS34/P150. They are also characterized by a slightly acidic pH (≈6.2), which causes many ligands to be uncoupled from their receptors and mix with internalized solute molecules (132).

At the SE, rapid sorting of cargo occurs, with internalized material destined for two distinct locations. It can be trafficked to late endosomes (LE) and lysosomes for degradation, or can be recycled back to the PM, either by a rapid pathway directly back to the PM, or via a slower recycling pathway, which firstly involves the transport to a long-lived organelle called perinuclear endocytic recycling compartment (ERC), and is adjacent to the microtubule-organizing center (MTOC) (132). These recycling routes are termed “fast recycling pathway” and “slow recycling pathway”, respectively (133).

2.2.1. Late endosomal-lysosomal degradation

During the process termed endosomal maturation, SEs acquire the characteristics of late endosomes (LEs) or multivesicular bodies (MVBs), such as a more acidic luminal pH (≈5.5) or acid hydrolases. LEs are typically enriched in the lipids PI(3,5)P_2 and 2’2-dioleoyl lysobisphosphatidic acid (LBPA). SE to LE maturation also involves the acquisition of RAB7, the marker for LEs, and SNAREs that are specific to LEs (129).

A key event in endosomal maturation is the replacement of RAB5 by RAB7, in a highly coordinated process termed Rab conversion. RAB5, together with PI(3)P, recruits a complex

containing the proteins Mon1/SAND1 and Ccz1/CCZ1 to SEs. Mon1/SAND1 promotes RAB5 inactivation by displacing its activator Rabex-5, while Ccz1/CCZ1 activates RAB7. RAB7 then recruits TBC2, a RAB5-inactivating protein that further decreases RAB5 activity, resulting in the dissociation of RAB5 effectors such as EEA1 and their replacement with RAB7 effectors which define late endosomal function (134). For example, the RAB7 effector WDR91 has been shown to inhibit PI 3-kinase activity, the enzyme that generates PI(3)P on endosomes (135), and the interaction of RAB7 with RILP is necessary for endosomal translocation along microtubules towards the cell center, where lysosomal fusion occurs (136).

Moreover, determinants of lysosome-targeted proteins, such as conjugated ubiquitin, are recognized by the sorting machinery of SEs and promote the formation of a series of invaginations which generate intraluminal vesicles (ILVs), thus allowing the separation of the material destined for degradation. The regions containing these vesicles separate themselves from tubular SE, giving rise to free MVBs. In contrast to SEs, MVBs are spherical structures with a diameter of ≈0.5 μm and a homogenous content of 50 nm diameter ILVs (137). The mechanism driving ILV formation is not fully understood, although it is known that the endosomal sorting complex required for transport (ESCRT) is a key player in this process (138), and the interaction of the ESCRT machinery with lipids of the underlying membrane through accessory proteins has been suggested to be important for ILV formation. For example, Alix provides a link between LBPA and ESCRT (139).

There are four different complexes: ESCRT-0,-I,-II,-III. ESCRT-0, -I, and -II contain ubiquitin-binding domains which allow for the interactions with ubiquitinated cargo. A model to explain their participation in MVB formation has been recently suggested. ESCRT-0 self-assembles to SEs and forms domains of clustered cargo, ESCRT -I and -II deform the membrane into buds, and finally ESCRT-III is recruited to the bud neck and efficiently cleaves it (140). The ATPase Vps4 promotes ESCRT dissociation from the membrane before inward vesiculation occurs (141).

MVBs eventually fuse with lysosomes and deliver their cargo either by a kiss-and-run mechanism, which releases intravesicular content through a transient, nm-sized pore, or by direct and permanent fusion (142). In any case, a hybrid organelle referred to as

endolysosome would form, from which the lysosome has to be reformed via a maturation process (142). Fusion usually occurs in the perinuclear region of the cell, as MVBs and lysosomes are concentrated near the MTOC (143).

Homotypic and heterotypic fusion events between these organelles require the recruitment of the homotypic fusion and vacuole protein sorting (HOPS) complex, which allows for organelle tethering. Its recruitment is dependent on the RAB7 counterpart in yeast, but seems to be RAB7-independent in mammals, in which Arl8b and RILP would mediate the process (144). Tethering also requires the participation of N-ethyl-maleimide-sensitive factor (NSF) and soluble NSF attachment proteins (SNAPs). This step is followed by the formation of the trans-SNARE complex, which bridges across the two organelles. The presence of VAMP8 within the trans-SNARE complex is important for homotypic LE fusion, while VAMP7 is required for heterotypic fusion events. The release of lumenal Ca^{2+}, through a currently unknown mechanism, finally leads to phospholipid bilayer fusion (143).

The fusion of LEs with lysosomes would consume lysosomes, and therefore a reformation process is necessary to recover these organelles. Contrary to LEs, lysosomes are electron-dense structures, and condensation of their content has been reported to be driven by lumenal Ca^{2+} release (145).

At the molecular level, the absence of mannose-6-phosphate receptors (M6PRs), present in LEs and hybrid organelles, is the major characteristics of lysosomes. In mammalian cells, newly synthesized acid hydrolases are tagged with mannose-6-phosphate (M6P) in the cis-Golgi, which allows them to bind to M6PRs in the TGN. The bound hydrolases are delivered to endosomes, where they dissociate from the receptors due to their acidic pH. M6PRs are recycled from LEs back to the Golgi via the retromer, which will be further explained below, while the hydrolases continue to lysosomes (143).

Lysosomes are the major degradative compartments of eukaryotic cells, degrading a variety of substances, such as proteins, nucleic acids, oligosaccharides and lipids into their building blocks, due to the action of a series of hydrolytic enzymes with optimal efficiency at the highly acidic pH of lysosomes (≈5) (146). The main constituents of the lysosomal membrane are the highly sialylated lysosomal associated membrane proteins LAMP1, 2 and

3, as well as lysosomal integral membrane proteins (LIMPs), which form a glycocalix-like layer protecting the membrane against hydrolases (147) and, importantly, some lysosomal membrane proteins play specific roles. For instance, LAMP2A acts as a receptor for chaperone-mediated autophagy (CMA) substrates, and LIMP2 mediates the transport of β-glucocerebrosidase to lysosomes, where ligand and receptor dissociate. Moreover, LAMP proteins likely participate in lysosomal motility, as their deficiency shifts lysosomal localization to the periphery, thus reducing their possibility to fuse with LEs and autophagosomes (148).

The epidermal growth factor receptor (EGFR) pathway has been traditionally used to study degradative trafficking, although this receptor can also be recycled back to the PM, depending on stimulation conditions (as further explained below). The targeting of transmembrane receptors to LEs/lysosomes allows signal termination and makes cells unresponsive until their PM is replenished by new receptors (149).

2.2.2. Endocytic recycling

Whilst the maturing SE moves to the cell center to fuse with lysosomes, molecules destined to be recycled back to the PM are efficiently removed by the pinching off of narrow tubules, which can be directly or indirectly transported to the PM, following a fast or a slow recycling pathway, respectively (150). RAB4, RAB5 and RAB11 play roles in regulating recycling, although the mechanisms are not completely understood. A study by Zerial's group indicates that these proteins would segregate into distinct microdomains which would determine the final destination of the cargo (151). RAB4 can target receptors either to the PM or to the ERC. In order to undergo fast recycling, the receptor needs to be quickly switched from a RAB5- to a RAB4-containing microdomain on the same vesicle. Alternatively, it can be transported to a RAB4/RAB11 enriched microdomain to undergo transport to the ERC (152). Interestingly, RAB4 dysregulation has been demonstrated to affect trafficking along both recycling and degradative pathways, pointing towards an important role of this protein in the correct functioning of SEs (153).

In the slow recycling pathway, the tubules emanating from SEs carry their cargo to the perinuclear region of the cell, where they likely fuse with recycling endosomes (REs). REs

are enriched in RAB11 and RAB8 family proteins, RAB22A, ARF6, EHD1 and MICAL-L1 (132). They often have a tubular shape and form a complex network known as the ERC. The ERC is a collection of tubules with diameters of about 60 nm, which are associated with microtubules and are located near the MTOC in many cell types, although in others, including neurons, the ERC is more dispersed (154). Contrary to LEs and lysosomes, the ERC is a long-lived compartment and transport from it requires the formation of intermediate carriers. After vesicles originating from SEs reach the ERC, a process of budding and fission is hypothesized to occur, and the released vesicles are transported to the PM along microtubules (155), a process which seems to be mediated by the RAB11-interacting protein KIF13, a plus-end directed kinesin motor (156).

Endocytic recycling allows the cell to maintain components of the PM, for example signaling receptors and transporters, to respond to new ligands and signals. Much of what is known about endocytic recycling comes from studies of transferrin (Tfn), an iron-binding protein that facilitates iron uptake, and the Tfn receptor (TfnR). Unlike most ligands, Tfn does not dissociate from its receptor in the slightly acidic environment of SEs and remains bound to it throughout the recycling pathway, being released upon returning to the PM (157). Kinetic studies confirmed that Tfn can undergo recycling by two distinct routes: the fast recycling pathway ($t_{1/2}$= 5 min) and the slow recycling pathway ($t_{1/2}$= 15-30 min) (158).

2.2.3. EGFR trafficking

EGFR trafficking pathways deserve special consideration, as they have been widely used in this thesis as a readout to study the effects of PD-associated proteins on endomembrane trafficking.

The EGFR is a member of the ErbB family of signaling receptors, and is implicated in regulating normal growth and differentiation. Its dysregulation is associated with different types of cancers (159), and mice lacking EGFR develop a form of neurodegeneration affecting the frontal cortex and olfactory bulb (160).

In the absence of ligand, most EGFR molecules remain monomeric and inactive. Under these circumstances, inactive receptors are continuously internalized and quickly recycled back to the PM, ensuring their accumulation on the cell surface (161). EGFR is activated

upon ligand binding, which promotes receptor dimerization, resulting in trans-autophosphorylation on tyrosine residues located in its cytoplasmic domain, initiating the activation of various signaling pathways (161). Several EGFR ligands have been described so far, being epidermal growth factor (EGF) the best described and the most commonly used for EGFR trafficking studies (162). Other EGFR ligands include transforming growth factor-alpha, amphiregulin, epiregulin, betacellulin, heparin-binding epidermal growth factor-like growth factor and epigen (163).

EGFR activation leads to its internalization and trafficking to SEs, from where it can be either recycled back to the PM, or degraded in lysosomes. Ligand concentration has been shown to be a key factor affecting EGFR fate (164, 165). Under conditions of low ligand availability, activated EGFR is almost exclusively internalized by CME and recycled back to the PM. When the canonical endocytic route is saturated due to increased ligand concentration, CIE pathways have been suggested to be activated, rapidly targeting EGFR towards degradation (161). Other studies, however, showed that clathrin knockdown completely inhibited EGFR endocytosis, arguing against the participation of CIE in EGFR internalization (162). This controversy is likely due to differences in the expression levels of proteins that participate in EGFR endocytosis between the cell lines used, and further investigation will be needed to clarify the exact mechanisms implicated in EGFR endocytosis.

Independently of the pathway responsible for its internalization, EGFR targeting to degradation seems to be dependent on receptor ubiquitylation, which is promoted by high stimulus intensity. A certain threshold of receptor phosphorylation is required to recruit Cbl E3 ubiquitin ligases, while low intensity of ligand-induced stimulus offers less phosphorylated binding sites, which are preferentially occupied by signaling effectors. Once ubiquitylated, EGFR can be recognized by the ubiquitin-dependent adaptors of ESCRTs and sequestered into MVBs, which physically removes the signaling tail of the EGFR from the cytosol leading to signal termination, thus allowing the cells to efficiently cope with overstimulation (161).

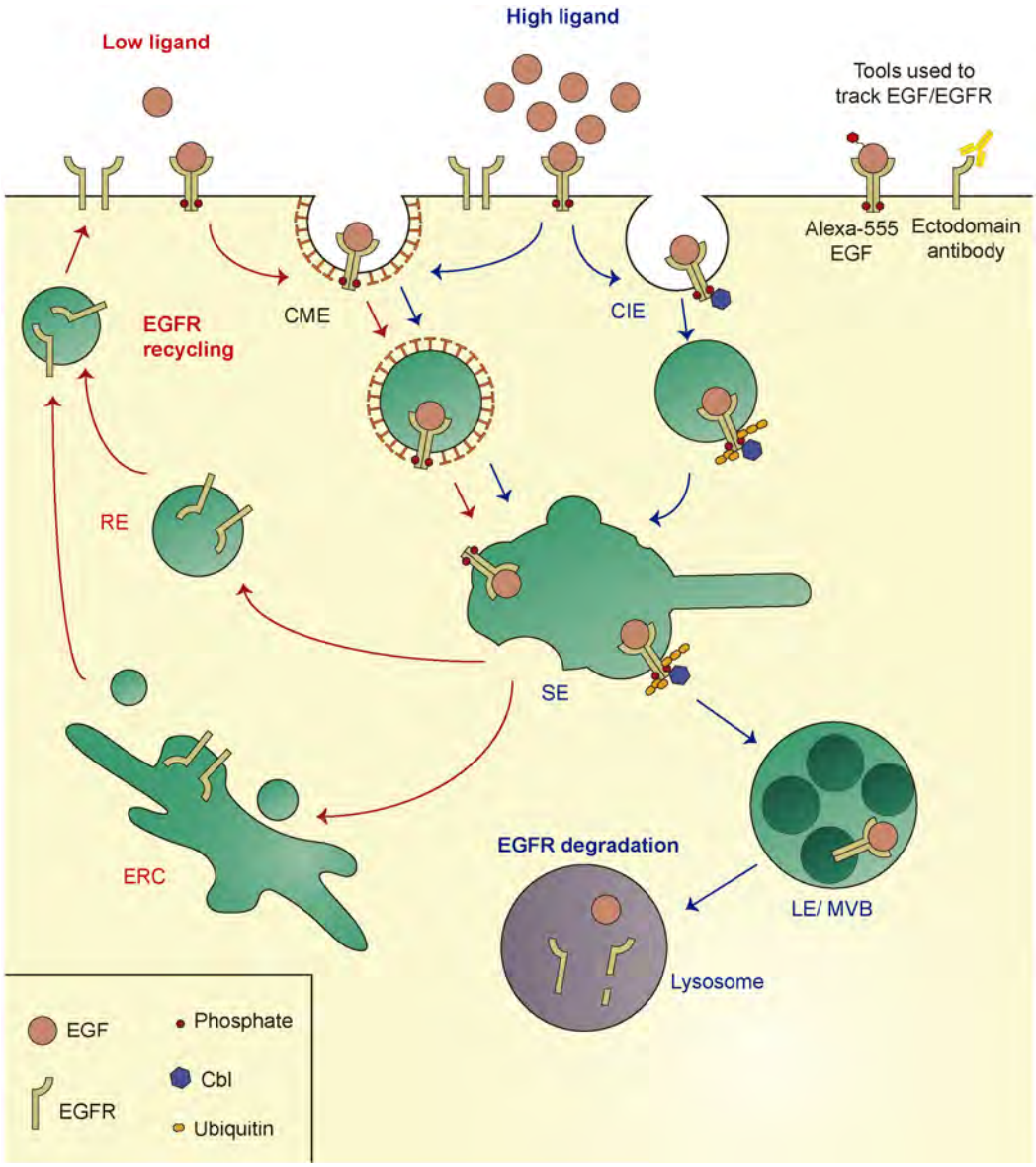

Fig. 4. EGFR trafficking under conditions of high and low EGF availability. Under conditions of low ligand availability, activated EGFR is almost exclusively internalized by CME and recycled back to the PM (red arrows), but when this pathway is saturated due to high EGF concentration, CIE pathways have been suggested to be activated, rapidly targeting EGFR towards degradation (blue arrows). In the presence of high stimulus intensity, the higher level of receptor phosphorylation promotes the recruitment of Cbl ubiquitin ligases and, once ubiquitylated, the EGFR can be recognized by the ubiquitin-dependent adaptors of ESCRTs and sequestered into MVBs. Low intensity of ligand-induced stimulus, however, offers less phosphorylated binding sites, which are preferentially occupied by signaling effectors, thus not allowing for Cbl recruitment. Tools used to study EGF/EGFR internalization in this thesis, namely fluorescently-labeled EGF or an antibody against the extracellular domain of the EGFR, are represented.

2.3. Cross-talk between endocytosis and the biosynthetic pathway

The TGN acts as the crossroad between the endocytic and biosynthetic pathways, representing both the starting point of the sorting of newly synthesized molecules and the arrival of proteins from endosomes via retromer. Traffic involving the TGN can be anterograde (to endosomes) or retrograde (from endosomes). Several proteins and lipids are delivered from the TGN to endolysosomes, including transmembrane sorting receptors, such as M6PRs and sortilins, which deliver hydrolytic enzymes, lysosomal membrane proteins and ion transporters (166). Regarding the retrograde pathway, the main cargoes are sorting receptors, SNAREs and other molecules whose functions depend on continuous retrieval back to the biosynthetic pathway. Interestingly, some plant and bacterial toxins such as Shiga, cholera, pertussis or ricin, also use the retromer pathway to exert cytotoxicity (167).

The best characterized cargo proteins that have been used to study the pathways between endosomes and the TGN are M6PRs. Clathrin-coated vesicles containing M6PRs form within the TGN and are directed towards endolysosomes. As mentioned above, the acidic pH of these organelles promotes the dissociation of the enzyme from the receptor. The enzyme continues its journey to the lysosome, where the low pH activates its degradative activity, whilst the receptor, which needs to be directed back to the TGN to start a new transport cycle, is transported back via the retromer complex (168).

The retromer is an evolutionary conserved complex consisting of two molecular modules: a heterotrimer composed of vacuolar protein sorting proteins VPS29, VPS35 and VPS26, called cargo selection complex, and the membrane-associated SNX-BAR dimer comprising the sorting nexins SNX1 or SNX2, and SNX5, SNX6 or SNX32, which contain PI(3)P binding domains able to interact with PI(3)P, and thus act in the retromer recruitment to endosomes. RAB7 also plays a key role in recruiting the retromer, by interacting with VPS35 in a guanine nucleotide-dependent way. Indeed, expression of dominant-negative RAB7 or RAB7 silencing were reported to cause retromer dissociation, inhibition of M6PR retrograde transport and missorting of acid hydrolases (144, 169).

Retrieval of M6PRs back to the TGN involves the recognition of a conserved W/F-L-M/V motif in the cytoplasmic tail of M6PR by VPS35 (170), and the functions of TIP47 and

RAB9. RAB9 is thought to define functionally distinct membrane domains on LEs, in which M6PRs concentrates. RAB9-positive vesicles subsequently bud off and, when in proximity to the TGN, are captured by tethering factors such as the Golgi-associated retrograde protein (GARP-I) and golgins, and finally fuse with the TGN in a process mediated by SNAREs (166).

2.4. Autophagy

Autophagy, the intracellular degradation process, is also sometimes included in the category of membrane trafficking for involving highly dynamic membrane organization. However, contrary to vesicle trafficking pathways, in which vesicles are generated from pre-existing organelles, autophagosomes are generated *de novo* (171). Three types of autophagy have been described in mammalian cells: macroautophagy, microautophagy and CMA, which differ in the way cytosolic components are delivered to lysosomes.

Macroautophagy (hereafter referred to as autophagy) is the best-characterized process, and consists of the engulfment of cytosolic components within autophagosomes and further degradation in lysosomes. This evolutionarily conserved pathway is key to maintain the cellular metabolism according to the cellular nutritional status, to remove dysfunctional organelles and misfolded protein aggregates, and to protect against invading pathogens, thus acting as a constitutive quality control pathway (172).

Autophagy is tightly regulated. It occurs constitutively, but can be markedly increased under certain circumstances. The classical example is mTOR-dependent autophagy, in which under starvation or nutrient deprivation circumstances, the mammalian target of rapamycin (mTOR) is inactivated leading to autophagy upregulation (173). It should be noted, however, that in mammalian cells autophagy can also be induced by mTOR-independent pathways (174).

The protein complex comprised of unc-51-like-kinase-1 (ULK-1), ATG13 and the focal adhesion kinase family-interacting protein of 200 kDa FIP200, plays a key role in autophagy induction. Indeed, mTOR functions, in part, by phosphorylating and inhibiting ULK-1 (175). The ULK-1 complex has been demonstrated to activate class III phosphoinositide 3-kinase (PI3K) and VPS34, required for early stages of autophagosome formation (176).

Upon autophagy induction, cytoplasmic components are trapped in a double membrane structure called autophagosome, whose origin is still under investigation, although different sources have been proposed, such as the PM, ER and mitochondria. It is possible that all these distinct locations contribute lipids and proteins to evolving autophasosomes, which subsequently mature through interactions with LEs and lysosomes (177–179).

The expansion of autophagosomes is mediated by two ubiquitin-like conjugation systems. One is the conjugation of ATG5 with the small ubiquitin-like protein ATG12, and the other is the covalent linkage of the cytosolic form of MAP1 light chain 3 (LC3-I) to phosphatidylethanolamine, generating the autophagosome membrane-bound form, LC3-II, the most commonly used autophagy marker (172).

Once formed, autophagosomes are transported on microtubules to the perinuclear region, where they fuse with LEs, creating a hybrid organelle called amphisome, or directly with lysosomes, giving rise to autophagolysosomes, wherein the vesicular products are degraded. Degraded products are then translocated to the cytoplasm, and to allow the maintenance of the cellular degradative capacity, lysosomes are subsequently reformed by budding off of tubules (proto-lysosomes) emanating from autolysosomes, although it remains to be elucidated how these nascent lysosomes convert into functional lysosomes (180, 181).

RAB7 is of fundamental importance for autophagosome maturation. Similarly to what happens in the endosomal pathway, RAB7 promotes autophagosome movement towards the perinuclear region by recruiting RILP. Moreover, it seems to control autophagosome-lysosome fusion by acting in concert with HOPS effectors and SNAREs (144).

The degradation of dysfunctional or superfluous mitochondria by autophagy is referred to as mitophagy, and it basically comprises all of the above-mentioned autophagy steps, such as phagophore formation, elongation, maturation and degradation of cargo. PINK1 and Parkin are fundamental for mitochondrial recruitment to autophagosomes. Mitochondrial depolarization activates PINK1, which phosphorylates Parkin and promotes its recruitment to depolarized mitochondria. Parkin subsequently ubiquitinates several mitochondrial outer membrane proteins, thus allowing them to be recognized by the ubiquitin-binding adaptor

protein p62. Finally, by binding LC3, p62 promotes the recruitment of damaged mitochondria to autophagosomes (182).

CMA is the process by which substrate proteins are selectively targeted to lysosomes and translocated into their lumen through the coordinated action of chaperones. CMA substrates contain a KFERQ-like motif in their amino acid sequence, which is recognized by the constitutive chaperone HSC70. This motif is often hidden in the folded protein and becomes exposed only upon unfolding. Once bound to the chaperone, the protein is targeted to the lysosomal surface, where it interacts with the cytosolic tail of a LAMP2 isoform, LAMP2A. This protein possesses a regulated lateral mobility that allows it to form a multimeric complex that mediates substrate translocation. By this mechanism, proteins can arrive to the lysosomal lumen without the need of intermediate cytosolic vesicles. CMA has an important role in protein quality control due to its ability to selectively remove single proteins from the cytosol (183, 184).

Finally, the least studied form of autophagy, microautophagy, can be defined as the direct uptake of cellular components into lysosomes through the invagination of the lysosomal membrane and subsequent vesicle scission into the lumen. It has been suggested that the main function of microautophagy is cell survival under nitrogen restriction conditions, as nitrogen deprivation induces microautophagy in yeast (185).

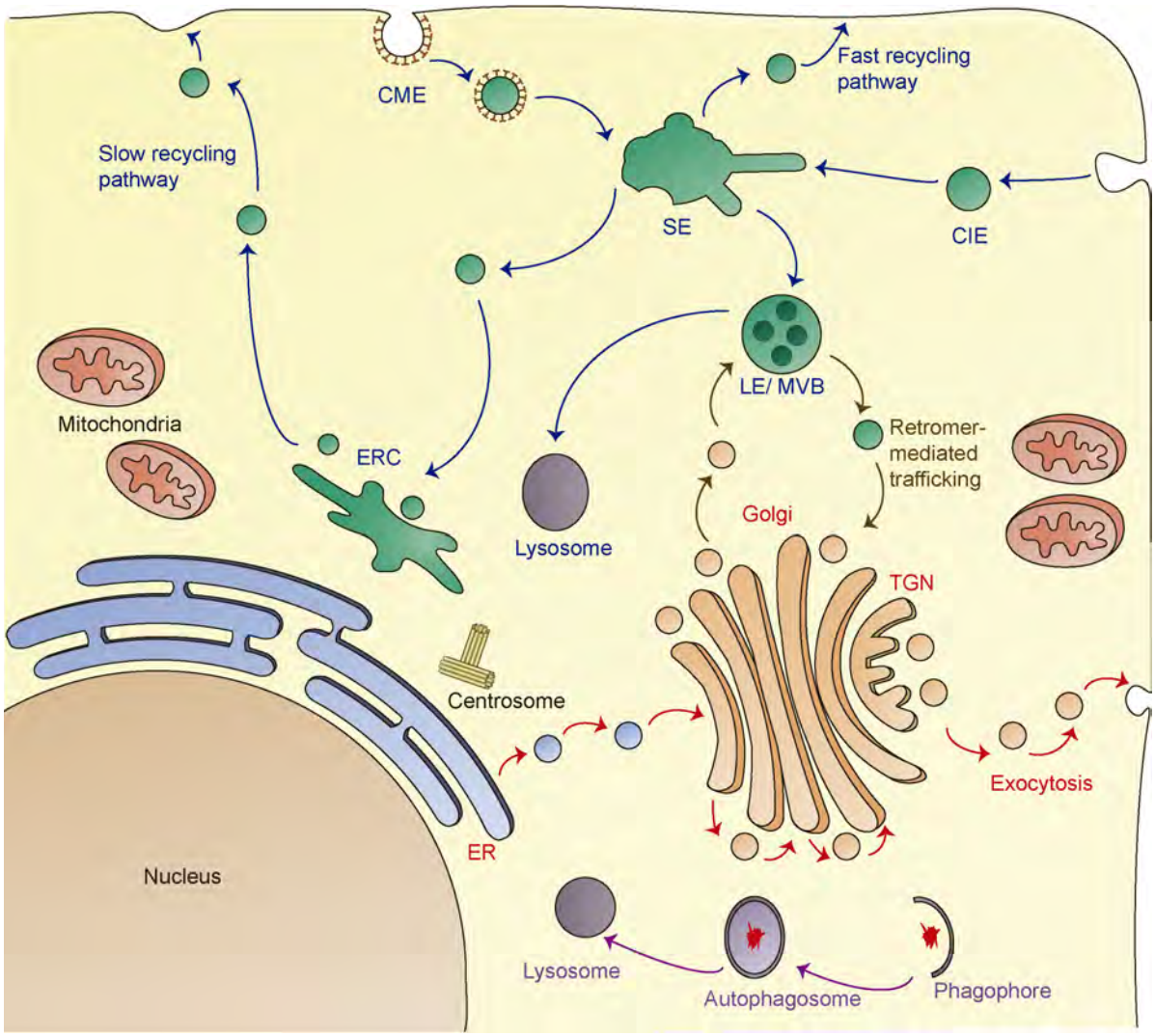

Fig. 5. Schematic representation of the different endomembrane trafficking pathways. In the endocytic pathway (blue arrows) extracellular substances are internalized either by clathrin-dependent or -independent mechanisms (CME and CIE, respectively). In SEs, the internalized material can be sorted for lysosomal degradation or recycled back to the PM, either by a slow or a fast recycling pathway. In the fast recycling pathway, the material goes directly back to the PM from SEs, while the slow recycling pathway firstly involves the transport to the ERC. On the other hand, in the biosynthetic/exocytotic pathway (red arrows), proteins synthesized in the ER are transported to the Golgi, progress through the different Golgi stacks and at the TGN are packaged into secretory vesicles which will fuse with the PM to release their contents. Proteins can also be retrogradely transported between Golgi stacks or from the Golgi to the ER (not represented here). Brown arrows represent the crosstalk between the endocytic and biosynthetic pathways, including anterograde transport from the TGN to endosomes, and retrograde transport from LEs to the TGN via the retromer complex. Macroautophagy, which consists of the engulfment of cytosolic components within autophagosomes and further degradation in lysosomes, is indicated with purple arrows.

3. RAB GTPases

As shown above, membrane trafficking pathways constitute a highly intricate and regulated system that connects the different cellular organelles, thus playing a critical role in the maintenance of cell homeostasis. Rab GTPases can be defined as the master regulators of intracellular vesicular trafficking. Through interactions with their multiple effectors, they coordinate basically all steps of intracellular trafficking, including the sorting of cargo and formation of transport vesicles, actin- and microtubule-dependent transport and membrane tethering.

The Rab family is part of the Ras superfamily of small GTPases and shows great evolutionary plasticity. The last eukaryotic common ancestor (LECA) expressed 20 Rab GTPases, a number which is unexpectedly large, probably indicating that the LECA had a complex set of organelles and trafficking steps. The 20 LECA Rabs can be classified into 6 large groups, mostly associated with a particular process: secretion (group I), EEs (group II), LEs (group III), recycling from endosomes to the PM (group IV), recycling from endosomes to Golgi (group V), and traffic associated with cilia and flagella (group VI). As eukaryotes diverged, some Rabs were lost in particular lineages, while others were gained, as a consequence of the loss or gain, respectively, of particular processes during specialization. No other set of membrane trafficking-associated proteins has experienced such a high degree of evolutionary plasticity, indicating that they underlie the diversity of organelle functions that exists between cell types and species (186).

3.1. Functional cycle

Rab GTPases function as molecular switches which are active in their GTP-bound state and inactive when bound to GDP. GTP binding causes a conformational change allowing for the interaction with the corresponding effectors and the activation of the pathways in which they are involved. Importantly, these changes in their activation state are coupled to changes in their membrane-bound state, and Rab GTPases exist in both soluble and membrane-bound pools. Rabs must be both GTP-bound and membrane-associated to be in an activated state.

Given the crucial role of Rab proteins in intracellular membrane trafficking, it is not surprising that their activation cycle is tightly controlled. Newly-synthesized Rabs bind Rab

escort proteins (REP1/2) and are prenylated at the C-terminus with one or (normally) two geranylgeranyl groups that function as membrane anchors. Most Rab proteins are prenylated by geranylgeranyl transferase type II (GGTII), which requires prior association of unprenylated Rabs with REP1/2. GGTII then dissociates from the complex, and REP1/2 chaperones the Rab to the membrane compartment in which it must exert its function (187).

Rab proteins undergo multiple cycles of membrane delivery and extraction. While the first membrane-association of newly synthetized Rabs is regulated by REP1/2, further membrane-association events are mediated by Rab GDP dissociation inhibitor (GDI1/2). GDI1/2 specifically recognizes GDP-bound Rabs and forms a soluble complex with them in the cytoplasm (188). GDI1/2 was suggested to require a membrane-associated GDI displacement factor (GDF) able to dissociate GDI1/2 from the Rab protein, thus promoting its membrane insertion. However, PRA1 and its yeast homolog Yip3 are the only GDFs that have been identified so far (189), and GDFs may not be necessary in all cases (188).

Once targeted to a membrane, Rabs can be activated by their respective guanine nucleotide exchange factors (GEFs), which promote the exchange of GDP with GTP. GEF binding promotes conformational changes in the Rab GTPase that open the nucleotide-binding pocket and subsequent GDP release. The excess of cytosolic GTP (≈1mM) relative to GDP ensures that GTP binds to the Rab protein as soon as GDP has been released, giving rise to an active GTPase which is resistant to membrane extraction. GEFs are very specific, binding only one or few Rab proteins. More than 40 Rab-GEFs have been identified so far, but presumably there exist many others, because around half of the currently known Rab proteins do not have an identified GEF (190). GEFs reported thus far belong to several structurally unrelated families, which makes the application of conventional homology search techniques difficult (191).

Upon membrane insertion and activation, Rab proteins are able to act upon their effectors and activate compartment-specific membrane trafficking events. Given their low intrinsic GTPase activity, conversion to their inactive forms is catalyzed by GTPase-activating proteins (GAPs). More than 40 different members have been reported in humans, and, contrary to Rab GEFs, GAPs belong to one major family, containing the TBC (Tre-2/Bub2/Cdc16) domain (188). The Rab3GAP complex is the only Rab GAP described thus

far that does not contain the TBC domain (192). TBC-containing GAPs stimulate GTP hydrolysis by a dual finger mechanism, in which the Gln-finger helps positioning a water molecule, while the Arg-finger stabilizes the partial negative charge on the GTP γ-phosphate. Interestingly, GAPs have been shown to act promiscuously towards several Rabs *in vitro*, although they achieve specificity *in vivo* (193), probably due to additional regulatory factors or to their subcellular localization.

Finally, GDP-bound Rabs lose affinity for effector molecules and display increased affinity for GDI1/2, which is followed by membrane extraction, generating stable complexes which act as a cytosolic reservoir of Rab proteins.

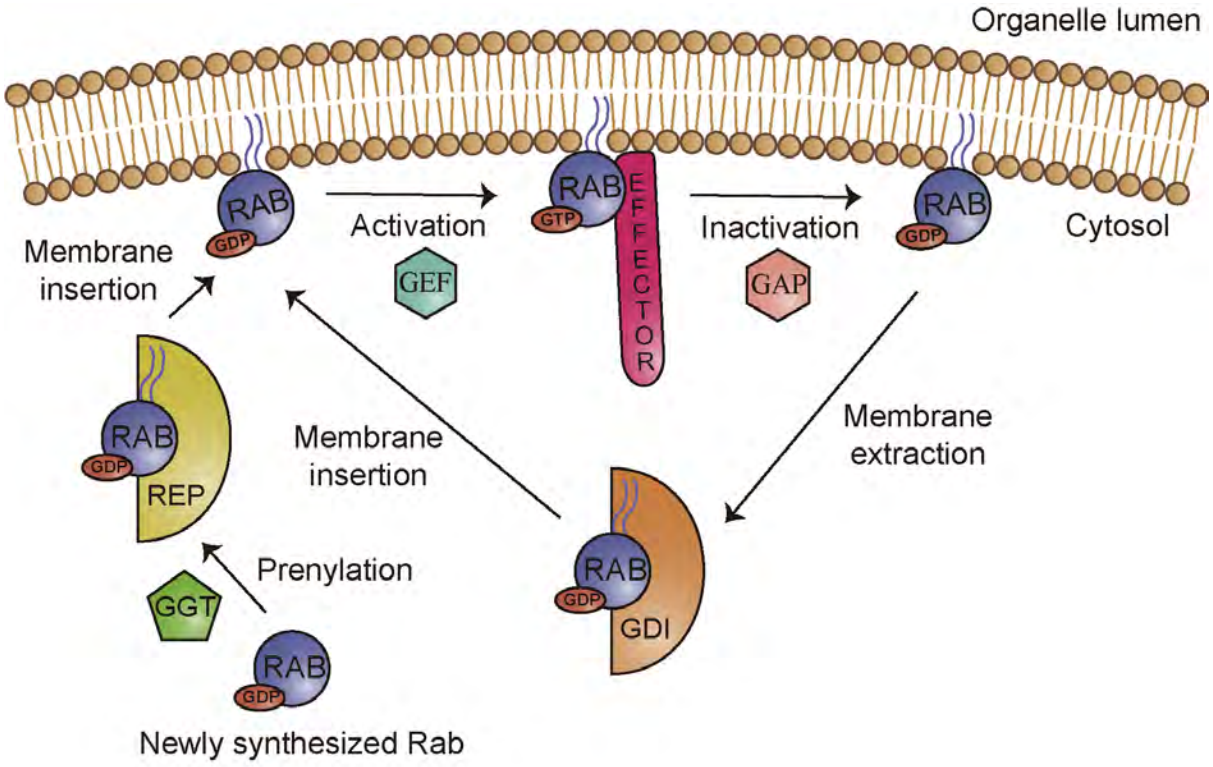

Fig. 6. Rab GTPase cycle. Newly synthesized and inactive Rab proteins bind to REP and become prenylated by GGT. The prenylated Rab can then be inserted into a particular membrane compartment, where a GEF promotes the exchange of GDP for GTP, thus activating the protein. Once one the membrane, the GTP-bound Rab can recognize multiple effectors and activate their specific functionalities. A GAP then converts Rab back to its inactive GDP-bound form, which is not able to interact with its effectors and is extracted from the membrane by GDI. Rab proteins undergo multiple cycles of GDI-mediated membrane delivery and extraction.

3.2. Structural features

Rab proteins are globular and contain a six-stranded β-sheet (β1-6), with five parallel strands and one anti-parallel strand, flanked by five α-helices (α1-5) in parallel configuration. The N- and C-termini are defined by β-1 and α-5, respectively (194). Two regions, called switch I (between α1/β2) and switch II (between β3/β4), experience a conformational change upon nucleotide exchange, adopting an ordered conformation when GTP-bound, and a less well-defined conformation in the diphosphate state. Six conserved sequence motifs surround the nucleotide-binding site: three phosphate-binding motifs (PM1-3) and three guanine-binding motifs (G1-3) (193).

The switch I domain interacts with the β-phosphate of both GDP and GTP, and contains an invariant threonine that binds Mg^{2+}, a cofactor required for high-affinity binding and hydrolysis of nucleotides (195). The switch II domain does not bind to GDP, but interacts with the γ-phosphate of GTP by the glycine residue of its conserved DTAGQ/T/H motif (191). Superimpositions of Rab structures in their active form show the main structural heterogeneity in their switch domains and the α3/β5 loop, located adjacent to the switch II domain (196). Switch regions are crucial for effector recognition, as this interaction takes place in the GTP-bound state of the Rab protein (197), and for interaction with regulators, including REP1/2, GDI1/2 and GEFs, which preferentially interact with the GDP-bound form (198).

The C-terminal region is highly variable between different Rabs, and thus is termed hypervariable domain. It has been postulated to be involved in Rab subcellular localization by mediating the interaction with specific membrane compartments (199). However, some studies suggest that membrane targeting involves multiple Rab regions (200, 201), and may be mediated by the localization of their GEFs or by posttranslational modifications (202, 203).

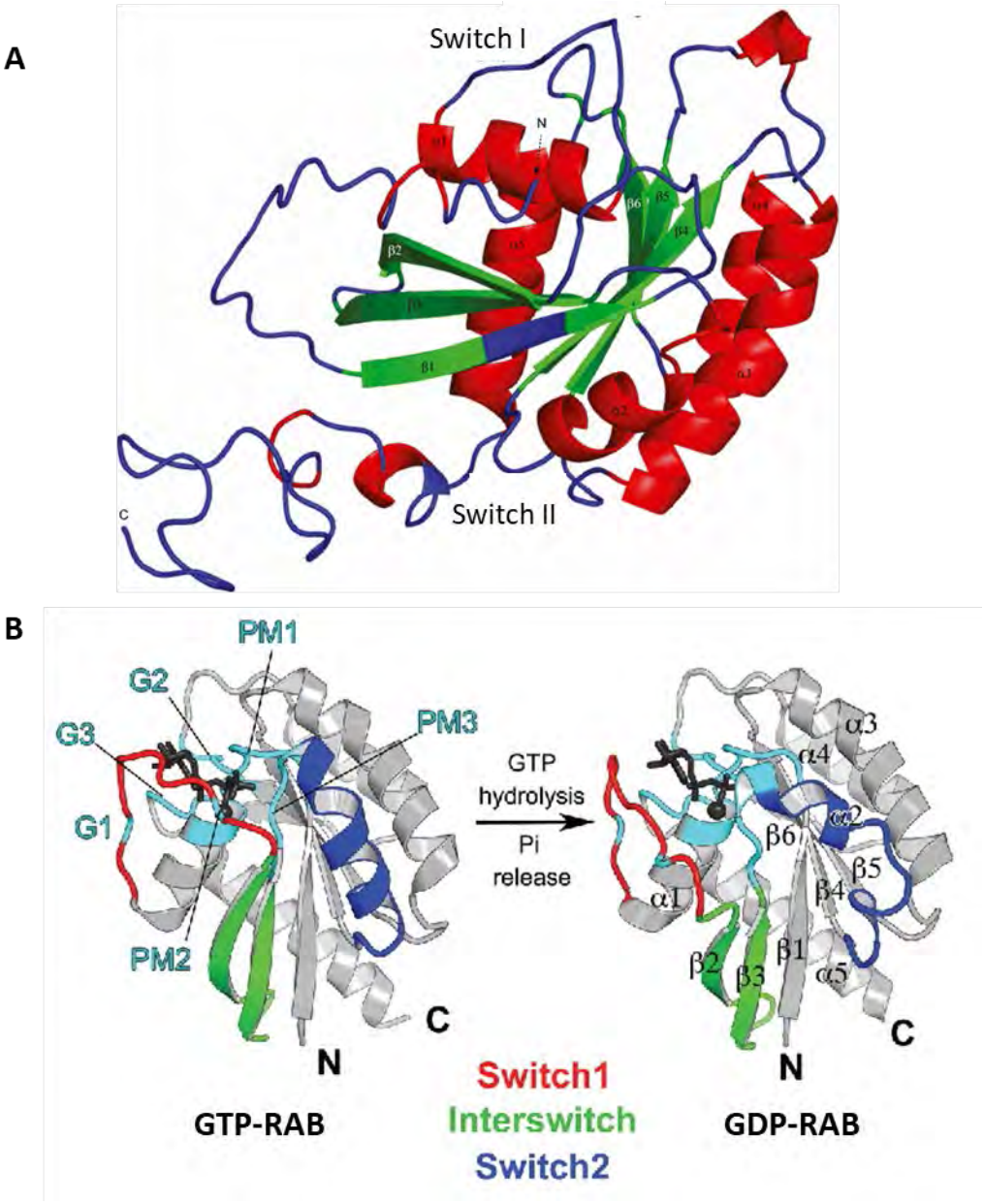

Fig. 7. Structural features of Rab GTPases. **(A)** Ribbon drawing of RAB3A to illustrate the main structural features of a Rab GTPase. The barrel-shaped core consists of 5 α-helices (in red), and the wall of the barrel is filled with 6 β-sheets (in green). The functional specificity of Rab is determined by switch I and II regions, which are important for the interactions with effectors and regulatory proteins. Adapted from (194). **(B)** Structure of GTP- and GDP-bound Sec4p, which were the first Rab structures determined in both nucleotide-bound states. Switch regions adopt an ordered conformation in the GTP-bound state and a less ordered conformation in the diphosphate state. The conserved motifs sorrounding the nucleotide-binding site are indicated in cyan. Switch I, switch II and interswitch (sequence between the two switches) are represented in red, blue and green, respectively. Adapted from (193).

3.3. Cellular distribution and functions

There are at least 63 different Rab proteins in humans, of which around three-quarters associate with endocytic organelles. Rabs recruit specific effectors to specific membrane compartments to which they associate in their active form and assemble the molecular machinery to mediate membrane trafficking. Sometimes, Rabs occupy different microdomains of a given membrane compartment. For example, RAB4, RAB5 and RAB11 can be observed segregated on a single endosome in live cells (151), and RAB7 and RAB9 also define distinct microdomains on LEs (204).

Rabs function in basically all steps of intracellular vesicular trafficking. RAB1 regulates ER-Golgi traffic (205), while RAB2 plays a role in retrograde trafficking from the Golgi to the ER (206). RAB6 exerts its function in retrograde intra-Golgi and Golgi to ER trafficking and, at least in some cell models, in anterograde Golgi-to-PM trafficking (207, 208). RAB5 regulates CCV uncoating, their fusion with SEs, and homotypic fusion events within SEs (209). RAB7 regulates transport from early to late endosomes and lysosomes, allows retromer recruitment and has a function in autophagy regulation, as described in the previous section (210). RAB7L1/ RAB29 is important for the maintenance of TGN integrity, and also participates in primary cilium growth and retromer-mediated trafficking (100, 211, 212). RAB4 and RAB11 regulate the transport along the fast and slow recycling pathways, respectively (213, 214), and RAB35 has also been shown to promote endocytic recycling (215). RAB9 regulates cargo transport from LEs to the TGN (216). RAB8 and RAB10 play a role in biosynthetic traffic from the TGN to the PM, trafficking from the ERC and in ciliogenesis (217–219). RAB12 has been suggested to participate in exocytosis and in an unconventional degradative pathway from REs to lysosomes, important for Tfn degradation, and it also favors autophagosome movement towards lysosomes (220, 221). RAB18 is required for normal ER structure and also participates in lipid droplet formation (222, 223). RAB33 mediates phagophore formation, whereas RAB24 is important for autophagosome maturation (224). RAB32 and RAB38 are involved in post-Golgi transport of key enzymes during melanogenesis (225), and RAB32 also controls mitochondrial fission (226).

Most Rab GTPases are ubiquitous, but some are restricted to specific cell types. In humans, 24 Rab proteins are specific to or enriched in the central nervous system, and their

functions include the regulation of neural development, neurite growth, axonal transport and synaptic vesicles (227). For example, RAB3A and RAB27B are rather exclusively expressed in neurons, and play a role in synaptic vesicle exocytosis (228).

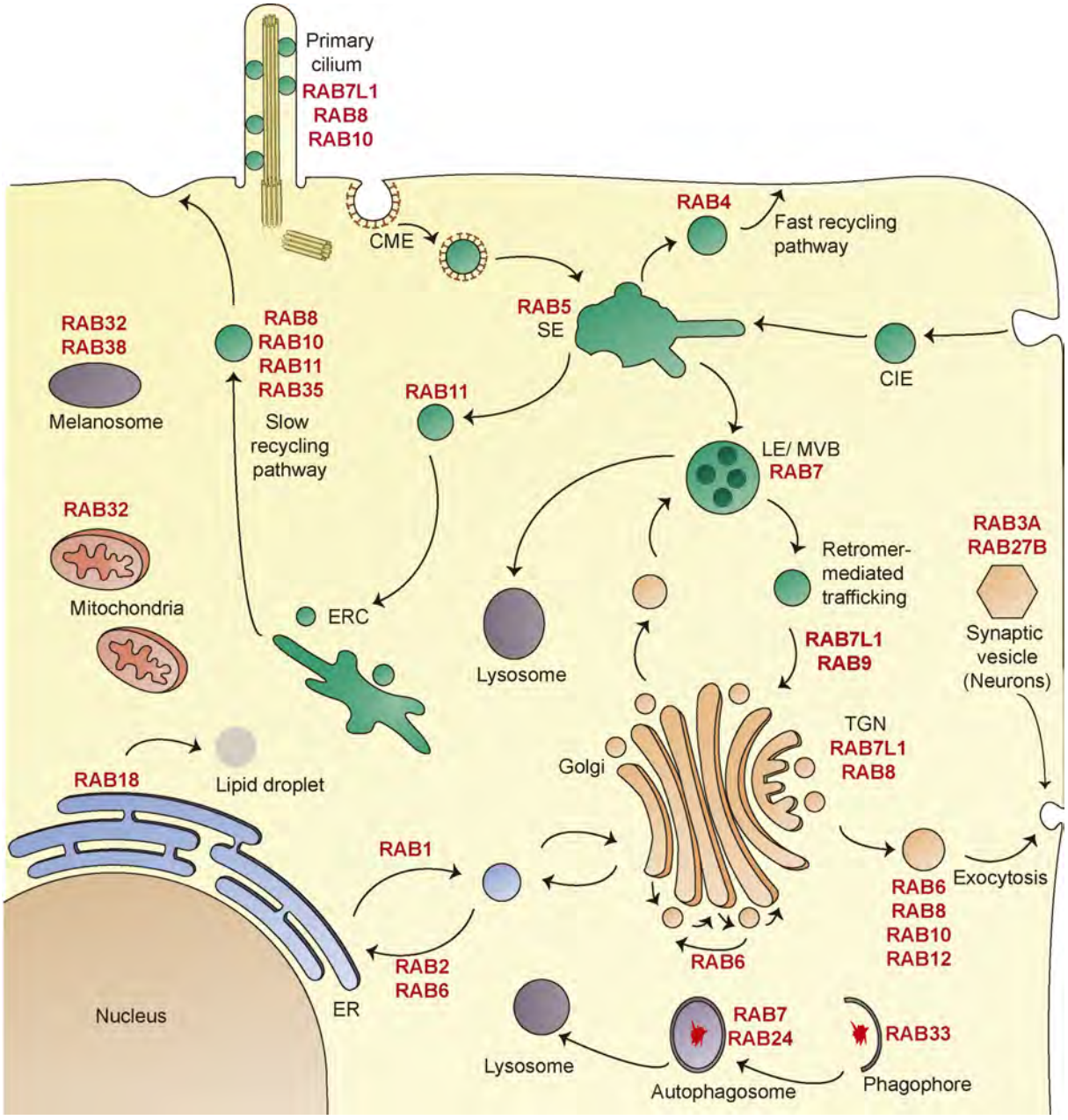

Fig. 8. Intracellular localization and functions of Rab GTPases. Rabs are implicated in all steps of intracellular vesicular trafficking. Here, the best characterized Rab proteins, as well as the most important Rabs for LRRK2 function (as further explained below), are represented. RAB1 regulates ER-Golgi traffic, while RAB2 plays a role in retrograde trafficking from the Golgi to the ER. RAB6 exerts its function in retrograde and anterograde trafficking involving the Golgi. RAB5 regulates CCV uncoating, their fusion with SEs, and homotypic fusion events within SEs. RAB7 regulates transport from EEs to LEs

and lysosomes, allows retromer recruitment, and has a function in autophagy regulation. RAB7L1 is important for TGN integrity, and participates in retromer regulation and ciliogenesis. RAB4 and RAB11 regulate the transport along the fast and slow recycling pathways, respectively, and RAB35 also promotes endocytic recycling. RAB9 regulates cargo transport from LEs to the TGN. RAB8 and RAB10 play a role in biosynthetic traffic from the TGN to the PM, trafficking from the ERC, and in ciliogenesis. RAB12 has been suggested to participate in exocytosis and in an unconventional degradative pathway from REs to lysosomes (not shown), and it also favors autophagosome movement towards lysosomes. RAB18 is required for normal ER structure and participates in lipid droplet formation. RAB33 mediates phagophore formation, whereas RAB24 is important for autophagosome maturation. RAB32 and RAB38 are involved in the post-Golgi transport of key enzymes during melanogenesis, and RAB32 also controls mitochondrial fission. RAB3A and RAB27B are predominantly expressed in neurons, and play a role in synaptic vesicle exocytosis.

3.4. Rab effectors

Rab effectors are proteins which specifically interact with a GTP-bound Rab GTPase. This way, Rab can act as molecular switches which activate the processes in which they are involved in when in their GTP-bound form. A few cases of Rabs binding to putative effectors in their GDP-bound state have also been described, such as protrudin interacting preferentially with GDP-RAB11 (229), but these studies need to be evaluated with great care, as they could represent an artefact of incomplete nucleotide exchange *in vitro* (230).

A great number of effectors for Rabs have been identified, including molecular tethers, fusion regulators, kinases, phosphatases, components of membrane contact sites and Rab regulators. The number of effectors for an individual Rab protein is growing rapidly, and a given Rab may have more than 30 effector proteins (231).

Effectors recognize the switch I-interswitch-switch II surface, which allows for specific interaction with the GTP-bound form of the Rab. Recent evidence suggests that subtle variations within this region confer specificity for effector recognition, thus permitting discrimination between different active Rab GTPases in spite of their overall structural similarity. For instance, a conserved hydrophobic triad of aromatic amino acids within this conserved surface plays a role in binding specificity, with their side chain orientations being influenced by surrounding variable residues. Moreover, non-conserved regions of Rab proteins may further account for effector binding specificity. Importantly, the recruitment of Rab proteins to distinct organelles or to specific microdomains within these organelles by

their regulatory proteins allows for the coupling of a given Rab with specific effectors localized in the proximity, further contributing to specificity (193, 232).

Interestingly, effector proteins can couple distinct Rab GTPases in network cascades, thereby linking their respective localizations and functions, allowing for the coordination of trafficking events. A typical example are Rab GEF cascades, in which one Rab, in its GTP-bound form, recruits the GEF that activates the next Rab protein in a specific trafficking pathway. An example is the transition from early to late endosomes, which has been previously described in this introduction. RAB5 recruits the HOPS complex, which contains VPS39, a GEF for RAB7, allowing RAB7 recruitment and maturation into a late endosomal compartment (233). Additionally, Rab GAP cascades, in which a GAP that inactivates the previous Rab is recruited only after the next Rab on the pathway has been activated, have been documented (234).

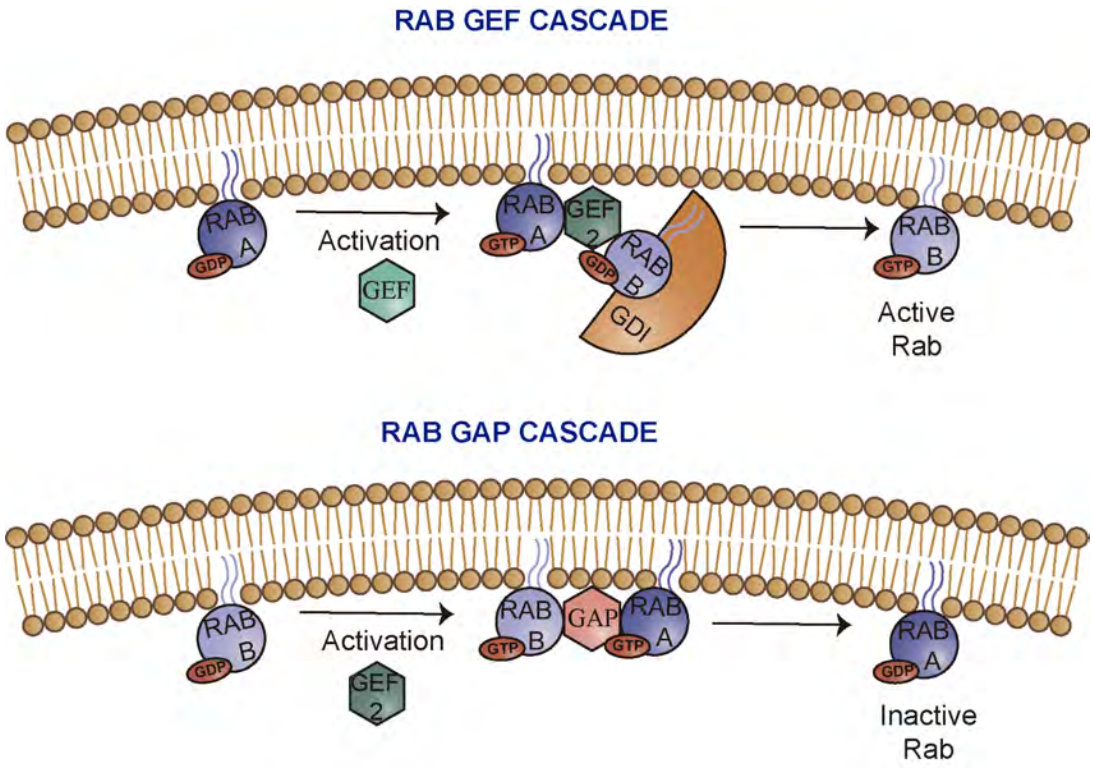

Fig. 9. Rab GEF and GAP cascades. Rab GEF cascades consist of a Rab protein (RAB A), which in its GTP-bound form, recruits the GEF (GEF 2) that activates the next Rab protein (RAB B) in a specific trafficking pathway. On the other hand, in Rab GAP cascades, a GAP that inactivates the previous Rab (RAB A) is recruited only after the next Rab (RAB B) on the pathway has been activated. Rab GEF and GAP cascades permit the coupling of distinct Rab GTPases in network cascades.

3.5. Rabs and PD

Rab protein dysfunction has been linked to a variety of human diseases. For example, mutations in RAB18A cause the recessive developmental disorder Warburg Micro syndrome (235), characterized by brain, eye and endocrine abnormalities, while Charcot-Marie-Tooth type 2B is a rare peripheral neuropathy caused by mutations in RAB7 (236). Mutations in RAB23 are responsible for Carpenter Syndrome characterized by congenital malformations (237), and mutations in RAB27 cause Griscelli Syndrome type 2, characterized by hypopigmentation and immune system abnormalities (238). Moreover, Rab regulators and effectors have been associated with diseases. Mutations in GDI1 cause a rare form of X-linked intellectual disability (239), whereas mutations in REP1 are linked to choroideremia, and X-linked chrorioretinal degeneration which causes blindness (240).

Several loss of function mutations in RAB39B have been identified as a rare cause of PD, and are also linked to symptoms atypical for PD cases such as intellectual disability (96). RAB39B is enriched in brain tissue, with the exogenously expressed protein showing a Golgi-like localization (241). Although its functions are not well-known, it has been recently shown to be involved in surface transport of the AMPA receptor subunit GluA2 through its effector PICK1 (242). Moreover, the protein complex composed of C9ORF72, WDR41 and SMCR8, implicated in autophagy regulation, has GEF activity towards RAB39B, as well as RAB8. Loss of C9ORF72 impairs autophagy, and the expression of a constitutively active form of RAB39B rescues this effect (243). Consequently, RAB39B could be playing a role in neuronal autophagy, and its loss could impair the ability to clear protein aggregates and result in α-syn accumulation. Indeed, widespread LB pathology in *postmortem* tissue of an individual carrying a loss-of-function mutation has been described (96).

Additionally, several PD-related genes have been reported to interact with Rabs. For instance, a subset of Rab proteins, including RAB1, RAB3A, RAB8A and RAB11, are known to modulate α-syn-mediated aggregation and toxicity (244–246). Various Rab proteins, including RAB5B, RAB7, RAB7L1, RAB32, RAB38 and RAB8A have been reported to interact with LRRK2 (100, 247–251). Importantly, the phosphorylation status of some Rabs is regulated by the enzymatic activities of PD-related proteins. For example, LRRK2 phosphorylates RAB3A/B/C/D, RAB8A/B, RAB10, RAB12, RAB43 and RAB35

(83, 252), and PINK1 has been shown to indirectly regulate the phosphorylation of RAB8A, RAB8B and RAB13 (253).

4. RAB8

RAB8 is a 24 kDa Rab GTPase displaying high homology with the yeast protein SEC4 involved in post-Golgi traffic (254). In humans, there are two isoforms sharing 80% homology, named RAB8A and RAB8B, which display a different expression pattern (255). RAB8B is mostly expressed in the spleen, testis and brain, whereas RAB8A is more ubiquitous and shows lower expression levels in the organs where RAB8B is more abundant (256). Among mammalian Rabs, the most closely related Rabs to RAB8 are RAB10 and RAB13 (257).

4.1. Regulation

Several GEFs for RAB8A have been identified, including Rabin8 (258), GRAB (259), and C9ORF72 (243). Amongst them, Rabin8 is the best studied one, and is involved in an activation cascade. Specifically, Rabin8 is recruited to membranes by GTP-bound RAB11, where it activates RAB8 (260). Similarly, a RAB11-GRAB-RAB8 cascade has been reported (261). Described proteins with GAP activity towards RAB8 comprise TBC1D1 (262), TBC1D4 (263), TBC1D30 (264), and TBC1D17. TBC1D17 has been shown to be recruited by the RAB8 effector optineurin to cause the inactivation of RAB8 (265).

A series of RAB8 effectors have been reported, and their characterization has allowed the identification of the cellular pathways in which RAB8 plays a role. Identified effectors include MICAL-3 (266), MICAL-L1 (267), JRAB/MICAL-L2 (268), CEP290 (269), optineurin (270), otoferlin (271), rabaptin5 (272), OCRL1 (273), and cenexin3 (264).

4.2. RAB8 functions

RAB8 is involved in regulating different membrane trafficking pathways, including endocytic recycling, trafficking from the TGN to the PM, and primary cilium formation.

RAB8 has been reported to localize to a tubular ERC and to participate in a membrane-recycling pathway which allows the recycling of internalized membrane back to the PM, a process which is crucial for the formation of new cell surface domains, and inhibition of RAB8 results in the accumulation of vesicles with membrane originating from the PM (274). Importantly, RAB8-mediated recycling of internalized membrane back to the PM plays a role in cell migration. It is crucial for the formation of new cell protrusions, defined as cell surface domains with a leading edge containing filopodia and lamellipodia, structures that mediate cell migration. Overexpression of RAB8 promotes protrusion formation. Conversely, in RAB8-deficient cells, a cessation of this membrane-recycling pathway stops migration and promotes cell-cell adhesion (274, 275).

The role of RAB8 in ERC-to-PM transport has also been related to protein recycling. For example, the recruitment to tubular membranes within the ERC of both RAB8 and EHD1, a protein implicated in the regulation of endocytic trafficking from the ERC to the PM, is mediated by MICAL-L1, and together they control the recycling of beta1 integrin to the PM (267). These proteins also participate in Tfn recycling. Indeed, RAB8 depletion has been shown to inhibit the trafficking of Tfn and the TfnR to the ERC (274) and similarly, knockdown of its effector optineurin impairs Tfn translocation to the ERC (270).

RAB8-dependent recycling was suggested to promote endosomal cholesterol removal (276, 277). RAB8 overexpression lowered cholesterol accumulation in a human fibroblast line carrying mutations causing Niemann-Pick type C, a disease in which cholesterol and sphingolipids accumulate in LEs. In contrast, RAB8 depletion was associated with the accumulation of cholesterol in LEs. Experiments using fluorescently-labeled sterol show that it can be detected in the ERC as a previous step to sterol efflux from the cell, which supports a role for ERC-localized RAB8 in cholesterol removal (276).

The delivery of vesicles to the ciliary membrane during ciliogenesis, the process by which primary cilia assemble, is another important function of RAB8 (278). The primary cilium is a sensory organelle that transmits signals from the extracellular environment and is formed at the apical cell surface as a result of a nucleation process originating from the centrosome/basal body (279). Targeting of RAB8 to maturing cilia is achieved by the RAB11-Rabin8 cascade. After ciliogenesis induction, RAB11 is recruited to the

pericentrosomal region, a process which is dependent on the mother centriole appendage protein cenexin3 and a phosphoinositide 3-kinase (PI3K-C2), which generates a pool of phosphatidylinositol 3-phosphate at the base of the cilium necessary for RAB11 activation. RAB11 recruits and activates Rabin8, with the subsequent recruitment and activation of RAB8, promoting the transport and fusion of RAB8-positive carriers at the ciliary base (280, 281). Based on the proximity of the centrosome to the Golgi, ciliary vesicles were initially suggested to be derived from the Golgi, although the implication of the ERC-related proteins EHD1, EHD3 and RAB11 in early ciliogenesis steps supports an ERC origin for ciliary vesicles. In addition, ciliary vesicles were shown to carry exogenously introduced smoothened, which is a transmembrane protein specifically localized in cilia, further supporting the implication of endocytic recycling pathways in ciliogenesis (282, 283).

In addition to its function in endocytic recycling, RAB8 localizes to the TGN and has a role in secretion. It has been found on secretory vesicles colocalizing with RAB6 in HeLa cells and, although not needed for their budding or motility, it is required for the docking and fusion steps (266). Moreover, insulin-induced translocation of the glucose transporter GLUT4 to the cell surface has been reported to be dependent on RAB8 in muscle cells (284). Further evidence for a role of RAB8 in exocytosis comes from the fact that optineurin has been demonstrated to be involved in constitutive secretion (285).

RAB8 is also implicated in polarized membrane trafficking in different cell types. Specifically, it plays a role in the polarized localization of apical cell surface proteins, and the RAB11-Rabin8-RAB8 cascade has been demonstrated to promote epithelial polarization by controlling apical exocytosis in intestinal epithelial cells (260, 286). Furthermore, it mediates the apical trafficking of digestive enzymes in acinar cells of the pancreas (287).

Importantly, in neuronal cells, RAB8-mediated membrane trafficking events are needed for neurite outgrowth. Indeed, neurite outgrowth is prevented when inhibiting RAB8, as a result of a decrease in the number of vesicles undergoing anterograde transport into neurites (288). RAB8 is also involved in AMPA receptor trafficking at postsynaptic terminals (289).

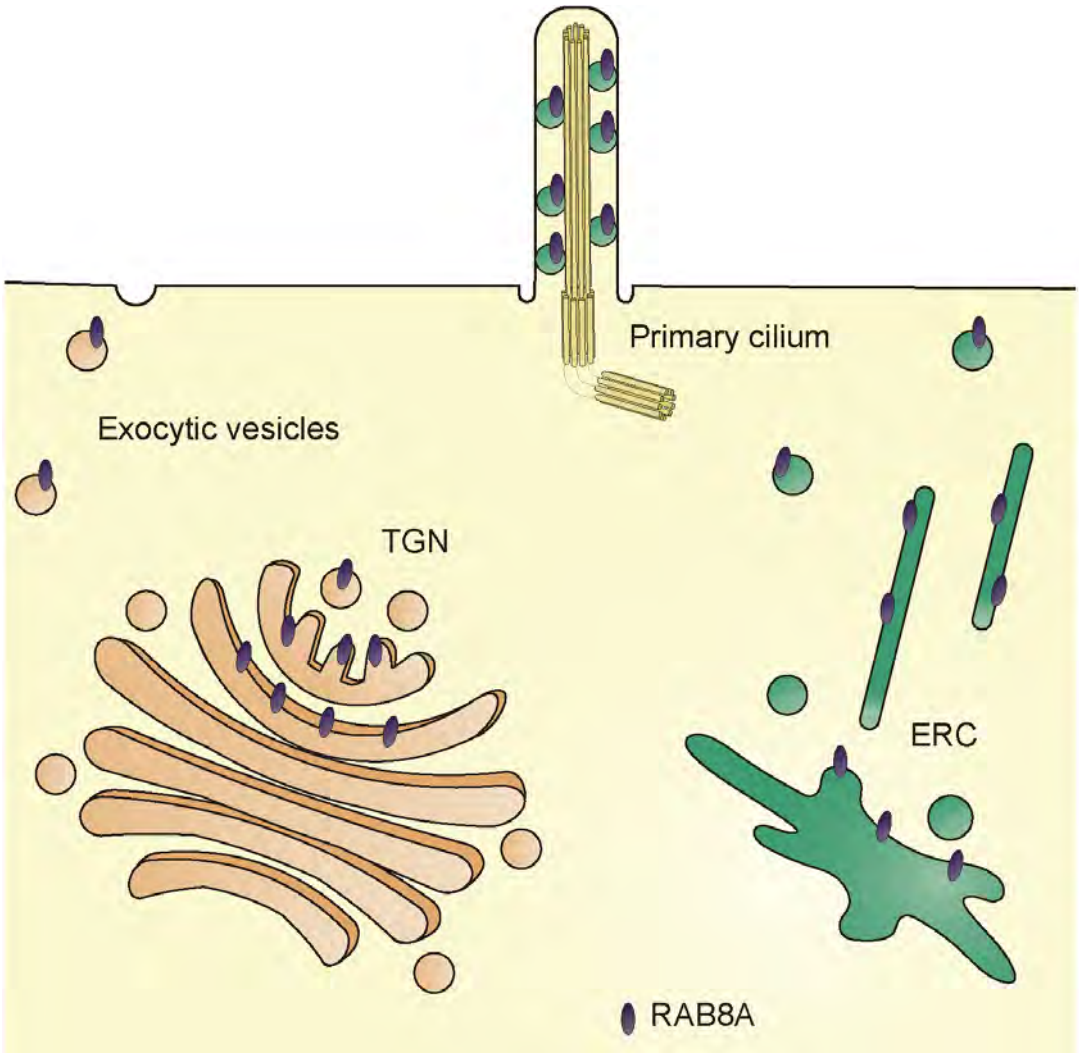

Fig. 10. RAB8A intracellular localization and functions. RAB8 can be found in different cellular compartments, including the TGN, exocytic vesicles, primary cilium and ERC. It is involved in regulating endocytic recycling from the ERC to the PM, important for membrane and protein recycling, constitutive and regulated secretion in different cell types, and in the delivery of ciliary vesicles to maturing primary cilia.

5. LRRK2: A LINK BETWEEN RAB GTPASES AND PD

In 2004, mutations in the LRRK2 gene were found to cause an autosomal-dominant form of PD in several families (290–292). Furthermore, variations in LRRK2 were found to increase risk for PD, indicating that it also plays a role in the sporadic form of the disease. LRRK2 mutations are the most common genetic cause of PD, accounting for ≈ 10% of familial PD and ≈ 4% of sporadic PD cases (293). Indeed, the G2019S mutation on its own

accounts for ≈ 2-5% of familial PD and ≈ 1-2 % of sporadic PD cases in the European population (294–296). However, in certain ethnicities, such as Ashkenazi Jewish and North African Berbers, its prevalence is much higher, being responsible for ≈ 20 and ≈ 42% of PD cases, respectively (297, 298).

The penetrance of LRRK2 mutations is incomplete. For example, the international LRRK2 consortium determined the penetrance of the G2019S mutation to be 28% at 59, 51% at 69 and 74% at 79 years (299), although this may vary depending on the ethnic group (300). Homozygous LRRK2 carriers are similar to heterozygous carriers, and also show incomplete penetrance (301). Therefore, genetic background and environmental factors seem to play an important role in the development of LRRK2-PD.

More recently, variations in LRRK2 were revealed as a PD risk factor by GWAS (90), suggesting that LRRK2 contribution to the disease may have been underestimated.

Importantly, LRRK2-related PD, although pleomorphic (291), is clinically and neurochemically largely indistinguishable from sporadic PD, such that understanding the cellular mechanisms altered by pathogenic LRRK2 may also shed light on the most common, sporadic form of the disease.

5.1. Expression and localization

LRRK2 is ubiquitously expressed, although it shows higher expression levels in certain organs such as the kidney or lung. It is also highly expressed in immune cells like lymphocytes, dendritic cells and macrophages. In the mammalian brain, LRRK2 is expressed at highest levels in neurons of the cortex, striatum and hippocampus, and lower levels in other regions such as the SNpc (302).

Regarding its subcellular localization, LRRK2 is predominantly cytosolic, but has also been detected in a variety of membrane compartments by immunofluorescence or cell fractionation studies, including the neck of caveolae, microvilli, MVBs, autophagosomes, lysosomes and the Golgi (303–305). In neurons, LRRK2 can also be present in synaptic vesicles (250, 306, 307).

It is important to note that the large pool of cytosolic LRRK2 may mask the membrane-associated pool, and it raises the issue of cytosolic LRRK2 precipitation onto membranes during fixation. To overcome these challenges, Dario Alessi and colleagues have employed a liquid nitrogen coverslip freeze-thaw protocol that depletes cytosolic proteins (304), which would be of interest to use so as to confirm the previously reported localizations of LRRK2. Moreover, due to the low levels of endogenous LRRK2 expression in the majority of cell types, most localization studies have been performed under overexpression conditions, and low overexpression levels should be assured in order to avoid possible artefacts. Importantly, distinct membranous localizations may further be triggered by specific interactors and/or stimuli, such as the reported LRRK2 recruitment to the Golgi by RABL1 (304) or to lysosomes under conditions of lysosomal stress (305). Consequently, they may not represent the localization of steady-state LRRK2 under endogenous conditions.

5.2. Structure and enzymatic activities

LRRK2 is a large protein (286kDa and 2527 aminoacids) belonging to the ROCO family, and is characterized by the presence of a ROC (Ras-of-complex) GTPase, a COR (C-terminal of ROC), and a kinase domain (308). Apart from such catalytic core comprised of a GTPase and kinase domain, it contains a series of protein-protein interaction domains, such as N-terminal armadillo, ankyrin and leucine-rich repeats, as well as C-terminal WD40 repeats (309).

The closest LRRK2 homolog is leucine-rich repeat kinase 1 (LRRK1), which shares a similar overall domain structure and 45% sequence similarity with LRRK2. However, no link between LRRK1 variants and PD has been established thus far, and both proteins seem to have different interactors and act on different pathways (310, 311).

Importantly, the major disease-segregating mutations within LRRK2 are located in the central catalytic region, including R1441C/G/H and N1437H in the ROC domain, Y1699C in the COR domain, and G2019S and I2020T in the kinase domain (312), which suggests that the dysregulation of these enzymatic activities could account for the pathogenic effect of the mutated proteins. Amongst them, the most frequently occurring mutation is G2019S, which has been reported to increase kinase activity two- to three- fold *in vitro* (313). Pathogenic

mutations in the ROC and COR domains display increased GTP binding and decreased GTP hydrolysis, resulting in both cases in an increase in the amount of GTP-bound LRRK2 (314, 315). Although none of the pathogenic mutations in the ROC or COR domains were shown to enhance kinase activity using *in vitro* phosphorylation assays, a recent study using *in vivo* approaches demonstrated that they display increased kinase activity as well (83). Consequently, all pathogenic mutants converge on enhancing LRRK2 kinase activity. The reason for the apparent discrepancy between *in vitro* and *in vivo* results could be the existence of other proteins which are not present *in vitro* and could influence LRRK2 activity in cells. For example, RAB7L1 was recently found to cause the activation of all the pathogenic LRRK2 mutations tested, although the mechanism is currently unknown (316).

The fact that increased LRRK2 kinase activity mediates neuronal toxicity (317), suggesting a toxic gain-of-function mechanism, points towards LRRK2 kinase inhibitors as potential disease-modifying drugs. First-generation inhibitors such as LRRK2-IN-1, CZC-54252, and CZC-25146 were reasonably selective against LRRK2, although they were unable to cross the blood-brain barrier (318). Moreover, LRRK2-IN-1 caused off-target effects related to inflammatory pathways (319). Second-generation inhibitors, including MLi-2 from Merck, PF-06447475 and PF-06685360 from Pfizer, and GNE-7915 and GNE-0877 from Genentech, are brain-permeable and show higher potency and selectivity (320). However, pharmacological kinase inhibition of LRRK2 has been reported to cause the abnormal accumulation of lamellar bodies (lysosome-related organelles which secrete pulmonary surfactants) in type II pneumocytes in non-human primates (321), which could be a safety liability for human clinical trials. However, these morphological changes may not be related to impaired organ function or toxicity. Indeed, a recent study showed that PF-06685360 induced morphological alterations characterized by darkened kidneys and accumulation of hyaline droplets in the proximal tubular epithelium of rats. However, these changes were reversible and no kidney toxicity or impaired kidney function was observed even after 12 weeks of treatment (322).

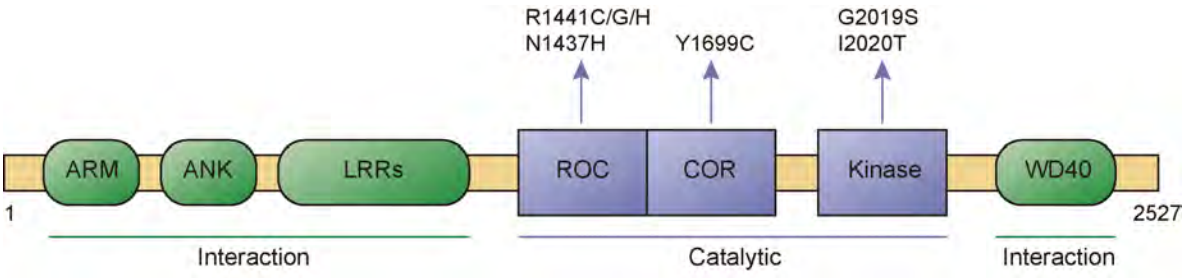

Fig. 11. LRRK2 structure and domains, indicating the major pathogenic mutations. LRRK2 is a large protein (286 kDa and 2527 aminoacids) which consists of a catalytic core comprising a ROC (Ras-of-complex) GTPase, a COR (C-terminal of ROC) and a kinase domain, and a series of protein-protein interaction domains such as N-terminal armadillo, ankyrin and leucine-rich repeats, as well as C-terminal WD40 repeats. The major disease-segregating mutations are located in the central catalytic region, including R1441C/G/H and N1437H in the ROC domain, Y1699C in the COR domain, and G2019S and I2020T in the kinase domain.

5.3. Intramolecular regulation of LRRK2

LRRK2 contains many serine and threonine residues, several of which have been reported to be phosphorylated. Depending on whether they are phophorylated by LRRK2 itself or by other kinases, they can be classified as autophosphorylation sites or as cellular phosphorylation sites, respectively. Although many autophosphorylation sites have been proposed *in vitro*, up to date only three have been confirmed in a cellular context, including T1410, T1503 and S1292. Cellular phosphorylation sites comprise S910, S935, S955 and S973, and amongst the potential upstream kinases responsible for their phosphorylation are casein kinase 1α, inhibitor of nuclear factor κB (IKK)-related kinases, and protein kinase A. Protein phosphatase 1α is the only phosphatase identified to affect the cellular phosphorylation sites to date (323).

PD-related mutations have been shown to impact upon the phosphorylation status of LRRK2. For example, S1292 autophosphorylation is enhanced by various pathogenic mutations and can be used as an indicator of LRRK2 kinase activity in cells (324). Additionally, most pathogenic mutations cause the dephosphorylation of the N-terminal cellular phosphorylation sites S910, S935, S955 and S973, although the mechanism remains unclear. Interestingly, these phosphorylation sites are also rapidly dephosphorylated in cells and tissues after treatment with LRRK2 kinase inhibitors, and abolishment of S935

phosphorylation has been used as a reliable readout for the efficacy of kinase inhibitors (325). Dephosphorylation of these phosphosites results in loss of 14-3-3 interactions, and in cells transiently expressing LRRK2, also in a change of LRRK2 localization to cytoplasmic accumulations and filamentous structures (325).

Another layer of regulation for LRRK2 is dimerization, which has been shown to be crucial for the activation of LRRK2. *In vivo*, LRRK2 is mostly monomeric within the cytosol, with dimers or higher-order oligomers predominantly associated with membranes. Pathogenic mutants show increased propensity to form dimers (326), supporting the idea that the active conformation may be the dimer.

LRRK2 has been suggested to belong to a group of G-proteins activated by nucleotide-dependent dimerization (GAD). GADs are characterized by their low nucleotide affinity and the dependence of their GTPase activity on dimerization, as a protomer would stimulate GTPase hydrolysis in the neighboring protomer. Consistently, the hydrolysis rate of monomeric LRRK2 is more than 700-fold slower than that of the dimeric form. Although a putative GEF and two GAPs have been characterized for LRRK2, it is not clear whether these proteins would modulate the GTPase cycle of LRRK2 in a conventional manner. In fact, due to its lower nucleotide affinity (μM range) compared to other GTPases, LRRK2 is not expected to be strictly dependent on GEFs for activation (327).

Another interesting aspect of LRRK2 regulation is the crosstalk between its enzymatic activities. Although LRRK2 is a functional GTPase, it is unclear how GTPase activity contributes to disease pathogenesis. The GTPase domain could serve to regulate kinase activity, as GTP-binding deficient mutants are kinase inactive, and GTP-binding has been shown to increase LRRK2 kinase activity (328–330). Reciprocally, kinase activity may regulate GTPase activity via autophosphorylation, as the *in vitro* phosphorylation of certain residues in the ROC domain enhances GTP hydrolysis (331, 332). However, isolated ROC domains were used, and evidence is lacking in the context of the full-length protein (333).

5.4. LRRK2 interactors

Almost 300 LRRK2 interactors have been described to date. However, there are many limitations to these studies. Firstly, most data come from *in vitro* systems, and the many

LRRK2 protein-protein interaction domains may make LRRK2 prone to bind to a variety of proteins with which it may not interact under physiological conditions. Indeed, the preservation and stoichiometry of protein-protein interactions is known to be highly dependent on experimental conditions and sample processing (334). Furthermore, due to the large size of the LRRK2 protein, several data were obtained using fragments, mainly the WD40 repeat containing domain (residues 2124-2527), the ROC domain (residues 1328-1513), or bigger fragments containing the whole C-terminal region (residues 970-2527) (335). These interactions need to be confirmed with the full-length protein under native conditions. Finally, due to its ubiquitous tissue expression, LRRK2 may have distinct interacting partners depending on the cell type analyzed and, possibly, the developmental state (336). However, validation in disease-relevant cell types is lacking for the majority of the reported LRRK2 interactors.

As a result of these limitations, most of the protein partners identified for LRRK2 have not been independently confirmed and indeed, when considering only the interactions validated in more than one publication or at least by 2 different experimental approaches in the same publication, the number of interactors becomes limited to 62 (336).

The identification of LRRK2 interactors is of great interest, as it sheds light on the functions of the protein. Interestingly, many of these partners are implicated in intracellular trafficking events. Amongst them, of special importance are Rab proteins. Using a yeast two-hybrid approach, RAB5B was first nominated as a LRRK2 interactor (250). The *Drosophila* LRRK2 homolog was also demonstrated to interact with RAB5 and RAB7 upon overexpression (248). However, RAB7 did not co-immunoprecipitate with LRRK2 in HEK293 cells under overexpression conditions (337), so this interaction may be restricted to the *Drosophila* homolog. The examination of genetic interactions in human brain expression data suggested an interaction between RAB7L1 and LRRK2 (100), which was further confirmed by high-throughput screening using recombinant proteins (338). Finally, LRRK2 was suggested to physically interact with RAB32 and RAB38 by yeast two-hybrid screening, and the interaction with endogenous LRRK2 was validated for overexpressed RAB32 by GFP-Trap analysis (247).

Another set of well characterized LRRK2 interactors include chaperones and adaptor proteins. For instance, a SILAC-based study found 14-3-3 proteins highly enriched in LRRK2 immunoprecipitates (339), and subsequent studies confirmed this interaction (340, 341). Importantly, this interaction was validated with endogenous levels of both LRRK2 and 14-3-3 proteins isolated from mouse tissue (339). 14-3-3 proteins are a family of chaperones which regulate the subcellular localization and function of a vast number of binding partners (342). Phosphorylation of LRRK2 S910 and S935 is required for 14-3-3 binding, and kinase inhibitors (340) and pathogenic mutations (341) showing decreased phosphorylation at these residues cause reduced 14-3-3 binding, most likely due to a conformational change in LRRK2 that abolishes the interaction and leaves these phosphosites accessible to phosphatases (325).

Cytoskeletal components such as actin, actin-binding proteins, tubulin and microtubule-interacting proteins (343) have also been reported as LRRK2 interactors by several groups, although confirmation with endogenous LRRK2 is missing in the majority of cases.

Finally, various interactors with roles in cell signaling have been proposed (344), and altering these interactions by pathogenic LRRK2 may have downstream consequences on many cellular processes. For example, LRRK2 was demonstrated to interact with various components of the Wingless signaling pathway (Wnt), such as dishevelled proteins 1, -2 and -3, low-density lipoprotein receptor-related protein 6 (LRP6) and β-catenin, by co-immunoprecipitation from the cytosolic fraction of mouse brain. Importantly, pathogenic mutations in LRRK2 seem to disrupt these interactions and, as Wnt signaling regulates more than 400 genes involved in cell growth, apoptosis, inflammation, synaptogenesis and synaptic function in mature neurons, these pathways could be impaired by mutant LRRK2 (345, 346).

5.5. LRRK2 substrates

The identification of LRRK2 kinase substrate has been one of the major goals in LRRK2 research, and much effort has been directed to it in the past years. Although many potential substrates were proposed, these studies were limited to *in vitro* approaches or to cell models overexpressing LRRK2, and evidence in a physiological context was lacking. However,

using phosphoproteomics together with genetic, biochemical and pharmacological approaches, Dario Alessi's laboratory identified a subset of Rab GTPases as LRRK2 kinase substrates, with RAB8A and RAB10 being the most prominent ones (83). A further systematic analysis of the Rab protein family identified 14 Rab proteins as LRRK2 substrates under co-overexpression conditions: RAB3A/B/C/D, RAB5A/B/C, RAB7L1, RAB8A/B, RAB10, RAB12, RAB35 and RAB43. Of these Rabs, 10 were phosphorylated under mutant LRRK2 overexpression and endogenous Rab conditions (RAB3A/B/C/D, RAB8A/B, RAB10, RAB12, RAB35 and RAB43), and only 4 under endogenous LRRK2 and Rab conditions (RAB8A, RAB10, RAB35 and RAB43) (252).

The LRRK2 phosphorylation site is an evolutionary conserved residue within the switch II domain, which is implicated in GDP/GTP exchange, as well as interactions with regulator and effector proteins as described above, suggesting that LRRK2 phosphorylation may impair these interactions (187). Indeed, RAB8A phosphorylation at T72 blocked the ability of its GEF Rabin8 to catalyze GDP displacement. Moreover, mutation of this residue to glutamic acid to mimic a phosphorylated state interfered with RAB8A binding to most of its effectors and to GDI1/2 and the GAP TBC1D15 (83). In contrast, a few proteins including RILPL1 and RILPL2, which participate in ciliogenesis, bind to only phosphorylated RAB8 and RAB10 with high affinity (252). Interestingly, all LRRK2 pathogenic mutants increased LRRK2 phosphorylation *in vivo* (83). Altogether, these findings suggest a scenario in which elevated LRRK2 kinase activity contributes to PD development by inducing the hyperphosphorylation of a subset of Rab proteins, which will disrupt their interactions with effectors and subsequently alter the trafficking pathways in which they are implicated.

Importantly, other groups have independently confirmed the phosphorylation of some of these Rab proteins by LRRK2. For instance, by performing *in vitro* kinase assays with 45 human Rabs, RAB1A/B, RAB3C, RAB8A/B and RAB35 were identified as LRRK2 substrates, and by using phospho-state-specific antibodies, the phosphorylation of RAB1A, RAB8A and RAB35 by LRRK2 was validated in HEK293 cells (347).

The identification of physiological LRRK2 substrates has been a milestone in LRRK2 research, opening the door to the use of Rab phosphorylation as a biomarker to assess LRRK2 kinase activity in patients, as well as the effects of LRRK2 kinase inhibitors in

preclinical and clinical trials. Indeed, RAB10 dephosphorylation takes place within 1-2 minutes upon addition of LRRK2 inhibitors, which is markedly more rapid than the dephosphorylation of the traditional LRRK2 biomarker sites S935 and S1292 which require 40-80 minutes (348). In this context, a reduction of RAB10 phosphorylation was detected after treatment with LRRK2 kinase inhibitors in human peripheral blood mononuclear cells (349). Similarly, using a newly developed phospho-state-specific antibody and immunoblot analysis, phosphorylated RAB10 was detected in human peripheral blood neutrophils, with a dramatic decrease upon LRRK2 inhibitor treatment (350). Another recent report using both peripheral blood mononuclear cells and neutrophils further confirmed RAB10 phosphorylation as a valid potential biomarker in LRRK2 inhibitor clinical trials (351).

However, as the initial screens identifying a subset of Rabs as LRRK2 kinase substrates were performed in mouse embryonic fibroblasts, and given the fact that Rab expression patterns vary amongst distinct cell types, future studies will be important to determine which Rabs are subject to LRRK2 phosphorylation in the different cell types, especially in PD-relevant tissues, and whether there are other cell-type specific substrates.

5.6. LRRK2 disease models

5.6.1. Invertebrates

Both *Caenorhabditis elegans* and *Drosophila melanogaster* have been used to study LRRK2 pathogenesis. They contain a single orthologue of mammalian LRRK1/LRRK2, which may not behave exactly as human LRRK2 (352). These model organisms have well-defined nervous systems that allow the exploration of basic mechanistic pathways which might underpin complex human disorders (353).

C. elegans Lrk-1 is located in the Golgi complex and is crucial for the polarized trafficking of synaptic vesicle proteins to axons. In Lrk-1 deletion mutants, synaptic vesicle proteins mislocalize to both presynaptic and dendritic endings in neurons (354). Other loss-of-function studies in *C. elegans* revealed that loss of Lrk-1 increases the sensitivity to the ER stressor tunicamycin, suggesting a functional link between LRRK2 and ER stress (355).

On the other hand, transgenic C. *elegans* overexpressing human LRRK2 in DA neurons shows age-dependent DA neurodegeneration, accompanied by behavioral defects and locomotor dysfunction, with the pathogenic mutations R1441C and G2019S causing a more severe phenotype than wild-type LRRK2 (356, 357). Interestingly, overexpression of the GTP-binding deficient mutant, K1347A, or the use of LRRK2 kinase inhibitors, protects against pathogenic LRRK2-induced neurodegeneration in this model, supporting that GTPase and kinase activities play important roles in LRRK2-linked neurodegeneration (357).

Several LRRK2 *Drosophila* models, including knockout (KO) and LRRK2 transgenic, have been generated thus far, and they have proven useful to unravel pathways implicated in PD pathogenesis, identify LRRK2 interactors and perform drug candidate screenings (353).

The majority of KO and loss-of-function mutant studies suggest that the *Drosophila* homolog of LRRK2, dLRRK, has almost no effect on DA neuron survival and is also dispensable for resistance to oxidative stress. In contrast, overexpression of both human LRRK2 and dLRRK pathogenic mutations causes DA neuron loss and age-dependent impairment in locomotor activity (358). Other phenotypes observed in flies expressing the G2019S pathogenic mutant include altered autophagy, elevated apoptosis and mitochondrial disorganization (359).

5.6.2. Rodent models

Much effort has been placed in developing rodent models for human disorders including PD, as they possess a more sophisticated CNS as compared to invertebrate models, and generally higher conservation of homologs with the human disease-causing genes. However, whereas several strategies have been used to develop LRRK2 rodent models, none of the currently available models is able to faithfully recapitulate the DA neuron loss and motor impairment observed in the human disease.

On the one hand, LRRK2 KO mice are viable and live to adulthood, showing no DA neurodegeneration, which suggests that PD caused by LRRK2 mutations is not due to a loss-of-function mechanism. Importantly, age-dependent kidney changes have been observed in these mice, with increased vacuolization in proximal tubule cells and progressive darkening of the organ. Kidneys also display an accumulation of α-syn and ubiquitinated protein

aggregates, which may arise from autophagy-lysosomal defects. These alterations, however, did not seem to correlate with increased kidney toxicity or lack of functionality. Moreover, an increase in the number and size of lamellar bodies in type II pneumocytes was observed in these mice (360–366).

Apart from the reported changes in peripheral organs, the observations from KO mice suggest that LRRK2 plays little if any role in DA neuron survival. However, a possible explanation could be that LRRK2 functions may be compensated by LRRK1, which is relatively abundant in the brain (367). Indeed, recently generated LRRK1/2 double-KO mice displayed age-dependent neurodegeneration, with a 22% loss of DA neurons in the SNpc at 15 months (368).

On the other hand, several transgenic techniques have been used to develop mouse models expressing LRRK2 WT or pathogenic mutants, including conventional (369–372), bacterial artificial chromosome (BAC) transgenic (373–375), tet-inducible transgenic (376, 377) and knock-in (KI) techniques (361, 378–380). Only two of the current transgenic LRRK2 models exhibit age-dependent SNpc DA neurodegeneration (370, 371), with one model showing 20% DA loss at 20 months of age (371) and the other one 50% loss at 16 months (370) of age. Both models were generated by conventional transgenic techniques, introducing the G2019S mutation under the PDGF-β promoter. The existence of neurodegeneration and differences between phenotypes could be due to distinct levels of transgene overexpression.

In this regard, KI models, in which only the endogenous protein is present, bearing physiological levels of expression, represent the most appropriate context to study the effect of pathogenic LRRK2. Although KI models do not display DA neuron loss, some PD-related phenotypes, such as impaired dopamine neurotransmission, axonal pathology and motor deficits have been described (379, 381, 382). The lack of DA neurodegeneration could be due to compensatory mechanisms during mouse development that prevent DA neuron loss, for example mediated by LRRK1.

Viral-mediated LRRK2 delivery through recombinant viral vectors has allowed targeting specific neuronal populations, such as SNpc DA neurons, and importantly, this approach

bypasses the development of compensatory mechanisms, as gene transfer takes place during adulthood. Herpes Simplex Virus- and adenovirus-mediated models overexpressing G2019S LRRK2 have been generated, and they show robust DA neurodegeneration, with up to 50% DA neuron loss (383, 384), likely due to the non-physiological levels of protein expression.

Nowadays, the same technologies which have been traditionally used to generate mouse models are available for rats. Rats offer many advantages over mice: their physiology is more similar to humans, they are more intelligent and can perform more complicated tasks, and due to their larger size, they are easier to manipulate and monitor. Recently, both LRRK2 KO (385–388) and transgenic rat (389–391) models have been developed. The observed phenotypes are consistent with the ones described in mice, with KO and transgenic rats displaying no significant DA neuron loss. Impaired dopamine release, age-dependent motor deficits and cognitive impairment were observed in some transgenic rat models.

Taken together, the research carried out with rodent models indicates that, and possibly because of the short lifespan of these animals, overexpression of pathogenic LRRK2 is the only way to induce neurodegeneration. However, models expressing physiological levels of pathogenic LRRK2 could be ideal to study early mechanisms involved in PD development.

5.6.3. Cell models

Although lacking the cellular diversity of the brain and the complexity of synaptic networks, cell culture models offer certain advantages over animal models. Firstly, genetic and pharmacological manipulations are far less complicated and time consuming, and pathogenic phenotypes are easier to detect and analyze, allowing for rapid large scale testing and high-throughput screening for drug candidates. Finally, specific cell types such as DA neurons can be studied in isolation to analyze cell-autonomous mechanisms which may contribute to disease.

Non-neuronal cell lines such as human embryonic kidney (HEK-293) and HeLa cells, derived from epitheloid cervix carcinoma, are routinely used as a first approach to study LRRK2 biological effects (341, 392–395), as they can be efficiently transfected. Achieving high overexpression levels, HEK293 are particularly suitable for proteomics and interaction

studies. However, the main drawback of these cell lines is that they lack a neuronal phenotype.

Neuronal-like cell lines, especially SH-SY5Y, derived from human neuroblastoma, are also commonly used. SH-SY5Y are catecholaminergic and develop neurite-like processes when differentiated by retinoic acid or growth factors (396). As an alternative, primary neurons derived from transgenic or KO rodent models can be obtained (397). However, there may be variability between cultures prepared at different times and by different researchers due to variations in tissue preparation and processing.

Cells from patients comprise important model systems as well, as they provide the opportunity to study LRRK2 pathology in a human context and in the real genetic background of the disease, even though genetic variability amongst patients may make cellular readouts more variable. Primary dermal skin fibroblasts obtained from age- and sex-matched control and LRRK2 patients have been traditionally employed (398, 399). Importantly, fibroblasts can be converted into induced pluripotent stem cells (iPSCs), which can potentially differentiate into any cell type, including DA neurons. Although still a costly and time-consuming process, iPSC research has experienced a great boom in the past years and several LRRK2 iPSC models have been generated (400). Importantly, recent progress in genome editing technologies allows for the generation of isogenic iPSC pairs differing in a single point mutation, thus providing a way to analyze the cellular and molecular consequences of monogenetic risk factors (401).

More recently, other cell types have emerged as models for LRRK2-associated PD. These include astrocytes (402) and microglia (403) from transgenic animals, due to their high levels of LRRK2 expression and the growing evidence indicating that neuroinflammation plays a role in PD pathogenesis, and peripheral immune cells from LRRK2 PD patients, which also show high expression levels and could potentially be used to detect biomarkers from blood samples (404). Epstein-Barr virus-immortalized lymphoblasts derived from LRRK2 PD patients have also proven useful for screening of LRRK2 kinase inhibitors (405).

The use of cellular systems has shed light on the mechanisms underlying LRRK2 pathogenicity, with some common denominators found in the different cell systems, such as alterations in autophagy, as further explained below.

5.7. Cellular and molecular pathways

Although much progress has been made since the discovery of LRRK2-related PD, there are still many unanswered questions regarding both the physiological and neurotoxic functions of LRRK2. LRRK2 has been associated with many different cellular processes, which could be partly due to the preferential phosphorylation of select kinase substrates and/or its vast network of interactors. Moreover, given the diversity of models and experimental approaches used, it is not known whether some of the reported phenotypes are cell type-specific. Here I will summarize current knowledge of LRRK2 functions, with special focus on endomembrane trafficking pathways, which are especially relevant for this dissertation.

5.7.1. Immune system

Multiple lines of evidence support a role for LRRK2 in systemic as well as CNS inflammatory processes.

As explained above, there is a close link between neuroinflammation and PD, and both PD patients and animal models of PD show higher levels of activated microglia, which remain phagocytic for a longer time (406). Recent studies in rodent models suggest a role for LRRK2 in microglial motility and inflammatory response, although the underlying mechanisms remain to be clarified (406). Interestingly, inflammation increased LRRK2 expression in microglia, while kinase inhibition or LRRK2 knockdown attenuated the microglial inflammatory response, as measured by TNFα secretion and nitric oxide synthase induction (407).

The fact that substantial levels of LRRK2 expression exist in different types of peripheral immune cells, including monocytes, neutrophils, B lymphocytes and, upon activation, T lymphocytes, points towards a general role for LRRK2 in systemic immunity (408). Indeed, LRRK2 polymorphisms have been associated with Crohn’s disease, an autoimmune disorder

(409), and leprosy, an infection caused by *Mycobacterium leprae* (410). In addition, pro-inflammatory signals such as interferon-γ (IFN-γ) or lipopolysaccharide (LPS) have been shown to up-regulate LRRK2 expression in immune cells. For example, IFN-γ activation has a direct effect on the LRRK2 promoter region, containing binding sites for IFN-response factors (411). Furthermore, LRRK2 has been linked to pathways implicated in cytokine production. LRRK2 overexpression was shown to activate the transcription of NF-κβ in luciferase reporter assays. This transcription factor regulates the expression of several proinflammatory cytokines such as TNFα, IL-6 and IL-12. LRRK2 has also been proposed to negatively regulate NFAT transcription by decreasing its nuclear translocation, although the consequences of this effect remain to be elucidated (408).

Recently, Tansey and colleagues reported that LRRK2 levels are higher in immune cells (B cells, T cells and monocytes) of sporadic PD patients as compared to age-matched controls, and this correlates with increased release of pro-inflammatory cytokines from PD patient monocytes and T cells, thus suggesting that LRRK2 levels in peripheral cells could constitute a biomarker for diagnosing and monitoring PD progression (412). Dzamko's group, however, reported similar LRRK2 levels in peripheral blood mononuclear cells from controls and PD patients, whereas LRRK2 was significantly increased in sporadic PD neutrophils (351). In contrast, another study by Sammler and colleagues failed to detect increased LRRK2 levels in neutrophils in either LRRK2-PD or sporadic PD patients, which may be explained by LRRK2 undergoing considerable proteolytic degradation in neutrophil extracts (350). The observed discrepancies may be due to the different experimental approaches, although the possibility that there are cell type-specific differences cannot be excluded. The potential use of LRRK2 levels in immune cells as a biomarker for PD is currently unclear and will require more investigation.

Whilst further work towards elucidating the precise mechanisms is warranted, current data suggest a role for LRRK2 in immune cell homeostasis, and alterations in LRRK2 function may result in a pro-inflammatory environment, contributing to tissue damage and neurodegeneration associated with aging.

5.7.2. Cytoskeleton and centrosome

Alterations in neurite outgrowth and branching have been consistently observed in cellular models of pathogenic LRRK2 (413), indicating possible cytoskeletal alterations. Although the exact mechanism(s) remain currently unknown, numerous studies have provided evidence for a role of LRRK2 in modulating the cytoskeleton.

As mentioned above, LRRK2 has been reported to interact with several cytoskeletal proteins (343). Furthermore, all pathogenic LRRK2 mutants except for G2019S were found to decorate microtubules under overexpression conditions, and this association was shown to be dependent on GTP binding rather than on kinase activity by Blanca Ramírez *et al.* (414). However, the molecular determinants responsible for this association, as well as its consequences, remain to be elucidated, with some studies suggesting changes in microtubule stability (343).

Apart from establishing cell shape, the cytoskeleton plays important roles in various cellular processes, including cell migration, division, intracellular organization, and vesicular trafficking events (415). Thus, alterations of cytoskeletal dynamics caused by pathogenic LRRK2 could further aggravate the LRRK2-related membrane trafficking deficits. In line with this, De Vos and colleagues found that the pathogenic variants R1441C and Y1699C, by associating with deacetylated microtubules, inhibited axonal transport in primary neurons and in *Drosophila*, while modulating microtubule acetylation could reverse the axonal transport defects (416).

Recently, centrosomal alterations have been proposed to contribute to LRRK2-mediated neurodegeneration (417). The centrosome is the main microtubule organizing center in most animal cells, and is important for several cellular processes such as cell polarity and division (418). Madero-Pérez *et al.* reported that pathogenic LRRK2 caused centrosomal cohesion deficits in dividing cells, as well as alterations in centrosome positioning in non-dividing cells, which correlated with defects in neurite outgrowth and polarized cell migration. Importantly, these centrosomal alterations were caused, at least in part, by LRRK2-mediated phosphorylation of RAB8A (417).

Furthermore, the centrosome is crucial for ciliogenesis, as the mother centriole constitutes the basal body of the primary cilium (418), and centrosomal alterations could account for defects in primary cilium formation. Indeed, a link between LRRK2 and ciliogenesis was recently established. Pfeffer and colleagues reported that pathogenic LRRK2 interfered with ciliogenesis in a manner dependent on RAB10 and RILPL1, and showed decreased ciliation in cholinergic neurons in the striatum of pathogenic LRRK2 transgenic mice. LRRK2 inhibition in mouse embryonic fibroblasts correlated with an increase in the response to Shh signaling, as measured by the expression of GLI1, the transcription factor triggered by this pathway. As cilia are essential in intracellular signal transduction of Sonic Hedgehog (Shh), the authors proposed that decreased ciliation would impair the ability of these cells to respond to Shh from DA neurons, associated with a decreased secretion of neuroprotective factors towards DA neurons, thereby contributing to DA neurodegeneration in a non-cell-autonomous manner (419). Although this is an attractive hypothesis, direct evidence is missing. Moreover, defects in ciliation in other cells types important for DA neuron survival, such as astrocytes, were not assessed in this study, and further work will be necessary to determine the contribution of altered ciliogenesis to LRRK2-related PD.

5.7.3. Autophagy and endolysosomal alterations

Autophagy alterations are one of the most commonly reported effects of pathogenic LRRK2 (420), although the variety of models and approaches employed has produced complex and sometimes controversial results, and the exact mechanism(s) underlying LRRK2-mediated autophagy defects remain unclear.

Research carried out with KO rodent models suggests a physiological role for LRRK2 in autophagy. Autophagic alterations in kidney cells were reported, which showed an age-dependent biphasic response, with increased autophagy (as measured by the accumulation of LC3-II) at 7 months and reduced autophagy at 20 months, accompanied by the accumulation of α-syn and lysosome-like structures (365). Another KO model displayed similar alterations in the kidneys, even though there were no changes in LC3-II levels (361). Interestingly, an accumulation of lamellar bodies was also observed in type II pneumocytes in this model.

Likewise, LRRK2 KO rats develop age-dependent accumulation of lysosomes in the kidneys, as well as lamellar bodies in lungs (385, 386).

Apart from such animal models, numerous cell systems have corroborated an effect for LRRK2 on autophagy. For example, silencing the essential autophagy proteins ATG7 and ATG8 was shown to rescue the neurite shortening phenotype caused by overexpressed G2019S mutant in SHSY5Y cells (421). Further evidence for a role of LRRK2 in autophagy was provided by subcellular localization studies, in which cells overexpressing low levels of pathogenic LRRK2 presented LRRK2 localization to MVBs and autophagic vacuoles (303). LRRK2 knockdown was reported to cause an increase of LC3-II levels in HEK293 cells (303). Likewise, LRRK2 kinase inhibitors lead to the accumulation of LC3-II positive autophagosomes (422), although another study reported the opposite effect in microglial cells (423). Strikingly, overexpression of mutant LRRK2 caused the same phenotype in HEK293 and SHSY5Y, with an accumulation of autophagosomes (402, 421, 424).

Data from patient-derived fibroblasts indicate the existence of autophagic alterations under endogenous LRRK2 conditions. Fibroblasts carrying the G2019S mutation were reported to have increased basal autophagy, which was dependent on abnormal activity of the MEK1/3 pathway (424). Another study demonstrated that G2019S, R1441G and Y1699C carriers show an impaired response to starvation-induced autophagy (402). Finally, iPSC-derived dopaminergic neurons from G2019S LRRK2 fibroblasts showed an accumulation of autophagosomes, which was due to decreased autophagosome clearance rather than increased autophagosome formation (425).

Gómez-Suaga et al. proposed that the increase in autophagosome numbers observed under conditions of LRRK2 kinase domain overexpression in HEK293 was mediated by elevated cytosolic calcium levels, resulting from altered NAADP-mediated calcium release from lysosomes, which would activate the calcium-dependent protein kinase kinase-β (CaMKK)/ adenosine monophosphate (AMP)-activated protein kinase (AMPK) pathway. Interestingly, they also showed that pathogenic LRRK2 caused a partial alkalinization of lysosomal pH (426).

Subsequent studies also observed endolysosomal alterations in the presence of mutant LRRK2, with changes in localization, number, size or functionality of endolysosomes. For instance, expression of the pathogenic mutants R1441C, Y1699C and G2019S in astrocytes caused enlarged, non-functional lysosomes, although contrary to the previous report their pH was more acidic (427). Another study reported perinuclear clustering and enlargement of endolysosomes in the presence of the G2019S mutation using *Drosophila* as a model (248). Furthermore, Patel and colleagues observed similar alterations in fibroblasts from patients carrying the G2019S mutations, which showed enlarged lysosomes clustered around the nucleus. Interestingly, these alterations could be corrected by inhibiting two-pore channel 2 (TPC2), a protein suggested to be involved in lysosomal Ca^{2+} release (398). Moreover, LaVoie and colleagues reported lysosomal alterations in cortical neurons from G2019S KI mice, which had reduced lysosomal protein expression, higher lysosomal pH and abnormal morphology compared to lysosomes in neurons from WT animals (428).

More recently, upregulating LRRK2 was reported to have an effect on maintaining lysosomal homeostasis under conditions of lysosomal overload stress in different cell models. LRRK2 was translocated to lysosomes upon chloroquine treatment, where it was proposed to phosphorylate RAB8A and RAB10, with the subsequent recruitment of their effectors EHBP1 and EHBP1L1 to regulate lysosomal homeostasis by two mechanisms: reverting lysosomal enlargement mediated by chloroquine and promoting lysosomal exocytosis (305).

Finally, another direct effect of LRRK2 on lysosomal functioning was reported by Ana María Cuervo's group. By using patient-derived neuronal cells, mutant LRRK2 was shown to interfere with CMA, by disrupting the formation of the LAMP2A translocation complex in the lysosome. As α-syn is degraded by this pathway, CMA impairment may result in α-syn accumulation and cell toxicity, suggesting a link between mutant LRRK2 and α-syn pathology (429).

Although they must be interpreted with caution due to the variety of models and experimental approaches employed, the majority of available data suggest that LRRK2 may have a physiological role in autophagosome formation, and pathogenic LRRK2 may simultaneously block autophagosome clearance and alter lysosomal function, leading to the

accumulation of undegraded material and lysosome-like structures. How these two events are related is not clear. Further work will be needed to clarify whether autophagy dysfunction is directly caused by pathogenic LRRK2, or a downstream consequence of altered lysosomal function, and whether some apparent discrepancies could be explained by cell-type specific mechanisms. The recent identification of p62 as a LRRK2 kinase substrate (430) may indicate that autophagy defects could be, at least in part, directly mediated by LRRK2, although the consequences of such phosphorylation event need to be further elucidated.

5.7.4. Other endomembrane trafficking pathways

Another vesicular trafficking pathway regulated by LRRK2 includes the transit of vesicles to and from the Golgi. Overexpression of VPS35 was shown to rescue the toxic effects of pathogenic LRRK2 in flies and rat primary neurons (100), pointing towards a link between LRRK2 and retromer-mediated trafficking. Interestingly, these two proteins were shown to physically interact by co-immunoprecipitation (100), and more recently the pathogenic and inactivating mutation D620N in VPS35 was demonstrated to increase LRRK2-mediated Rab phosphorylation in a series of models, including mouse embryonic fibroblasts, mouse tissues, monocytes and neutrophils from PD patients (431).

Further supporting a link between LRRK2 and retromer-mediated membrane trafficking, a constitutively active form of RAB9 was shown to rescue the autophagy/lysosomal phenotype in mutant *Drosophila* (432). In addition, both G2019S LRRK2 and RAB7L1 silencing caused lysosomal swelling and accumulation of M6PR in primary neurons in a manner similar to VPS35 silencing, and these defects could be reverted upon overexpression of VPS35 or RAB7L1 (100). RAB7L1 knockdown also resulted in a reduction of VPS35 and VPS29 levels, suggesting that it plays a role in proper retromer formation (100). An independent study reported altered subcellular distribution and decreased half-life of M6PR in the presence of both G2019S LRRK2 and inactive RAB7L1 mutants in SH-SY5Y cells (433).

Strikingly, Cookson and colleagues observed that RAB7L1 recruited LRRK2 to the Golgi, resulting in Golgi fragmentation and aberrant Golgi clustering (249), thus suggesting that RAB7L1 would promote the pathogenic effects of mutant LRRK2 rather than reverting

them, in contrast to the above mentioned studies on retromer trafficking. Subsequent reports further observed an effect of the RAB7L1-LRRK2 axis on Golgi integrity (211), and interestingly RAB7L1-mediated recruitment of LRRK2 to the Golgi was shown to promote its kinase activity (304, 316). However, it is possible that the effects of RAB7L1 on Golgi fragmentation and retromer-mediated trafficking could be due to different mechanisms. Indeed, RAB7L1 was also shown to recruit LRRK2 to stressed lysosomes, where it would exert a positive function by maintaining lysosomal homeostasis (305). Alternatively, RAB7L1-mediated disruption of the Golgi may be dependent on overexpression levels or on cell type.

Apart from retrograde trafficking, LRRK2 may have an effect on anterograde trafficking from the ER to the Golgi, as it has been reported to interact with Sec16a, a component of ER exit sites, in HeLa cells and hippocampal neurons. As these sites are important for the export of dendritic proteins, loss of LRRK2 would impair the trafficking of glutamate receptors to the cell surface (434).

Moreover, LRRK2 KO rats were shown to exhibit alterations in lamellar body exocytosis in lung cells (435), suggesting a possible role in exocytosis. Indeed, LRRK2 has been proposed to participate in synaptic vesicle exocytosis. Overexpression of G2019S LRRK2 was shown to result in reduced readily-releasable vesicle numbers and exocytosis rate in hippocampal neurons, which was suggested to be due to LRRK2-mediated phosphorylation of SNAPIN, which is part of the SNARE complex and implicated in neurotransmitter release, although such phosphorylation event was only reported in *vitro* and under overexpression conditions (436). Further supporting a role for LRRK2 in this process, Greggio's group identified NSF, also implicated in synaptic vesicle exocytosis, as a LRRK2 kinase substrate by *in vitro* phosphorylation assays, showing that phosphorylated NSF displayed enhanced ATP hydrolysis and SNARE complex dissociation *in vitro*, although the consequences were not tested *in vivo* (437). However, other studies reported no effect of pathogenic LRRK2 on synaptic vesicle exocytosis (438), thus it is not clear with the currently available data whether LRRK2 participates in this process.

LRRK2 has also been described to play a role in early and late endocytic events. On the one hand, both LRRK2 knockdown and mutant LRRK2 were shown to impair synaptic

vesicle endocytosis in primary neurons, and this effect was rescued by RAB5B (250). LRRK2-mediated phosphorylation of several proteins involved in synaptic endocytosis, such as endophilin A, synaptojanin 1 or auxilin (439, 440) was proposed, although it has not been validated *in vivo*. LRRK2-mediated phosphorylation of synaptojanin 1 resulted in decreased interaction with endophilin, necessary for synaptic vesicle endocytosis, and both G2019S LRRK2 and loss of function of synaptojanin 1 caused similar alterations in this process (439). Moreover, LRRK2-mediated phosphorylation of auxilin was demonstrated to alter its ability to bind clathrin during synaptic vesicle endocytosis, which would result in inefficient dopamine packaging due to the inability of properly regenerating synaptic vesicles. Interestingly, auxilin overexpression was shown to rescue the pathogenic phenotypes in mutant LRRK2 iPSC-derived dopaminergic neurons (441).

Finally, Gómez-Suaga *et al.* demonstrated an effect for LRRK2 on late endocytic steps by studying EGFR trafficking. Pathogenic LRRK2 caused a delay in EGFR degradation in HeLa cells, which was rescued by active RAB7A. Importantly, pull-down studies in HEK293 and fibroblasts from patients showed reduced RAB7A activity in the presence of G2019S LRRK2, although the underlying mechanism remains unknown (399).

Altogether, the above-mentioned studies indicate a central role for LRRK2 in regulating vesicular trafficking pathways, either by directly impinging on these pathways, or indirectly, for example via centrosomal and/or microtubule alterations.

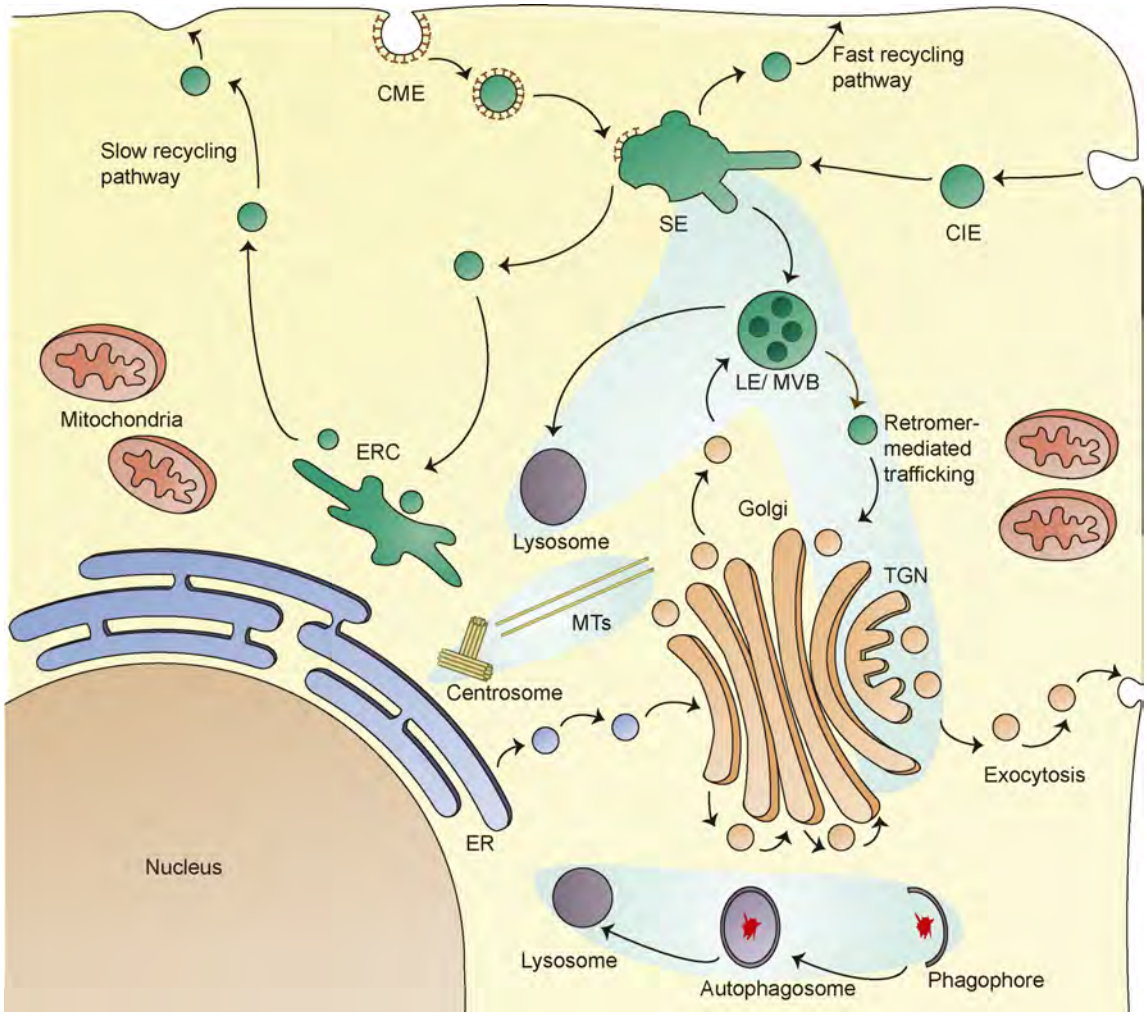

Fig. 12. LRRK2 functions in endomembrane trafficking. LRRK2 has been consistently shown to play a role in autophagy, retromer-mediated trafficking, TGN integrity, endocytosis and lysosomal functioning, thus having a central role in the regulation of intracellular vesicular trafficking, which would be impaired by pathogenic mutations. Moreover, alterations in the centrosome and/or microtubules in the presence of pathogenic LRRK2 could further contribute to endomembrane trafficking deficits. The sites of LRRK2 action are represented as blue shadows.

The role of LRRK2 in the regulation of different vesicular trafficking events is consistent with the major contribution of altered membrane trafficking to PD pathogenesis and the emerging importance of Rab GTPases in this disease, even though the precise molecular mechanisms remain largely unknown. In the present work, we aimed to determine a mechanistic link between the LRRK2-mediated phosphorylation of RAB8A, one of the major LRRK2 kinase substrates, and deficits in endocytic trafficking, one of the main trafficking pathways affected by pathogenice LRRK2.

IV. OBJECTIVES

1. Determine whether deficits in endolysosomal trafficking caused by mutant LRRK2 correlate with phosphorylation of RAB7A, the Rab GTPase crucial for endolysosomal trafficking steps.

2. Analyze whether LRRK2-mediated endolysosomal trafficking deficits are rescued upon RAB8A expression, and whether this is dependent on the activation or phosphorylation status of RAB8A.

3. Determine whether upregulation of the RAB11-Rabin8 cascade which activates RAB8A reverts the LRRK2-mediated endolysosomal defects.

4. Determine whether knockdown of RAB8A mimicks the effects of pathogenic LRRK2 on endolysosomal trafficking.

5. Analyze whether loss of RAB8A decreases RAB7A activity.

6. Evaluate whether the endocytic alterations caused by pathogenic LRRK2 or the absence of RAB8A cause accumulation of internalized material in an alternative intracellular membrane compartment.

7. Determine whether the accumulation of endocytosed material in an alternative compartment is accompanied by a deficit in endocytic recycling.

8. Analyse whether such possible trafficking alterations are rescued by active RAB7A expression.

9. Determine whether dominant-negative RAB7A expression phenocopies the alterations in membrane trafficking caused by mutant LRRK2 expression or loss of RAB8A.

V. MATERIAL AND METHODS

DNA constructs and site-directed mutagenesis

Double-myc tagged wildtype or pathogenic LRRK2 constructs have been previously described (399), and triple flag-tagged LRRK2 constructs have been previously described as well (442). DNA was prepared from bacterial cultures grown at 28 °C (at 37 °C for RAB constructs) using a midiprep kit (Promega) according to manufacturer´s instructions. GFP-RAB7A, GFP-RAB7A-Q67L and GFP-RAB7A-T22N constructs have been previously described (399). Human GFP-RAB18, GFP-RAB18-Q67L and GFP-RAB18-S22N were a generous gift from J. Presley (McGill University, Montreal, Canada). Human GFP-RAB11 and GFP-RAB11-S25N were gifts from Richard Pagano (Addgene plasmids #12674, #12678) (443), and GFP-RAB11-Q70L was generated by site-directed mutagenesis (QuickChange, Stratagene). Human GFP-RAB8A, GFP-RAB8A-Q67L and GFP-RAB8A-T22N were gifts from Maxence Nachury (Addgene plasmids #24898, #24899, #24900) (278), and GFP-RAB8A-T72A, GFP-RAB8A-T72D and GFP-RAB8A-T72E were generated by site-directed mutagenesis (QuickChange, Stratagene). An siRNA-resistant form of RAB8A (417) was generated by introducing three silent mutations into the target sequence of the seed region of the RAB8A siRNA (Ambion, ThermoFisher, ID s8679, cat. nr 4390824). Specifically, the original sequence 5´-GCAAGAGAATTAAACTGCA-3´ was mutated to 5´-GCAAGAGAATTAAGTTACA-3´. Human GFP-Rabin8 was a gift from Keith Mostov (Addgene plasmid #26726) (260), and human GFP-RAB4 was a gift from Marci Scidmore (Addgene plasmid #49434) (444). Human GFP-RAB9 was a gift from Richard Pagano (Addgene plasmid #12663) (443). For generation of the distinct flag-tagged RAB proteins for *in vitro* phosphorylation studies, the respective RAB inserts were PCR amplified with flanking EcoRI and BamHI restriction enzyme sites at the 5´ and 3´ ends, respectively, and the resultant PCR products used to subclone into the EcoRI/BamHI sites of a 3xflag-vector (SigmaAldrich). All 3xflag-tagged RAB8A constructs were generated by Gibson Assembly master Mix (New England Biolabs). In all cases, the identity of constructs was verified by sequencing the entire coding region.

Cell culture and transfection

HeLa cells were cultured and transfected as previously described (399). Briefly, cells were cultured in 100 mm dishes in full medium (DMEM containing 10% fetal bovine serum, non-essential amino acids and high glucose) at 37 °C in 5 % CO_2. Confluent cells were harvested using 0.05 % trypsin and 0.02 mM EDTA in PBS and subcultured at a ratio of 1:4 - 1:6. Cells were plated onto 6-well plates and the following day, at 70-80 % confluency, transfected using Lipofectamine 2000 (Invitrogen) according to manufacturer´s specifications for 4 h in DMEM, followed by replacement with fresh full medium. Double transfections were performed using 4 μg of LRRK2 plasmids and 1 μg of plasmids of interest. Transfected cells were replated the next day at a 1:2 ratio onto coverslips in 24-well plates. Proteins were expressed for 48 hours before analysis as described below.

Knockdown of RAB8A by RNA interference

HeLa cells were seeded in 6-well plates at 30-40 % confluence one day prior to transfection such that they were 70-80 % confluent the following day. They were transfected with 25 nM siRNA and 1 μg of GFP-RAB7-Q67L or GFP-RAB4 as indicated using 4 μl of jetPRIME Transfection Reagent (Polyplus-Transfection SA, no 114-15) in 200 μl jetPRIME buffer. The mix was incubated for 15 min at room temperature and added to 2 ml of full medium per well of a 6-well plate. For knockdown experiments in the presence of wildtype or siRNA-resistant mRFP-RAB8A variants, cells were transfected with 50 nM of the indicated siRNA using 4 l of jetPRIME transfection reagent. Four hours later, media was replaced with fresh DMEM, and cells transfected with 1 μg of the indicated RAB8A constructs using Lipofectamine 2000 according to manufacturer´s instructions, followed by media replacement 4 h later. In all cases, cells were passaged 24 h later and processed for Western blot analyis or fluorescent EGF binding and internalization assays 48 h after transfection. RNAi reagents included Silencer Select Negative Control no. 1 siRNA (Ambion, ThermoFisher, cat. nr 4390843) and Silencer Select RAB8A (Ambion, ThermoFisher, ID s8679, cat. nr 4390824). The latter has been validated using TaqMan Gene Expression Analysis and was found to result in around a 95 % reduction of mRNA levels 48 hours post-transfection (ThermoFisher). Knockdown efficacy of this siRNA reagent was

confirmed by Western blotting with a sheep polyclonal RAB8A antibody which specifically detects RAB8A (antibody S969D, mrcppureagents.dundee.ac.uk).

Immunofluorescence and laser confocal imaging

HeLa cells were fixed using 4 % paraformaldehyde (PFA) in PBS for 20 min at room temperature, permeabilized in 0.5 % Triton X-100/PBS for 3 x 5 min, and incubated in blocking buffer (10 % goat serum, 0.5 % Triton X-100/PBS) for 1 h. Coverslips were incubated with primary antibody in blocking buffer for 1 h at room temperature, followed by washes in 0.5 % Triton X-100/PBS and incubation with secondary antibodies for 1 h. Coverslips were washed in PBS and mounted in mounting medium with DAPI (Vector Laboratories). For staining with the anti-LAMP1 antibody, 0.5 % Triton X-100 was replaced by 0.05 % saponin. Primary antibodies included mouse monoclonal anti-LAMP1 (1:200, Santa Cruz Biotechnology, 20011), rabbit polyclonal anti-beta COP (1:200, Thermo Fisher, PA1-061) rabbit polyclonal anti-TfnR (1:100, Thermo Fisher, PA5-27739) and a mouse monoclonal anti-EGFR antibody against the extracellular domain of the EGFR (1:200, Santa Cruz, sc-120). Secondary antibodies included Alexa488-conjugated goat anti-mouse (1:2000, Invitrogen), Alexa594-conjugated goat anti-mouse (1:2000, Invitrogen) and Alexa594-conjugated goat anti-rabbit (1:2000, Invitrogen), respectively. To determine the localization of all GFP-tagged RAB protein variants in the absence of antibody staining, cells were fixed, briefly permeabilized in 0.5 % Triton X-100/PBS for 3 min, washed in PBS and mounted as described above.

Images were acquired on a Leica TCS-SP5 confocal microscope using a 63x 1.4 NA oil UV objective (HCX PLAPO CS). Single excitation for each wavelength separately was used throughout all acquisitions (488 nm Argon Laser line and a 500-545 nm emission band pass; 543 HeNe laser line and a 556-673 nm emission band pass; 405 nm UV diode and a 422-466 nm emission band pass). The same laser settings and exposure times were used for image acquisition of individual experiments to be quantified. Ten to 15 image sections of selected areas were acquired with a step size of 0.4 μm, and z-stack images analyzed and processed using Fiji.

Alexa-EGF binding and uptake assays

Binding and uptake assays were performed essentially as described (399). Transfected HeLa cells were re-seeded onto coverslips the day after transfection and serum starved for 16 h. The following day, medium was replaced with fresh, serum-free medium containing 100 ng/ml Alexa555-EGF (Invitrogen) at 4 °C, which allows ligand binding to the receptor but prevents internalization. Alternatively, 100 ng/ml Alexa488-EGF (Invitrogen) were employed for experiments with siRNA-resistant or wildtype mRFP-RAB8A constructs. Control cells were washed twice with PBS followed by acid stripping (0.5 M NaCl, 0.2 M acetic acid, pH 2.5) for 3 min at 4 °C to confirm that labelled EGF was only surface-bound under those conditions. Upon binding, cells were washed twice with ice-cold PBS and transferred to pre-warmed serum-free medium to allow uptake of bound Alexa555-EGF/Alexa488-EGF. At the indicated times, cells were fixed with 4 % PFA in PBS for 15 min at room temperature, and softly permeabilized with 0.5 % Triton X-100/PBS for 3 min before mounting with DAPI.

To measure the total number of Alexa555-EGF/Alexa488-EGF structures per cell, cells were circled, and a modified NIH Fiji macro (GFP-LC3 macro) was employed. At least 20 and up to 100 independent cells were analysed for each condition and experiment, and analysis was done by an observer blind to conditions.

For intensity analyses, integrated densities of 30 to 50 cells per condition were determined, background-corrected and normalized to 250 μm^2 to correct for differences in cell size. Intensity per punctum was then determined by dividing the integrated density of the punctae by the number of punctae (445, 446). Analysis was performed using Fiji by an observer blind to conditions.

Immunofluorescence-based EGFR recycling assays

Recycling assays were done as previously described (447). Briefly, transfected HeLa cells were seeded onto poly-L-lysine-coated coverslips the day after transfection, and serum-starved overnight. The following day, cells were pretreated with 50 µg/ml cycloheximide (Calbiochem, 239765) in serum-free medium for 1 h at 37 °C to block novel protein synthesis. Cells were treated with 20 ng/ml non-labelled EGF for 20 min at 4 °C in serum-

free medium in the presence of cycloheximide to allow EGF binding to the receptor. Upon binding, cells were washed twice with ice-cold PBS, and then transferred to pre-warmed serum-free medium containing cycloheximide, and shifted to 37 °C for 10 min to allow for EGFR internalization (pulse). After the pulse, a mild acidic wash (pH 4.5) was performed on ice, followed by two washes with ice-cold PBS. Subsequently, cells were incubated in serum-free medium containing cycloheximide at 37 °C to allow for EGFR recycling back to the PM, measured at different time points (chase; 15min, 30 min, 60 minutes). At the indicated times, cells were fixed with 4 % PFA in PBS for 15 min, followed by blocking with 10 % goat serum in PBS, and immunostaining with an EGFR antibody directed against the extracellular domain of the EGFR (1:200, Santa Cruz, sc-120), followed by staining with an Alexa488-coupled secondary antibody. Permeabilization was omitted from all steps to visualize only surface EGFR. For intensity quantifications, pictures were acquired the same day with the same settings, and analysis was performed with Fiji. Integrated densities of 30 to 50 cells per condition were determined, background-subtracted and normalized to 250 μm^2 to correct for differences in cell size.

In vivo imaging and colocalization analysis

For live cell fluorescence microscopy to determine colocalization of fluorescent EGF with the various RAB proteins in the absence or presence of pathogenic LRRK2, transfected cells were re-seeded onto 35-mm glass-bottom dishes (IBIDI Biosciences) 24 h after transfection. For analysis of colocalization with fluorescent EGF, cells were serum-starved overnight. The next day, medium was replaced by phenol-free, serum-free DMEM (GIBCO), and cells were incubated with 100 ng/ml Alexa647-EGF (Invitrogen) for 20 min at 4 °C to allow for fluorescent EGF surface binding. Subsequently, cells were washed twice in ice-cold PBS and incubated for 20 min at 37 °C to allow for internalization of bound EGF before image acquisition.

Cells were imaged on a Leica TCS-SP5 confocal microscope using a 63x 1.4 NA oil UV objective (HCX PLAPO CS) by acquiring individual z-stack images corresponding to the cell center. The JACoP plugin of Fiji was used for the quantification of colocalization of the different GFP-tagged RAB proteins with Alexa647-EGF. After thresholding, the percentage of colocalization was obtained by calculating the Mander´s coefficients [M1 for red channel

(Alexa647-EGF)], and the percentage of colocalization was obtained by M1 x 100 (399). A total number of 15-20 independent cells were analyzed per condition per experiment.

Cell extracts and Western blotting

Cells were collected 48 h after transfection, washed in PBS and resuspended in cell lysis buffer (1% SDS in PBS containing 1 mM PMSF, 1 mM Na_3VO_4 and 5 mM NaF). Extracts were sonicated, boiled, and centrifuged at 13500 rpm for 10 min at 4 °C. Protein concentration of supernatants was estimated using the BCA assay (Pierce), and extracts immediately resolved by SDS-PAGE, transferred to nitrocellulose membranes, and probed with primary antibodies overnight at 4 °C. Antibodies used for immunoblotting included a rabbit polyclonal anti-GFP (1:2000, Abcam, ab6556), a mouse monoclonal anti-GAPDH (1:2000, Abcam, ab9484), a mouse monoclonal anti-LRRK2 (1:1000, NeuroMab, 75-253), a mouse monoclonal anti-RAB8A antibody (1:1000, BD Biosciences, 610844), a mouse monoclonal anti-tubulin antibody (clone DM1A, 1:10000, Sigma), a sheep polyclonal anti-RAB8A antibody (1:500, S969D, mrcppureagents.dundee.ac.uk), a rabbit polyclonal anti-RAB7 antibody (1:1000, Sigma, R4779), a mouse monoclonal anti-RAB11 antibody (1:1000, BD Biosciences, 610656) and a KO-validated rabbit monoclonal anti-RAB4 antibody (1:1000, Abcam, ab109009). Membranes were washed and incubated with secondary antibodies (anti-rabbit HRP-conjugated antibody (1:2000, Dako Cytomation) or anti-mouse HRP-conjugated antibody (1:2000, Dako Cytomation)) for 60 min at room temperature, followed by detection using ECL reagents (Roche Diagnostic GmbH). A series of timed exposures were undertaken to ensure that densitometric analyses were performed at exposures within the linear range, films were scanned, and densitometric analysis performed using QuantityOne (Bio-Rad).

Determination of EGFR steady-state levels and EGFR degradation

For determination of steady-state levels and EGFR degradation, we employed HEK293T cells, as overexpression and transfection efficiencies are higher than in HeLa cells (399). HEK293T cells were cultured and transfected overnight using 6 µl lipoD reagent (SignaGen Laboratories, SL100688) and 2 µg of flag-tagged LRRK2 DNA (300 ng for pCMV), as previously described (417). The following day, cells were split into poly-L-lysine-coated 6-

well plates, and were processed 48 hours after transfection. For determination of steady-state levels of endogenous EGFR, cells were washed in ice-cold PBS and collected by scraping and mechanical disruption. Cells were centrifuged at 5000 rpm for 2 min at 4 °C, and the cell pellet resuspended in 100 µl lysis buffer (10% SDS, 1 mM PMSF in PBS). Samples were sonicated, centrifuged at 10´000 rpm for 10 min at 4 °C, and supernatants (25 µg total protein) analyzed by SDS-PAGE and Western blotting using a mouse monoclonal anti-flag antibody (1:500, Sigma, F1804), a rabbit monoclonal anti-EGFR antibody (1:1000, Cell Signaling, D38B1), or a mouse monoclonal anti-tubulin antibody (clone DM1A, 1:10000, Sigma) as loading control.

For determination of EGFR degradation, HEK293T cells were transfected and plated onto poly-L-lysine-coated 6 well plates, and degradation assays performed 48 hours after transfection. Cells were serum-starved for 1 hour in the presence of 1 µg/ml cycloheximide, followed by incubation with 100 ng/ml non-labeled EGF (Sigma, E9644) for 20 min at 4 °C in serum-free medium containing cycloheximide. After washing in ice-cold PBS, time point 0 was collected by cell scraping. For the remaining time points, cells were incubated in serum-free medium containing cycloheximide at 37 °C for distinct periods of time (30 min, 60 min, 90 min) followed by cell scraping, and cell extracts prepared and analyzed by SDS-PAGE and Western blotting as described above.

GST-RILP pulldown assays and active RAB7 determination

GST-RILP pulldown assays were essentially performed as described (399, 448). Briefly, GST-RILP vector was transformed into *E. coli* strain BL21, and 250 ml of LB inoculated with a 1 ml overnight culture grown at 37 °C to an OD of 0.6-0.8. Isopropyl-1-thio-β-D-galactopyranoside (EMD Biosciences) (0.5 mM) was added and bacteria induced for protein production for 3-4 h at 28 °C. Bacterial cells were pelleted, washed with cold PBS and cell pellets frozen at -20 °C. Pellets were resuspended in 5 ml ice-cold purification buffer (25 mM Tris-HCl, pH 7.4, 150 mM NaCl, 0.5 mM EDTA, 1 mM dithiothreitol, 0.1 % Triton X-100 and 1 mM PMSF), and lysates were sonicated and cleared by centrifugation. Supernatant was diluted with another 5 ml of ice-cold purification buffer, and GST-RILP purified using 300 µl of a pre-equilibrated 50 % slurry of glutathione-Sepharose 4B beads (GE Healthcare) and incubation for 1 h at 4 °C on a rotary wheel. Beads were washed with purification buffer,

resuspended to a 50 % slurry, and kept at 4 °C. A sample (5 µl) was separated by SDS-PAGE and analyzed by Coomassie brilliant blue staining to determine protein purity, and protein concentration estimated by BCA assay (Pierce). Beads were used with cell lysates within 2 days of preparation. Transfected HEK293T cells (one 10 cm diameter dish per assay) were collected by centrifugation, washed in PBS, resuspended in pulldown buffer (20 mM HEPES, pH 7.4, 100 mM NaCl, 5 mM $MgCl_2$, 1 % Triton X-100 and 1 mM PMSF) and lysates cleared by centrifugation at 13500 rpm for 10 min at 4 °C. GST-RILP pulldown assays were performed in 1 ml pulldown buffer containing 300 µg of cell lysate and 60 µl of 50 % slurry beads pre-equilibrated in pulldown buffer. Beads were incubated on a rotary wheel overnight at 4 °C, washed twice with ice-cold pulldown buffer, and bound proteins eluted by adding 40 µl of 1 x sample buffer/β-mercaptoethanol and boiling for 4 min at 95 °C prior to separation by SDS-PAGE.

Alternatively, active RAB7 levels were determined with a RAB7 activation assay kit (NewEast Biosciences) according to manufacturer´s specifications and as previously described (449). Briefly, cells were transfected as described above, and lysates (2 mg total protein) immunoprecipitated with a conformation-specific anti-RAB7-GTP mouse monoclonal antibody (NewEast Biosciences, 26923) bound to protein A/G-agarose, and the precipitated RAB7-GTP was detected by immunoblotting with a non-conformation-specific rabbit polyclonal anti-RAB7 antibody (1:1000, Sigma, R4779). As a positive control, extracts were incubated with 100 µM GTPγS (NewEast Biosciences, 30302) for 30 min at 30 ºC to activate all available RAB7 prior to immunoprecipitation.

Cell culture, transient transfection and protein purification

HEK-293T cells were maintained in DMEM supplemented with 10 % fetal bovine serum and 1×penicillin/streptomycin at 37 ºC and in a 5 % CO_2 atmosphere. Cells were transfected with the 3X-FLAG-RABs, or with wildtype or G2019S 3X-FLAG-LRRK2 plasmid DNAs, using polyethylenimine (PEI) with a DNA:PEI ratio of 1:2 (w/w). Cells were harvested 72 h post-transfection for biochemical assays.

Cells were lysed in buffer A (20 mM Tris-HCl pH 7.5, 150 mM NaCl, 1 mM EDTA, 2.5 mM $Na_4O_7P_2$, 1 mM β-glycerophosphate, 1 mM $NaVO_4$, 0.5% Tween-20, protease inhibitor

cocktail, 1×Complete Mini Protease Inhibitor cocktail (Roche Applied Sciences)). Cleared lysates (1 ml) were incubated with anti-FLAG-M2-agarose beads (Sigma) by rotating overnight at 4 °C. Resin complexes were washed with different buffers (twice with 20 mM Tris–HCl, 500 mM NaCl, 0.5 % Tween 20; twice with 20 mM Tris–HCl, 300 mM NaCl, 0.5 % Tween 20; twice with 20 mM Tris–HCl, 150 mM NaCl, 0.5 % Tween 20; twice with 20 mM Tris–HCl, 150 mM NaCl, 0.1 % Tween 20; and twice with 20 mM Tris–HCl, 150 mM NaCl, 0.02 % Tween 20), and proteins were eluted in kinase buffer (25 mM Tris-HCl pH 7.5, 5 mM β-glycerophosphate, 2 mM dithiothreitol, 0.1 mM Na_3VO_4, 10 mM $MgCl_2$, 0.02 % Tween 20 and 150 ng/µl of 3X-FLAG peptide) for 45 min at 4 °C with shaking. Eluted proteins were resolved by SDS–PAGE and stained with Coomassie G-250 to verify protein purity. RAB and LRRK2 protein concentrations were estimated by densitometry against a standard curve of increasing concentrations of bovine serum albumin (BSA) (20, 50, 100 and 150 ng/µl).

Phosphorylation assays

Phosphorylation reactions were performed either in the presence or the absence of 1 µM of the LRRK2-kinase inhibitor PF 06447475 (Tocris Bioscience). Reactions were performed in kinase buffer in the presence of 30 nM LRRK2 and 300 nM of the respective RAB proteins, and with [33P]-γ-ATP (1 µCi/reaction; Perkin Elmer) and 200 µM of cold ATP (Sigma-Aldrich) at 30 °C for 1 h in a final volume of 30 µl. Reactions were terminated with 4×Laemmli buffer and boiling at 95°C for 10 min. Phosphorylation reaction samples were resolved on pre-cast 4–20% SDS–PAGE gels (Biorad) and transferred onto PVDF membranes. Incorporated radioactivity was detected by phosphorscreen and Cyclone acquisition (Perkin Elmer), and the same membranes were probed with HRP-conjugated anti-FLAG antibody to confirm equal protein loading.

Statistical analysis

All data are expressed as means ± s.e.m., data were analyzed by one-way ANOVA with Tukey´s post hoc test, and $P < 0.05$ was considered significant.

VI. RESULTS

LRRK2 phosphorylates RAB8A, but not RAB7A

Since the phosphorylation of RAB8A has been suggested to cause its inactivation (83), we wondered whether pathogenic LRRK2 may cause the reported decrease in RAB7A activity (21) via direct phosphorylation. When comparing the phosphorylation of different RAB proteins *in vitro*, RAB8A was found to serve as an efficient LRRK2 kinase substrate (Fig. 13A-C). In addition, and as previously described (83), phosphorylation of RAB8A was increased with the pathogenic G2019S variant as compared to wildtype LRRK2, and was largely abolished when mutating the identified LRRK2 phosphorylation site (T72A) (Fig. 13C). In contrast, other RAB proteins tested, including RAB7A, were not phosphorylated to a significant degree (Fig. 13B). Therefore, the previously reported LRRK2-mediated deficit in endolysosomal trafficking (399) does not seem to be due to direct LRRK2-mediated phosphorylation and concomitant inactivation of RAB7A.

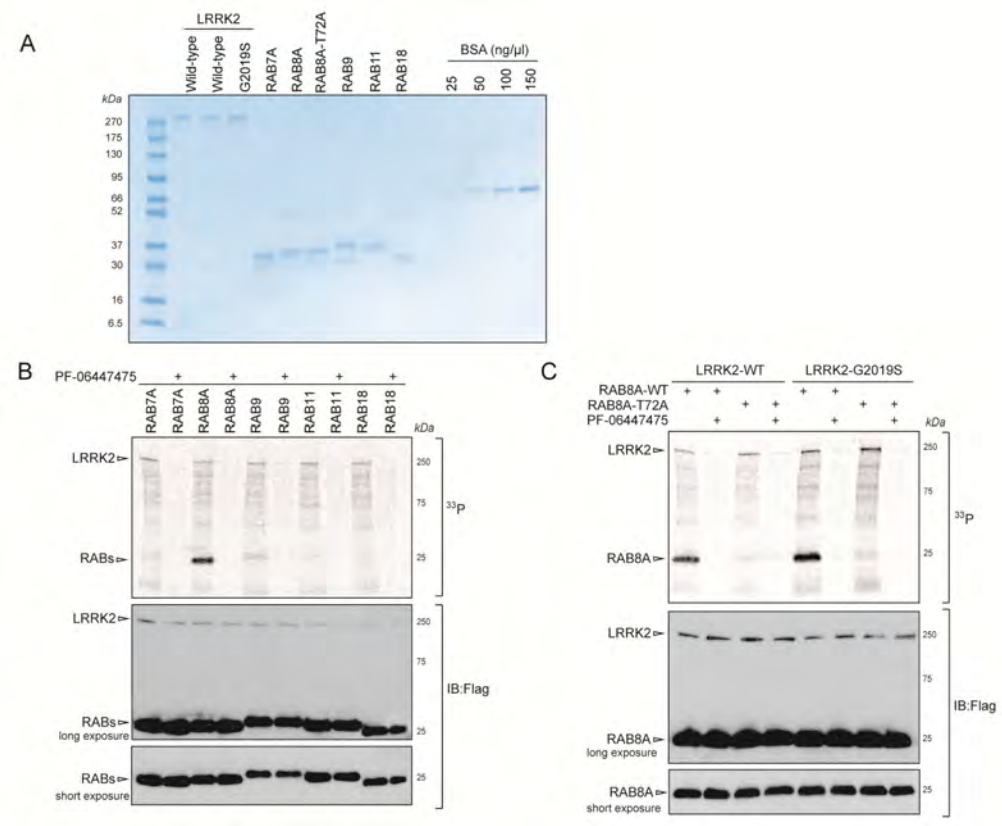

Fig. 13. LRRK2 phosphorylates RAB8A but not endolysosomal RAB7A/RAB9 proteins. **(A)** Representative Coomassie blue stained SDS-PAGE of purified 3x-flag-tagged LRRK2 or 3x-flag-tagged RAB proteins after 3xflag peptide elution. Protein concentration was estimated by a calibration curve with BSA standards of known concentrations. **(B)** In vitro radioactive kinase assays of 3x-flag-tagged wildtype LRRK2 and 3x-flag-tagged RAB7A, RAB8A, RAB9, RAB11 or

RAB18, purified from HEK293T cells (1:10 ratio of LRRK2:Rab proteins). Incorporated radioactivity was revealed by phosphoscreen (upper panel), and total protein loading by anti-flag (IB:Flag) immunoblotting (lower panel). LRRK2 kinase inhibitor PF 06447475 was used at 1 μM to confirm LRRK2-specific phosphorylation. **(C)** In vitro radioactive kinase assays of 3x-flag-tagged wildtype or G2019S LRRK2 in the presence of either 3x-flag-tagged wildtype RAB8A or phosphodeficient RAB8A-T72A as indicated. Incorporated radioactivity was revealed by phosphoscreen (upper panel), and total protein loading by anti-flag (IB:Flag) immunoblotting (lower panel). LRRK2 kinase inhibitor PF 06447475 was used at 1 μM to confirm LRRK2-specific phosphorylation.

G2019S LRRK2-mediated endolysosomal trafficking deficits are rescued by a RAB11-Rabin8-RAB8A cascade

Upon binding of EGF, the EGFR is internalized by clathrin-mediated endocytosis, and sorted to lysosomes for degradation in a manner dependent on RAB7 (450). EGFR surface availability can be assessed by binding of Alexa555-EGF to cells at 4 °C, and endocytic trafficking and degradation followed by quantification of endocytosed Alexa555-EGF over time. HeLa cells were co-transfected with GFP and with either myc-tagged or flag-tagged G2019S LRRK2, or with a flag-tagged kinase-inactive variant (G2019S-K1906M) of pathogenic LRRK2, respectively, followed by assessment of binding and degradation of fluorescently labeled EGF. Binding of Alexa555-EGF at 4 °C was reduced in the presence of either myc-tagged or flag-tagged G2019S LRRK2, but not a kinase-inactive version thereof, indicating that it was tag-independent and due to the LRRK2 kinase activity (Fig. 14A,B). Upon incubation of cells at 37 °C for either 10 min or 30 min to monitor fluorescent EGF degradation, a pronounced delay in the clearance of Alexa555-EGF per cell was observed in the presence of G2019S, but not kinase-inactive G2019S-K1906M LRRK2, respectively (Fig. 14C,D). A similar pathogenic LRRK2-mediated deficit in EGF clearance was observed when quantifying intracellular fluorescent EGF-positive punctae per area, with no change in the fluorescence intensity of the individual dots (Fig. 14E,F). To further corroborate that the increase in intracellular fluorescent EGF was due to impaired EGFR degradation, biochemical EGFR degradation assays were performed in transfected HEK293T cells expressing G2019S or kinase-inactive G2019S-K1906M LRRK2, respectively. Pathogenic LRRK2 expression did not alter steady-state EGFR expression levels (Fig. 14G). However, and as previously described (399), cells expressing G2019S LRRK2 displayed a deficit in

EGFR degradation as compared to cells expressing kinase-inactive G2019S-K1906M LRRK2 (Fig. 14H,I). Therefore, pathogenic LRRK2 interferes with the endolysosomal trafficking and degradation of EGF and the EGFR.

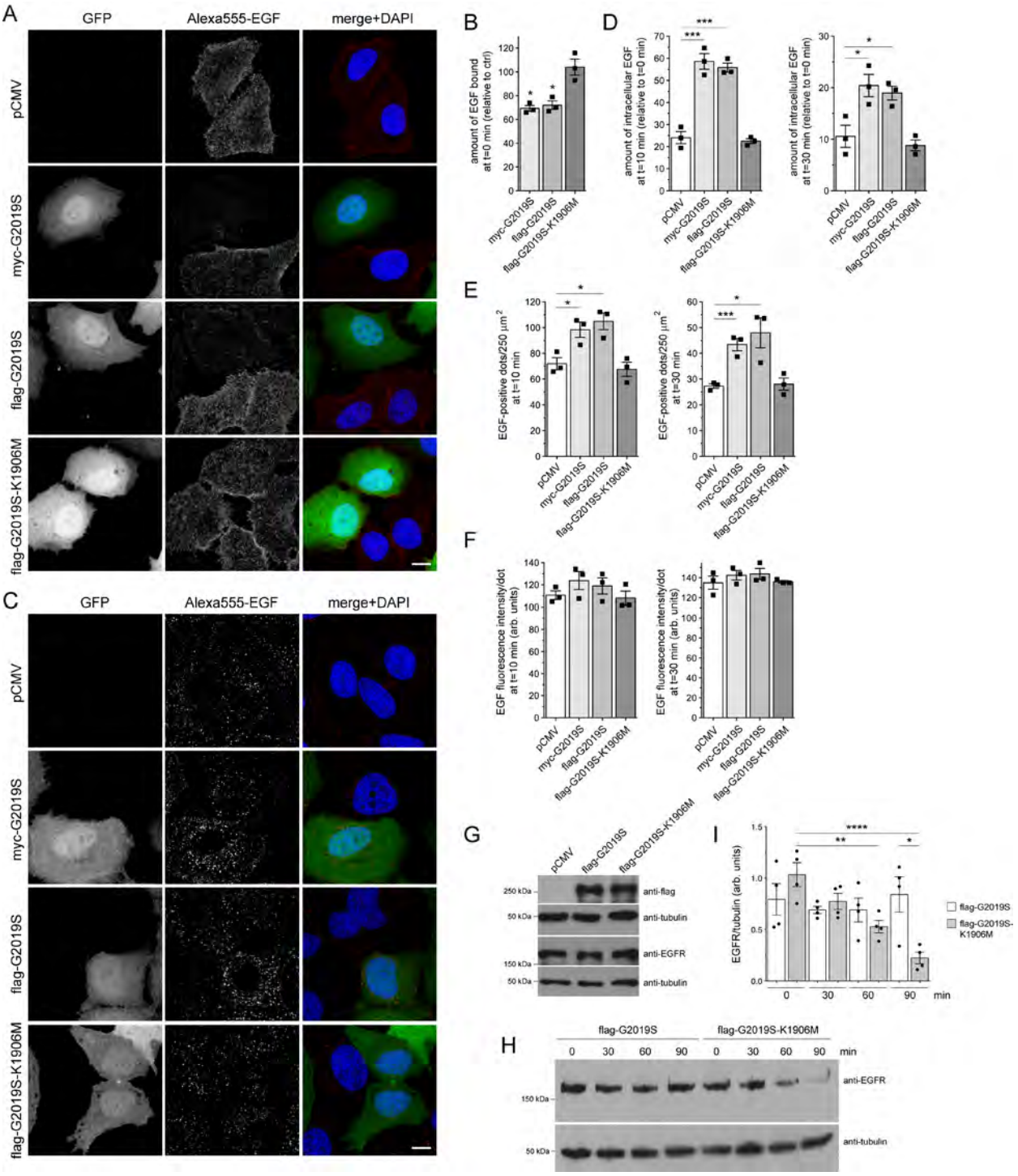

Fig. 14. Pathogenic G2019S LRRK2, but not a kinase-inactive G2019S-K1906M variant, causes a deficit in EGF binding and degradation. **(A)** HeLa cells were transfected with either pCMV, or co-transfected with GFP and either myc-tagged G2019S LRRK2, flag-tagged G2019S or G2019S-K1906M LRRK2 as indicated, incubated with Alexa555-EGF for 30 min at 4 °C, washed to remove unbound fluorescent EGF, and fixed and processed as described in Materials and Methods. Scale bar, 10 μm. **(B)** Quantification of surface-bound fluorescent EGF (t=0 min) of cells transfected with the various constructs as indicated, and normalized to EGF surface binding of pCMV-transfected cells (ctrl). N=3 independent experiments. *P < 0.05. **(C)** HeLa cells transfected with the indicated constructs were allowed to bind Alexa555-EGF at 4 °C, washed to remove unbound fluorescent EGF, and then shifted to 37 °C for 10 min to allow for the internalization and degradation of fluorescent EGF. Scale bar, 10 μm. **(D)** Quantification of Alexa555-EGF was performed after 10 min (left) and 30 min (right) upon internalization, and normalized to the amount of Alexa555-EGF binding for each condition at t=0 min, thus reflecting the percentage of internalized bound fluorescent EGF. N=3 independent experiments. *P < 0.05; ***P < 0.005. **(E)** Quantification of the total number of fluorescent EGF-positive punctae per 250 μm2 upon expression of distinct constructs as indicated, after 10 min (left) and 30 min (right) of internalization. N=3 independent experiments. *P < 0.05; ***P < 0.005. **(F)** Since the immunofluorescence signal intensity directly correlates to the size of the individual structures, signal intensity per punctum was quantified at 10 min (left) and 30 min (right) upon internalization, which revealed no change amongst the different conditions, further indicating a deficit in EGF degradation, rather than an increase in the amount of internalized fluorescent EGF per cell. **(G)** HEK293T cells were transfected with the indicated constructs, followed by analysis of endogenous EGFR expression levels. **(H)** HEK293T cells were transfected with either pathogenic G2019S LRRK2 or with kinase-inactive G2019S-K1906M variant, serum-starved for 1 h in the presence of cycloheximide to block novel protein synthesis, and EGFR internalization stimulated with non-labelled EGF for the indicated time points. Cell extracts were analyzed by Western blotting for EGFR levels, and tubulin used as loading control. **(I)** Quantification of EGFR degradation in HEK293T cells transfected with either G2019S LRRK2 or G2019S-K1906M, at distinct time points as indicated, and with values normalized to tubulin as loading control. N=4 independent experiments. *P < 0.05; **P < 0.01; ****P < 0.001.

We next wondered how these LRRK2-mediated endolysosomal trafficking deficits may be modulated by RAB8A. In HeLa cells, GFP-tagged wildtype RAB8A and GTP-locked, constitutively active RAB8A-Q67L were largely localized to a tubular endocytic recycling compartment partially overlapping with TfnR, with tubular localization more evident in live or in fixed but only briefly permeabilized cells (Fig. 15A-C). In contrast, GDP-locked inactive RAB8A-T22N was cytosolic and not properly targeted to a tubular recycling compartment (Fig. 15B). When expressed on their own, neither RAB8A nor RAB8A-Q67L caused alterations in EGF binding or EGFR trafficking, whilst RAB8A-T22N caused a modest decrease in EGF surface binding and a slight delay in EGFR degradation, evident only at t=30 min (Fig. 16A,B). Importantly, the pathogenic G2019S LRRK2-mediated decrease in EGF binding and the delay in EGFR trafficking were fully rescued when expressing RAB8A-Q67L (Fig. 16C,D). This was not observed with wildtype RAB8A or with RAB8A-T22N (Fig. 16C,D), although both wildtype and RAB8A-Q67L were expressed to similar degrees (Fig. 15E), and none of the RAB8A variants interfered with the co-expression of G2019S LRRK2 (Fig. 17A,B). In this cell system, and taking into account a roughly 50 % transfection efficiency, overexpression of LRRK2 constructs was about 1-1.5-fold above endogenous levels, and overexpression of RAB8A around 2.5-4-fold above endogenous levels, respectively (Fig. 15D,E).

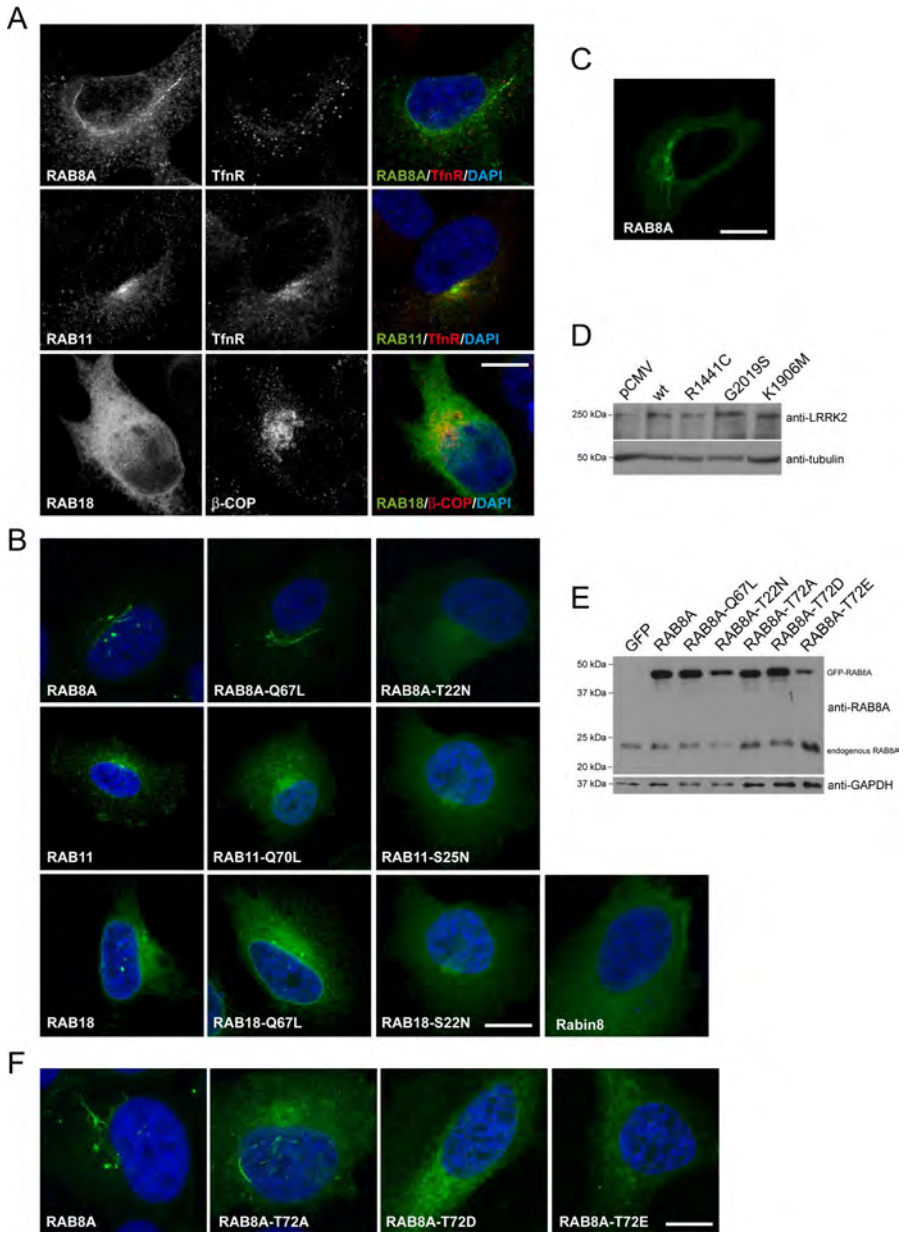

Fig. 15. Subcellular localization and expression levels of different RAB proteins. **(A)** HeLa cells were transfected with GFP-tagged RAB constructs as indicated, and stained with antibodies against a marker for endolysosomes (LAMP1), endocytic recycling compartment (TfnR) or trans-Golgi (b-COP). Scale bar, 10 μm. **(B)** HeLa cells were transfected with GFP-tagged RAB constructs as indicated. To maintain proper membrane association of the different RAB proteins, cells were fixed but only briefly permeabilized before mounting with DAPI. Scale bar, 10 μm. **(C)** Individual z-stack of live HeLa cell transfected with GFP-RAB8A. Scale bar, 10 μm. **(D)** HeLa cells were transfected with either empty vector (pCMV) or the indicated GFP-tagged LRRK2 constructs, and cell extracts (30 μg) analyzed by Western blotting for LRRK2 protein levels, and for tubulin as loading control. **(E)** HeLa cells were transfected with either GFP, or GFP-tagged RAB8A constructs as indicated, and cell extracts (30 μg) analyzed by Western blotting for RAB8A, and for GAPDH as loading control. **(F)** Example of HeLa cells transfected with the indicated GFP-tagged RAB8A variants, fixed and mounted with DAPI (blue). Scale bar, 10 μm.

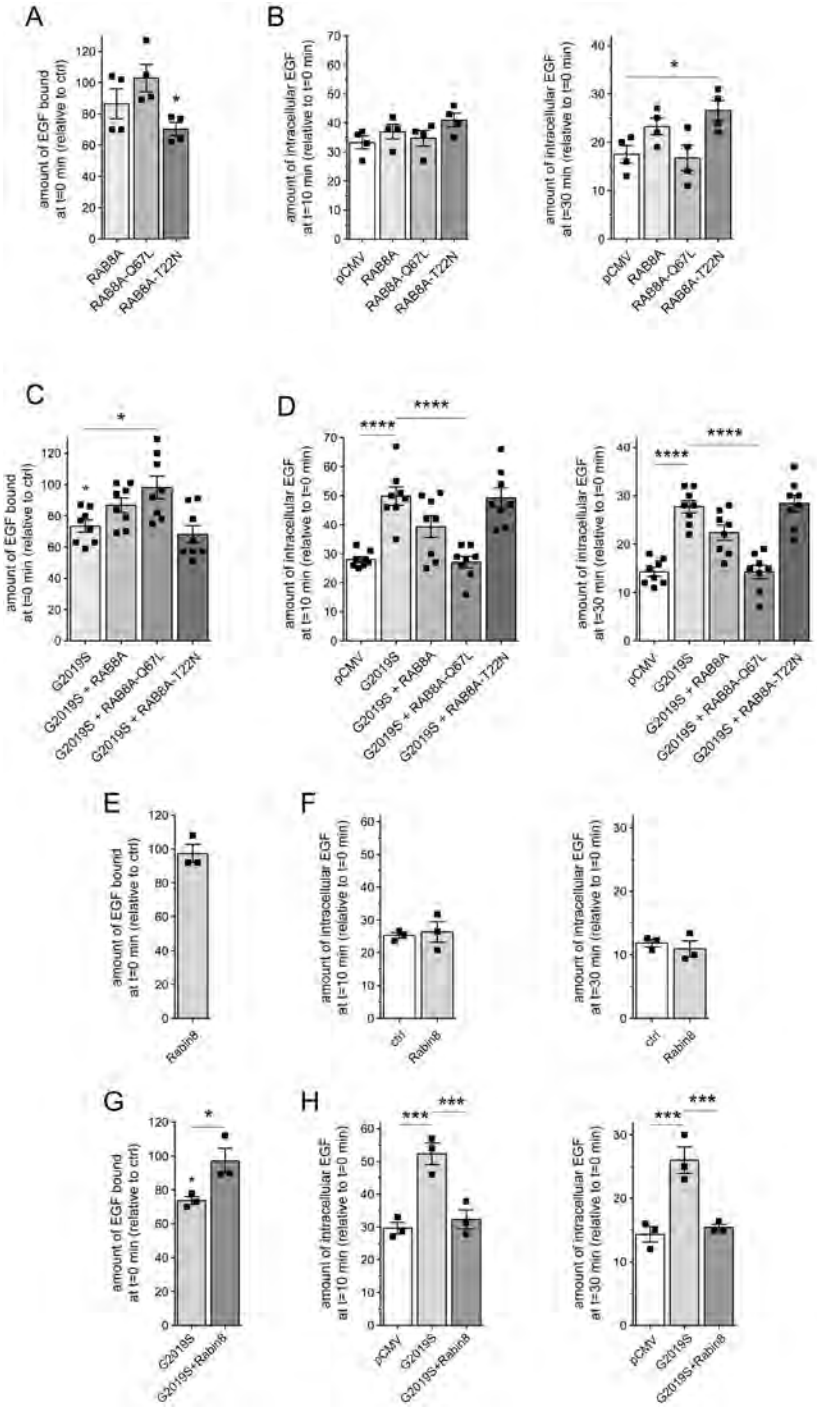

Fig. 16. Active RAB8A and Rabin8 rescue the LRRK2-mediated deficit in EGF binding and degradation. **(A)** HeLa cells were transfected with either empty pCMV vector (ctrl) or the indicated RAB8A constructs, followed by quantification of the amount of surface-bound fluorescent EGF. N=4 independent experiments. *P < 0.05. **(B)** Cells were transfected as indicated, followed by quantification of internalized Alexa555-EGF in transfected cells after 10 min (left) and 30 min (right) of internalization. Values are normalized to the amount of Alexa555-EGF binding at t=0. N=4 independent experiments. *P < 0.05. **(C)** Cells were co-transfected with G2019S LRRK2 and the indicated RAB8A constructs, and surface-bound fluorescent EGF quantified. N=8 independent experiments. *P < 0.05. **(D)** Cells were co-transfected with G2019S LRRK2

and the indicated RAB8A constructs, followed by quantification of internalized Alexa555-EGF after 10 min (left) and 30 min (right) of internalization. N=8 independent experiments. ****P < 0.001. **(E)** Cells were transfected with either empty pCMV vector (ctrl) or with Rabin8, and surface-bound fluorescent EGF quantified. N=3 independent experiments. **(F)** Cells were transfected as indicated, followed by quantification of internalized fluorescent EGF at 10 min (left) and 30 min (right). N=3 independent experiments. **(G)** Cells were transfected with either empty pCMV vector (ctrl), or co-transfected with G2019S pathogenic LRRK2 and either pCMV vector or Rabin8 as indicated, and surface-bound fluorescent EGF quantified. N=3 experiments. *P < 0.05. **(H)** Cells were transfected as indicated, followed by quantification of internalized fluorescent EGF as described above. N=3 independent experiments. ***P < 0.005.

Rabin8 functions as a GEF for RAB8A and activates it by catalyzing GDP release for subsequent GTP loading (258). Conversely, Rabin8 is activated by RAB11, which controls vesicle exit from recycling REs (260, 278, 280, 451). However, it remains unknown whether such cascade operates in all RAB8A-dependent membrane trafficking events. We therefore tested whether Rabin8 or RAB11 could rescue the LRRK2-mediated deficit in endolysosomal trafficking. Overexpressed Rabin8 was largely cytosolic (Fig. 15B) and had no effect on endolysosomal trafficking when expressed on its own (Fig. 16E,F). However, Rabin8 expression rescued the G2019S LRRK2-mediated deficits in EGF binding and degradation (Fig. 16G,H) without interfering with the expression levels of G2019S LRRK2 (Fig. 17C), indicating that activating endogenous RAB8A by Rabin8 expression also rescues the LRRK2-mediated endolysosomal trafficking defects.

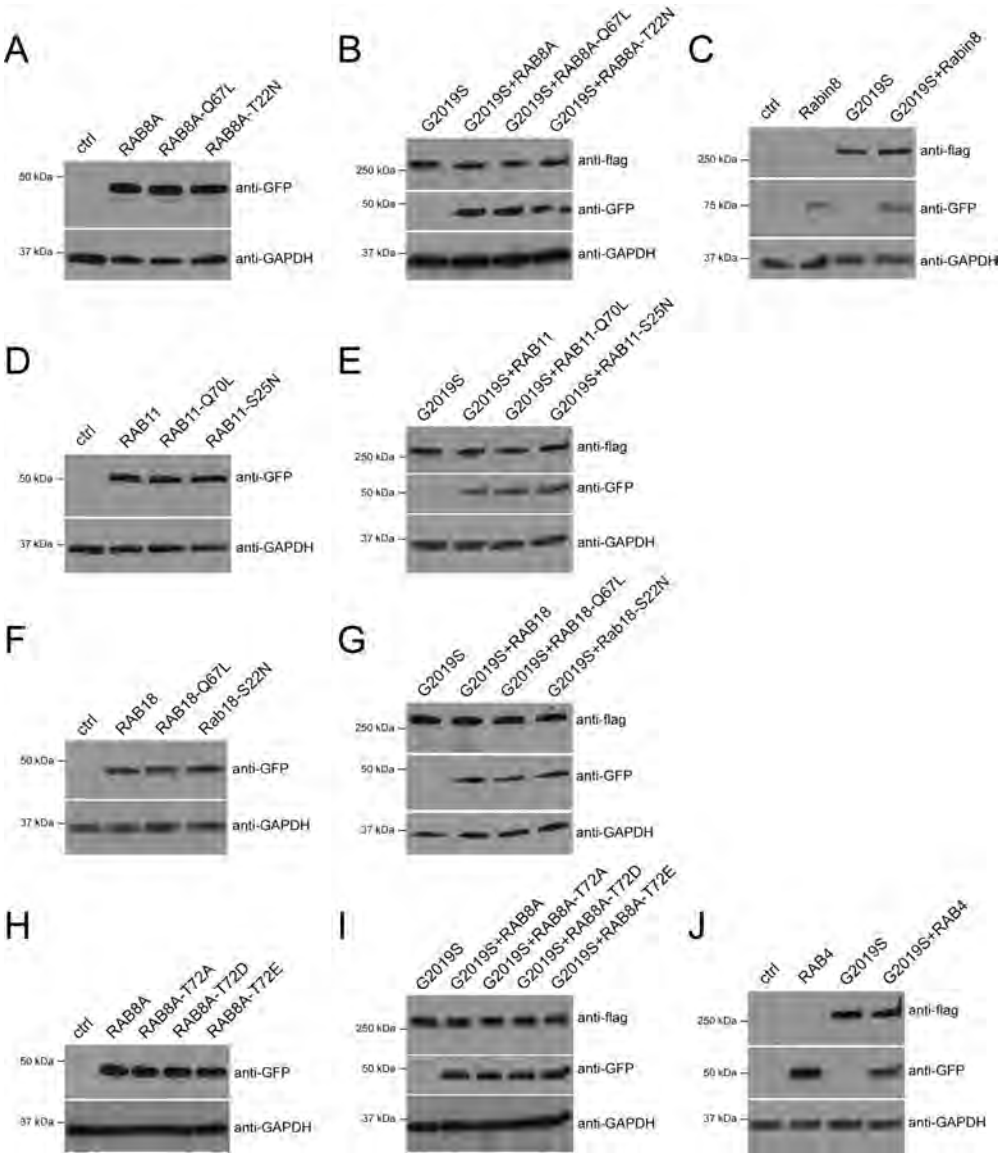

Fig. 17. Expression and co-expression levels of various RAB proteins with G2019S LRRK2. **(A)** HeLa cells were transfected with GFP-tagged RAB8A constructs as indicated, and cell extracts (30 µg) analyzed by Western blotting for GFP, and for GAPDH as loading control. **(B)** HeLa cells were transfected with flag-G2019S along with the indicated GFP-tagged RAB8A constructs as indicated, and cell extracts (30 µg) analyzed by Western blotting for flag, GFP, and for GAPDH as loading control. **(C)** HeLa cells were transfected with GFP-tagged Rabin8, flag-G2019S, or co-transfected as indicated, and cell extracts (30 µg) analyzed by Western blotting for flag, GFP, and for GAPDH as loading control. **(D)** Same as **(A)**, but cells transfected with GFP-tagged RAB11 constructs as indicated. **(E)** Same as **(B)**, but cells co-transfected with flag-G2019S and the GFP-tagged RAB11 constructs as indicated. **(F)** Same as **(A)**, but cells transfected with GFP-tagged RAB18 constructs as indicated. **(G)** Same as **(B)**, but cells co-transfected with flag-G2019S and GFP-tagged RAB18 constructs as indicated. **(H)** Same as **(A)**, but cells transfected with GFP-tagged RAB8A constructs as indicated. **(I)** Same as **(B)**, but cells co-transfected with flag-G2019S and GFP-tagged RAB8A constructs as indicated. **(J)** Cells were transfected with GFP-tagged RAB4, flag-G2019S, or co-transfected as indicated, and cell extracts (30 µg) analyzed by Western blotting for flag, GFP, and for GAPDH as loading control.

We next analyzed the effects of RAB11 on the LRRK2-mediated deficits in EGFR trafficking. GFP-tagged RAB11 colocalized with TfnR (Fig. 15A). Both wildtype and GTP-locked active RAB11 (RAB11-Q70L) were membrane-associated, whilst GDP-locked inactive RAB11 (RAB11-S25N) was largely cytosolic (Fig. 15B). When co-expressed with pathogenic LRRK2, both wildtype and active, but not inactive RAB11 rescued the deficit in EGF binding and degradation (Fig. 18A,B), whilst none of them had an effect on their own (Fig. 18C,D), even though expressed to comparable degrees and not altering the expression levels of G2019S LRRK2 (Fig. 17D,E). As another means to show that the effects reported here were specific, we analyzed the role of RAB18, an ER-resident RAB protein (452). RAB18 was localized to a reticular pattern reminiscent of the ER as well as the nuclear envelope (Fig. 15A,B) (452). Neither wildtype, GTP-locked (RAB18-Q67L), nor GDP-locked RAB18 (RAB18-S22N) could rescue the pathogenic LRRK2-mediated deficits (Fig. 18E,F), and they also displayed no effect on their own (Fig. 18G,H), even though expressed to similar degrees and not affecting the levels of co-expressed G2019S LRRK2 (Fig. 17F,G). Altogether, these data indicate that the RAB11-Rabin8-RAB8A cascade specifically rescues the endolysosomal trafficking defects associated with pathogenic LRRK2.

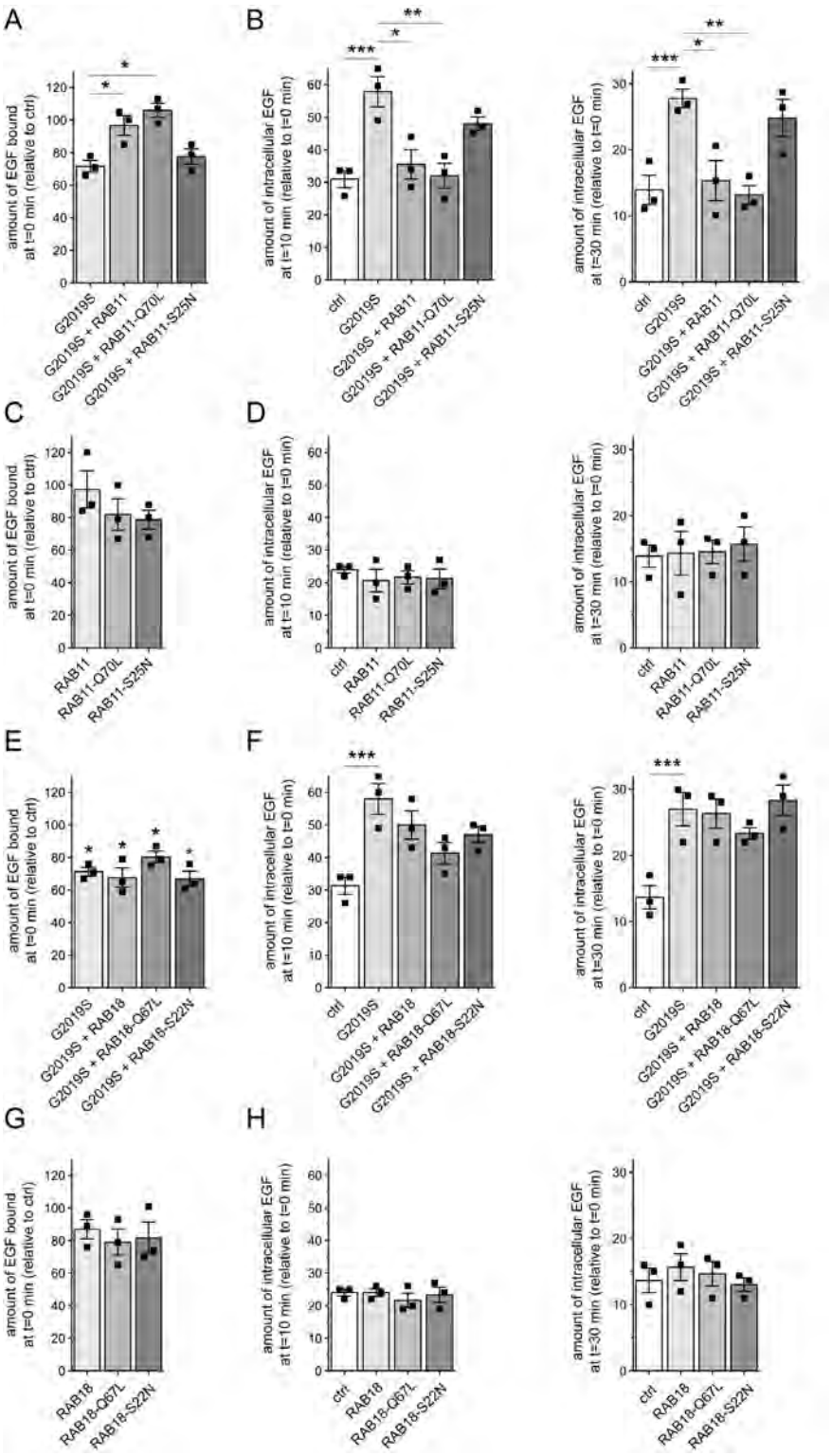

Fig. 18. RAB11 rescues the LRRK2-mediated delay in EGFR trafficking. **(A)** HeLa cells were co-transfected with G2019S LRRK2 and the indicated RAB11 constructs, and surface-bound fluorescent EGF quantified. N=3 independent experiments. *P < 0.05. **(B)** Cells were transfected with either empty pCMV vector (ctrl), or co-transfected with G2019S LRRK2 and the indicated RAB11 constructs, followed by quantification of internalized fluorescent EGF at 10 min (left) and 30 min (right).

N=3 independent experiments. *P < 0.05; **P < 0.01; ***P < 0.005. **(C)** Cells were transfected with either empty pCMV vector (ctrl) or the indicated RAB11 constructs, and the amount of surface-bound fluorescent EGF quantified. N=3 independent experiments. **(D)** Cells were transfected as indicated, followed by quantification of internalized EGF at 10 min (left) and 30 min (right). N=3 independent experiments. **(E)** Cells were transfected with either empty pCMV vector (ctrl), or co-transfected with G2019S LRRK2 and the indicated RAB18 constructs, and surface-bound fluorescent EGF quantified. N=3 independent experiments. *P < 0.05. **(F)** Cells were transfected as indicated, followed by quantification of internalized fluorescent EGF at 10 min (left) and 30 min (right). N=3 independent experiments. ***P < 0.005. **(G)** Same as in **(E)**, but cells transfected with either empty pCMV vector (ctrl) or the indicated RAB18 constructs. N=3 independent experiments. **(H)** Same as in **(F)**, but cells transfected with either empty pCMV vector (ctrl) or the indicated RAB18 constructs. N=3 independent experiments.

G2019S LRRK2-mediated endolysosomal trafficking deficits are mimicked by knockdown of RAB8A

We reasoned that if LRRK2-mediated phosphorylation of RAB8A causes its inactivation, a phosphomimetic RAB8A variant should be unable to rescue the delay in EGFR degradation. Thus, we expressed wildtype RAB8A, the phosphodeficient RAB8A-T72A variant or the phosphomimetic RAB8A-T72D/RAB8A-T72E variants, respectively. Whilst wildtype RAB8A was largely localized to a tubular recycling compartment, the phosphomimetic variants displayed a prominently cytosolic localization, and the phosphodeficient RAB8A variant was also partially cytosolic (Fig. 15F). With the exception of RAB8A-T72E, none of these variants significantly altered EGF binding or EGFR degradation when expressed on their own (Fig. 19A,B), with all constructs apart from RAB8A-T22N and RAB8A-T72E expressed to similar degrees (Fig. 15E). However, the phosphodeficient, but not the phosphomimetic RAB8A versions, fully rescued the effect of pathogenic LRRK2 (Fig. 19C,D) without altering the co-expression levels of G2019S LRRK2 (Fig. 17H,I).

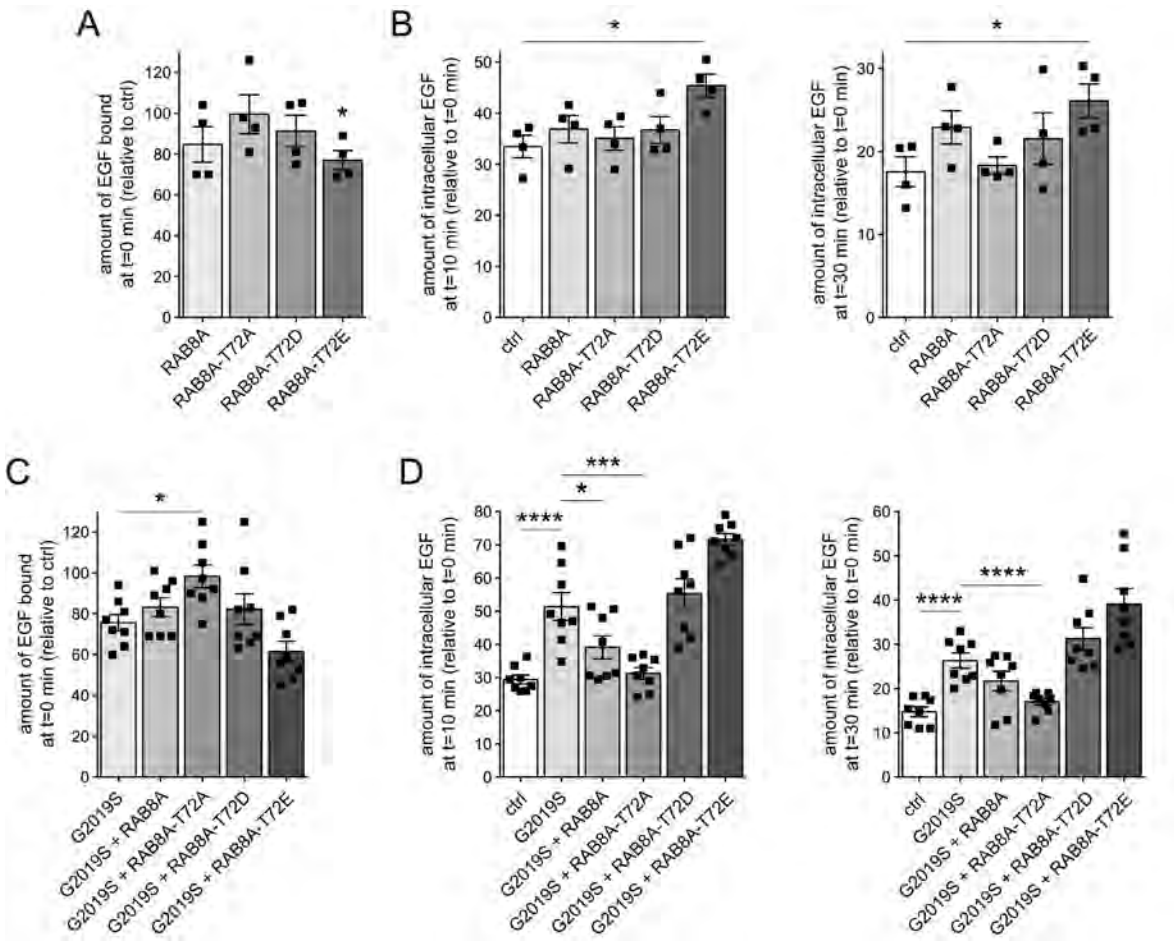

Fig. 19. Phosphodeficient RAB8A, but not wildtype or phosphomimetic RAB8A variants revert the LRRK2-mediated effects on EGFR trafficking. **(A)** HeLa cells were transfected with either empty pCMV vector (ctrl) or the indicated RAB8A constructs, and surface-bound fluorescent EGF quantified. N=4 independent experiments. *P < 0.05. **(B)** Cells were transfected with the indicated constructs, followed by quantification of internalized fluorescent EGF. N=4 independent experiments. *P < 0.05. **(C)** Cells were co-transfected with G2019S LRRK2 and the indicated RAB8A constructs, and surface-bound fluorescent EGF quantified. N=8 independent experiments. *P < 0.05. **(D)** Cells were transfected with the indicated constructs, and internalized fluorescent EGF quantified at 10 min (left) and 30 min (right). N=8 independent experiments. *P < 0.05; ***P < 0.005; ****P < 0.001.

Various studies indicate that phosphodeficient and phosphomimetic RAB8A may not be able to properly mimick the dephosphorylated and phosphorylated status of RAB8A, respectively (83, 252, 417, 419). Therefore, and as another means to analyze the effect of LRRK2-mediated RAB8A inactivation on EGF binding and EGFR trafficking, we performed siRNA experiments. Specific siRNA of RAB8A caused a >80% decrease in RAB8A protein levels 48h post-transfection (Fig. 20A,B). Strikingly, RAB8A knockdown caused a pronounced deficit in EGF surface binding and EGFR degradation (Fig. 20C,D). Moreover, the deficits induced upon siRNA of RAB8A could be rescued when overexpressing active, GTP-locked RAB7A (RAB7A-Q67L) (Fig. 20E,F). Knockdown of RAB8A was not associated with a change in the steady-state levels of several other RAB proteins including RAB7A (Fig. 21A), indicating that the deficits in endolysosomal trafficking are not due to off-target effects on RAB7A protein levels. In addition, an siRNA-resistant version of RAB8A (417), but not wildtype, siRNA-sensitive RAB8A, rescued the effect of RAB8A knockdown on EGF binding and EGFR trafficking (Fig. 22A-D), further indicating that the effects were due to the specific knockdown of RAB8A.

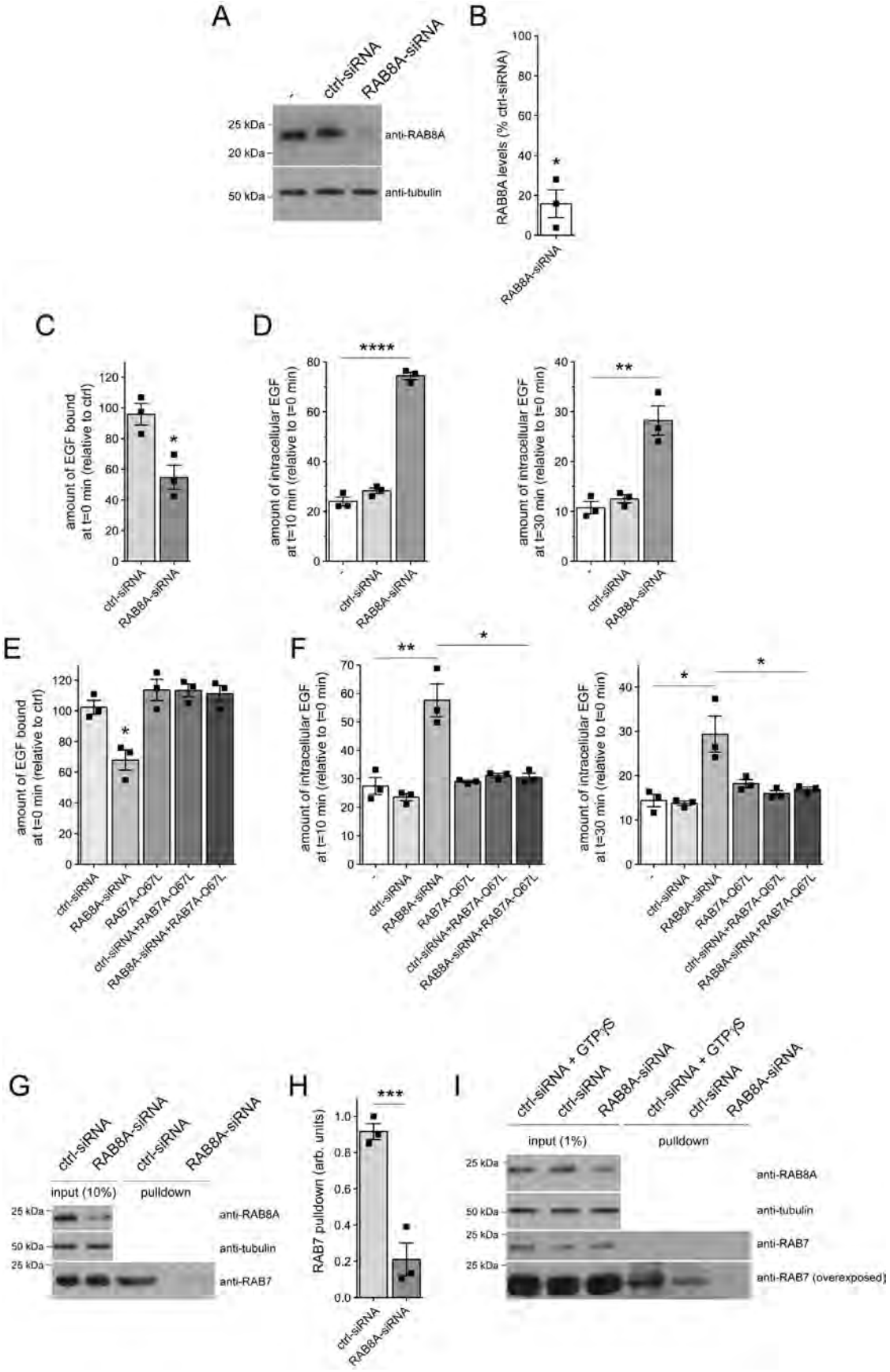
A
ctrl-siRNA
RAB8A-siRNA
25 kDa
20 kDa
anti-RAB8A
50 kDa
anti-tubulin
B
RAB8A levels (% ctrl-siRNA)
RAB8A-siRNA
C
amount of EGF bound at t=0 min (relative to ctrl)
ctrl-siRNA
RAB8A-siRNA
D
amount of intracellular EGF at t=10 min (relative to t=0 min)
amount of intracellular EGF at t=30 min (relative to t=0 min)
E
amount of EGF bound at t=0 min (relative to ctrl)
RAB7A-Q67L
ctrl-siRNA+RAB7A-Q67L
RAB8A-siRNA+RAB7A-Q67L
F
amount of intracellular EGF at t=10 min (relative to t=0 min)
amount of intracellular EGF at t=30 min (relative to t=0 min)
G
input (10%)
pulldown
anti-RAB8A
anti-tubulin
anti-RAB7
H
RAB7 pulldown (arb. units)
I
ctrl-siRNA + GTPγS
input (1%)
pulldown
anti-RAB8A
anti-tubulin
anti-RAB7
anti-RAB7 (overexposed)

Fig. 20. Knockdown of RAB8A mimicks the endolysosomal trafficking deficits mediated by G2019S LRRK2. **(A)** HeLa cells were either non-transfected (-), or transfected with ctrl-siRNA or RAB8A-siRNA, and cell extracts (30 μg) analysed by Western blotting for RAB8A protein levels and tubulin as loading control. **(B)** Quantification of the type of experiments depicted in **(A)**. RAB8A levels in the presence of RAB8A-siRNA were normalized to levels in the presence of ctrl-siRNA. N=3 independent experiments. *P < 0.05. **(C)** Cells were either left untreated (-), or transfected with ctrl-siRNA or RAB8A-siRNA, and surface-bound fluorescent EGF quantified. N=3 independent experiments. *P < 0.05. **(D)** Cells were either left untreated (-), or transfected with ctrl-siRNA or RAB8A-siRNA, followed by quantification of internalized fluorescent EGF at 10 min (left) and 30 min (right). N=3 independent experiments. **P < 0.01; ****P < 0.001. **(E)** Cells were either left untreated, or co-transfected with ctrl-siRNA or RAB8A-siRNA in the absence or presence of GFP-tagged active RAB7A (RAB7A-Q67L), and surface-bound fluorescent EGF quantified. N=3 independent experiments. *P < 0.05. **(F)** Cells were either left untreated, or co-transfected with ctrl-siRNA or RAB8A-siRNA in the absence or presence of RAB7A-Q67L, and internalized fluorescent EGF quantified at 10 min (left) and 30 min (right). N=3 independent experiments. *P < 0.05; **P < 0.01. **(G)** Cells were either treated with ctrl-siRNA or RAB8A-siRNA as indicated, and the RAB7-binding domain of RILP coupled to GST was used to pulldown the GTP-bound form of RAB7 from cell lysates (300 μg). Input (10 %) was run alongside pulldowns to demonstrate equal levels of total RAB7 protein in ctrl-siRNA or RAB8A-siRNA treated cells, and the levels of RAB8A and tubulin analyzed on a separate gel. **(H)** Experiments of the type depicted in **(G)** were quantified, and the amount of RAB7 isolated by GST-RILP expressed relative to input. N=3 independent experiments, * P < 0.005. **(I)** Cells were either treated with ctrl-siRNA or RAB8A-siRNA as indicated, and a conformation-specific antibody used to immunoprecipitate active RAB7 from cell lysates (2 mg). As a positive control, ctrl-siRNA-treated cell extracts were incubated with 100 μM GTPγS to activate RAB7A before immunoprecipitation. Input (1%) was run alongside pulldowns to demonstrate equal levels of total RAB7 protein in ctrl-siRNA or RAB8A-siRNA treated cells, and the levels of RAB8A and tubulin analyzed on a separate gel.

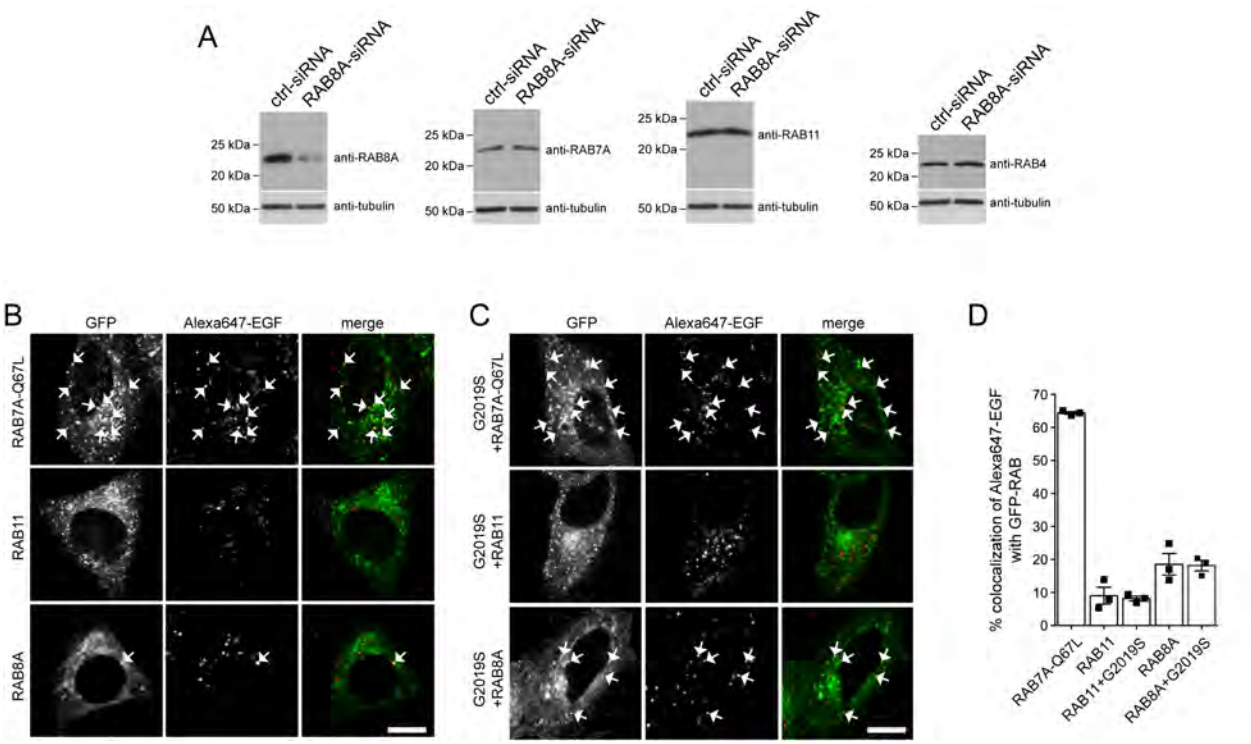

Fig. 21. Specificity of RAB8A knockdown, and lack of Alexa647-EGF accumulation in RAB8A- or RAB11-positive compartments. **(A)** HeLa cells were treated with ctrl-siRNA or RAB8A-siRNA, and extracts subjected to Western blotting against various RAB proteins as indicated. **(B)** Cells were transfected with GFP-tagged RAB proteins as indicated, loaded with Alexa647-EGF for 20 min and followed by live imaging. Arrows indicate colocalization. Scale bar, 10 µm. **(C)** Cells were transfected with GFP-tagged RAB proteins and G2019S LRRK2 as indicated, loaded with Alexa647-EGF for 20 min followed by live imaging. Arrows indicate colocalization. Scale bar, 10 µm. **(D)** Quantification of colocalization of Alexa647-EGF with GFP-tagged RAB proteins in the absence or presence of G2019S LRRK2 as indicated (Manders coefficient 1 x 100). N=3 independent experiments.

To gain direct evidence for a change in RAB7A activity upon siRNA of RAB8A, we employed an effector pulldown assay using the RAB7-binding domain of RILP to selectively isolate RAB7-GTP from cell lysates (399, 448). Pulldown assays were performed from either non-treated cells, or cells treated with control siRNA or with RAB8A-siRNA, respectively (Fig. 20G,H). The fraction of endogenous RAB7 bound to GTP was drastically reduced upon RAB8A knockdown (Fig. 20G,H), similar to what we previously described for G2019S LRRK2 (21). As an alternative means, active RAB7 was immunoprecipitated from cell extracts previously treated with control siRNA or RAB8A siRNA using a conformation-specific antibody (449), which also showed a significant decrease of active RAB7 upon

RAB8A knockdown (Fig. 20I). Therefore, loss of RAB8A function effectively phenocopies the pathogenic G2019S LRRK2-mediated defects in endolysosomal trafficking by decreasing RAB7 activity (21).

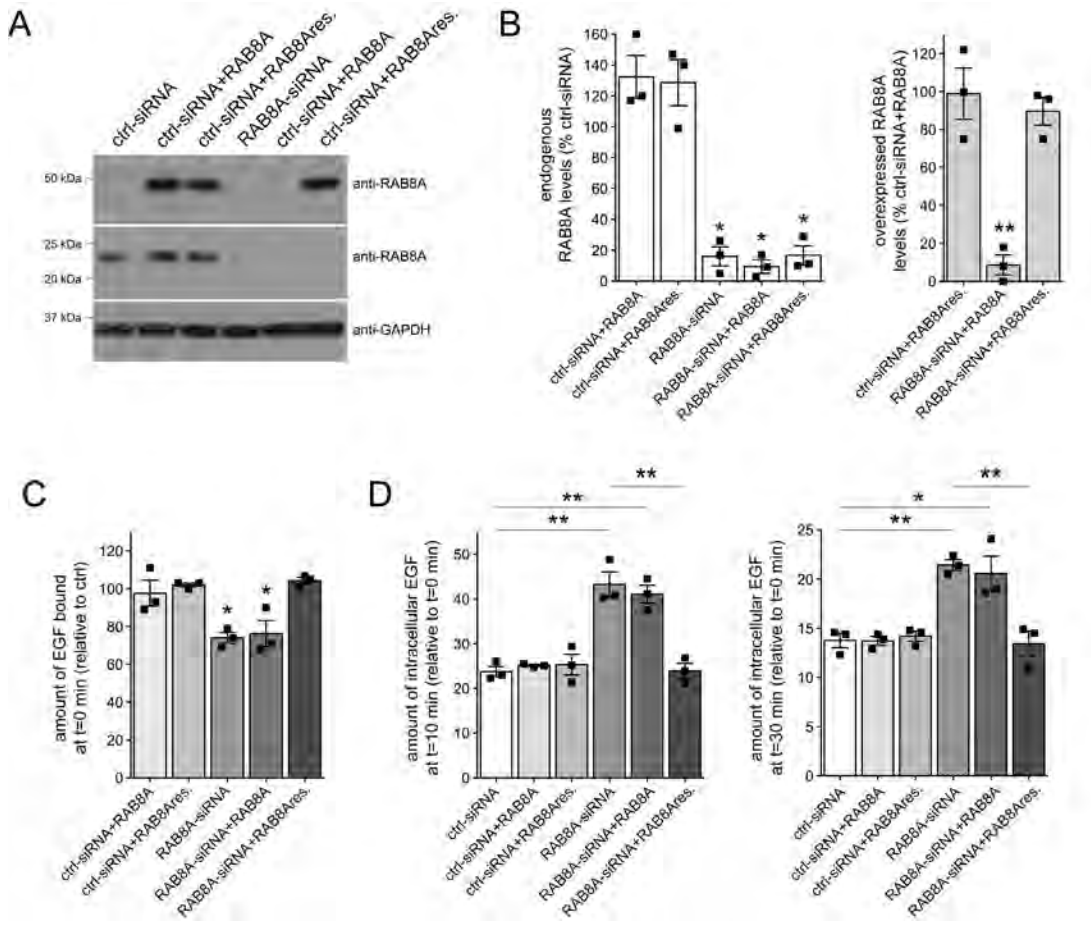

Fig. 22. siRNA-resistant RAB8A variant rescues the G2019S LRRK2-mediated endolysosomal trafficking deficits. **(A)** HeLa cells were either transfected with ctrl-siRNA or RAB8A-siRNA, and either with wildtype mRFP-RAB8A (RAB8A) or an siRNA-resistant version of mRFP-RAB8A (RAB8res.), and cell extracts (30 µg) analyzed by Western blotting for mRFP-RAB8A levels, endogenous RAB8A levels and GAPDH as loading control. **(B)** Quantification of the type of experiments depicted in **(A)**. Endogenous RAB8A levels (left) were normalized to levels in the presence of ctrl-siRNA, and overexpressed mRFP-RAB8A levels (right) normalized to levels in the presence of ctrl-siRNA and wildtype RAB8A (RAB8A). N=3 independent experiments. *P < 0.05; **P < 0.01. **(C)** Cells were either transfected with ctrl-siRNA or RAB8A-siRNA in the presence or absence of wildtype or siRNA-resistant mRFP-RAB8A as indicated, and surface-bound fluorescent Alexa488-EGF quantified. N=3 independent experiments. *P < 0.05. **(D)** Cells were either transfected with ctrl-siRNA or RAB8A-siRNA in the presence or absence of wildtype or siRNA-resistant mRFP-RAB8A as indicated, followed by quantification of internalized fluorescent Alexa488-EGF at 10 min (left) and 30 min (right). N=3 independent experiments. * P < 0.05; ** P < 0.01.

G2019S LRRK2 or RAB8A knockdown cause accumulation of EGF in a RAB4 compartment

We next wondered whether the delay in EGF degradation in the presence of pathogenic LRRK2 may reflect a redistribution of EGF into a non-endolysosomal vesicular compartment, thereby precluding its efficient degradation. As expected, the active version of endolysosomal RAB7A extensively colocalized with Alexa647-EGF 20 min upon internalization (Fig. 21B-D). In contrast, colocalization of fluorescent EGF with RAB8A or RAB11 was minor, and was not altered in the presence of G2019S LRRK2 (Fig. 21B-D), suggesting that pathogenic LRRK2 did not cause the accumulation of EGF in RAB8A or RAB11-positive endocytic recycling compartments, respectively.

Crosstalk between both the recycling and degradative endosomal trafficking pathways has been described to converge on an endocytic RAB4-positive compartment (453). We therefore next analyzed for possible changes in the colocalization of EGF with GFP-tagged RAB4. Expression of RAB4 did not affect EGF binding or EGFR trafficking in either the absence or presence of G2019S LRRK2 (Fig. 23A,B), and did not alter G2019S LRRK2 expression levels (Fig. 17J). However, when quantifying the colocalization of Alexa647-EGF with GFP-tagged RAB4 in live mock-transfected versus pathogenic LRRK2-transfected cells, a significant increase was observed in G2019S LRRK2-expressing cells (Fig. 23C,D). Similarly, there was a significant increase in the accumulation of fluorescent EGF in a RAB4-positive compartment upon siRNA of RAB8A as compared to control siRNA (Fig. 23E,F). These data indicate that either G2019S LRRK2 expression or RAB8A inactivation causes alterations in endolysosomal trafficking events culminating in the accumulation of EGF in a non-degradative, RAB4-positive recycling compartment.

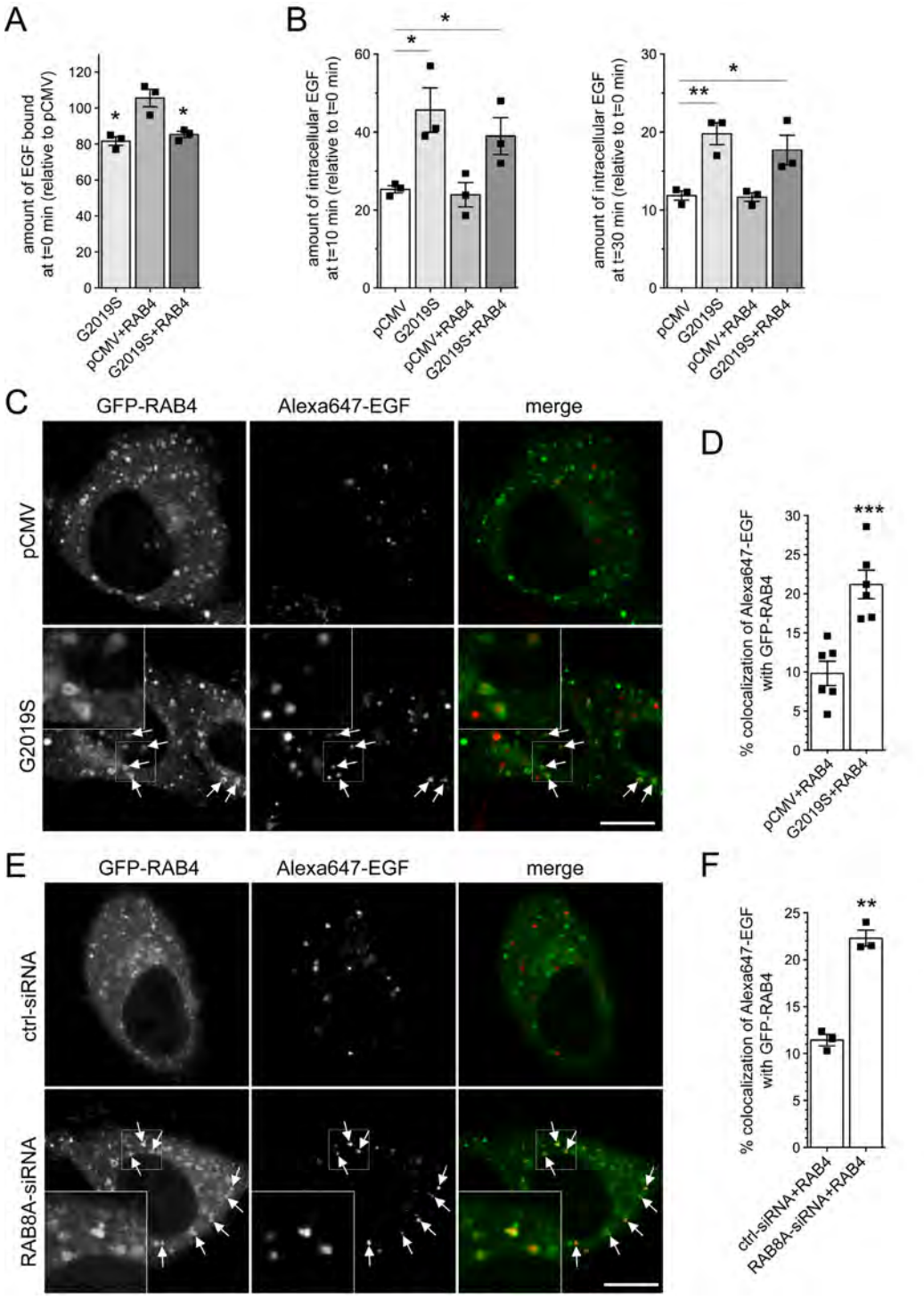

Fig. 23. Pathogenic LRRK2 or knockdown of RAB8A cause accumulation of EGF in a RAB4-positive endocytic compartment. **(A)** HeLa cells were transfected with either empty pCMV vector or pathogenic LRRK2, or co-transfected with GFP-tagged RAB4, and surface-bound fluorescent EGF quantified. N=3 independent experiments. *P < 0.05. **(B)** Cells were transfected as indicated, followed by quantification of internalized fluorescent EGF at 10 min (left) and 30 min (right). N=3 independent experiments. *P < 0.05; **P < 0.01. **(C)** Example of HeLa cells co-transfected with GFP-RAB4 and either

empty pCMV vector or pathogenic LRRK2. Live pictures were taken 20 min upon fluorescent EGF internalization, and arrows point to GFP-RAB4-positive vesicles containing Alexa647-EGF. Scale bar, 10 μm. **(D)** Quantification of colocalization of Alexa647-EGF with GFP-RAB4 (Manders coefficient 1 x 100) from 15-20 cells per experiment. N=6 independent experiments. ***P < 0.005. **(E)** Example of HeLa cells cotransfected with GFP-RAB4 and either ctrl-siRNA or RAB8A-siRNA. Live pictures were taken as described above. Arrows point to GFP-RAB4-positive vesicles containing Alexa647-EGF. Scale bar, 10 μm. **(F)** Quantification of colocalization of Alexa647-EGF with GFP-RAB4 (Manders coefficient 1 x 100) from 15-20 cells per experiment. N=3 independent experiments. **P < 0.01.

G2019S LRRK2 causes a deficit in EGFR recycling

The observed accumulation of fluorescent EGF in a RAB4-positive compartment suggests that pathogenic LRRK2 may cause additional alterations in endocytic recycling events. Since the concentration of EGF ligand is known to influence the balance between lysosomal degradation and recycling of the receptor, we next used low ligand concentrations to favor receptor recycling, together with an antibody against the extracellular domain of the EGFR in the absence of permeabilization to visualize only surface EGFR (447). Cells were co-transfected with mRFP and either pathogenic G2019S LRRK2 or kinase-inactive G2019S-K1906M, serum-starved and incubated on ice with 20 ng/ml non-labelled EGF for 20 min in the presence of cycloheximide to prevent novel protein synthesis (steady state). Cells were then shifted to 37 °C which allows them to internalize EGFR (pulse), followed by a chase for various time points to assess EGFR recycling rates back to the cell surface (chase). As observed for fluorescent EGF surface binding, the antibody against the extracellular domain of the EGFR revealed a decrease in EGFR surface levels under steady-state conditions in cells expressing G2019S LRRK2, but not kinase-inactive G2019S-K1906M, respectively (Fig. 24A,B), even though both were expressed to similar degrees (Fig. 24C). Shifting cells to 37 °C caused receptor internalization in all cases, but after a 15-min chase, cells showed differential EGFR recycling rates back to the cell surface, with an impairment in the presence of G2019S LRRK2, but not the kinase-inactive G2019S-K1906M variant (Fig. 24B). Quantification of the fluorescence intensity of EGFR on the cell surface showed that the receptor did not recycle to the cell surface even upon prolonged chase times (Fig. 24B). These data indicate that pathogenic LRRK2 causes not only a deficit in endolysosomal trafficking, but also a defect in endocytic EGFR recycling.

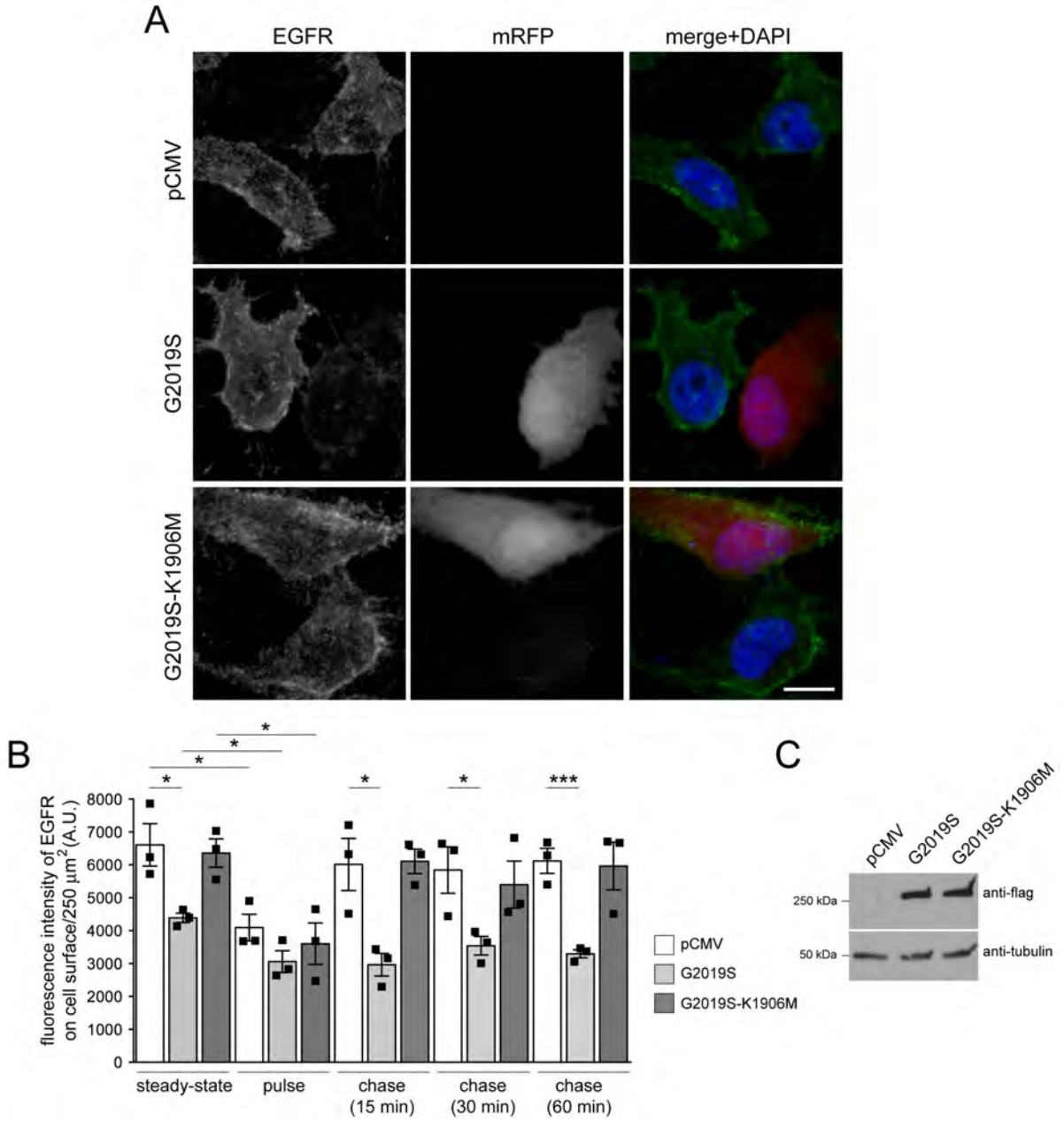

Fig. 24. Pathogenic G2019S LRRK2 causes a deficit in EGFR recycling. **(A)** Example of HeLa cells transfected with pCMV, or cotransfected with mRFP and either G2019S or kinase-inactive G2019S-K1906M LRRK2, and stained with an antibody against the extracellular domain of the EGFR in the absence of permeabilization to visualize only surface EGFR. Scale bar, 10 µm. **(B)** Quantification of fluorescence intensity of surface levels of EGFR at t=0 min (steady-state), upon triggering internalization of the EGFR (pulse), or upon chase for various time points to assess recycling rates (chase), as described in Materials and Methods. N=3 independent experiments. *P < 0.05; ***P < 0.005. **(C)** HeLa cells were transfected as indicated, and cell extracts (30 µg) analyzed by Western blotting for flag-tagged LRRK2 levels and tubulin as loading control.

Mistargeting of EGF into a RAB4 compartment and endocytic recycling deficits mediated by either G2019S LRRK2 or RAB8A knockdown are rescued upon active RAB7A expression

Since expression of active RAB7A rescued the endolysosomal EGFR trafficking deficits observed upon either siRNA of RAB8A or upon G2019S LRRK2 expression (399), we wondered whether active RAB7A expression would also lead to a reversal in the accumulation of fluorescent EGF in a RAB4-positive compartment, and a rescue of the endocytic EGFR recycling deficit. Quantification of the colocalization of Alexa647-EGF with GFP-tagged RAB4 upon siRNA of RAB8A was rescued when co-expressing active RAB7A-Q67L, but not wildtype or inactive RAB7A-T22N versions, respectively, even though all constructs were expressed to similar degrees (Fig. 25A-C). Furthermore, siRNA of RAB8A caused a decrease in EGFR surface levels and endocytic recycling deficits of the EGFR, which were rescued upon co-expression of active RAB7A-Q67L, but not wildtype or inactive RAB7A-T22N versions, respectively (Fig. 25D). Similarly, expression of active, but not wildtype or inactive RAB7A caused a reversal in the accumulation of fluorescent EGF in a RAB4-positive compartment upon pathogenic G2019S LRRK2 expression, with constructs expressed to similar degrees (Fig. 26A-C). In addition, the LRRK2-mediated decrease in EGFR surface levels and the endocytic recycling deficits of the EGFR were rescued by active, but not wildtype or inactive RAB7A versions, respectively (Fig. 26D). Thus, pathogenic LRRK2 expression causes a defect in endolysosomal degradation which is accompanied by mistargeting of EGF into a RAB4 compartment and by a deficit in endocytic recycling, all phenocopied by knockdown of RAB8A and rescued in the presence of active RAB7A.

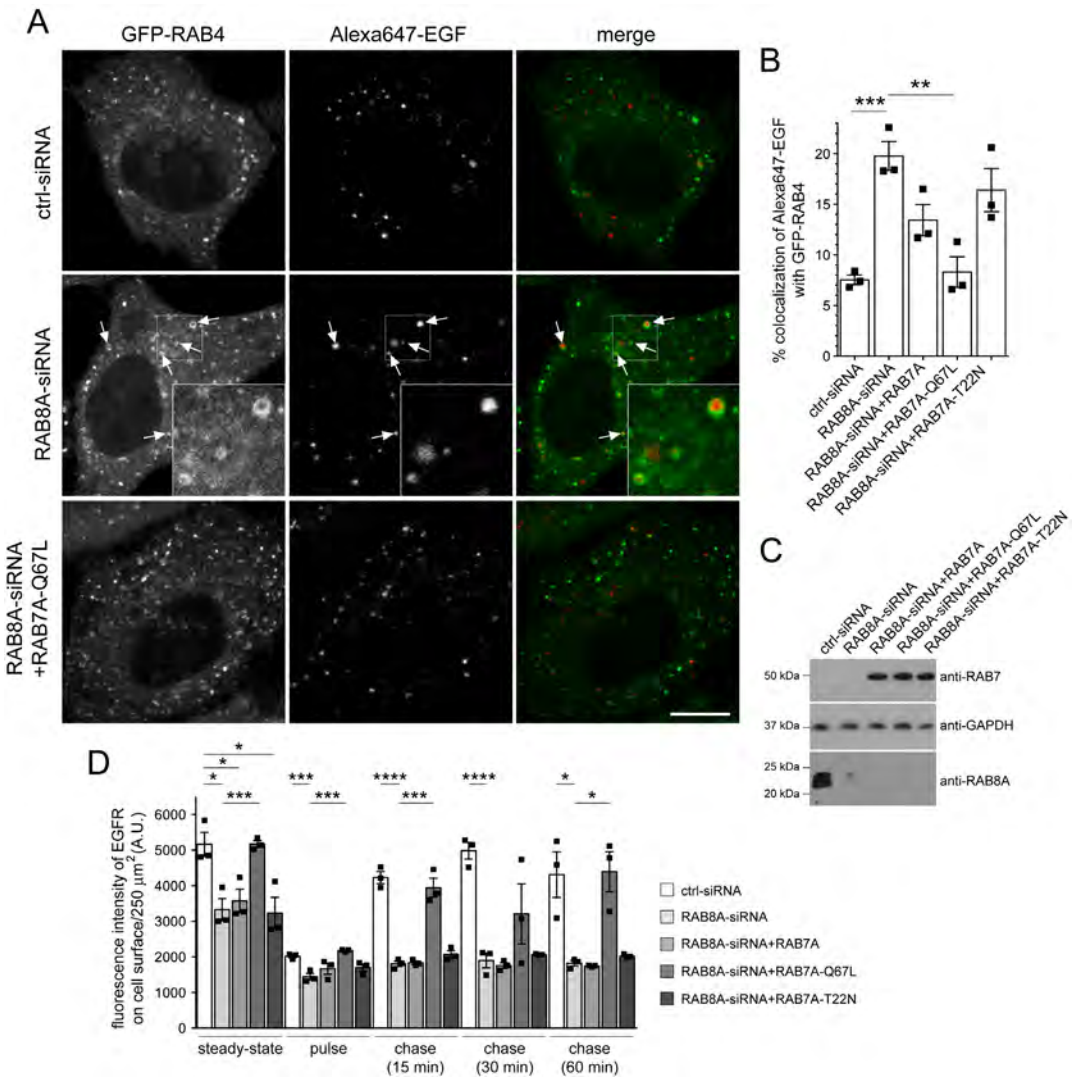

Fig. 25. Accumulation of EGF in a RAB4-positive endocytic compartment and deficits in EGFR recycling due to knockdown of RAB8A are rescued by active RAB7A expression. **(A)** Example of HeLa cells cotransfected with GFP-RAB4 and either ctrl-siRNA or RAB8A-siRNA, with or without RAB7A-Q67L expression as indicated. Live pictures were taken 20 min upon fluorescent EGF internalization, and arrows point to GFP-RAB4-positive vesicles containing Alexa647-EGF. An independent picture (543 HeNe laser line) was acquired to confirm co-expression of the distinct mRFP-tagged RAB7A constructs in all cases. Scale bar, 10 µm. **(B)** Quantification of colocalization of Alexa647-EGF with GFP-RAB4 and either ctrl-siRNA or RAB8A-siRNA, in the presence or absence of distinct RAB7A constructs as indicated (Manders coefficient 1 x 100) from 15-20 cells per experiment. N=3 independent experiments. **P < 0.01; *** P < 0.005. **(C)** HeLa cells were treated with ctrl-siRNA or RAB8A-siRNA as indicated, transfected with the indicated RAB7A constructs, and cell extracts (30 µg) analysed by Western blotting for RAB8A protein levels, mRFP-RAB7A protein levels (anti-RAB7 antibody) and GAPDH as loading control. **(D)** HeLa cells were treated with either ctrl-siRNA or RAB8A-siRNA as indicated, with or without co-transfection with the indicated RAB7A constructs. EGFR recycling assays were performed as described in Materials and Methods, revealing a deficit in EGFR surface levels and EGFR recycling upon RABA-siRNA, which was rescued upon expression of active RAB7A. N=3 independent experiments. *P < 0.05; ***P < 0.005; ****P < 0.001.

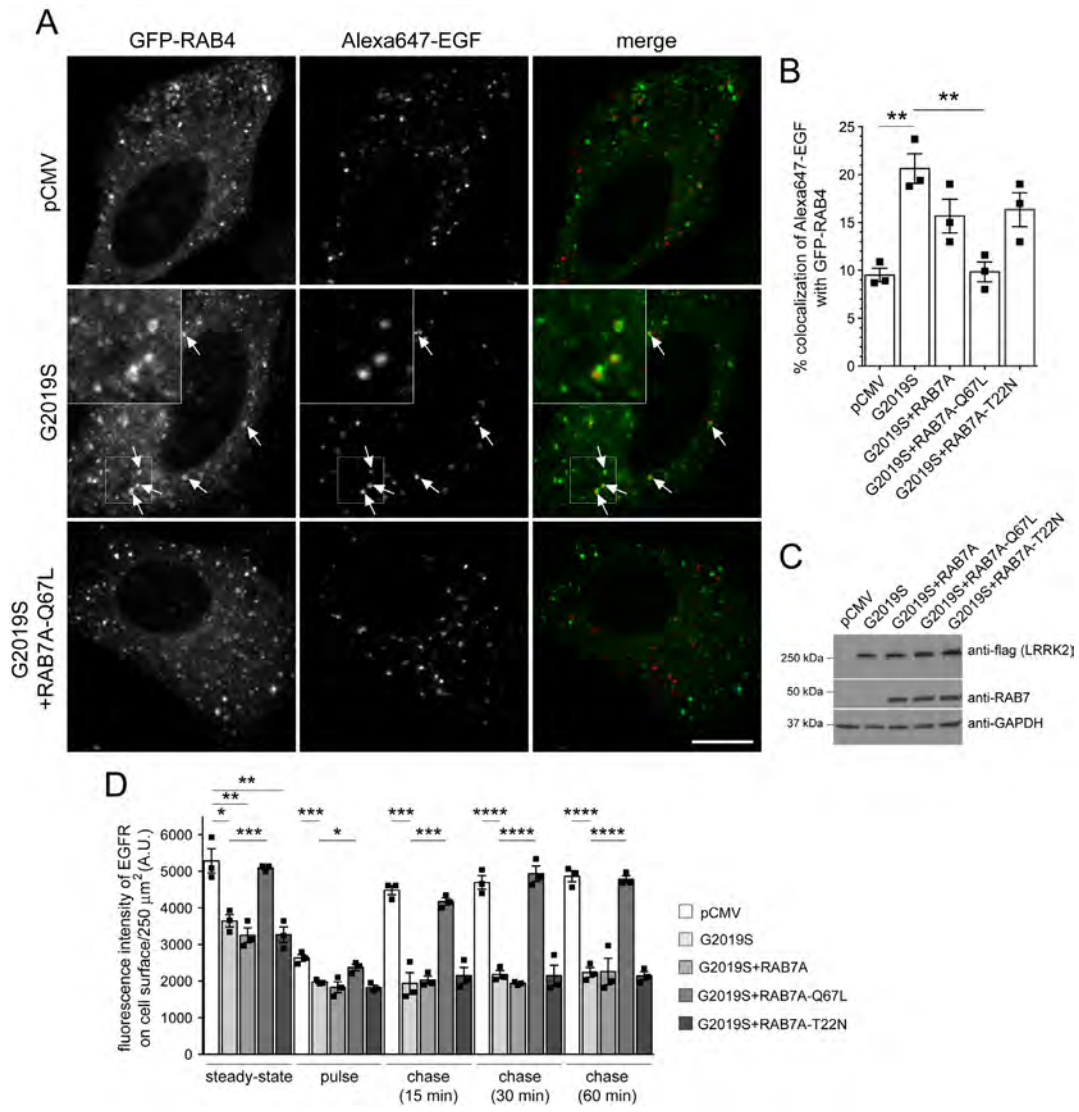

Fig. 26. Accumulation of EGF in a RAB4-positive endocytic compartment and deficits in EGFR recycling due to G2019S LRRK2 expression are rescued by active RAB7A expression. **(A)** Example of HeLa cells co-transfected with GFP-RAB4 and either empty pCMV vector or pathogenic LRRK2, with or without RAB7A-Q67L expression as indicated. Live pictures were taken 20 min upon fluorescent EGF internalization, and arrows point to GFP-RAB4-positive vesicles containing Alexa647-EGF. An independent picture (543 HeNe laser line) was acquired to confirm co-expression of the distinct mRFP-tagged RAB7A constructs in all cases. Scale bar, 10 µm. **(B)** Quantification of colocalization of Alexa647-EGF with GFP-RAB4 in cells co-expressing empty pCMV vector, or G2019S LRRK2, in the presence or absence of mRFP-tagged RAB7A constructs as indicated (Manders coefficient 1 x 100), from 15-20 cells per experiment. N=3 independent experiments. **P < 0.01. **(C)** HeLa cells were transfected with the indicated constructs, and cell extracts (30 µg) analysed by Western blotting for flag-tagged G2019S-LRRK2, mRFP-RAB7A protein levels (anti-RAB7 antibody) and GAPDH as loading control. **(D)** HeLa cells were transfected with either empty pCMV vector or pathogenic G2019S LRRK2, in the presence or absence of mRFP-tagged RAB7A constructs as indicated, and EGFR surface levels and EGFR recycling determined at the indicated time points. N=3 independent experiments. *P < 0.05; **P < 0.01; ***P < 0.005; ****P < 0.001.

Dominant-negative RAB7A causes accumulation of EGF in a RAB4 compartment and endocytic recycling deficits which are rescued by active RAB8A

Finally, we wondered whether decreasing active RAB7A levels *per se* may account for the mistargeting of the EGFR into a RAB4A compartment and endocytic recycling deficits, as observed upon pathogenic LRRK2 expression or knockdown of RAB8A. Expression of dominant-negative RAB7A (RAB7A-T22N) (144) interfered with EGF surface binding and EGFR degradation, which was rescued upon overexpression of active RAB8A (Fig. 27A,B). Further, expression of dominant-negative RAB7A, but not wildtype or catalytically active RAB7A (RAB7A-Q67L), caused accumulation of EGF in a RAB4 compartment (Fig. 27C,D), which was rescued upon overexpression of active RAB8A (Fig. 27E,F). Similarly, dominant-negative RAB7A caused a decrease in EGFR surface levels and EGFR recycling, which was rescued upon overexpression of active RAB8A (Fig. 27G). Thus, decreasing RAB7A activity causes the same trafficking deficits as observed upon pathogenic LRRK2 expression or knockdown of RAB8A, and such effects can be rescued by either active RAB7A or RAB8A expression, respectively. Altogether, our data indicate that G2019S LRRK2 expression causes inactivation of RAB8A, associated with inactivation of RAB7A and followed by alterations in endolysosomal trafficking events culminating in the accumulation of EGF in a non-degradative, RAB4-positive recycling compartment, as well as impaired endocytic recycling.

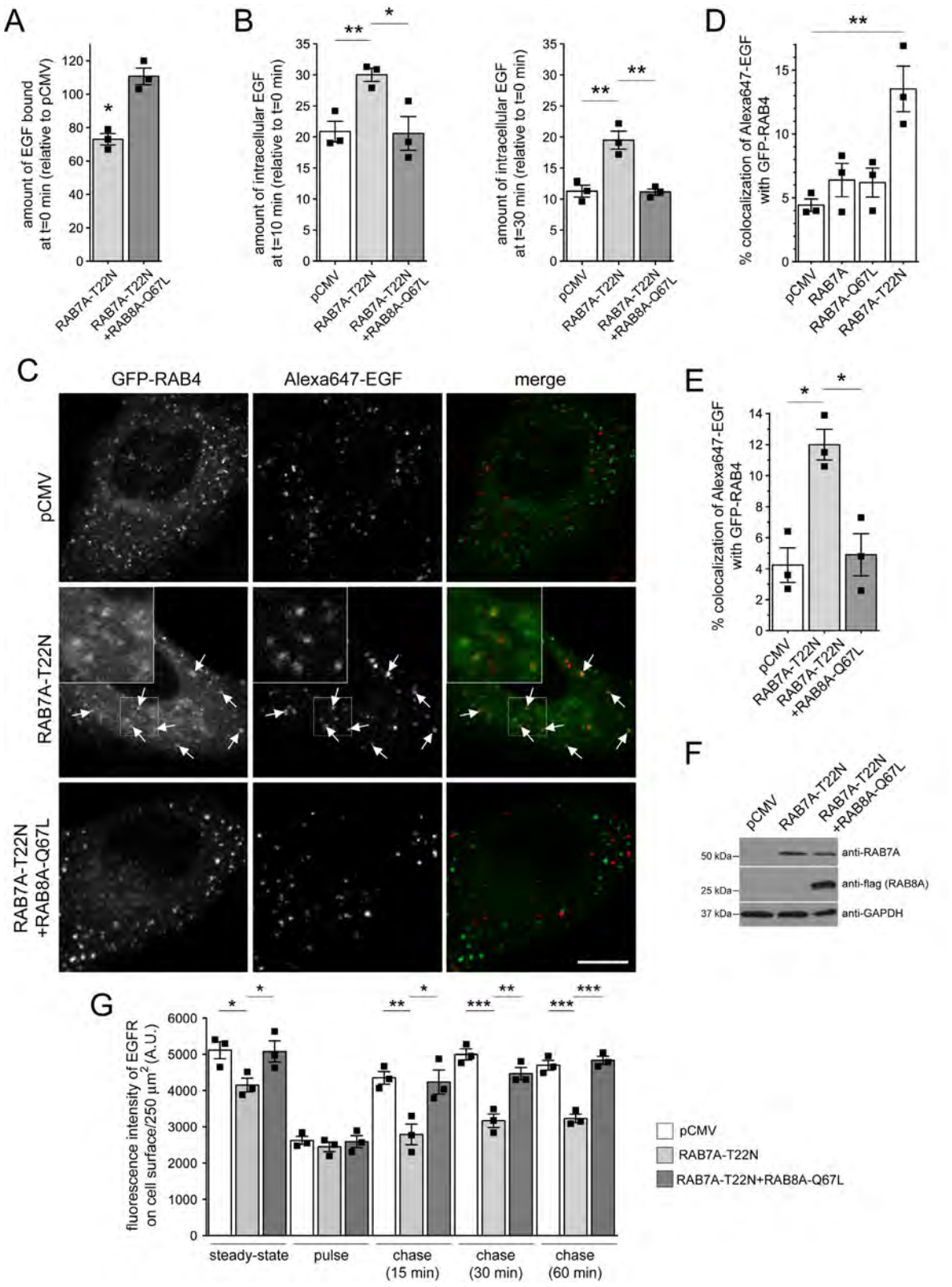

Fig. 27. Expression of dominant-negative RAB7A causes defects in EGFR trafficking, accumulation of EGF in a RAB4-positive endocytic compartment, and deficits in EGFR recycling, which are reversed upon active RAB8A expression. **(A)**

HeLa cells were transfected with either empty pCMV vector (ctrl), or with dominant-negative RAB7A (RAB7A-T22N) in the presence or absence of active RAB8A (RAB8A-Q67L), and surface-bound fluorescent EGF quantified. N=3 independent experiments. *P < 0.05. **(B)** Cells were transfected with the indicated constructs, followed by quantification of internalized fluorescent EGF at 10 min (left) and 30 min (right). N=3 independent experiments. *P < 0.05; **P < 0.01. **(C)** Example of HeLa cells cotransfected with GFP-RAB4 and either mRFP-RAB7A-T22N, or with mRFP-RAB7A-T22N and flag-tagged RAB8A-Q67L as indicated. Live pictures were taken 20 min upon fluorescent EGF internalization, and arrows point to GFP-RAB4-positive vesicles containing Alexa647-EGF. An independent picture (543 HeNe laser line) was acquired to confirm co-expression of the mRFP-tagged RAB7A constructs in all cases. Scale bar, 10 μm. **(D)** Quantification of colocalization of Alexa647-EGF with GFP-RAB4, in the presence or absence of the distinct RAB7A constructs as indicated (Manders coefficient 1 x 100) from 15-20 cells per experiment. N=3 independent experiments. ** P < 0.01. **(E)** Quantification of colocalization of Alexa647-EGF with GFP-RAB4 in the presence or absence of RAB7A-T22N and RAB8A-Q67L constructs as indicated (Manders coefficient 1 x 100) from 15-20 cells per experiment. N=3 independent experiments. * P < 0.05. **(F)** HeLa cells were transfected with the indicated constructs, and cell extracts (30 μg) analysed by Western blotting for mRFP-tagged RAB7A-T22N, flag-tagged RAB8A-Q67L and GAPDH as loading control. **(G)** HeLa cells were transfected with either empty pCMV vector or dominant-negative RAB7A-T22N, in the absence or presence of RAB8A-Q67L, and EGFR surface levels and EGFR recycling determined at the indicated time points. N=3 independent experiments. *P < 0.05; **P < 0.01; ***P < 0.005.

VII.DISCUSSION

The present work establishes a mechanistic connection between LRRK2-mediated RAB8A phosphorylation and deficits in endocytic trafficking caused by mutant LRRK2. Both pathogenic LRRK2 and RAB8A knockdown altered degradative and recycling trafficking events, resulting in the accumulation of endocytosed EGF/EGFR in a RAB4-positive compartment. RAB8A phosphorylation and concomitant inactivation may thus form the basis for how pathogenic LRRK2 leads to endolysosomal alterations, a key pathogenic phenotype in PD.

Effect of pathogenic LRRK2 on RAB8A and membrane trafficking alterations

We confirmed RAB8A as a prominent LRRK2 substrate *in vitro*, in contrast to other RAB proteins, including RAB7A and RAB11, which were not phosphorylated by LRRK2. Moreover, we corroborated T72 as the major phosphorylation site within RAB8A, as previously shown by Dario Alessi's group. This residue lies within the switch II domain, a highly conserved region which is important for Rab interactions (187).

We used the well-established EGFR trafficking assay to study endocytic degradative trafficking events. Using this cellular assay, pathogenic LRRK2 was previously found to cause a deficit in EGF surface binding, as well as a delay in EGFR degradation, in a manner dependent on RAB7A inactivation (399).

We showed that a mutant version of RAB8A mimicking the permanently active GTP-bound form rescued the pathogenic LRRK2-mediated delay in EGFR degradation, as well as the reduced EGF surface binding, suggesting that these effects may be at least in part mediated by a deficit in the amount of active RAB8A. Similarly, the components of the activation cascade for RAB8A, RAB11 and Rabin8, rescued the effect of mutant LRRK2, which indicates that activating endogenous RAB8A is enough to revert the endolysosomal trafficking deficits. Altogether, these data suggest that pathogenic LRRK2 may cause an inactivation of RAB8A *in vivo*, probably by a direct phosphorylation event, which would result in a loss-of-function phenotype for RAB8A-mediated intracellular membrane trafficking events.

Studies of protein phosphorylation often employ amino acid substitutions to generate phosphomimetic (T-to-D or T-to-E) or phosphodeficient (T-to-A) versions of proteins. When

using a T72E version of RAB8A, LRRK2-mediated phosphorylation of RAB8A was suggested to cause its inactivation, as this variant displayed decreased binding to the key regulatory proteins Rabin8 and GDI1/2 and to several effectors *in vitro* (252, 417). Indeed, in our hands the phosphomimetic RAB8A variants were unable to rescue the LRRK2-mediated deficits, and were largely cytosolic. Similar observations have been previously described for RAB7A (454). RAB7A was shown to be phosphorylated on an equivalent residue (S72) in the switch II region, and a phosphomimetic RAB7A version displayed impaired interaction with GDI1/2 and the RAB7A GEF Mon1-Ccz1, and was also localized to the cytoplasm (454).

The T72D and T72E variants of RAB8A did not display a significant effect *per se* on EGFR trafficking, and thus were not able to mimic a pathogenic version of LRRK2. However, there are some concerns related to the use of phosphomimetic mutants, and data obtained with them have to be taken with great caution. For example, the negative charge of the phosphate group is much larger than that of the negatively charged aminoacids E and D, with a single negative charge. Moreover, phosphorylation-dependent protein interactions, due to their unique size and charge properties, may not be properly mimicked by aminoacid substitutions (455). In this context, previous studies indicate that RAB8A-T72D and RAB8A-T72E cannot reproduce a phosphorylated state of RAB8A (417, 419). While phosphorylated RAB8A could be detected on/around the centrosome by a phosphorylation state-specific antibody, phosphomimetic RAB8A was not localized to the centrosome (417). Moreover, and contrary to the phosphorylated form, RAB8A-T72E failed to show enhanced interaction with GFP-RILPL1 (419). Consequently, phosphomimetic variants of RAB8A may represent inactive forms of the protein, which could explain why they are not able to effectively reproduce the effect of pathogenic LRRK2 on degradative trafficking.

On the other hand, the phosphodeficient variant RAB8A-T72A rescued the effect of pathogenic LRRK2. Pfeffer and colleagues showed that this mutant lacked primary cilia localization, displaying altered localization to the Golgi complex, and was unable to rescue the decreased ciliation phenotype observed in RAB8A KO cells, thus representing a loss-of-function version of RAB8A (419). Although we did not observe such Golgi localization in HeLa cells under our experimental conditions, RAB8A-T72A displayed less localization to

the tubular recycling compartment as compared to WT or constitutively active RAB8A versions. Although reduced, the tubular localization of RAB8A-T72A may indicate that it is at least partly functional and thus able to rescue the pathogenic effect of G2019S LRRK2 on EGFR trafficking, at least in HeLa cells.

Due to the caveats of employing phosphomimetic and phosphodeficient protein variants, we performed knockdown studies as an alternative means to test for the role of pathogenic LRRK2 on regulating RAB8A activity. Interestingly, RAB8A knockdown mimicked the mutant LRRK2-mediated alterations in endomembrane trafficking, supporting the conclusion that pathogenic LRRK2 causes a loss-of-function phenotype of RAB8A in the context of membrane trafficking events. Similarly, LRRK2-mediated phosphorylation of RAB8A was shown to cause a deficit in protein transport and/or signaling defects at cilia (252, 419), consistent with a loss-of-function phenotype. Strikingly, phosphorylated RAB8A was found to be absent from the ERC and aberrantly accumulate in a pericentrosomal/centrosomal compartment in the presence of pathogenic LRRK2 (417), indicating that altered intracellular localization may contribute to RAB8A loss-of-function.

As previously described for G2019S LRRK2 (399), the deficits in EGFR trafficking caused by RAB8A knockdown were rescued by overexpression of an active form of RAB7A. Moreover, RAB8A knockdown caused a dramatic decrease in the amount of endogenous active RAB7A, as demonstrated by both GST-RILP pull-down assays and a conformation-specific antibody recognizing GTP-RAB7A. How a decrease in RAB8A activity and/or levels upon siRNA may impair RAB7A functioning remains unclear. A variety of scenarios are possible, including direct competition for shared GEFs or GAPs. The former mechanism seems unlikely, as currently identified GEFs for RAB8A include Rabin8, GRAB and MSS4 (258, 259, 456, 457), whilst the main GEF for RAB7 is the Mon1-Ccz1 complex (458, 459). Alternatively, the two Rab proteins may compete for GAPs. Identified GAPs for RAB8A include TBC1D4 (460) and the TBC-domain-containing protein EPI64 (461), whilst GAPs for RAB7 include TBC1D2/armus (462), TBC1D5 (463) and TBC1D15 (448, 464). However, GAPs display a certain promiscuity, with little correlation between their Rab binding and Rab-GAP activity (465, 466). In this context, it is interesting to note that TBC1D15 was found to preferentially interact with phosphodeficient as compared to

phosphomimetic RAB8A (83). While further work will be required to address this possibility, it is tempting to speculate that LRRK2-mediated phosphorylation of RAB8A may result in decreased interaction with TBC1D15, allowing it to act upon RAB7A (Fig. 28), analogous to the recently reported retromer-mediated regulation of RAB7A activity via TBC1D5 (467).

In this specific study, Jiménez-Orgaz *et al.* showed that the active form of RAB7A is mostly found on endolysosomes, while inactive RAB7A is localized to different membrane compartments such as mitochondria, ER and Golgi, and this balance between inactive and active RAB7A is lost in the absence of TBC1D5, with the hyperactivated small GTPase massively accumulating in endolysosomes and causing deficits in autophagosome formation around damaged mitochondria during parkin-mediated mitophagy (467). In the future, it would be interesting to analyze for possible changes in the colocalization of endogenous RAB7A with distinct membrane compartments in the presence of pathogenic LRRK2 or upon knockdown of RAB8A. Alternatively, it is possible that this mechanism is specific for TBC1D5 and related to retromer-mediated regulation of RAB7A activity. On the other hand, TBC1D15 is associated with RAB7A inhibition during mitophagy (468), and its effect may be restricted to this pathway, although other phenotypes such as lysosomal fragmentation have been associated with TBC1D15 (448).

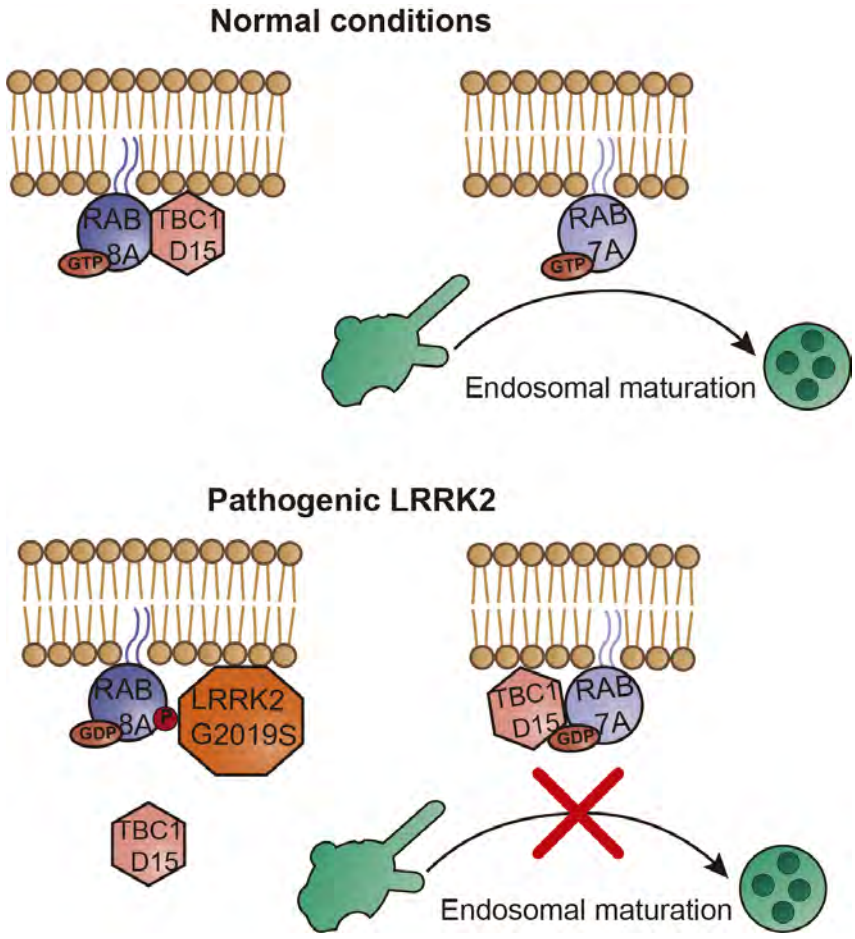

Fig. 28. LRRK2-mediated phosphorylation of RAB8A may cause a decrease in RAB7A activity via TBC1D15. TBC1D15, a RAB7A GAP, preferentially interacts with phosphodeficient as compared to phosphomimetic RAB8A. Under normal conditions, there is a balance between the amount of TBC1D15 interacting with RAB8A or with RAB7A, which allows RAB7A to exert its normal functions. In contrast, pathogenic LRRK2-mediated phosphorylation of RAB8A may result in decreased interaction with TBC1D15, which would then act upon RAB7A causing its inactivation and inhibiting its normal cellular roles.

A variety of other mechanisms may be responsible for the decrease in RAB7A activity reported in the presence of pathogenic LRRK2. For example, Rab proteins are known to associate with ion channels (469), and the release of ions through these channels may regulate Rab activity. In fact, calcium release through the endolysosomal channel P2Xa was demonstrated to cause an increase in RAB11 GAP activity, and the subsequent downregulation of RAB11 activity (470). Interestingly, pathogenic LRRK2 has been related to enhanced activity of another lysosomal calcium channel, TPCN2, resulting in increased

lysosomal calcium release (398, 426), which may impact upon RAB7A activity, similarly to the described calcium-mediated downregulation of RAB11 activity. Although TPCN2 has been suggested to be modulated by RAB7A activity (471, 472), the enhanced TPCN2 activity in the presence of pathogenic LRRK2 may cause a concomitant calcium-mediated decrease in overall RAB7A activity. Apart from RAB7A, other Rab proteins including the LRRK2 substrates RAB8A and RAB10 have been shown to interact with TPCN2 (471), and it is tempting to speculate that LRRK2-mediated phosphorylation of these Rab proteins could alter TPCN2 activity and result in calcium-mediated decrease in RAB7A activity. In the future, it would be interesting to determine whether RAB8A knockdown also causes alterations in endolysosomal calcium release similar to what has been described for pathogenic LRRK2.

A recent proteomics study has identified proteins which preferentially interact with phosphorylated RAB8A, as well as proteins whose interactions are weakened/lost when RAB8A is phosphorylated (252). These data allow for the formulation of additional hypotheses. For example, phosphorylated RAB8A was preferentially shown to interact with EHBP1L1, which is known to bind to only GTP-bound RAB8A. Selective binding of phosphorylated RAB8A to EHBP1L1 may decrease the amount of EHBP1L1 able to act on non-phosphorylated RAB8A, which is expected to cause mistrafficking of apical membrane proteins into lysosomes (473). Whilst the link to RAB7A remains unclear, it would be interesting to determine whether there are alterations in RAB7 activity in EHBP1L1 knockout cells, or whether the observed LRRK2-mediated trafficking deficit can be rescued when overexpressing EHBP1L1.

On the other hand, phosphorylated RAB8A has been shown to lose interaction with various proteins, most prominently WDR81/WDR91 (252). These proteins function as a complex, and WDR81 knockout cells have been shown to display a deficit in EGFR degradation by impairing endolysosomal fusion (474). Thus, a loss of interaction of phosphorylated RAB8A with WDR81/WDR91 may contribute to the LRRK2-induced trafficking deficits we observed. In addition, as described in the introduction, WDR91 has been reported as a RAB7A effector, and its loss increases endosomal PI(3)P levels and blocks endosomal-lysosomal membrane trafficking (135). Finally, phosphorylated RAB8A

has also been shown to display decreased interaction with OCRL1 (252), an inositol-5-phosphatase involved in endocytosis (475). Thus, it would be interesting to determine whether pathogenic LRRK2 may cause alterations in endosomal phosphatidylinositol levels via some of the above-mentioned mechanisms.

The finding that deficits in RAB8A, a RAB protein which functions at the endocytic recycling compartment, cause alterations in late endocytic degradative trafficking seems puzzling at first. However, several reports have revealed crosstalk between the recycling and degradative trafficking pathways involving a RAB4-positive compartment. For example, overexpression of dominant-negative RAB4 variants was found to alter both endocytic recycling as well as degradation (153). Moreover, a GAP for RAB4 regulates both TfnR recycling as well as degradative EGFR trafficking (476). Similarly, the Rho GAP DLC3 was shown to be required for the proper lysosomal degradation of the EGFR and, in the absence of DLC3, EGFR was found accumulated in RAB4-positive vesicles (453). These data indicate the presence of a dynamic and intricate crosstalk between recycling and degradative membrane trafficking pathways which converge onto a RAB4-positive recycling compartment. We therefore examined the colocalization of EGF with GFP-tagged RAB4, and observed increased colocalization both in the presence of the G2019S variant of LRRK2 and in the absence of RAB8A. We also attempted to determine the colocalization of EGF/EGFR with endogenous RAB4. However, two distinct commercially available anti-RAB4 antibodies were unable to detect endogenous RAB4 under various different immunocytochemistry/permeabilization conditions tested (Fig. 29).

Our results suggest that endocytosed material aberrantly accumulates in a RAB4-positive compartment, thus precluding its efficient degradation. Given the fact that RAB4 also localizes to SEs (151), where it has been suggested to play an important role in cargo sorting (477), it remains possible that the observed RAB4-positive compartment corresponds mostly to SEs, and that EGF accumulation in this compartment would simply reflect the delay in degradation due to decreased RAB7A activity in the presence of G2019S LRRK2 or knockdown of RAB8A. Since previous studies from the laboratory have shown a lack of accumulation of EGF in a RAB5-positive compartment upon pathogenic LRRK2 expression (399), this possibility seems unlikely though.

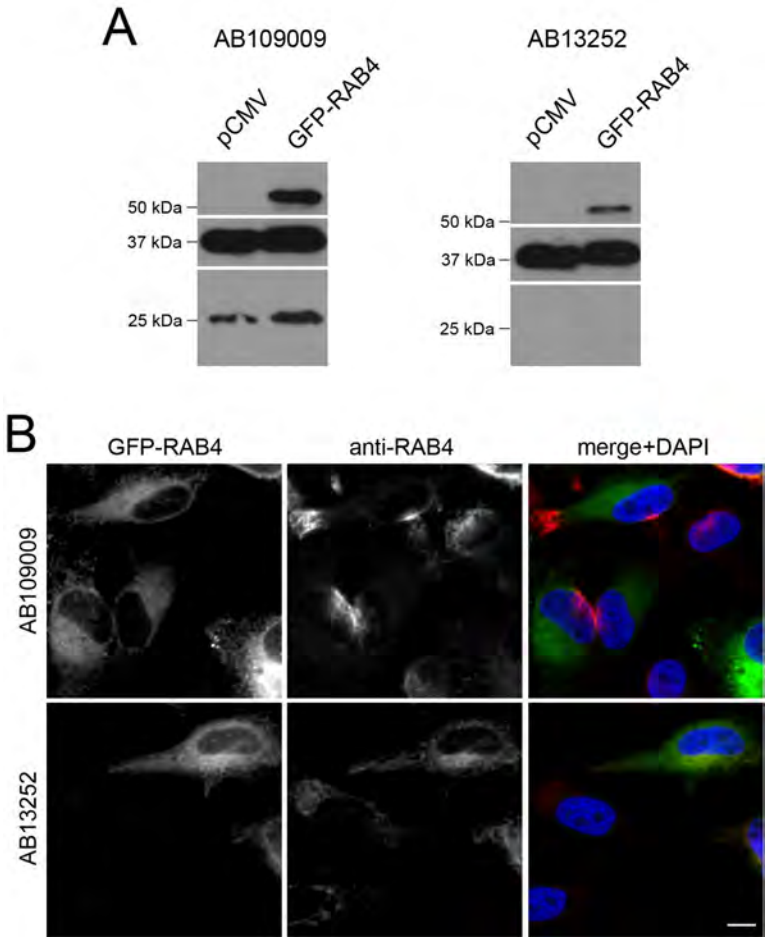

Fig. 29. Test by WB and immunocytochemistry of two commercially available anti-RAB4 antibodies. **(A)** HeLa cells were transfected with the indicated constructs, and 40 µg of extracts analyzed by Western blotting for the detection of endogenous RAB4 or GFP-tagged RAB4, as well as GAPDH as loading control. Only the AB109009 antibody (Abcam) was able to detect endogenous RAB4 by Western blotting, whilst both antibodies could detect overexpressed GFP-RAB4. **(B)** HeLa cells were transfected as indicated, and fixed cells were stained using the indicated anti-RAB4 antibodies. Only the AB13252 antibody (Abcam) could detect GFP-RAB4, the signal intensity being weak and only slightly increased as compared to the signal obtained in non-transfected cells. Scale bar, 10 µm.

Thus, the accumulation of EGF in a RAB4-positive compartment suggests that pathogenic LRRK2 or RAB8A knockdown may alter endocytic recycling. Indeed, in both cases the recycling of the EGFR back to the PM is compromised, which could be responsible for the decrease in steady-state levels of the EGFR at the PM, and reduced EGF surface binding observed when overexpressing pathogenic LRRK2 or knocking down RAB8A.

Interestingly, and as observed for EGF/EGFR degradation deficits, the mistargeting of EGF into a RAB4-positive compartment and the defects in EGFR recycling by either G2019S LRRK2 expression or knockdown of RAB8A were rescued upon active RAB7A expression. Conversely, expression of dominant-negative RAB7A caused identical deficits in endolysosomal EGF trafficking associated with the accumulation of EGF in a RAB4-positive compartment, and deficits in EGFR recycling, which were rescued by active RAB8A. These data are consistent with the idea that pathogenic LRRK2 causes a phosphorylation-mediated loss of proper RAB8A functioning and a concomitant decrease in RAB7A activity, the latter of which contributes to the observed trafficking deficits. The data further suggest a complex and mutual crosstalk between RAB8A and RAB7A, whose mechanistic underpinning will require further investigation.

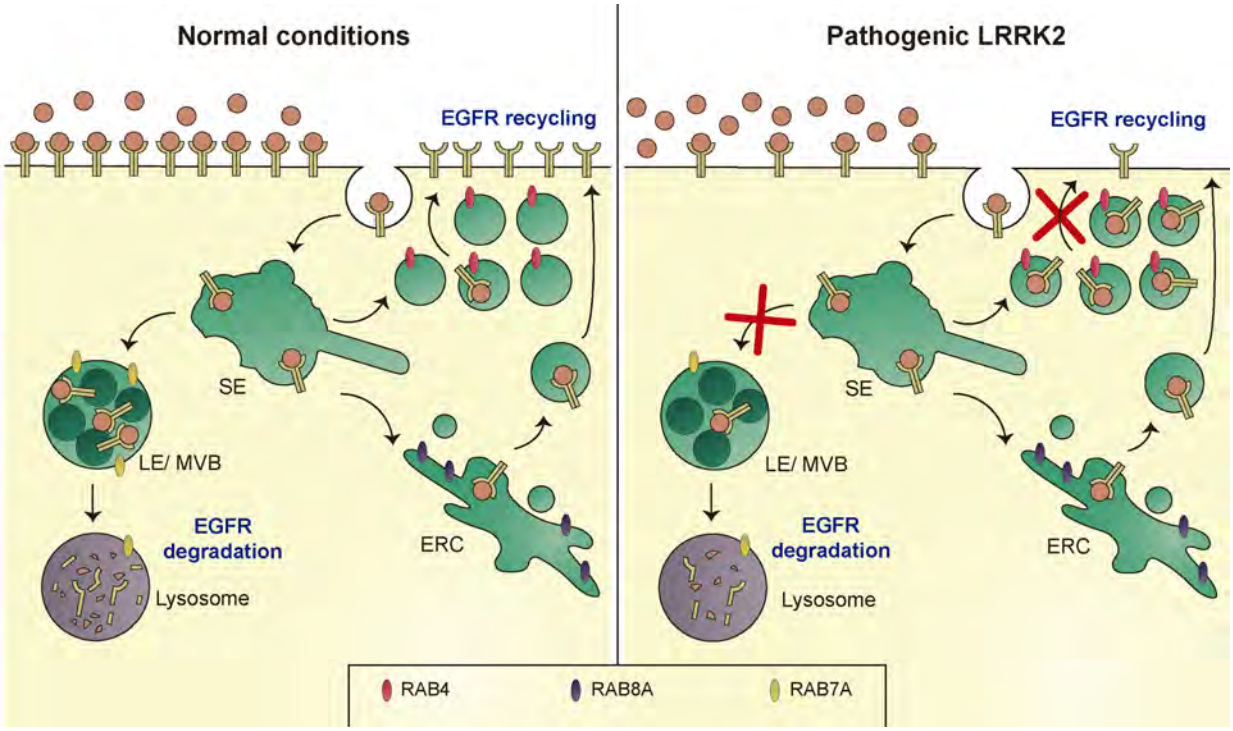

Fig. 30. Model for pathogenic LRRK2 action on EGFR trafficking. In the absence of pathogenic LRRK2, both recycling and degradation of the EGFR occur normally, as explained in the introduction. However, pathogenic LRRK2 disrupts EGFR recycling and degradation by impairing the functions of the GTPases RAB7A and RAB8A, resulting in EGF/EGFR accumulation in a RAB4-positive compartment.

Membrane trafficking deficits and PD

Neurons are highly polarized cells and their extremely arborized cellular architecture imposes a great burden on membrane trafficking. Specifically, SNpc DA neurons have one of the most dense arborizations of all neurons, with up to 150,000 presynaptic terminals per neuron (478). They depend on membrane trafficking for neurotransmission, and to maintain the balance between recycling and degradation of synaptic vesicles or protein cargoes such as neurotransmitters or receptors. It is not surprising then that alterations in these pathways lead to different forms of neurodegeneration (479).

In the case of PD, as previously explained in the introduction, a considerable number of genes, both familial or risk factors, have roles in endomembrane trafficking pathways (103), and it is possible that the number of PD-related genes implicated in vesicular trafficking has been greatly underestimated, due to the small effect sizes of risk loci not reaching GWAS significance. Indeed, a recent report using GWAS data from 18,869 PD cases and 22,452 controls to study the contribution of pathway-specific SNPs, demonstrated that the endocytic membrane trafficking pathway contributes to the heritability of PD outside of what is explained by GWAS (101). Nineteen genes were identified in this study, and importantly nine of them are involved in cargo degradation, which highlights the relevance of the endocytic pathway for PD risk (101).

Regarding LRRK2, previous studies in various non-neuronal as well as neuronal cell types have shown that pathogenic LRRK2 causes endolysosomal defects, even though most of these studies have employed endolysosomal morphological alterations as a readout for the pathogenic LRRK2-mediated deficits (248, 398, 425, 427, 428, 480). In contrast, our studies, by probing alterations in the trafficking of the EGFR in a non-neuronal cell line, have allowed us to precisely dissect the dynamic alterations in the trafficking steps altered by pathogenic LRRK2.

Interestingly, LRRK2 has also been related to altered trafficking of neuronal receptors. For example, both LRRK2 knockout or the pathogenic R1441C LRRK2 variant were shown to impair the activity-dependent trafficking of the NMDA glutamate receptors, which

correlated with the dispersion of SEC16A from ER exit sites, and alterations in COP-II-mediated trafficking from the ER to the Golgi (434).

Moreover, G2019S LRRK2 was reported to cause an increase in DA receptor D1 levels on the cell membrane which parallels a decrease in the vesicle pool in SH-SY5Y cells and mice (481), and is due to impaired receptor internalization (482). In addition, pathogenic LRRK2 causes a decrease in the degradation of DA receptor D2 and its accumulation in the Golgi compartment, which probably interferes with receptor recycling to the PM (482), similarly to what we have reported for EGFR trafficking.

Dopamine receptors belong to two classes: D1-like (D1 and D5) and D2-like (D2, D3 and D4) receptors, based on their properties to stimulate or inhibit, respectively, adenylyl cyclase. This enzyme catalyzes cyclic AMP production, with the subsequent activation of PKA and downstream phosphorylation of various intracellular targets, thus altering cellular functioning. For example, the D1-PKA pathway has been shown to increase the surface expression of both AMPA and NMDA glutamate receptors, although the underlying mechanism is not clear. Moreover, PKA phosphorylation promotes the opening of L-type calcium channels and the subsequent calcium entry. As a result, D1 and D2 receptors show functional antagonism, with D1 signaling enhancing dendritic excitability and glutamatergic signaling, while D2 signaling would have the opposite effect in striatal neurons. The balance between the two types of receptors allows for the modulation of the cortical and thalamic glutamatergic signals impinging upon the striatal neural population, and forms the basis of voluntary motor control (483, 484). Consequently, increased D1 and decreased D2 surface levels in the presence of pathogenic LRRK2 may result in enhanced excitability and calcium entry associated with excitatory glutamatergic input, and may lead to excitotoxicity.

Collectively, these data suggest that the endocytic alterations caused by pathogenic LRRK2 would alter neurotransmitter receptor trafficking, with downstream consequences for neurotransmission and proper neuronal functioning.

Endocytic alterations could also directly interfere with lysosomal composition and functionality. After ER synthesis, lysosomal membrane proteins usually follow the secretory route to the PM prior to being re-internalized by endocytosis (485). Altered trafficking of

these proteins to lysosomes would result in alterations in lysosomal function and positioning, with the subsequent decrease in their degradative capacity, apart from defects in the specific pathways in which these proteins are implicated, such as CMA in the case of LAMP2A or the transport of β-glucocerebrosidase to lysosomes in the case of LIMP1. Interestingly, as noted in the introduction, the genes coding for LAMP3 and LIMP1 have been identified as risk factors for PD.

In addition, due to the low rate of adult neurogenesis, neurons are particularly dependent on proper degradative trafficking to maintain their homeostasis and functionality through their extended lifetime. Altered lysosomal functioning will interfere with α-syn degradation, exacerbating its accumulation and toxicity (486). Indeed, PD-associated mutations related to lysosomal biology have been shown to increase α-syn toxicity. For example, the loss of ATP13A2 impairs lysosomal function leading to α-syn accumulation (487), and heterozygous mutations in GBA were shown to decrease α-syn degradation and promote neurotoxicity (488). Pathogenic LRRK2 overexpression was also demonstrated to cause α-syn accumulation in different models (489), even though the exact mechanism(s) remain unknown. Interestingly, increased intracellular levels of α-syn promote its release via exocytosis, and extracellular α-syn can subsequently be endocytosed by neighboring neurons (486), thus spreading the pathology. In this context, the endocytic deficits caused by pathogenic LRRK2 would preclude efficient α-syn targeting to lysosomes, further contributing to neurodegeneration in PD.

It is also important to note that a role for glial dysfunction in PD pathogenesis has emerged, and endomembrane trafficking alterations caused by pathogenic LRRK2 in these cells may also contribute to neurodegeneration. Several studies showed that toxic α-syn species released by stressed neurons can be efficiently internalized by astrocytes and trafficked to lysosomes for degradation (490–492). However, continuous α-syn uptake would be detrimental due to the overwhelming of the endolysosomal machinery in astrocytes, already compromised under pathological conditions, leading to the accumulation of non-digested α-syn aggregates in these cells (490, 492). Further supporting the crucial role of astrocytes in α-syn clearance and neuroprotection, a recent study reported that iPSC-derived astrocytes from G2019S LRRK2 PD patients promoted the appearance of PD-related

phenotypes, including abnormal α-syn accumulation, in control iPSC-derived DA neurons co-cultured with them. Conversely, control astrocytes partially prevented the appearance of disease-related phenotypes in DA neurons carrying the G2019S mutation in co-culture (493). These data indicate that astrocytes may play both an active role in promoting neuronal α-syn-related neuronal degeneration, as well as a neuroprotective role. It will be interesting to determine whether the observed LRRK2-mediated events in astrocytes correlate with changes in RAB8 phosphorylation and impaired RAB7A activity, and whether they are mimicked by knockdown of RAB8A. In addition, it would be interesting to establish EGFR degradation assays in astrocytes (494) derived from control and G2019S KI mice to corroborate the trafficking deficits we observed also in this cellular model system.

RAB protein phosphorylation and PD

Several lines of evidence point towards an important role for RAB8A in PD. For example, the phosphorylation status of RAB8A is not only modulated by LRRK2, but also by the PD-related kinase PINK1 (253). Overexpression of RAB8A rescues α-syn-induced neuronal toxicity (244), and depletion of TMEM230, another PD-linked gene product, causes a decrease in RAB8A levels associated with deficits in retromer-mediated trafficking and Golgi-derived vesicle secretion (495). Thus, all currently available data indicate that reduced RAB8A protein levels and/or altered RAB8A phosphorylation/activation correlate with various cellular alterations related to PD pathogenesis.

Our study demonstrates for the first time a novel role for a pathogenic LRRK2-mediated inactivation of RAB8A which impairs endolysosomal trafficking and correlates with a decrease in RAB7A activity. Given the central role of RAB7A in several membrane trafficking pathways, including endosomal maturation, autophagosomal maturation, mitophagy, retromer recruitment and lysosome biogenesis (144), a decrease in its activity would be expected to impinge on the proper functioning of these pathways.

Importantly, RAB8A phosphorylation has also been related to other phenotypes caused by pathogenic LRRK2, including lipid storage (251), centrosomal deficits (417) and ciliogenesis (419), suggesting that it may play a central role in LRRK2-mediated PD.

Given the central role of LRRK2 in altering autophagy, it will be important to determine whether the autophagic alterations observed in both cellular and animal models of LRRK2 PD are also mediated, at least in part, by RAB8A. Various studies suggest a link between RAB8A and autophagy. For example, its effector optineurin is a selective autophagy adaptor which binds polyubiquitinated cargoes to autophagosomes (496). Moreover, reduced expression of C9ORF72, a GEF for RAB8A, leads to autophagy dysfunction in neuronal cultures (497). In addition, RAB8B, and to a lesser extent RAB8A, were shown to have a role in the maturation of *Mycobacterium*-containing autophagosomes (498). Finally, inhibiting or depleting OCRL1, another RAB8A effector, leads to the accumulation of lysosomal PI(4,5)P2 and subsequent inhibition of the lysosomal calcium channel mucolipin-1, involved in autophagosome-lysosome fusion, thus promoting autophagosome accumulation (499). RAB8A knockdown experiments could be performed to analyze whether silencing RAB8A reproduces the effect of pathogenic LRRK2 in terms of autophagy. Given the role of RAB7A in autophagy, a concomitant reduction in RAB7A activity may contribute to the phenotypes, which therefore may be rescued upon active RAB7A overexpression.

In addition, a role for RAB8A in cytokine release (500) and vesicular trafficking to the immune synapse has been reported. TLR activation in macrophages promotes the formation of specific membrane signaling domains, to which RAB8A is recruited by a currently unknown mechanism. There, it interacts with its effector PI3Kγ and promotes AKT-dependent signaling to limit the production of proinflammatory cytokines, thus suppressing the inflammatory response. Indeed, an inhibitor of PI3Kγ resulted in enhanced expression of proinflammatory cytokines in response to lipopolysaccharide (500, 501). Importantly, increased release of pro-inflammatory cytokines from monocytes and T cells from PD patients carrying pathogenic LRRK2 has been reported (412), and it would be of interest to evaluate whether RAB8A loss-of-function contributes to this phenotype both in peripheral and central immune system cells. Additionally, alterations in secretory or recycling pathways due to RAB8A knockdown could further impair the immune responses. For instance, RAB8A regulates the delivery of recycling T-cell receptors to the immune synapse, with dominant-negative RAB8A impairing this process (502), and it is likely that the delivery of

other receptors or cytokines to the PM is also altered as a result of the trafficking deficits caused by LRRK2-mediated phosphorylation of RAB8A.

RAB8A was previously shown to directly interact with α-syn, causing a decrease in its toxicity and ameliorating neuron loss in *Drosophila* (503). It remains possible that LRRK2-mediated phosphorylation of RAB8A could contribute to the accumulation of toxic species of α-syn due to an altered localization/ability of the phosphorylated form of RAB8A to interact with α-syn, apart from its role to impair degradative trafficking. It would be interesting to test for a differential interaction of α-syn with phosphorylated versus non-phosphorylated RAB8A, or to determine the effects of a possible additional deficit in EGFR degradation in the presence of both α-syn and pathogenic LRRK2. In this context, it is interesting to note that LRRK2 was suggested to promote α-syn propagation by phosphorylating RAB35 (504). Immunocytochemical analysis of the neocortex of mice treated with a LRRK2 kinase inhibitor revealed decreased colocalization between α-syn and RAB35 as compared to vehicle-treated mice. Moreover, increased colocalization of α-syn with the lysosomal marker cathepsin D was observed in the inhibitor-treated cells, indicating that LRRK2-mediated phosphorylation of RAB35 may prevent its interaction with α-syn, thus facilitating the lysosomal clearance of α-syn (504). However, direct evidence of RAB35 phosphorylation is missing in this study, and it will be important to show differential interactions between α-syn and dephosphorylated versus phosphorylated RAB35 using phosphorylated protein, rather than merely phosphomimetic mutants.

The involvement of other LRRK2 substrates in the endocytic trafficking alterations observed in this study remains to be determined as well. For example, RAB10 participates in some of the pathways in which RAB8A plays a role, including exocytic trafficking, recycling and ciliogenesis (505). While they have a similar function in exocytosis and recycling, it was recently shown that they play opposing roles in ciliogenesis, with RAB8 promoting and RAB10 inhibiting normal cilia formation. Pathogenic LRRK2 was shown to inhibit ciliogenesis via RAB10 phosphorylation in a toxic gain-of-function fashion, favoring the binding of phospho-RAB10 to RILPL1 (419). Therefore, it will be interesting to determine the effect of RAB10 knockdown on the endocytic trafficking of the EGFR, as similar

alterations may be expected given the redundant roles of these GTPases in endocytic and secretory trafficking.

Finally, we have tested the effect of another RAB protein, RAB7L1, on the trafficking pathway of the EGFR. Our preliminary data indicate that RAB7L1 knockdown mimics the deficits caused by pathogenic LRRK2, while RAB7L1 overexpression rescues the pathogenic LRRK2-mediated alterations in EGFR trafficking. These data are consistent with previous studies indicating that RAB7L1 overexpression rescues the pathogenic LRRK2-induced shortening of neurite length (100), but contradict other studies indicating that RAB7L1 promotes Golgi recruitment and activation of LRRK2, and increases LRRK2-mediated phosphorylation of RAB8A and RAB10 (249, 304). However, our preliminary data suggest that RAB7L1 expression also rescues the LRRK2-mediated deficits of EGFR trafficking in the presence of brefeldin A, which indicates that this phenotype is independent of the Golgi-related functions of RAB7L1. Importantly, a recent study showed that RAB7L1 can recruit LRRK2 and its substrate Rabs to stressed lysosomes, where they play a positive role by promoting lysosomal homeostasis (305), and it remains possible that a similar mechanism could be responsible for the observed effect of RAB7L1 on endocytic EGFR trafficking. In this regard, it will be interesting to analyze RAB7L1 localization either in the presence or absence of pathogenic LRRK2 under the exact conditions of our EGFR assays once antibodies suitable for immunocytochemistry of endogenous RAB7L1 become available. In addition, it will be important to determine whether RAB7L1 activates LRRK2 kinase activity in our assay system, by determining alterations in the phosphorylation status of RAB8 and RAB10 via Western blotting techniques.

Some Rabs may function in a tissue-specific manner. For example, RAB8A is critical for GLUT4 exocytosis in muscle cells (460), whilst this function appears to be mostly dependent on RAB10 in adipocytes (506). It is important to note that the studies identifying a series of Rab GTPases as LRRK2 kinase substrates were performed in MEFs (83), and it will be crucial to determine which Rabs are enriched in PD-relevant tissue, and which of them are subject to LRRK2 phosphorylation in the different tissues.

Interestingly, several lines of evidence suggest that Rab protein phosphorylation by LRRK2 may also be relevant for other familial forms of PD, as well as for the most common

sporadic form of the disease. For instance, the PD-associated D620N mutation in VPS35 enhances RAB8A, RAB10 and RAB12 phosphorylation in mice, as well as RAB10 phosphorylation in neutrophils and monocytes from PD patients carrying this mutation (431). Moreover, increased LRRK2-mediated phosphorylation of RAB10 has been observed in brain tissue from patients with idiopathic PD, as well as in two toxin-induced rat models of the disease (507). Assessing RAB10 phosphorylation in human neutrophils was suggested to serve as biomarker for on-target kinase inhibition (350), even though RAB10 phosphorylation levels were found to be similar in controls and PD patients (350, 351), suggesting that this readout cannot serve as biomarker for patient stratification purposes based on abnormal LRRK2 kinase activity.

Finally, the fact that pathogenic LRRK2 impairs the activity of Rabs opens the door to alternative therapeutic approaches which may complement and/or replace LRRK2 kinase inhibitors. For example, RAB8A and/or RAB7A activation, by modulating the effects of their GAPs or GEFs, may serve as attractive therapeutic drug strategies for LRRK2-related PD. Furthermore, if the involvement of Rab proteins in sporadic PD is confirmed, compounds targeting their activity could also be used to treat the most common sporadic form of the disease.

VIII. CONCLUSIONS/CONCLUSIONES

1. RAB7A is not a kinase substrate for LRRK2 *in vitro*, indicating that the reported LRRK2-mediated decrease in RAB7A activity and concomitant alterations in endomembrane trafficking are not due to direct LRRK2-mediated RAB7A phosphorylation.

2. Expression of active or phosphodeficient, but not phosphomimetic RAB8A, rescues the mutant LRRK2-mediated effects on endolysosomal membrane trafficking.

3. The endolysosomal trafficking deficits caused by pathogenic LRRK2 are rescued upon upregulation of the RAB11-Rabin8 cascade which activates RAB8A.

4. Knockdown of RAB8A mimicks the effects of pathogenic LRRK2 expression on endolysosomal trafficking, and can be rescued by overexpression of an active form of RAB7A.

5. Knockdown of RAB8A causes a decrease in RAB7A activity as assessed by an effector pulldown assay or immunoprecipitation using a conformation-specific antibody.

6. Mutant LRRK2 or knockdown of RAB8A cause accumulation of internalized material in a RAB4-positive early recycling compartment preventing its efficient degradation.

7. Pathogenic LRRK2 or knockdown of RAB8A lead to a deficit in endocytic recycling.

8. The accumulation of internalized material in a RAB4-positive compartment, as well as the recycling defects upon pathogenic LRRK2 expression or knockdown of RAB8A are rescued upon expression of active RAB7A.

9. Expression of dominant-negative RAB7A interferes with endolysosomal degradation and recycling and causes accumulation of internalized material in a RAB4-positive compartment which is rescued upon expression of active RAB8A, thus phenocopying the effects of mutant LRRK2 expression or knockdown of RAB8A.

1. RAB7A no es sustrato de la actividad quinasa de LRRK2 *in vitro*, lo cual indica que la disminución de la actividad de RAB7A provocada por LRRK2 patogénica y las alteraciones resultantes en el tráfico intracelular de membranas no son causadas por fosforilación directa de RAB7A por LRRK2.

2. La expresión de RAB8A catalíticamente activo o fosfodeficiente, pero no fosfomimético, rescata los efectos de LRRK2 mutante en el tráfico intracelular de membranas.

3. La cascada de activación de RAB8A, conformada por RAB11 y Rabin8, revierte las alteraciones en el tráfico vesicular provocadas por LRRK2 patogénica.

4. El silenciamiento de RAB8A altera el tráfico intracelular de membranas de manera similar a LRRK2 patogénica, pudiendo dichas alteraciones ser rescatadas por la sobreexpresión de la forma activa de RAB7A.

5. El silenciamiento de RAB8A disminuye la actividad de RAB7A, determinada tanto por ensayos de *pull-down* empleando un efector de RAB7A como por inmunoprecipitación con un anticuerpo específico de la conformación activa.

6. Tanto LRRK2 patogénica como el silenciamiento de RAB8A causan la acumulación del material endocitado en un compartimento vesicular positivo para RAB4, evitando una eficiente degradación lisosomal del mismo.

7. LRRK2 mutante o el silenciamiento de RAB8A provocan defectos en el reciclaje endocítico.

8. La acumulación de material internalizado en un compartimento positivo para RAB4, así como las alteraciones en el reciclaje endocítico provocadas por la expresión de LRRK2 patogénica o por el silenciamiento de RAB8A son rescatadas por una forma catalíticamente activa de RAB7A.

9. La expresión de un mutante dominante negativo de RAB7A interfiere con las rutas vesiculares degradativa y de reciclaje y resulta en la acumulación del material internalizado en un compartimento positivo para RAB4, siendo estos efectos rescatados por la expresión de una forma activa de RAB8A. De esta manera, RAB7A dominante

negativo fenocopia las alteraciones provocadas por LRRK2 mutante o por el silenciamiento de RAB8A sobre el tráfico intracelular de membranas.

IX. REFERENCES

1. Obeso,J.A., Stamelou,M., Goetz,C.G., Poewe,W., Lang,A.E., Weintraub,D., Burn,D., Halliday,G.M., Bezard,E., Przedborski,S., *et al.* (2017) Past, present, and future of Parkinson's disease: A special essay on the 200th Anniversary of the Shaking Palsy. *Mov. Disord.*, **32**, 1264–1310.

2. Reeve,A., Simcox,E. and Turnbull,D. (2014) Ageing and Parkinson's disease: Why is advancing age the biggest risk factor? *Ageing Res. Rev.*, **14**, 19–30.

3. Dorsey,E., Constantinescu,R., Thompson,J., Biglan,K., Holloway,R. and Kieburtz,K. (2007) Projected number of people with Parkinson disease in the most poplous natios, 2005 through 2030. *Neurology*, **68**, 384–386.

4. Dauer,W. and Przedborski,S. (2003) Parkinson's disease: Mechanisms and models. *Neuron*, **39**, 889–909.

5. Wakabayashi,K., Tanji,K., Odagiri,S., Miki,Y., Mori,F. and Takahashi,H. (2013) The Lewy body in Parkinson's disease and related neurodegenerative disorders. *Mol. Neurobiol.*, **47**, 495–508.

6. Wakabayashi,K., Tanji,K., Mori,F. and Takahashi,H. (2007) The Lewy body in Parkinson's disease: Molecules implicated in the formation and degradation of α-synuclein aggregates. *Neuropathology*, **27**, 494–506.

7. Jankovic,J. (2008) Parkinson's disease: Clinical features and diagnosis. *J. Neurol. Neurosurg. Psychiatry*, **79**, 368–376.

8. Cheng,H.C., Ulane,C.. and Burke,R.. (2010) Clinical progression in Parkinson's disease and the neurobiology of Axons. *Ann. Neurol.*, **67**, 715–725.

9. Giguère,N., Burke Nanni,S. and Trudeau,L.-E. (2018) On Cell Loss and Selective Vulnerability of Neuronal Populations in Parkinson's Disease. *Front. Neurol.*, **9**, 455.

10. Barone,P. (2010) Neurotransmission in Parkinson's disease: Beyond dopamine. *Eur. J. Neurol.*, **17**, 364–376.

11. Kalia,L. V. and Lang,A.E. (2015) Parkinson's disease. *Lancet*, **386**, 896–912.

12. Surmeier,D.J., Obeso,J.A. and Halliday,G.M. (2017) Selective neuronal vulnerability in Parkinson disease. *Nat. Rev. Neurosci.*, **18**, 101–113.

13. Dawson,T.M. (2008) Non-autonomous cell death in Parkinson's disease. *Lancet Neurol.*, **7**, 474–475.

14. Connolly,B.S. and Lang,A.E. (2014) Pharmacological treatment of Parkinson disease: A review. *JAMA - J. Am. Med. Assoc.*, **311**, 1670–1683.

15. Charles,D., Konrad,P.E., Ph,D., Neimat,J.S., Molinari,L., Tramontana,M.G., Ph,D., Finder,S.G., Ph,D., Gill,C.E., *et al.* (2015) NIH Public Access. **20**, 731–737.

16. Smith,Y., Wichmann,T., Factor,S.A. and Delong,M.R. (2012) Parkinson's disease therapeutics: New developments and challenges since the introduction of levodopa. *Neuropsychopharmacology*, **37**, 213–246.

17. Langston,J., Ballard,P., Tetrud,J. and Irwin,I. (1983) Chronic Parkinsonism in humans due to a product of meperidine-analog synthesis. *Science (80-.).*, **219**, 979–980.

18. Langston,J.W., Forno,L.S., Rebert,C.S. and Irwin,I. (1984) Selective nigral toxicity after systemic administration of 1-methyl-4-phenyl 1-1,2,3,6, tetrahydropyridine (MPTP) in the squirrel monkey. *Brain Res.*, **292**, 390–394.

19. Betarbet,R. and MacKenzie,G. (2000) Chronic systems pesticide exposure reproduces features of parkinson. *Nat. Neurosci.*, **3**, 1301–1306.

20. Polymeropoulos,M.H., Lavedan,C., Leroy,E., Ide,S.E., Dehejia,A., Dutra,A., Pike,B., Root,H., Rubenstein,J., Boyer,R., *et al.* (1997) Mutation in the α-synuclein gene identified in families with Parkinson's disease. *Science*, **276**, 2045–2047.

21. Spillantini,M.G., Schmidt,M.L., Lee,V.M.-Y., Trojanowski,J.Q., Jakes,R. and Goedert,M. (1997) alpha-Synuclein in Lewy bodies. *Nature*, **388**, 839–840.

22. Chartier-Harlin,M.C., Dachsel,J.C., Vilariño-Güell,C., Lincoln,S.J., Leprêtre,F., Hulihan,M.M., Kachergus,J., Milnerwood,A.J., Tapia,L., Song,M.S., *et al.* (2011) Translation initiator EIF4G1 mutations in familial parkinson disease. *Am. J. Hum.*

Genet., **89**, 398–406.

23. Leroy,E., Boyer,R., Auburger,G., Leube,B., Ulm,G., Mezey,E., Harta,G., Brownstein,M.J., Jonnalagada,S., Chernova,T., *et al.* (1998) The ubiquitin pathway in Parkinson's disease. *Nature*, **395**, 451–452.

24. Lautier,C., Goldwurm,S., Dürr,A., Giovannone,B., Tsiaras,W.G., Pezzoli,G., Brice,A. and Smith,R.J. (2008) Mutations in the GIGYF2 (TNRC15) Gene at the PARK11 Locus in Familial Parkinson Disease. *Am. J. Hum. Genet.*, **82**, 822–833.

25. Smith,L., Mullin,S. and Schapira,A.H.V. (2017) Insights into the structural biology of Gaucher disease. *Exp. Neurol.*, **298**, 180–190.

26. Sidransky,E., Nalls,M.A., Ph,D., Aasly,J.O., Annesi,G., Barbosa,E.R., Bar-shira,A., Berg,D., Bras,J., Brice,A., *et al.* (2010) Multi-center analysis of glucocerebrosidase mutations in Parkinson disease. *N Engl J Med.*, **361**, 1651–1661.

27. Simón-Sánchez,J., Schulte,C., Bras,J.J.M., Sharma,M., Gibbs,J.R., Berg,D., Paisan-Ruiz,C., Lichtner,P., Scholz,S.W., Hernandez,D.G., *et al.* (2009) Genome-wide association study reveals genetic risk underlying Parkinson's disease. *Genet.*, **41**, 1308–1312.

28. Wang,Y. and Mandelkow,E. (2016) Tau in physiology and pathology. *Nat. Rev. Neurosci.*, **17**, 5–21.

29. Golub,Y., Berg,D., Calne,D.B., Pfeiffer,R.F., Uitti,R.J., Stoessl,A.J., Wszolek,Z.K., Farrer,M.J., Mueller,J.C., Gasser,T., *et al.* (2009) Genetic factors influencing age at onset in LRRK2-linked Parkinson disease. *Park. Relat. Disord.*, **15**, 539–541.

30. Jakes,R., Spillantini,M.G. and Goedert,M. (1994) Identification of two distinct synucleins from human brain. *FEBS Lett.*, **345**, 27–32.

31. Burré,J., Sharma,M., Tsetsenis,T., Buchman,V., Etherton,M.R. and Südhof,T.C. (2010) Alpha-synuclein promotes SNARE-complex assembly in vivo and in vitro. *Science*, **329**, 1663–7.

32. Conway,K.A., Lee,S.-J., Rochet,J.-C., Ding,T.T., Williamson,R.E. and Lansbury,P.T. (2000) Acceleration of oligomerization, not fibrillization, is a shared property of both α-synuclein mutations linked to early-onset Parkinson's disease: Implications for pathogenesis and therapy. *Proc. Natl. Acad. Sci.*, **97**, 571-576.

33. Tokuda,T., Qureshi,M.M., Ardah,M.T., Varghese,S., Shehab,S.A.S., Kasai,T., Ishigami,N., Tamaoka,A., Nakagawa,M. and El-Agnaf,O.M.A. (2010) Detection of elevated levels of α-synuclein oligomers in CSF from patients with Parkinson disease. *Neurology*, **75**, 1766-1770.

34. Park,M.J., Cheon,S.-M., Bae,H.-R., Kim,S.-H. and Kim,J.W. (2011) Elevated levels of α-synuclein oligomer in the cerebrospinal fluid of drug-naïve patients with Parkinson's disease. *J. Clin. Neurol.*, **7**, 215–222.

35. Ingelsson,M. (2016) Alpha-synuclein oligomers-neurotoxic molecules in Parkinson's disease and other Lewy body disorders. *Front. Neurosci.*, **10**, 408.

36. Gosavi,N., Lee,H., Lee,J.S., Patel,S. and Lee,S. (2002) Golgi fragmentation occurs in the cells with prefibrillar alpha-synuclein aggregates and precedes the formation of fibrillar inclusion J. Biol. Chem, **277**, 48984–48992.

37. Bridi,J.C. and Hirth,F. (2018) Mechanisms of α-Synuclein Induced Synaptopathy in Parkinson's Disease. *Front. Neurosci.*, **12**, 80.

38. Kordower,J.H., Chu,Y., Hauser,R.A., Freeman,T.B. and Olanow,C.W. (2008) Lewy body-like pathology in long-term embryonic nigral transplants in Parkinson's disease. *Nat. Med.*, **14**, 504–506.

39. Li,J.Y., Englund,E., Holton,J.L., Soulet,D., Hagell,P., Lees,A.J., Lashley,T., Quinn,N.P., Rehncrona,S., Björklund,A., *et al.* (2008) Lewy bodies in grafted neurons in subjects with Parkinson's disease suggest host-to-graft disease propagation. *Nat. Med.*, **14**, 501–503.

40. Danzer,K.M., Kranich,L.R., Ruf,W.P., Cagsal-Getkin,O., Winslow,A.R., Zhu,L., Vanderburg,C.R. and McLean,P.J. (2012) Exosomal cell-to-cell transmission of alpha

synuclein oligomers. *Mol. Neurodegener.*, **7**, 42.

41. Danzer,K.M., Krebs,S.K., Wolff,M., Birk,G. and Hengerer,B. (2009) Seeding induced by α-synuclein oligomers provides evidence for spreading of α-synuclein pathology. *J. Neurochem.*, **111**, 192–203.

42. Rocha,E.M., De Miranda,B. and Sanders,L.H. (2018) Alpha-synuclein: Pathology, mitochondrial dysfunction and neuroinflammation in Parkinson's disease. *Neurobiol. Dis.*, **109**, 249–257.

43. Braak,H., Tredici,K. Del, Rüb,U., de Vos,R.A.I., Jansen Steur,E.N.H. and Braak,E. (2003) Staging of brain pathology related to sporadic Parkinson's disease. *Neurobiol. Aging*, **24**, 197–211.

44. Rietdijk,C.D., Perez-Pardo,P., Garssen,J., van Wezel,R.J.A. and Kraneveld,A.D. (2017) Exploring Braak's hypothesis of parkinson's disease. *Front. Neurol.*, **8**.

45. Chandra,R., Hiniker,A., Kuo,Y.-M., Nussbaum,R.L. and Liddle,R.A. (2017) α-Synuclein in gut endocrine cells and its implications for Parkinson's disease. *JCI Insight*, **2**, 1–13.

46. Puspita,L., Chung,S.Y. and Shim,J.-W. (2017) Oxidative stress and cellular pathologies in Parkinson's disease. *Mol. Brain*, **10**, 53.

47. Schapira, a H., Cooper,J.M., Dexter,D., Jenner,P., Clark,J.B. and Marsden,C.D. (1989) Mitochondrial complex I deficiency in Parkinson's disease. *Lancet*, **1**, 1269.

48. Schapira,A.H. V., Cooper,J.M., Dexter,D., Clark,J.B., Jenner,P. and Marsden,C.D. (1990) Mitochondrial Complex I Deficiency in Parkinson's Disease. *J. Neurochem.*, **54**, 823–827.

49. Hattingen,E., Magerkurth,J., Pilatus,U., Mozer,A., Seifried,C., Steinmetz,H., Zanella,F. and Hilker,R. (2009) Phosphorus and proton magnetic resonance spectroscopy demonstrates mitochondrial dysfunction in early and advanced Parkinson's disease. *Brain*, **132**, 3285–3297.

50. Smeyne,R.J. and Jackson-Lewis,V. (2005) The MPTP model of Parkinson's disease.

Mol. Brain Res., **134**, 57–66.

51. Pickrell,A.M. and Youle,R.J. (2015) The roles of PINK1, Parkin, and mitochondrial fidelity in parkinson's disease. *Neuron*, **85**, 257–273.

52. Schapira,A.H. V (2007) Mitochondrial dysfunction in Parkinson's disease. *Cell Death Differ.*, **14**, 1261–1266.

53. Quinlan,C.L., Perevoshchikova,I. V, Hey-Mogensen,M., Orr,A.L. and Brand,M.D. (2013) Sites of reactive oxygen species generation by mitochondria oxidizing different substrates. *Redox Biol.*, **1**, 304–312.

54. Bosco,D.A., Fowler,D.M., Zhang,Q., Nieva,J., Powers,E.T., Wentworth Jr,P., Lerner,R.A. and Kelly,J.W. (2006) Elevated levels of oxidized cholesterol metabolites in Lewy body disease brains accelerate α-synuclein fibrilization. *Nat. Chem. Biol.*, **2**, 249.

55. Nakabeppu,Y., Tsuchimoto,D., Yamaguchi,H. and Sakumi,K. (2007) Oxidative damage in nucleic acids and Parkinson's disease. *J. Neurosci. Res.*, **85**, 919–934.

56. Lotharius,J. and Brundin,P. (2002) Pathogenesis of parkinson's disease: Dopamine, vesicles and α-synuclein. *Nat. Rev. Neurosci.*, **3**, 932–942.

57. Guo,J.T., Chen,A.Q., Kong,Q., Zhu,H., Ma,C.M. and Qin,C. (2008) Inhibition of Vesicular Monoamine Transporter-2 Activity in a-Synuclein Stably Transfected SH-SY5Y Cells. *Cell Mol Neurobiol*, **28**, 35–47.

58. Ambrosi,G., Cerri,S. and Blandini,F. (2014) A further update on the role of excitotoxicity in the pathogenesis of Parkinson ' s disease. *J Neural Transm*, **121**, 849.

59. Gao,H., Zhu,H., Song,C., Lin,L., Xiang,Y., Yan,Z.-H., Bai,G.-H., Ye,F.-Q. and Li,X.-K. (2013) Metabolic Changes Detected by Ex Vivo High Resolution H NMR Spectroscopy in the Striatum of 6-OHDA-Induced Parkinson ' s Rat. *Mol Neurobiol*, **47**, 123–130.

60. di Michele,F., Luchetti,S., Bernardi,G., Romeo,E. and Longone,P. (2013) Neurosteroid and neurotransmitter alterations in Parkinson's disease. *Front. Neuroendocrinol.*, **34**,

132–142.

61. Rodriguez,M.C., Obeso,J.A. and Olanow,C.W. (1998) Subthalamic nucleus-mediated excitotoxicity in Parkinson's disease: a target for neuroprotection. *Ann. Neurol.*, **44**, S175-88.

62. Mark,L.P., Prost,R.W., Ulmer,J.L., Smith,M.M., Daniels,D.L., Strottmann,J.M., Brown,W.D. and Hacein-Bey,L. (2001) Pictorial review of glutamate excitotoxicity: Fundamental concepts for neuroimaging. *Am. J. Neuroradiol.*, **22**, 1813–1824.

63. Dong,X.X., Wang,Y. and Qin,Z.H. (2009) Molecular mechanisms of excitotoxicity and their relevance to pathogenesis of neurodegenerative diseases. *Acta Pharmacol. Sin.*, **30**, 379–387.

64. Meredith,G.E. and Rademacher,D.J. (2012) MPTP Mouse Models of Parkinson ' s Disease: An Update. *J Park. Dis*, **1**, 19–33.

65. Amor,S., Puentes,F., Baker,D. and Van Der Valk,P. (2010) Inflammation in neurodegenerative diseases. *Immunology*, **129**, 154–169.

66. Doorn,K.J., Moors,T., Drukarch,B., van de Berg,W.D.J., Lucassen,P.J. and van Dam,A.M. (2014) Microglial phenotypes and toll-like receptor 2 in the substantia nigra and hippocampus of incidental Lewy body disease cases and Parkinson's disease patients. *Acta Neuropathol. Commun.*, **2**, 1–17.

67. Schapansky,J., Nardozzi,J. and LaVoie,M. (2015) The complex relationships between microglia, alpha-synuclein, and LRRK2 in Parkinson's disease. **302**, 74–88.

68. Sulzer,D., Alcalay,R.N., Garretti,F., Cote,L., Kanter,E., Agin-Liebes,J., Liong,C., McMurtrey,C., Hildebrand,W.H., Mao,X., *et al.* (2017) T cells from patients with Parkinson's disease recognize α-synuclein peptides. *Nature*, **546**, 656–661.

69. Hakimi,M., Selvanantham,T., Swinton,E., Padmore,R.F., Tong,Y., Kabbach,G., Venderova,K., Girardin,S.E., Dennis,E., Scherzer,C.R., *et al.* (2011) Parkinson's disease-linked LRRK2 is expressed in circulating and tissue immune cells and upregulated following recognition of microbial structures. **118**, 795–808.

70. Chu,K., Zhou,X. and Luo,B.Y. (2012) Cytokine gene polymorphisms and Parkinson's disease: a metaanalysis. *Can. J. Neurol. Sci.*, **39**, 58–64.

71. Hamza,T.H., Zabetian,C.P., Tenesa,A., Laederach,A., Montimurro,J., Yearout,D., Kay,D.M., Doheny,K.F., Paschall,J., Pugh,E., *et al.* (2010) Common genetic variation in the HLA region is associated with late-onset sporadic Parkinson's disease. *Nat. Genet.*, **42**, 781–785.

72. Sanchez-Guajardo,V., Febbraro,F., Kirik,D. and Romero-Ramos,M. (2010) Microglia Acquire Distinct Activation Profiles Depending on the Degree of α-Synuclein Neuropathology in a rAAV Based Model of Parkinson's Disease. *PLoS One*, **5**, e8784.

73. Barkholt,P., Sanchez-Guajardo,V., Kirik,D. and Romero-Ramos,M. (2012) Long-term polarization of microglia upon α-synuclein overexpression in nonhuman primates. *Neuroscience*, **208**, 85–96.

74. Watson,M.B., Richter,F., Lee,S.K., Gabby,L., Wu,J., Masliah,E., Effros,R.B. and Chesselet,M.-F. (2012) Regionally-specific microglial activation in young mice over-expressing human wildtype alpha-synuclein. *Exp. Neurol.*, **237**, 318–334.

75. Stokholm,M.G., Iranzo,A., Østergaard,K., Serradell,M., Otto,M., Svendsen,K.B., Garrido,A., Vilas,D., Borghammer,P., Santamaria,J., *et al.* (2017) Assessment of neuroinflammation in patients with idiopathic rapid-eye-movement sleep behaviour disorder: a case-control study. *Lancet Neurol.*, **16**, 789–796.

76. Machado,A., Herrera,A.J., Venero,J.L., Santiago,M., de Pablos,R.M., Villarán,R.F., Espinosa-Oliva,A.M., Argüelles,S., Sarmiento,M., Delgado-Cortés,M.J., *et al.* (2011) Inflammatory Animal Model for Parkinson's Disease: The Intranigral Injection of LPS Induced the Inflammatory Process along with the Selective Degeneration of Nigrostriatal Dopaminergic Neurons. *ISRN Neurol.*, **2011**, 476158.

77. Kortekaas,R., Leenders,K.L., van Oostrom,J.C.H., Vaalburg,W., Bart,J., Willemsen,A.T.M. and Hendrikse,N.H. (2005) Blood–brain barrier dysfunction in parkinsonian midbrain in vivo. *Ann. Neurol.*, **57**, 176–179.

78. Tansey,M.G. and Romero-Ramos,M. (2018) Immune system responses in Parkinson's disease: Early and dynamic. *Eur. J. Neurosci.*, **49**, 364-383.

79. Brochard,V., Combadière,B., Prigent,A., Laouar,Y., Perrin,A., Beray-Berthat,V., Bonduelle,O., Alvarez-Fischer,D., Callebert,J., Launay,J.-M., *et al.* (2009) Infiltration of CD4+ lymphocytes into the brain contributes to neurodegeneration in a mouse model of Parkinson disease. *J. Clin. Invest.*, **119**, 182–192.

80. Lira,A., Kulczycki,J., Slack,R., Anisman,H. and Park,D.S. (2011) Involvement of the Fc gamma receptor in a chronic N-methyl-4-phenyl-1,2,3,6-tetrahydropyridine mouse model of dopaminergic loss. *J. Biol. Chem.*, **286**, 28783–28793.

81. Kannarkat,G.T., Boss,J.M. and Tansey,M.G. (2013) The role of innate and adaptive immunity in Parkinson's disease. *J. Parkinsons. Dis.*, **3**, 493–514.

82. Chandra,S., Gallardo,G., Fernández-Chacón,R., Schlüter,O.M. and Südhof,T.C. (2005) α-Synuclein cooperates with CSPα in preventing neurodegeneration. *Cell*, **123**, 383–396.

83. Steger,M., Tonelli,F., Ito,G., Davies,P., Trost,M., Vetter,M., Wachter,S., Lorentzen,E., Duddy,G., Wilson,S., *et al.* (2016) Phosphoproteomics reveals that Parkinson's disease kinase LRRK2 regulates a subset of Rab GTPases. *Elife*, **5**, 1–28.

84. Mazzulli,J.R., Xu,Y., Sun,Y., Knight,A.L., Mclean,P.J., Caldwell,A., Sidransky,E., Grabowski,G.A. and Krainc,D. (2012) NIH Public Access. **146**, 37–52.

85. Do,C.B., Tung,J.Y., Dorfman,E., Kiefer,A.K., Drabant,E.M., Francke,U., Mountain,J.L., Goldman,S.M., Tanner,C.M., Langston,J.W., *et al.* (2011) Web-based genome-wide association study identifies two novel loci and a substantial genetic component for parkinson's disease. *PLoS Genet.*, **7**.

86. Tsunemi,T., Hamada,K. and Krainc,D. (2014) ATP13A2/PARK9 Regulates Secretion of Exosomes and -Synuclein. *J. Neurosci.*, **34**, 15281–15287.

87. Ramirez,A., Heimbach,A., Gründemann,J., Stiller,B., Hampshire,D., Cid,L.P., Goebel,I., Mubaidin,A.F., Wriekat,A.L., Roeper,J., *et al.* (2006) Hereditary parkinsonism with dementia is caused by mutations in ATP13A2, encoding a lysosomal type 5 P-type

ATPase. *Nat. Genet.*, **38**, 1184–1191.

88. Korvatska,O., Strand,N.S., Berndt,J.D., Strovas,T., Chen,D.H., Leverenz,J.B., Kiianitsa,K., Mata,I.F., Karakoc,E., Greenup,J.L., *et al.* (2013) Altered splicing of ATP6AP2 causes X-linked parkinsonism with spasticity (XPDS). *Hum. Mol. Genet.*, **22**, 3259–3268.

89. Lesage,S., Drouet,V., Majounie,E., Deramecourt,V., Jacoupy,M., Nicolas,A., Cormier-Dequaire,F., Hassoun,S.M., Pujol,C., Ciura,S., *et al.* (2016) Loss of VPS13C Function in Autosomal-Recessive Parkinsonism Causes Mitochondrial Dysfunction and Increases PINK1/Parkin-Dependent Mitophagy. *Am. J. Hum. Genet.*, **98**, 500–513.

90. Nalls,M.A., Pankratz,N., Lill,C.M., Do,C.B., Hernandez,D.G., Saad,M., Destefano,A.L., Kara,E., Bras,J., Sharma,M., *et al.* (2014) Large-scale meta-analysis of genome-wide association data identifies six new risk loci for Parkinson's disease. *Nat. Genet.*, **46**, 989–993.

91. Zavodszky,E., Seaman,M.N.J., Moreau,K., Jimenez-Sanchez,M., Breusegem,S.Y., Harbour,M.E. and Rubinsztein,D.C. (2014) Mutation in VPS35 associated with Parkinson's disease impairs WASH complex association and inhibits autophagy. *Nat. Commun.*, **5**, 1–16.

92. Vilariño-Güell,C., Rajput,A., Milnerwood,A.J., Shah,B., Szu-Tu,C., Trinh,J., Yu,I., Encarnacion,M., Munsie,L.N., Tapia,L., *et al.* (2014) DNAJC13 mutations in Parkinson disease. *Hum. Mol. Genet.*, **23**, 1794–1801.

93. Edvardson,S., Cinnamon,Y., Ta-Shma,A., Shaag,A., Yim,Y.I., Zenvirt,S., Jalas,C., Lesage,S., Brice,A., Taraboulos,A., *et al.* (2012) A deleterious mutation in DNAJC6 encoding the neuronal-specific clathrin-uncoating Co-chaperone auxilin, is associated with juvenile parkinsonism. *PLoS One*, **7**, 4–8.

94. Quadri,M., Fang,M., Picillo,M., Olgiati,S., Guido,J., Graafland,J., Wu,B., Xu,F., Erro,R., Amboni,M., *et al.* (2013) Mutation in the SYNJ1 gene associated with autosomal recessive, early-onset Parkinsonism. *Human Mutation*, **34**, 1208-1315.

95. Krebs,C.E., Karkheiran,S., Powell,J.C., Cao,M., Makarov,V., Darvish,H., Di Paolo,G., Walker,R.H., Shahidi,G.A., Buxbaum,J.D., *et al.* (2013) The sac1 domain of SYNJ1 identified mutated in a family with early-onset progressive parkinsonism with generalized seizures. *Hum. Mutat.*, **34**, 1200–1207.

96. Wilson,G.R., Sim,J.C.H., McLean,C., Giannandrea,M., Galea,C.A., Riseley,J.R., Stephenson,S.E.M., Fitzpatrick,E., Haas,S.A., Pope,K., *et al.* (2014) Mutations in RAB39B cause X-linked intellectual disability and early-onset parkinson disease with α-synuclein pathology. *Am. J. Hum. Genet.*, **95**, 729–735.

97. Deng,H., Shi,Y., Yang,Y., Ahmeti,K.B., Miller,N., Huang,C., Cheng,L., Zhai,H., Deng,S., Nuytemans,K., *et al.* (2018) *Nat. Genet*. **48**, 733–739.

98. Satake,W., Nakabayashi,Y., Mizuta,I., Hirota,Y., Ito,C., Kubo,M., Kawaguchi,T., Tsunoda,T., Watanabe,M., Takeda,A., *et al.* (2009) Genome-wide association study identifies common variants at four loci as genetic risk factors for Parkinson's disease. *Nat. Genet.*, **41**, 1303–1307.

99. International Parkinson Disease Genomics Consortium (2011) Imputation of sequence variants for identification of genetic risks for Parkinson's disease: a meta-analysis of genome-wide association studies. *Lancet*, **377**, 641–649.

100. MacLeod,D.A., Rhinn,H., Kuwahara,T., Zolin,A., Di Paolo,G., MacCabe,B.D., Marder,K.S., Honig,L.S., Clark,L.N., Small,S.A., *et al.* (2013) RAB7L1 Interacts with LRRK2 to Modify Intraneuronal Protein Sorting and Parkinson's Disease Risk. *Neuron*, **77**, 425–439.

101. Bandres-Ciga,S., Saez-Atienzar,S., Bonet-Ponce,L., Billingsley,K., Vitale,D., Blauwendraat,C., Gibbs,J.R., Pihlstrøm,L., Gan-Or,Z., *et al.* (2019) The endocytic membrane trafficking pathway plays a major role in the risk of Parkinson's disease. *Mov. Disord.*, **0**.

102. Youle,R.J. and Narendra,D.P. (2011) Mechanisms of mitophagy. *Nat. Rev. Mol. Cell Biol.*, **12**, 9–14.

103. Abeliovich,A. and Gitler,A.D. (2016) Defects in trafficking bridge Parkinson's disease pathology and genetics. *Nature*, **539**, 207–216.

104. Levine,B. and Klionsky,D.J. (2004) Development by self-digestion: Molecular mechanisms and biological functions of autophagy. *Dev. Cell*, **6**, 463–477.

105. Cuervo,A.M., Stafanis,L., Fredenburg,R., Lansbury,P.T. and Sulzer,D. (2004) Impaired degradation of mutant α-synuclein by chaperone-mediated autophagy. *Science*, **305**, 1292–1295.

106. Chauhan,A. and Jeans,A.F. (2015) Is parkinson's disease truly a prion-like disorder? An appraisal of current evidence. *Neurol. Res. Int.*, **2015**.

107. Enns,C. (1999) Overview of Protein Trafficking in the Secretory and Endocytic Pathways. *Curr. Protoc. Cell Biol.*, **3**, 15.1.1-15.1.10.

108. Bonifacino,J.S. and Glick,B.S. (2004) The Mechanisms of Vesicle Budding and Fusion ganelles of the pathway. Such observations inspired the vesicular transport hypothesis, which states that the transfer of cargo molecules between organelles of the. *Cell*, **116**, 153–166.

109. Ramirez,O.A. and Couve,A. (2011) The endoplasmic reticulum and protein trafficking in dendrites and axons. *Trends Cell Biol.*, **21**, 219–227.

110. Burgoyne,R.D. and Morgan,A. (2004) Exocytosis. In Meyers,R.A. (ed), *Encyclopedia of Molecular Cell Biology and Molecular Medicine*,. Wiley-VCH Verlag GmbH & Co. KGaA, Weinheim, pp. 305–327.

111. Lodish H, Berk A, Zipursky SL, et al. (2000). Molecular Cell Biology. 4th edition. New York: W. H. Freeman. Section 17.3, Overview of the Secretory Pathway.

112. Sprangers,J. and Rabouille,C. (2015) SEC16 in COPII coat dynamics at ER exit sites. *Biochem. Soc. Trans.*, **43**, 97-103.

113. Bard,F. and Malhotra,V. (2006) The Formation of TGN-to-Plasma-Membrane Transport Carriers. *Annu. Rev. Cell Dev. Biol.*, **22**, 439–455.

114. Duden,R. (2003) ER-to-Golgi transport: COP I and COP II function (Review). *Mol. Membr. Biol.*, **20**, 197–207.

115. Wu,B. and Guo,W. (2015) The Exocyst at a Glance. *J. Cell Sci.*, **128**, 2957–2964.

116. Martin-Urdiroz,M., Deeks,M.J., Horton,C.G., Dawe,H.R. and Jourdain,I. (2016) The Exocyst Complex in Health and Disease. *Front. cell Dev. Biol.*, **4**, 24.

117. Gerber,S.H. and Südhof,T.C. (2002) Molecular Determinants of Regulated Exocytosis. *Diabetes*, **51**, S3-S11.

118. Chieregatti,E. and Meldolesi,J. (2005) Regulated exocytosis: new organelles for non-secretory purposes. *Nat. Rev. Mol. Cell Biol.*, **6**, 181.

119. Blott,E.J. and Griffiths,G.M. (2002) Secretory lysosomes. *Nat. Rev. Mol. Cell Biol.*, **3**, 122.

120. Ravi,S., VanDemark,A.P. and Kiselyov,K. (2017) Regulation of Lysosomal Exocytosis by Oxidative Stress and Calcium Ions. *Biophys. J.*, **112**, 91a.

121. Miaczynska,M. and Stenmark,H. (2008) Mechanisms and functions of endocytosis. *J. Cell Biol.*, **180**, 7–11.

122. Alberts,B., Johnson,A., Lewis,J. and Al.,E. (2002) Transport into the Cell from the Plasma Membrane: Endocytosis. In *Molecular Biology of the Cell*. Garland Science, New York.

123. Doherty,G.J. and McMahon,H.T. (2009) Mechanisms of Endocytosis. *Annu. Rev. Biochem.*, **78**, 857–902.

124. Parkar,N.S., Akpa,B.S., Nitsche,L.C., Wedgewood,L.E., Place,A.T., Sverdlov,M.S., Chaga,O. and Minshall,R.D. (2009) Vesicle Formation and Endocytosis: Function, Machinery, Mechanisms, and Modeling. *Antioxid. Redox Signal.*, **11**, 1301–1312.

125. Mayor,S., Parton,R.G. and Donaldson,J.G. Clathrin-independent pathways of endocytosis. *Cold Spring Harb. Perspect. Biol.*, **6**, a016758.

126. Rosales,C. and Uribe-Querol,E. (2017) Phagocytosis: A Fundamental Process in Immunity. *Biomed Res. Int.*, **2017**, 9042851.

127. McMahon,H.T. and Boucrot,E. (2011) Molecular mechanism and physiological functions of clathrin-mediated endocytosis. *Nat. Rev. Mol. Cell Biol.*, **12**, 517–533.

128. Eisenberg,E. and Greene,L.E. (2007) Multiple Roles of Auxilin and Hsc70 in Clathrin-Mediated Endocytosis. *Traffic*, **8**, 640–646.

129. Huotari,J. and Helenius,A. (2011) Endosome maturation. *EMBO J.*, **30**, 3481–3500.

130. Klumperman,J. and Raposo,G. (2014) The complex ultrastructure of the endolysosomal system. *Cold Spring Harb. Perspect. Biol.*, **6**, 1–22.

131. Jovic,M., Sharma,M., Rahajeng,J. and Caplan,S. (2010) The early endosome: a busy sorting station for proteins at the crossroads. *Histol. Histopathol.*, **25**, 99–112.

132. Naslavsky,N. and Caplan,S. (2018) The enigmatic endosome – sorting the ins and outs of endocytic trafficking. *J. Cell Sci.*, **131**, jcs216499.

133. Taguchi,T. (2013) Emerging roles of recycling endosomes. *J. Biochem.*, **153**, 505–510.

134. Casanova,J.E. and Winckler,B. (2017) A new Rab7 effector controls phosphoinositide conversion in endosome maturation. *J. Cell Biol.*, **216**, 2995–2997.

135. Liu,K., Xing,R., Jian,Y., Gao,Z., Ma,X., Sun,X., Li,Y., Xu,M., Wang,X., Jing,Y., *et al.* (2017) WDR91 is a Rab7 effector required for neuronal development. *J. Cell Biol.*, **216**, 3307–3321.

136. Jordens,I., Fernandez-Borja,M., Marsman,M., Dusseljee,S., Janssen,L., Calafat,J., Janssen,H., Wubbolts,R. and Neefjes,J. (2001) The Rab7 effector protein RILP controls lysosomal transport by inducing the recruitment of dynein-dynactin motors. *Curr. Biol.*, **11**, 1680–1685.

137. Gruenberg,J. and Stenmark,H. (2004) The biogenesis of multivesicular endosomes. *Nat. Rev. Mol. Cell Biol.*, **5**, 317.

138. Schmidt,O. and Teis,D. (2012) The ESCRT machinery. *Curr. Biol.*, **22**, R116–R120.

139. Woodman,P.G. and Futter,C.E. (2008) Multivesicular bodies: co-ordinated progression to maturity. *Curr. Opin. Cell Biol.*, **20**, 408–414.

140. Wollert,T. and Hurley,J.H. (2010) Molecular mechanism of multivesicular body biogenesis by ESCRT complexes. *Nature*, **464**, 864–869.

141. Hanson,P.I., Roth,R., Lin,Y. and Heuser,J.E. (2008) Plasma membrane deformation by circular arrays of ESCRT-III protein filaments. *J. Cell Biol.*, **180**, 389-402.

142. Luzio,J.P., Parkinson,M.D.J., Gray,S.R. and Bright,N.A. (2009) The delivery of endocytosed cargo to lysosomes: Figure 1. *Biochem. Soc. Trans.*, **37**, 1019–1021.

143. Luzio,J.P., Pryor,P.R. and Bright,N.A. (2007) Lysosomes: fusion and function. *Nat. Rev. Mol. Cell Biol.*, **8**, 622.

144. Guerra,F. and Bucci,C. (2016) Multiple roles of the small GTPase Rab7. *Cells*, **5**.

145. Pryor,P.R., Mullock,B.M., Bright,N.A., Gray,S.R. and Luzio,J.P. (2000) The Role of Intraorganellar Ca²⁺In Late Endosome–Lysosome Heterotypic Fusion and in the Reformation of Lysosomes from Hybrid Organelles. *J. Cell Biol.*, **149**, 1053-1062.

146. Schulze,H., Kolter,T. and Sandhoff,K. (2009) Principles of lysosomal membrane degradation. Cellular topology and biochemistry of lysosomal lipid degradation. *Biochim. Biophys. Acta - Mol. Cell Res.*, **1793**, 674–683.

147. Winchester,B.G. (2001) Lysosomal membrane proteins. *Eur. J. Paediatr. Neurol.*, **5**, 11–19.

148. Schwake,M., Schröder,B. and Saftig,P. (2013) Lysosomal Membrane Proteins and Their Central Role in Physiology. *Traffic*, **14**, 739–748.

149. Gindhart,J.G. and Weber,K.P. (2009) Lysosome and Endosome Organization and Transport in Neurons. *Encycl. Neurosci.*, 10.1016/B978-008045046-9.00733-6.

150. Grant,B.D. and Donaldson,J.G. (2009) Pathways and mechanisms of endocytic recycling. *Nat Rev Mol Cell Biol.*, **10**, 597–608.

151. Sönnichsen,B., De Renzis,S., Nielsen,E., Rietdorf,J. and Zerial,M. (2000) Distinct membrane domains on endosomes in the recycling pathway visualized by multicolor imaging of Rab4, Rab5, and Rab11. *J. Cell Biol.*, **149**, 901–913.

152. M Zerial and H McBride (2001) Rab proteins as membrane organizers. *Nat. Rev. Mol. Cell Biol.*, **2**, 107–17.

153. McCaffrey,M.W., Bielli,A., Cantalupo,G., Mora,S., Roberti,V., Santillo,M., Drummond,F. and Bucci,C. (2001) Rab4 affects both recycling and degradative endosomal trafficking. *FEBS Lett.*, **495**, 21–30.

154. Xie,S., Bahl,K., Reinecke,J.B., Hammond,G.R. V., Naslavsky,N. and Caplan,S. (2016) The endocytic recycling compartment maintains cargo segregation acquired upon exit from the sorting endosome. *Mol. Biol. Cell*, **27**, 108–126.

155. Maxfield,F.R. and McGraw,T.E. (2004) Endocytic recycling. *Nat. Rev. Mol. Cell Biol.*, **5**, 121.

156. Delevoye,C., Miserey-Lenkei,S., Montagnac,G., Gilles-Marsens,F., Paul-Gilloteaux,P., Giordano,F., Waharte,F., Marks,M.S., Goud,B. and Raposo,G. (2014) Recycling endosome tubule morphogenesis from sorting endosomes requires the kinesin motor KIF13A. *Cell Rep.*, **6**, 445–454.

157. Dautry-Varsat,A. (1986) Receptor-mediated endocytosis: The intracellular journey of transferrin and its receptor. *Biochimie*, **68**, 375–381.

158. Sheff,D.R., Daro,E.A., Hull,M. and Mellman,I. (1999) The receptors recycling pathway contains two distinct populations of early endosomes with different sorting functions. *J. Cell Biol.*, **145**, 123–139.

159. Caldieri,G., Malabarda,M.G., Di Fiore,P.P. and Sigismund,S. (2018) EGFR Trafficking in Physiology and Cancer. *Prog Mol Subcell Biol*, **57**, 235–272.

160. Wagner,B., Natarajan,A., Grünaug,S., Kroismayr,R., Wagner,E.F. and Sibilia,M. (2006) Neuronal survival depends on EGFR signaling in cortical but not midbrain astrocytes. *EMBO J.*, **25**, 752–762.

161. Bakker,J., Spits,M., Neefjes,J. and Berlin,I. (2017) The EGFR odyssey – from activation to destruction in space and time. *J. Cell Sci.*, **130**, 4087–4096.

162. Henriksen,L., Grandal,M.V., Knudsen,S.L.J., van Deurs,B. and Grøvdal,L.M. (2013) Internalization Mechanisms of the Epidermal Growth Factor Receptor after Activation with Different Ligands. *PLoS One*, **8**.

163. Singh,B., Carpenter,G. and Coffey,R.J. (2016) EGF receptor ligands: recent advances. *F1000Research*, **5**, F1000 Faculty Rev-2270.

164. Madshus,I.H. and Stang,E. (2009) Internalization and intracellular sorting of the EGF receptor: a model for understanding the mechanisms of receptor trafficking. *J. Cell Sci.*, **122**, 3433–3439.

165. Tanaka,T., Zhou,Y., Ozawa,T., Okizono,R., Banba,A., Yamamura,T., Oga,E., Muraguchi,A. and Sakurai,H. (2018) Ligand-activated epidermal growth factor receptor (EGFR) signaling governs endocytic trafficking of unliganded receptor monomers by non-canonical phosphorylation. *J. Biol. Chem.*, **293**, 2288–2301.

166. Progida,C. and Bakke,O. (2016) Bidirectional traffic between the Golgi and the endosomes – machineries and regulation. *J. Cell Sci.*, 10.1242/jcs.185702.

167. Sannerud,R., Saraste,J. and Goud,B. (2003) Retrograde traffic in the biosynthetic-secretory route: Pathways and machinery. *Curr. Opin. Cell Biol.*, **15**, 438–445.

168. Li,C., Shah,S.Z.A., Zhao,D. and Yang,L. (2016) Role of the retromer complex in neurodegenerative diseases. *Front. Aging Neurosci.*, **8**, 1–12.

169. Seaman,M.N.J. (2012) The retromer complex - endosomal protein recycling and beyond. *J. Cell Sci.*, **125**, 4693–4702.

170. Cui,Y., Yang,Z. and Teasdale,R.D. (2018) The functional roles of retromer in

Parkinson's disease. *FEBS Lett.*, **592**, 1096–1112.

171. Noda,T. (2017) Autophagy in the context of the cellular membrane-trafficking system: the enigma of Atg9 vesicles. *Biochem. Soc. Trans.*, **45**, 1323–1331.

172. Amaya,C., Fader,C.M. and Colombo,M.I. (2015) Autophagy and proteins involved in vesicular trafficking. *FEBS Lett.*, **589**, 3343–3353.

173. Jung,C.H., Ro,S.-H., Cao,J., Otto,N.M. and Kim,D.-H. (2010) mTOR regualtion of autophagy. *FEBS Lett*, **584**, 1287–1295.

174. Sarkar,S. (2013) Regulation of autophagy by mTOR-dependent and mTOR-independent pathways: autophagy dysfunction in neurodegenerative diseases and therapeutic application of autophagy enhancers. *Biochem. Soc. Trans.*, **41**, 1103 LP-1130.

175. Wang,T. and Abrams,G.D. (2014) ULK-Atg13-FIP200 Complexes Mediate mTOR Signaling to the Autophagy Machinery. *Minerva Ortop. e Traumatol.*, **65**, 87–102.

176. Mercer,T.J., Gubas,A. and Tooze,S.A. (2018) A molecular perspective of mammalian autophagosome biogenesis. *J. Biol. Chem.*, **293**, 5386–5395.

177. Hamasaki,M., Furuta,N., Matsuda,A., Nezu,A., Yamamoto,A., Fujita,N., Oomori,H., Noda,T., Haraguchi,T., Hiraoka,Y., *et al.* (2013) Autophagosomes form at ER-mitochondria contact sites. *Nature*, **495**, 389–393.

178. Graef,M., Friedman,J.R., Graham,C., Babu,M. and Nunnari,J. (2013) ER exit sites are physical and functional core autophagosome biogenesis components. *Mol. Biol. Cell*, **24**, 2918–2931.

179. Rubinsztein,D.C., Shpilka,T. and Elazar,Z. (2012) Mechanisms of Autophagosome Biogenesis. *Curr. Biol.*, **22**, R29–R34.

180. Jahreiss,L., Menzies,F.M. and Rubinsztein,D.C. (2008) The itinerary of autophagosomes: From peripheral formation to kiss-and-run fusion with lysosomes. *Traffic*, **9**, 574–587.

181. Chen,Y. and Yu,L. (2017) Recent progress in autophagic lysosome reformation. *Traffic*,

18, 358–361.

182. Palikaras,K., Lionaki,E. and Tavernarakis,N. (2018) Mechanisms of mitophagy in cellular homeostasis, physiology and pathology. *Nat. Cell Biol.*, **20**, 1013–1022.

183. Cuervo,A.M. and Wong,E. (2013) Chaperone-mediated autophagy: roles in disease and aging. *Cell Res.*, **24**, 92.

184. Cuervo,A.M. (2010) Chaperone-mediated autophagy: selectivity pays off. *Trends Endocrinol. Metab.*, **21**, 142–150.

185. Jian,W.L. and Bao,L.J. (2012) Microautophagy: lesser-known self-eating. *Cell. Mol. Life Sci.*, **69**, 1125-1136.

186. Klöpper,T.H., Kienle,N., Fasshauer,D. and Munro,S. (2012) Untangling the evolution of Rab G proteins: implications of a comprehensive genomic analysis. *BMC Biol.*, **10**, 71.

187. Madero-Pérez,J., Fdez,E., Fernández,B., Lara Ordóñez,A.J., Blanca Ramírez,M., Romo Lozano,M., Rivero-Ríos,P. and Hilfiker,S. (2017) Cellular effects mediated by pathogenic LRRK2: homing in on Rab-mediated processes. *Biochem Soc Trans*, **45**, 147–154.

188. Müller,M.P. and Goody,R.S. (2018) Molecular control of Rab activity by GEFs, GAPs and GDI. *Small GTPases*, **9**, 5–21.

189. Sivars,U., Aivazian,D. and Pfeffer,S. (2005) Purification and Properties of Yip3/PRA1 as a Rab GDI Displacement Factor. *Methods Enzymol.*, **403**, 348–356.

190. Ishida,M., Oguchi,M.E. and Fukuda,M. (2016) Multiple Types of Guanine Nucleotide Exchange Factors (GEFs) for Rab Small GTPases Mini-review and Review. *Cell Struct. Funct.*, **41**, 61–79.

191. Cherfils,J. and Zeghouf,M. (2013) Regulation of Small GTPases by GEFs, GAPs, and GDIs. *Physiol. Rev.*, **93**, 269–309.

192. Nagano,F., Sasaki,T., Fukui,K., Asakura,T., Imazumi,K. and Takai,Y. (1998) Molecular cloning and characterization of the noncatalytic subunit of the Rab3 subfamily-specific

GTPase-activating protein. *J. Biol. Chem.*, **273**, 24781–24785.

193. Pylypenko,O., Hammich,H., Yu,I.-M. and Houdusse,A. (2018) Rab GTPases and their interacting protein partners: Structural insights into Rab functional diversity. *Small GTPases*, **9**, 22–48.

194. Veleri,S., Punnakkal,P., Dunbar,G.L. and Maiti,P. (2018) Molecular Insights into the Roles of Rab Proteins in Intracellular Dynamics and Neurodegenerative Diseases. *NeuroMolecular Med.*, **20**, 18–36.

195. Vetter,I.R. and Wittinghofer,A. (2001) The Guanine in Switch Three Dimensions. *Science*, **294**, 1299–1304.

196. Hutagalung,A.H. and Novick,P.J. (2011) Role of Rab GTPases in Membrane Traffic and Cell Physiology. *Physiol. Rev.*, **91**, 119–149.

197. Pfeffer,S.R. (2005) Structural clues to rab GTPase functional diversity. *J. Biol. Chem.*, **280**, 15485–15488.

198. Gabe Lee,M.T., Mishra,A. and Lambright,D.G. (2009) Structural mechanisms for regulation of membrane traffic by Rab GTPases. *Traffic*, **10**, 1377–1389.

199. Chavrier,P., Gorvel,J.P., Stelzer,E., Simons,K., Gruenberg,J. and Zerial,M. (1991) Hypervariable C-termmal domain of rab proteins acts as a targeting signal. *Nature*, **353**, 769–772.

200. Beranger,F.., Paterson,H.., Powers,S.., De Gunzburg,J.. and Hancock,J.F.. d (1994) The effector domain of Rab6, plus a highly hydrophobic C terminus, is required for Golgi apparatus localization. *Mol. Cell. Biol.*, **14**, 744–758.

201. Ali,B.R. (2004) Multiple regions contribute to membrane targeting of Rab GTPases. *J. Cell Sci.*, **117**, 6401–6412.

202. Pylypenko,O. and Goud,B. (2012) Posttranslational modifications of Rab GTPases help their insertion into membranes. *Proc. Natl. Acad. Sci.*, **109**, 5555–5556.

203. Blümer,J., Rey,J., Dehmelt,L., Maze,T., Wu,Y.W., Bastiaens,P., Goody,R.S. and

Itzen,A. (2013) RabGEFs are a major determinant for specific Rab membrane targeting. *J. Cell Biol.*, **200**, 287–300.

204. Barbero,P., Bittova,L. and Pfeffer,S.R. (2002) Visualization of Rab9-mediated vesicle transport from endosomes to the trans-Golgi in living cells. *J. Cell Biol.*, **156**, 511–518.

205. Segev,N., Mulholland,J. and Botstein,D. (1988) The yeast GTP-binding YPT1 protein and a mammalian counterpart are associated with the secretion machinery. *Cell*, **52**, 915–924.

206. Chavrier,P., Parton,R.G., Hauri,H.P., Simons,K. and Zerial,M. (1990) Localization of Low-Molecular-Weight Gtp Binding-Proteins to Exocytic and Endocytic Compartments. *Cell*, **62**, 317–329.

207. Martinez,O., Schmidt, a, Salaméro,J., Hoflack,B., Roa,M. and Goud,B. (1994) The small GTP-binding protein rab6 functions in inta-Golgi transport. *J. Cell Biol.*, **127**, 1575–1588.

208. Grigoriev,I., Splinter,D., Keijzer,N., Wulf,P.S., Demmers,J., Ohtsuka,T., Modesti,M., Maly,I. V, Grosveld,F., Hoogenraad,C.C., *et al.* (2007) Rab6 Regulates Transport and Targeting of Exocytotic Carriers. *Dev. Cell*, **13**, 305–314.

209. Bucci,C., Parton,R.G., Mather,I.H., Stunnenberg,H., Simons,K., Hoflack,B. and Zerial,M. (1992) The small GTPase rab5 function as a regulatory factor in the early endocytic pathway. *Cell*, **70**, 715–728.

210. Feng,Y., Press,B. and Wandinger-Ness,A. (1995) Rab 7: An important regulator of late endocytic membrane traffic. *J. Cell Biol.*, **131**, 1435–1452.

211. Wang,S., Ma,Z., Xu,X., Wang,Z., Sun,L., Zhou,Y., Lin,X., Hong,W. and Wang,T. (2014) A role of Rab29 in the integrity of the trans-Golgi network and retrograde trafficking of mannose-6-phosphate receptor. *PLoS One*, **9**, e96242–e96242.

212. Onnis,A., Finetti,F., Patrussi,L., Gottardo,M., Cassioli,C., Spanò,S. and Baldari,C.T. (2015) The small GTPase Rab29 is a common regulator of immune synapse assembly and ciliogenesis. *Cell Death Differ.*, **22**, 1687–1699.

213. Ullrich,O., Reinsch,S., Urbé,S., Zerial,M. and Parton,R.G. (1996) Rab11 regulates recycling through the pericentriolar recycling endosome. *J. Cell Biol.*, **135**, 913–924.

214. van der Sluijs,P., Hull,M., Webster,P., Mâle,P., Goud,B. and Mellman,I. (1992) The small GTP-binding protein rab4 controls an early sorting event on the endocytic pathway. *Cell*, **70**, 729–740.

215. Klinkert,K. and Echard,A. (2016) Rab35 GTPase: A Central Regulator of Phosphoinositides and F-actin in Endocytic Recycling and Beyond. *Traffic*, **17**, 1063–1077.

216. Lombardi,D., Soldati,T., Riederer,M.A., Goda,Y., Zerial,M. and Pfeffer,S.R. (1993) Rab9 functions in transport between late endosomes and the trans Golgi network. *EMBO J.*, **12**, 677–82.

217. Huber,L.A., Pimplikar,S., Parton,R.G., Virta,H., Zerial,M. and Simons,K. (1993) Rab8, a small GTPase involved in vesicular traffic between the TGN and the basolateral plasma membrane. *J. Cell Biol.*, **123**, 35–45.

218. Babbey,C.M., Ahktar,N., Wang,E., Chih-Hsiung Cheng,C., Grant,B.D. and Dunn,E.W. (2006) Rab10 Regulates Membrane Transport through Early Endosomes of Polarized Madin-Darby Canine Kidney Cells. *Mol. Biol. Cell*, **17**, 3156–3175.

219. Sato,T., Iwano,T., Kunii,M., Matsuda,S., Mizuguchi,R., Jung,Y., Hagiwara,H., Yoshihara,Y., Yuzaki,M., Harada,R., *et al.* (2014) Rab8a and Rab8b are essential for several apical transport pathways but insufficient for ciliogenesis. *J. Cell Sci.*, **127**, 422–431.

220. Matsui,T., Itoh,T. and Fukuda,M. (2011) Small GTPase Rab12 Regulates Constitutive Degradation of Transferrin Receptor. *Traffic*, **12**, 1432–1443.

221. Xu,J., Kozlov,G., McPherson,P.S. and Gehring,K. (2018) A PH-like domain of the Rab12 guanine nucleotide exchange factor DENND3 binds actin and is required for autophagy. *J. Biol. Chem.*, **293**, 4566–4574.

222. Gerondopoulos,A., Bastos,R.N., Yoshimura,S., Anderson,R., Carpanini,S., Aligianis,I.,

Handley,M.T. and Barr,F.A. (2014) Rab18 and a Rab18 GEF complex are required for normal ER structure. *J. Cell Biol.*, **205**, 707-720.

223. Xu,D., Li,Y., Wu,L., Li,Y., Zhao,D., Yu,J., Huang,T., Ferguson,C., Parton,R.G., Yang,H., *et al.* (2018) Rab18 promotes lipid droplet (LD) growth by tethering the ER to LDs through SNARE and NRZ interactions. *J. Cell Biol.*, **217**, 975-995.

224. Ao,X., Zou,L. and Wu,Y. (2014) Regulation of autophagy by the Rab GTPase network. *Cell Death Differ.*, **21**, 348–358.

225. Bultema,J.J., Ambrosio,A.L., Burek,C.L. and Di Pietro,S.M. (2012) BLOC-2, AP-3, and AP-1 proteins function in concert with Rab38 and Rab32 proteins to mediate protein trafficking to lysosome-related organelles. *J. Biol. Chem.*, **287**, 19550–19563.

226. Bui,M., Gilady,S.Y., Fitzsimmons,R.E.B., Benson,M.D., Lynes,E.M., Gesson,K., Alto,N.M., Strack,S., Scott,J.D. and Simmen,T. (2010) Rab32 Modulates Apoptosis Onset and Mitochondria-associated Membrane (MAM) Properties. *J. Biol. Chem.*, **285**, 31590–31602.

227. Ng,E.L. and Tang,B.L. (2008) Rab GTPases and their roles in brain neurons and glia. *Brain Res. Rev.*, **58**, 236–246.

228. Pavlos,N.J., Gronborg,M., Riedel,D., Chua,J.J.E., Boyken,J., Kloepper,T.H., Urlaub,H., Rizzoli,S.O. and Jahn,R. (2010) Quantitative Analysis of Synaptic Vesicle Rabs Uncovers Distinct Yet Overlapping Roles for Rab3a and Rab27b in Ca2+-Triggered Exocytosis. *J. Neurosci.*, **30**, 13441–13453.

229. Shirane,M. and Nakayama,K.I. (2006) Protrudin induces neurite formation by directional membrane trafficking. *Science (80-.).*, **314**, 818–821.

230. Pfeffer,S.R. (2013) Rab GTPase regulation of membrane identity. *Curr. Opin. Cell Biol.*, **25**, 414–419.

231. Christoforidis,S., McBride,H.M., Burgoyne,R.D. and Zerial,M. (1999) The rab5 effector EEA1 is a core component of endosome docking. *Nature*, **397**, 621–625.

232. Grosshans,B.L., Ortiz,D. and Novick,P. (2006) Rabs and their effectors: achieving specificity in membrane traffic. *Proc. Natl. Acad. Sci. U. S. A.*, **103**, 11821–11827.

233. Rink,J., Ghigo,E., Kalaidzidis,Y. and Zerial,M. (2005) Rab conversion as a mechanism of progression from early to late endosomes. *Cell*, **122**, 735–749.

234. Novick,P. (2016) Regulation of membrane traffic by Rab GEF and GAP cascades. *Small GTPases*, **7**, 252–256.

235. Bem,D., Yoshimura,S.-I., Nunes-Bastos,R., Bond,F.C., Kurian,M.A., Rahman,F., Handley,M.T.W., Hadzhiev,Y., Masood,I., Straatman-Iwanowska,A.A., *et al.* (2011) Loss-of-function mutations in RAB18 cause Warburg micro syndrome. *Am. J. Hum. Genet.*, **88**, 499–507.

236. Cogli,L., Piro,F. and Bucci,C. (2009) Rab7 and the CMT2B disease. *Biochem. Soc. Trans.*, **37**, 1027-1031.

237. H,H.C.H., Luen,T.B. and K,G.E.L. (2018) Rab23 and developmental disorders. *Rev. Neurosci.*, **29**, 849.

238. Meeths,M., Bryceson,Y.T., Rudd,E., Zheng,C., Wood,S.M., Ramme,K., Beutel,K., Hasle,H., Heilmann,C., Hultenby,K., *et al.* (2010) Clinical presentation of Griscelli syndrome type 2 and spectrum of RAB27A mutations. *Pediatr. Blood Cancer*, **54**, 563–572.

239. D'Adamo,P., Menegon,A., Lo Nigro,C., Grasso,M., Gulisano,M., Tamanini,F., Bienvenu,T., Gedeon,A.K., Oostra,B., Wu,S.-K., *et al.* (1998) Mutations in GDI1 are responsible for X-linked non-specific mental retardation. *Nat. Genet.*, **19**, 134.

240. Mitsios,A., Dubis,A.M. and Moosajee,M. (2018) Choroideremia: from genetic and clinical phenotyping to gene therapy and future treatments. *Ther. Adv. Ophthalmol.*, **10**, 2515841418817490.

241. Tang,B.L. (2017) Rabs, Membrane Dynamics, and Parkinson's Disease. *J. Cell. Physiol.*, **232**, 1626–1633.

242. Mignogna,M.L., Giannandrea,M., Gurgone,A., Fanelli,F., Raimondi,F., Mapelli,L., Bassani,S., Fang,H., Van Anken,E., Alessio,M., *et al.* (2015) The intellectual disability protein RAB39B selectively regulates GluA2 trafficking to determine synaptic AMPAR composition. *Nat. Commun.*, **6**, 6504.

243. Sellier,C., Campanari,M., Julie Corbier,C., Gaucherot,A., Kolb-Cheynel,I., Oulad-Abdelghani,M., Ruffenach,F., Page,A., Ciura,S., Kabashi,E., *et al.* (2016) Loss of C9ORF72 impairs autophagy and synergizes with polyQ Ataxin-2 to induce motor neuron dysfunction and cell death. *EMBO J.*, **35**, 1276–1297.

244. Gitler,A.D., Bevis,B.J., Shorter,J., Strathearn,K.E., Hamamichi,S., Su,L.J., Caldwell,K.A., Caldwell,G.A., Rochet,J.-C., McCaffery,J.M., *et al.* (2008) The Parkinson's disease protein alpha-synuclein disrupts cellular Rab homeostasis. *Proc. Natl. Acad. Sci. U. S. A.*, **105**, 145–50.

245. Cooper,A.A., Gitler,A.D., Cashikar,A., Haynes,C.M., Kathryn,J., Bhullar,B., Liu,K., Xu,K., Strathearn,K.E., Cao,S., *et al.* (2006) NIH Public Access. *Science*, **313**, 324–328.

246. Breda,C., Nugent,M.L., Estranero,J.G., Kyriacou,C.P., Outeiro,T.F., Steinert,J.R. and Giorgini,F. (2015) Rab11 modulates α-synuclein-mediated defects in synaptic transmission and behaviour. *Hum. Mol. Genet.*, **24**, 1077–1091.

247. Waschbüsch,D., Michels,H., Strassheim,S., Ossendorf,E., Kessler,D., Gloeckner,C.J. and Barnekow,A. (2014) LRRK2 transport is regulated by its novel interacting partner Rab32. *PLoS One*, **9**.

248. Dodson,M.W., Zhang,T., Jiang,C., Chen,S. and Guo,M. (2012) Roles of the Drosophila LRRK2 homolog in Rab7-dependent lysosomal positioning. *Hum. Mol. Genet.*, **21**, 1350–1363.

249. Beilina,A., Rudenko,I.N., Kaganovich,A., Civiero,L., Chau,H., Kalia,S.K., Kalia,L. V., Lobbestael,E., Chia,R., Ndukwe,K., *et al.* (2014) Unbiased screen for interactors of leucine-rich repeat kinase 2 supports a common pathway for sporadic and familial Parkinson disease. *Proc. Natl. Acad. Sci.*, **111**, 2626–2631.

250. Shin,N., Jeong,H., Kwon,J., Heo,H.Y., Kwon,J.J., Yun,H.J., Kim,C.H., Han,B.S., Tong,Y., Shen,J., *et al.* (2008) LRRK2 regulates synaptic vesicle endocytosis. *Exp. Cell Res.*, **314**, 2055–2065.

251. Yu,M., Arshad,M., Wang,W., Zhao,D., Xu,L. and Zhou,L. (2018) LRRK2 mediated Rab8a phosphorylation promotes lipid storage. *Lipids Health Dis.*, **17**, 34.

252. Steger,M., Diez,F., Dhekne,H.S., Lis,P., Nirujogi,R.S., Karayel,O., Tonelli,F., Martinez,T.N., Lorentzen,E., Pfeffer,S.R., *et al.* (2017) Systematic proteomic analysis of LRRK2-mediated rab GTPase phosphorylation establishes a connection to ciliogenesis. *Elife*, **6**, 1–22.

253. Lai,Y.-C., Kondapalli,C., Lehneck,R., Procter,J.B., Dill,B.D., Woodroof,H.I., Gourlay,R., Peggie,M., Macartney,T.J., Corti,O., *et al.* (2015) Phosphoproteomic screening identifies Rab GTPases as novel downstream targets of PINK1. *EMBO J.*, **34**, 2840–2861.

254. Chavrier,P., Vingron,M., Sander,C., Simons,K. and Zerial,M. (1990) Molecular cloning of YPT1/SEC4-related cDNAs from an epithelial cell line. *Mol. Cell. Biol.*, **10**, 6578–6585.

255. Armstrong,J., Thompson,N., Squire,J.H., Smith,J., Hayes,B. and Solari,R. (1996) Identification of a novel member of the Rab8 family from the rat basophilic leukemia cell line, RBL.2H3. *J. Cell Sci.*, **109**, 1265–1274.

256. Chen,S., Liang,M.C., Chia,J.N., Ngsee,J.K. and Ting,A.E. (2001) Rab8b and Its Interacting Partner TRIP8b Are Involved in Regulated Secretion in AtT20 Cells. *J. Biol. Chem.*, **276**, 13209–13216.

257. Pereira-Leal,J.B. and Seabra,M.C. (2001) Evolution of the Rab family of small GTP-binding proteins. *J. Mol. Biol.*, **313**, 889–901.

258. Hattula,K., Furuhjelm,J., Arffman,A. and Peränen,J. (2002) A Rab8-specific GDP/GTP Exchange Factor Is Involved in Actin Remodeling and Polarized Membrane Transport. *Mol. Biol. Cell*, **13**, 3268–3280.

259. Yoshimura,S.I., Gerondopoulos,A., Linford,A., Rigden,D.J. and Barr,F.A. (2010) Family-wide characterization of the DENN domain Rab GDP-GTP exchange factors. *J. Cell Biol.*, **191**, 367–381.

260. Bryant,D.M., Datta,A., Rodríguez-Fraticelli,A.E., PeräCurrency Signnen,J., Martín-Belmonte,F. and Mostov,K.E. (2010) A molecular network for de novo generation of the apical surface and lumen. *Nat. Cell Biol.*, **12**, 1035–1045.

261. Furusawa,K., Asada,A., Urrutia,P., Gonzalez-Billault,C., Fukuda,M. and Hisanaga,S. (2017) Cdk5 Regulation of the GRAB-Mediated Rab8-Rab11 Cascade in Axon Outgrowth. *J. Neurosci.*, **37**, 790–806.

262. Roach,W.G., Chavez,J.A., Mîinea,C.P. and Lienhard,G.E. (2007) Substrate specificity and effect on GLUT4 translocation of the Rab GTPase-activating protein Tbc1d1. *Biochem. J.*, **403**, 353–358.

263. Mîinea,C.P., Sano,H., Kane,S., Sano,E., Fukuda,M., Peränen,J., Lane,W.S. and Lienhard,G.E. (2005) AS160, the Akt substrate regulating GLUT4 translocation, has a functional Rab GTPase-activating protein domain. *Biochem. J.*, **391**, 87–93.

264. Yoshimura,S.I., Egerer,J., Fuchs,E., Haas,A.K. and Barr,F.A. (2007) Functional dissection of Rab GTPases involved in primary cilium formation. *J. Cell Biol.*, **178**, 363–369.

265. Vaibhava,V., Nagabhushana,A., Chalasani,M.L.S., Sudhakar,C., Kumari,A. and Swarup,G. (2012) Optineurin mediates a negative regulation of Rab8 by the GTPase-activating protein TBC1D17. *J. Cell Sci.*, **125**, 5026–5039.

266. Grigoriev,I., Yu,K. Lou, Martinez-Sanchez,E., Serra-Marques,A., Smal,I., Meijering,E., Demmers,J., Peränen,J., Pasterkamp,R.J., Van Der Sluijs,P., *et al.* (2011) Rab6, Rab8, and MICAL3 cooperate in controlling docking and fusion of exocytotic carriers. *Curr. Biol.*, **21**, 967–974.

267. Sharma,M., Giridharan,S.S., Rahajeng,J., Naslavsky,N. and Caplan,S. (2009) MICAL-L1 links EHD1 to tubular recycling endosomes and regulates receptor recycling. *Mol.*

Biol. Cell, **20**, 5181–5194.

268. Yamamura,R., Nishimura,N., Nakatsuji,H., Arase,S. and Sasaki,T. (2008) The interaction of JRAB/MICAL-L2 with Rab8 and Rab13 coordinates the assembly of tight junctions and adherens junctions. *Mol. Biol. Cell*, **19**, 971–983.

269. Tsang,W.Y., Bossard,C., Khanna,H., Peränen,J., Swaroop,A., Malhotra,V. and Dynlacht,B.D. (2008) CP110 Suppresses Primary Cilia Formation through Its Interaction with CEP290, a Protein Deficient in Human Ciliary Disease. *Dev. Cell*, **15**, 187–197.

270. Hattula,K. and Peränen,J. (2000) FIP-2, a coiled-coil protein, links Huntingtin to Rab8 and modulates, cellular morphogenesis. *Curr. Biol.*, **10**, 1603–1606.

271. Heidrych,P., Zimmermann,U., Breß,A., Pusch,C.M., Ruth,P., Pfister,M., Knipper,M. and Blin,N. (2008) Rab8b GTPase, a protein transport regulator, is an interacting partner of otoferlin, defective in a human autosomal recessive deafness form. *Hum. Mol. Genet.*, **17**, 3814–3821.

272. Omori,Y., Zhao,C., Saras,A., Mukhopadhyay,S., Kim,W., Furukawa,T., Sengupta,P., Veraksa,A. and Malicki,J. (2008) Elipsa is an early determinant of ciliogenesis that links the IFT particle to membrane-associated small GTPase Rab8. *Nat. Cell Biol.*, **10**, 437–444.

273. Hou,X., Hagemann,N., Schoebel,S., Blankenfeldt,W., Goody,R.S., Erdmann,K.S. and Itzen,A. (2011) A structural basis for Lowe syndrome caused by mutations in the Rab-binding domain of OCRL1. *EMBO J.*, **30**, 1659–1670.

274. Hattula,K., Furuhjelm,J., Tikkanen,J., Tanhuanpaa,K., Laakkonen,P. and Peranen,J. (2006) Characterization of the Rab8-specific membrane traffic route linked to protrusion formation. *J. Cell Sci.*, **119**, 4866–4877.

275. Bravo-Cordero,J.J., Marrero-Diaz,R., Megías,D., Genís,L., García-Grande,A., García,M.A., Arroyo,A.G. and Montoya,M.C. (2007) MT1-MMP proinvasive activity is regulated by a novel Rab8-dependent exocytic pathway. *EMBO J.*, **26**, 1499–1510.

276. Linder,M.D., Uronen,R.-L., Maarit Hölttä-Vuori,M., van der Sluijs,P., Peränen,P. and Elina,I. (2007) Rab8-dependent Recycling Promotes Endosomal Cholesterol Removal in Normal and Sphingolipidosis Cells. *Mol. Biol. Cell*, **18**, 47–56.

277. Linder,M.D., Mäyränpää,M.I., Peränen,J., Pietilä,T.E., Pietiäinen,V.M., Uronen,R.L., Olkkonen,V.M., Kovanen,P.T. and Ikonen,E. (2009) Rab8 regulates ABCA1 cell surface expression and facilitates cholesterol efflux in primary human macrophages. *Arterioscler. Thromb. Vasc. Biol.*, **29**, 883–888.

278. Nachury,M. V., Loktev,A. V., Zhang,Q., Westlake,C.J., Peränen,J., Merdes,A., Slusarski,D.C., Scheller,R.H., Bazan,J.F., Sheffield,V.C., *et al.* (2007) A Core Complex of BBS Proteins Cooperates with the GTPase Rab8 to Promote Ciliary Membrane Biogenesis. *Cell*, **129**, 1201–1213.

279. Singla,V. and Reiter,J.F. (2006) The primary cilium as the cell's antenna: Signaling at a sensory organelle. *Science (80-.).*, **313**, 629–633.

280. Knödler,A., Feng,S., Zhang,J., Zhang,X., Das,A., Peranen,J. and Guo,W. (2010) Coordination of Rab8 and Rab11 in primary ciliogenesis. *Proc. Natl. Acad. Sci.*, **107**, 6346–6351.

281. Westlake,C.J., Baye,L.M., Nachury,M. V., Wright,K.J., Ervin,K.E., Phu,L., Chalouni,C., Beck,J.S., Kirkpatrick,D.S., Slusarski,D.C., *et al.* (2011) Primary cilia membrane assembly is initiated by Rab11 and transport protein particle II (TRAPPII) complex-dependent trafficking of Rabin8 to the centrosome. *Proc. Natl. Acad. Sci.*, **108**, 2759–2764.

282. Jo,H. and Kim,J. (2013) Itinerary of vesicles to primary cilia. *Animal Cells Syst. (Seoul).*, **17**, 221–227.

283. Lu,Q., Insinna,C., Ott,C., Stauffer,J., Pintado,P.A., Rahajeng,J., Baxa,U., Walia,V., Cuenca,A., Hwang,Y.-S., *et al.* (2015) Early steps in primary cilium assembly require EHD1/EHD3-dependent ciliary vesicle formation. *Nat. Cell Biol.*, **17**, 228–240.

284. Ishikura,S. and Klip,A. (2008) Muscle cells engage Rab8A and myosin Vb in insulin-

dependent GLUT4 translocation Ishikura S, Klip A. Muscle cells engage Rab8A and myosin Vb in insulin-dependent GLUT4 translocation. *Am J Physiol Cell Physiol*, **295**, 1016–1025.

285. Bond,L.M., Peden,A.A., Kendrick-Jones,J., Sellers,J.R. and Buss,F. (2011) Myosin VI and its binding partner optineurin are involved in secretory vesicle fusion at the plasma membrane. *Mol. Biol. Cell*, **22**, 54–65.

286. Sato,T., Mushiake,S., Kato,Y., Sato,K., Sato,M., Takeda,N., Ozono,K., Miki,K., Kubo,Y., Tsuji,A., *et al.* (2007) The Rab8 GTPase regulates apical protein localization in intestinal cells. *Nature*, **448**, 366–369.

287. Faust,F., Gomez-Lazaro,M., Borta,H., Agricola,B. and Schrader,M. (2008) Rab8 is involved in zymogen granule formation in pancreatic acinar AR42J cells. *Traffic*, **9**, 964–979.

288. Huber,L. a, Dupree,P. and Dotti,C.G. (1995) A deficiency of the small GTPase rab8 inhibits membrane traffic in developing neurons. *Mol. Cell. Biol.*, **15**, 918–924.

289. Gerges,N.Z., Backos,D.S. and Esteban,J.A. (2004) Local control of AMPA receptor trafficking at the postsynaptic terminal by a small GTPase of the Rab family. *J. Biol. Chem.*, **279**, 43870–43878.

290. Funayama,M., Hasegawa,K., Ohta,E., Kawashima,N., Komiyama,M., Kowa,H., Tsuji,S. and Obata,F. (2005) An LRRK2 mutation as a cause for the Parkinsonism in the original PARK8 family. *Ann. Neurol.*, **57**, 918–921.

291. Zimprich,A., Biskup,S., Leitner,P., Lichtner,P., Farrer,M., Lincoln,S., Kachergus,J., Hulihan,M., Uitti,R.J., Calne,D.B., *et al.* (2004) Mutations in LRRK2 cause autosomal-dominant parkinsonism with pleomorphic pathology. *Neuron*, **44**, 601–607.

292. Paisán-Ruíz,C., Jain,S., Evans,E.W., Gilks,W.P., Simón,J., Van Der Brug,M., De Munain,A.L., Aparicio,S., Gil,A.M., Khan,N., *et al.* (2004) Cloning of the gene containing mutations that cause PARK8-linked Parkinson's disease. *Neuron*, **44**, 595–600.

293. Lesage,S. and Brice,A. (2009) Parkinson's disease: From monogenic forms to genetic susceptibility factors. *Hum. Mol. Genet.*, **18**, 48–59.

294. Gilks,W.P., Abou-Sleiman,P.M., Gandhi,S., Jain,S., Singleton,A., Lees,A.J., Shaw,K., Bhatia,K.P., Bonifati,V., Quinn,N.P., *et al.* (2005) A common LRRK2 mutation in idiopathic Parkinson's disease. *Lancet*, **365**, 415–416.

295. Nichols,W., Pankratz,N., Hernandez,D., Paisanruiz,C., Jain,S., Halter,C., Michaels,V., Reed,T., Rudolph, a and Shults,C. (2005) Genetic screening for a single common mutation in familial Parkinson's disease. *Lancet*, **365**, 410–412.

296. Di Fonzo,A., Rohé,C.F., Ferreira,J., Chien,H.F., Vacca,L., Stocchi,F., Guedes,L., Fabrizio,E., Manfredi,M., Vanacore,N., *et al.* (2005) A frequent LRRK2 gene mutation associated with autosomal dominant Parkinson's disease. *Lancet*, **365**, 412–415.

297. Ozelius,L., Senthil,G., Saunders-Pullman,R., Ohmann,E., Deligtisch,A., Tagliati,M., Hunt,A., Klein,C., Henick,B., Hailpern,S., *et al.* (2006) LRRK2 G2019S as a Cause of Parkinson's Disease in North African Arabs. *N. Engl. J. Med.*, **354**, 422–423.

298. Lesage,S., Belarbi,S., Troiano,A., Condroyer,C., Hecham,N., Pollak,P., Lohman,E., Benhassine,T., Ysmail-Dahlouk,F., Dürr,A., *et al.* (2008) Is the common LRRK2 G2019S mutation related to dyskinesias in North African Parkinson disease? *Neurology*, **71**, 1550–1552.

299. Healy,D.G., Falchi,M., O'Sullivan,S.S., Bonifati,V., Durr,A., Bressman,S., Brice,A., Aasly,J., Zabetian,C.P., Goldwurm,S., *et al.* (2008) Phenotype, genotype, and worldwide genetic penetrance of LRRK2-associated Parkinson's disease: a case-control study. *Lancet Neurol.*, **7**, 583–590.

300. Hulihan,M.M., Ishihara-Paul,L., Kachergus,J., Warren,L., Amouri,R., Elango,R., Prinjha,R.K., Upmanyu,R., Kefi,M., Zouari,M., *et al.* (2008) LRRK2 Gly2019Ser penetrance in Arab-Berber patients from Tunisia: a case-control genetic study. *Lancet Neurol.*, **7**, 591–594.

301. Ishihara,L., Warren,L., Gibson,R., Amouri,R., Lesage,S., Dürr,A., Tazir,M.,

Wszolek,Z.K., Uitti,R.J., Nichols,W.C., *et al.* (2006) Clinical features of Parkinson disease patients with homozygous leucine-rich repeat kinase 2 G2019S mutations. *Arch. Neurol.*, **63**, 1250–1254.

302. Seol,W. (2010) Biochemical and molecular features of LRRK2 and its pathophysiological roles in Parkinson's disease. *BMB Rep.*, **43**, 233–244.

303. Alegre-Abarrategui,J., Christian,H., Lufino,M.M.P., Mutihac,R., Venda,L.L., Ansorge,O. and Wade-Martins,R. (2009) LRRK2 regulates autophagic activity and localizes to specific membrane microdomains in a novel human genomic reporter cellular model. *Hum. Mol. Genet.*, **18**, 4022–4034.

304. Purlyte,E., Dhekne,H.S., Sarhan,A.R., Gomez,R., Lis,P., Wightman,M., Martinez,T.N., Tonelli,F., Pfeffer,S.R. and Alessi,D.R. (2017) Rab29 activation of the Parkinson's disease-associated LRRK2 kinase. *EMBO J.*, **37**, e201798099.

305. Eguchi,T., Kuwahara,T., Sakurai,M., Komori,T., Fujimoto,T., Ito,G., Yoshimura,S., Harada,A., Fukuda,M., Koike,M., *et al.* (2018) LRRK2 and its substrate Rab GTPases are sequentially targeted onto stressed lysosomes and maintain their homeostasis. *Proc. Natl. Acad. Sci.*, **115**, E9115 LP-E9124.

306. Cookson MR (2016) Cellular functions of LRRK2 implicate vesicular trafficking pathways in Parkinson´s disease. *Biochem Soc Trans*, **44**, 1603–1610.

307. Piccoli,G., Condliffe,S.B., Bauer,M., Giesert,F., Boldt,K., De Astis,S., Meixner,A., Sarioglu,H., Vogt-Weisenhorn,D.M., Wurst,W., *et al.* (2011) LRRK2 Controls Synaptic Vesicle Storage and Mobilization within the Recycling Pool. *J. Neurosci.*, **31**, 2225–2237.

308. Civiero,L., Dihanich,S., Lewis,P.A. and Greggio,E. (2014) Genetic, structural, and molecular insights into the function of RAS of complex proteins domains. *Chem. Biol.*, **21**, 809–818.

309. Moore,D.J. (2008) The biology and pathobiology of LRRK2: Implications for Parkinson's disease. *Park. Relat. Disord.*, **14**, 92–98.

310. Langston,R.G., Rudenko,I.N. and Cookson,M.R. (2016) The function of orthologues of the human Parkinson's disease gene LRRK2 across species: implications for disease modelling in preclinical research. *Biochem. J.*, **473**, 221–232.

311. Reyniers,L., Del Giudice,M.G., Civiero,L., Belluzzi,E., Lobbestael,E., Beilina,A., Arrigoni,G., Derua,R., Waelkens,E., Li,Y., *et al.* (2014) Differential protein-protein interactions of LRRK1 and LRRK2 indicate roles in distinct cellular signaling pathways. *J. Neurochem.*, **131**, 239–250.

312. Islam,M.S. and Moore,D.J. (2017) Mechanisms of LRRK2-dependent neurodegeneration: role of enzymatic activity and protein aggregation. *Biochem Soc Trans.*, **45**, 163–172.

313. Liu,M., Kang,S., Ray,S., Jackson,J., Zaitsev,A.D., Gerber,S.A., Cuny,G.D. and Glicksman,M.A. (2011) Kinetic, mechanistic, and structural modeling studies of truncated wild-type leucine-rich repeat kinase 2 and the G2019S mutant. *Biochemistry*, **50**, 9399–9408.

314. Nguyen,A.P.T. and Moore,D.J. (2017) Understanding the GTPase Activity of LRRK2: Regulation, Function, and Neurotoxicity. *Adv. Neurobiol.*, **14**, 71–88.

315. Huang,X., Wu,C., Park,Y., Long,X., Hoang,Q.Q. and Liao,J. (2018) The Parkinson's disease–associated mutation N1437H impairs conformational dynamics in the G domain of LRRK2. *FASEB J.*, 10.1096/fj.201802031R.

316. Liu,Z., Bryant,N., Kumaran,R., Beilina,A., Abeliovich,A., Cookson,M.R. and West,A.B. (2018) LRRK2 phosphorylates membrane-bound Rabs and is activated by GTP-bound Rab7L1 to promote recruitment to the trans-Golgi network. *Hum. Mol. Genet.*, **27**, 385–395.

317. Smith,W.W., Pei,Z., Jiang,H., Dawson,V.L., Dawson,T.M. and Ross,C.A. (2006) Kinase activity of mutant LRRK2 mediates neuronal toxicity. *Nat. Neurosci.*, **9**, 1231–1233.

318. Chan,S.L. and Tan,E.-K. (2017) Targeting LRRK2 in Parkinson's disease: an update on

recent developments AU - Chan, Sharon L. *Expert Opin. Ther. Targets*, **21**, 601–610.

319. Luerman,G.C., Nguyen,C., Samaroo,H., Loos,P., Xi,H., Hurtado-Lorenzo,A., Needle,E., Stephen Noell,G., Galatsis,P., Dunlop,J., *et al.* (2014) Phosphoproteomic evaluation of pharmacological inhibition of leucine-rich repeat kinase 2 reveals significant off-target effects of LRRK-2-IN-1. *J. Neurochem.*, **128**, 561–576.

320. West,A.B. (2017) Achieving neuroprotection with LRRK2 kinase inhibitors in Parkinson disease. *Exp. Neurol.*, **298**, 236–245.

321. Fuji,R.N., Flagella,M., Baca,M., Baptista,M.A.S., Brodbeck,J., Chan,B.K., Fiske,B.K., Honigberg,L., Jubb,A.M., Katavolos,P., *et al.* (2015) Effect of selective LRRK2 kinase inhibition on nonhuman primate lung. *Sci. Transl. Med.*, **7**, 273ra15.

322. Andersen,M.A., Wegener,K.M., Larsen,S., Badolo,L., Smith,G.P., Jeggo,R., Jensen,P.H., Sotty,F., Christensen,K.V. and Thougaard,A. (2018) PFE-360-induced LRRK2 inhibition induces reversible, non-adverse renal changes in rats. *Toxicology*, **395**, 15–22.

323. Lobbestael,E., Zhao,J., Rudenko,I.N., Beylina,A., Gao,F., Wetter,J., Beullens,M., Bollen,M., Cookson,M.R., Baekelandt,V., *et al.* (2013) Identification of protein phosphatase 1 as a regulator of the LRRK2 phosphorylation cycle. *Biochem. J.*, **456**, 119–128.

324. Sheng,Z., Zhang,S., Bustos,D., Kleinheinz,T., Pichon,C.E. Le, Dominguez,S.L., Solanoy,H.O., Drummond,J., Zhang,X., Ding,X., *et al.* (2012) Ser 1292 Autophosphorylation Is an Indicator of LRRK2 Kinase Activity and Contributes to the Cellular Effects of PD Mutations. *Sci. Transl. Med.*, **4**.

325. De Wit,T., Baekelandt,V. and Lobbestael,E. (2018) LRRK2 Phosphorylation : Behind the Scenes. *Neuroscientist*, **24**, 486-500.

326. Sen,S., Webber,P.J. and West,A.B. (2009) Dependence of Leucine-rich Repeat Kinase 2 (LRRK2) Kinase Activity on Dimerization *J. Biol. Chem.*, **284**, 36346–36356.

327. Gilsbach,B.K. and Kortholt,A. (2014) Structural biology of the LRRK2 GTPase and

kinase domains: implications for regulation. *Front. Mol. Neurosci.*, **7**, 1–9.

328. West,A.B., Moore,D.J., Choi,C., Andrabi,S.A., Li,X., Dikeman,D., Biskup,S., Zhang,Z., Lim,K.L., Dawson,V.L., *et al.* (2007) Parkinson's disease-associated mutations in LRRK2 link enhanced GTP-binding and kinase activities to neuronal toxicity. *Hum. Mol. Genet.*, **16**, 223–232.

329. Ito,G., Okai,T., Fujino,G., Takeda,K., Ichijo,H., Katada,T. and Iwatsubo,T. (2007) GTP Binding Is Essential to the Protein Kinase Activity of LRRK2, a Causative Gene Product for Familial Parkinson's Disease. *Biochemistry*, **46**, 1380–1388.

330. Biosa,A., Trancikova,A., Civiero,L., Glauser,L., Bubacco,L., Greggio,E. and Moore,D.J. (2013) GTPase activity regulates kinase activity and cellular phenotypes of parkinson's disease-associated LRRK2. *Hum. Mol. Genet.*, **22**, 1140–1156.

331. Webber,P.J., Smith,A.D., Sen,S., Renfrow,M.B., Mobley,J.A. and West,A.B. (2011) Autophosphorylation in the leucine-rich repeat kinase 2 (LRRK2) GTPase domain modifies kinase and GTP-binding activities. *J. Mol. Biol.*, **412**, 94–110.

332. Greggio,E., Taymans,J.M., Zhen,E.Y., Ryder,J., Vancraenenbroeck,R., Beilina,A., Sun,P., Deng,J., Jaffe,H., Baekelandt,V., *et al.* (2009) The Parkinson's disease kinase LRRK2 autophosphorylates its GTPase domain at multiple sites. *Biochem. Biophys. Res. Commun.*, **389**, 449–454.

333. Liu,Z., Mobley,J.A., Delucas,L.J., Kahn,R.A. and West,A.B. (2016) LRRK2 autophosphorylation enhances its GTPase activity. *FASEB J.*, **30**, 336–347.

334. Salašová,A., Yokota,C., Potěšil,D., Zdráhal,Z., Bryja,V. and Arenas,E. (2017) A proteomic analysis of LRRK2 binding partners reveals interactions with multiple signaling components of the WNT / PCP pathway. *Mol. Neurodegener.*, 10.1186/s13024-017-0193-9.

335. Porras,P., Duesbury,M., Fabregat,A., Ueffing,M. and Orchard,S. (2015) A visual review of the interactome of LRRK2 : Using deep-curated molecular interaction data. *Proteomics*, **15**, 1390-1404.

336. Manzoni,C., Denny,P., Lovering,R.C. and Lewis,P.A. (2015) Computational analysis of the LRRK2 interactome. *PeerJ*, **3**, e778.

337. Madero-Pérez,J., Fernández,B., Lara Ordóñez,A.J., Fdez,E., Lobbestael,E., Baekelandt,V. and Hilfiker,S. (2018) RAB7L1-Mediated Relocalization of LRRK2 to the Golgi Complex Causes Centrosomal Deficits via RAB8A. *Front. Mol. Neurosci.*, **11**, 417.

338. Beilina,A., Rudenko,I.N., Kaganovich,A., Civiero,L., Chau,H. and Kalia,S.K. (2013) Unbiased screen for interactors of leucine-rich repeat kinase 2 supports a common pathway for sporadic and familial Parkinson disease. *Proc Natl Acad Sci U S A.*, **111**, 2626-2631.

339. Nichols,R.J., Dzamko,N., Morrice,N.A., Campbell,D.G., Deak,M., Ordureau,A., Macartney,T., Tong,Y., Shen,J., Prescott,A.R., *et al.* (2010) 14-3-3 binding to LRRK2 is disrupted by multiple Parkinson's disease-associated mutations and regulates cytoplasmic localization. *Biochem. J.*, **430**, 393–404.

340. Dzamko,N., Deak,M., Hentati,F., Reith,A.D., Prescott,A.R., Alessi,D.R. and Nichols,R.J. (2010) Inhibition of LRRK2 kinase activity leads to dephosphorylation of Ser(910)/Ser(935), disruption of 14-3-3 binding and altered cytoplasmic localization. *Biochem. J.*, **430**, 405–413.

341. Li,X., Wang,Q.J., Pan,N., Lee,S., Zhao,Y., Chait,B.T. and Yue,Z. (2011) Phosphorylation-dependent 14-3-3 binding to LRRK2 is impaired by common mutations of familial Parkinson's disease. *PLoS One*, **6**, e17153–e17153.

342. Shimada,T., Fournier,A.E. and Yamagata,K. (2013) Neuroprotective function of 14-3-3 proteins in neurodegeneration. *Biomed Res. Int.*, **2013**, 564534.

343. Civiero,L., Cogo,S., Biosa,A. and Greggio,E. (2018) The role of LRRK2 in cytoskeletal dynamics. *Biochem. Soc. Trans.*, **46**, 1653-1663.

344. Harvey,K. and Outeiro,T.F. (2018) The role of LRRK2 in cell signalling. *Biochem. Soc. Trans.*, **47**, 197-207..

345. Sancho,R.M., Law,B.M.H. and Harvey,K. (2009) Mutations in the LRRK2 Roc-COR tandem domain link Parkinson's disease to Wnt signalling pathways. *Hum. Mol. Genet.*, **18**, 3955–3968.

346. Berwick,D.C. and Harvey,K. (2012) LRRK2 functions as a Wnt signaling scaffold, bridging cytosolic proteins and membrane-localized LRP6. *Hum. Mol. Genet.*, **21**, 4966–4979.

347. Jeong,G.R., Jang,E.H., Bae,J.R., Jun,S., Kang,H.C., Park,C.H., Shin,J.H., Yamamoto,Y., Tanaka-Yamamoto,K., Dawson,V.L., *et al.* (2018) Dysregulated phosphorylation of Rab GTPases by LRRK2 induces neurodegeneration. *Mol. Neurodegener.*, **13**, 1–17.

348. Ito,G., Katsemonova,K., Tonelli,F., Lis,P., Baptista,M.A.S., Shpiro,N., Duddy,G., Wilson,S., Ho,P.W.-L., Ho,S.-L., *et al.* (2016) Phos-tag analysis of Rab10 phosphorylation by LRRK2: a powerful assay for assessing kinase function and inhibitors. *Biochem. J.*, **473**, 2671–2685.

349. Thirstrup,K., Dächsel,J.C., Oppermann,F.S., Williamson,D.S., Smith,G.P., Fog,K. and Christensen,K. V. (2017) Selective LRRK2 kinase inhibition reduces phosphorylation of endogenous Rab10 and Rab12 in human peripheral mononuclear blood cells. *Sci. Rep.*, **7**, 1–18.

350. Fan,Y., Howden,A.J.M., Sarhan,A.R., Lis,P., Ito,G., Martinez,T.N., Brockmann,K., Gasser,T., Alessi,D.R. and Sammler,E.M. (2017) Interrogating Parkinson's disease LRRK2 kinase pathway activity by assessing Rab10 phosphorylation in human neutrophils. *Biochem. J.*, **475**, 23-44.

351. Atashrazm,F., Hammond,D., Perera,G., Bolliger,M.F., Matar,E., Halliday,G.M., Schüle,B., Lewis,S.J.G., Nichols,R.J. and Dzamko,N. (2018) LRRK2-mediated Rab10 phosphorylation in immune cells from Parkinson's disease patients. *Mov. Disord.*

352. Yue,Z. (2009) LRRK2 in Parkinson's disease: in vivo models and approaches for understanding pathogenic roles. *FEBS J.*, **276**, 6445–6454.

353. Xiong,Y. and Yu,J. (2018) Modeling Parkinson's disease in Drosophila: What have we learned for dominant traits? *Front. Neurol.*, **9**.

354. Sakaguchi-Nakashima,A., Meir,J.Y., Jin,Y., Matsumoto,K. and Hisamoto,N. (2007) LRK-1, a C. elegans PARK8-Related Kinase, Regulates Axonal-Dendritic Polarity of SV Proteins. *Curr. Biol.*, **17**, 592–598.

355. Sämann,J., Hegermann,J., von Gromoff,E., Eimer,S., Baumeister,R. and Schmidt,E. (2009) Caenorhabditits elegans LRK-1 and PINK-1 act antagonistically in stress response and neurite outgrowth. *J. Biol. Chem.*, **284**, 16482–16491.

356. Saha,S., Guillily,M.D., Ferree,A., Lanceta,J., Chan,D., Ghosh,J., Hsu,C.H., Segal,L., Raghavan,K., Matsumoto,K., *et al.* (2009) LRRK2 modulates vulnerability to mitochondrial dysfunction in Caenorhabditis elegans. *J. Neurosci.*, **29**, 9210-9218.

357. Yao,C., El Khoury,R., Wang,W., Byrd,T.A., Pehek,E.A., Thacker,C., Zhu,X., Smith,M.A., Wilson-Delfosse,A.L. and Chen,S.G. (2010) LRRK2-mediated neurodegeneration and dysfunction of dopaminergic neurons in a Caenorhabditis elegans model of Parkinson's disease. *Neurobiol. Dis.*, **40**, 73–81.

358. Li,T., Yang,D., Sushchky,S., Liu,Z. and Smith,W.W. (2011) Models for LRRK2-linked parkinsonism. *Parkinsons. Dis.*, **2011**, 942412.

359. Hindle,S., Afsari,F., Stark,M., Middleton,C.A., Evans,G.J.O., Sweeney,S.T. and Elliott,C.J.H. (2013) Dopaminergic expression of the Parkinsonian gene LRRK2-G2019S leads to non-autonomous visual neurodegeneration, accelerated by increased neural demands for energy. *Hum. Mol. Genet.*, **22**, 2129–2140.

360. Andres-Mateos,E., Mejias,R., Sasaki,M., Li,X., Lin,B.M., Biskup,S., Zhang,L., Banerjee,R., Thomas,B., Yang,L., *et al.* (2009) Unexpected Lack of Hypersensitivity in LRRK2 Knock-Out Mice to MPTP (1-Methyl-4-Phenyl-1,2,3,6-Tetrahydropyridine). *J. Neurosci.*, **29**, 15846-15850.

361. Herzig,M., Kolly,C., Persohn,E., Theil,D., Schweizer,T., Hafner,T., Stemmelen,C., Troxler,T., Schmid,P., Danner,S., *et al.* (2011) LRRK2 protein levels are determined by

kinase function and are crucial for kidney and lung homeostasis in mice. *Hum. Mol. Genet.*, **20**, 4209–4223.

362. Hinkle,K.M., Yue,M., Behrouz,B., Dächsel,J.C., Lincoln,S.J., Bowles,E.E., Beevers,J.E., Dugger,B., Winner,B., Prots,I., *et al.* (2012) LRRK2 knockout mice have an intact dopaminergic system but display alterations in exploratory and motor co-ordination behaviors. *Mol. Neurodegener.*, **7**, 25.

363. Lin,X., Parisiadou,L., Gu,X.-L., Wang,L., Shim,H., Sun,L., Xie,C., Long,C.-X., Yang,W.-J., Ding,J., *et al.* (2009) Leucine-Rich Repeat Kinase 2 Regulates the Progression of Neuropathology Induced by Parkinson's-Disease-Related Mutant α-synuclein. *Neuron*, **64**, 807–827.

364. Paus,M., Kohl,Z., Ben Abdallah,N.M.-B., Galter,D., Gillardon,F. and Winkler,J. (2013) Enhanced dendritogenesis and axogenesis in hippocampal neuroblasts of LRRK2 knockout mice. *Brain Res.*, **1497**, 85–100.

365. Tong,Y., Giaime,E., Yamaguchi,H., Ichimura,T., Liu,Y., Si,H., Cai,H., Bonventre,J. V and Shen,J. (2012) Loss of leucine-rich repeat kinase 2 causes age-dependent bi-phasic alterations of the autophagy pathway. *Mol. Neurodegener.*, **7**, 2.

366. Tong,Y., Yamaguchi,H., Giaime,E., Boyle,S., Kopan,R., Kelleher,R.J. and Shen,J. (2010) Loss of leucine-rich repeat kinase 2 causes impairment of protein degradation pathways, accumulation of alpha-synuclein, and apoptotic cell death in aged mice. *Proc Natl Acad Sci USA*, **107**, 9879-9884.

367. Biskup,S., Moore,D.J., Rea,A., Lorenz-Deperieux,B., Coombes,C.E., Dawson,V.L., Dawson,T.M. and West,A.B. (2007) Dynamic and redundant regulation of LRRK2 and LRRK1 expression. *BMC Neurosci.*, **8**, 1–11.

368. Giaime,E., Tong,Y., Wagner,L.K., Yuan,Y., Huang,G. and Shen,J. (2017) Age-Dependent Dopaminergic Neurodegeneration and Impairment of the Autophagy-Lysosomal Pathway in LRRK-Deficient Mice. *Neuron*, **96**, 796–807.

369. Garcia-Miralles,M., Coomaraswamy,J., Häbig,K., Herzig,M.C., Funk,N., Gillardon,F.,

Maisel,M., Jucker,M., Gasser,T., Galter,D., *et al.* (2015) No Dopamine Cell Loss or Changes in Cytoskeleton Function in Transgenic Mice Expressing Physiological Levels of Wild Type or G2019S Mutant LRRK2 and in Human Fibroblasts. *PLoS One*, **10**, e0118947.

370. Chen,C.-Y., Weng,Y.-H., Chien,K.-Y., Lin,K.-J., Yeh,T.-H., Cheng,Y.-P., Lu,C.-S. and Wang,H.-L. (2012) (G2019S) LRRK2 activates MKK4-JNK pathway and causes degeneration of SN dopaminergic neurons in a transgenic mouse model of PD. *Cell Death Differ.*, **19**, 1623.

371. Ramonet,D., Daher,J.P.L., Lin,B.M., Stafa,K., Kim,J., Banerjee,R., Westerlund,M., Pletnikova,O., Glauser,L., Yang,L., *et al.* (2011) Dopaminergic Neuronal Loss, Reduced Neurite Complexity and Autophagic Abnormalities in Transgenic Mice Expressing G2019S Mutant LRRK2. *PLoS One*, **6**, e18568.

372. Tsika,E., Kannan,M., Foo,C.S.-Y., Dikeman,D., Glauser,L., Gellhaar,S., Galter,D., Knott,G.W., Dawson,T.M., Dawson,V.L., *et al.* (2014) Conditional expression of Parkinson's disease-related R1441C LRRK2 in midbrain dopaminergic neurons of mice causes nuclear abnormalities without neurodegeneration. *Neurobiol. Dis.*, **71**, 345–358.

373. Li,X., Patel,J.C., Wang,J., Avshalumov,M. V, Nicholson,C., Buxbaum,J.D., Elder,G.A., Rice,M.E. and Yue,Z. (2010) Enhanced striatal dopamine transmission and motor performance with LRRK2 overexpression in mice is eliminated by familial Parkinson's disease mutation G2019S. *J Neurosci*, **30**, 1788-1797.

374. Li,Y., Liu,W., Oo,T.F., Wang,L., Tang,Y., Jackson-Lewis,V., Zhou,C., Geghman,K., Bogdanov,M., Przedborski,S., *et al.* (2009) Mutant LRRK2(R1441G) BAC transgenic mice recapitulate cardinal features of Parkinson's disease. *Nat Neurosci*, **12**, 826-828.

375. Melrose,H.L., Dachsel,J.C., Behrouz,B., Lincoln,S.J., Yue,M., Hinkle,K.M., Kent,C.B., Korvatska,E., Taylor,J.P., Witten,L., *et al.* (2010) Impaired dopaminergic neurotransmission and microtubule-associated protein tau alterations in human LRRK2 transgenic mice. *Neurobiol Dis*, **40**, 503-517.

376. Lin,X., Parisiadou,L., Gu,X.L., Wang,L., Shim,H., Sun,L., Xie,C., Long,C.X.,

Yang,W.J., Ding,J., *et al.* (2009) Leucine-rich repeat kinase 2 regulates the progression of neuropathology induced by Parkinson's-disease-related mutant alpha-synuclein. *Neuron*, **64**, 807-827.

377. Sgobio,C., Xie,C., Yu,J., Sun,L., Lin,X., Gu,X., Cai,H., Liu,G., Parisiadou,L., Sastry,N., *et al.* (2015) Selective expression of Parkinson's disease-related Leucine-rich repeat kinase 2 G2019S missense mutation in midbrain dopaminergic neurons impairs dopamine release and dopaminergic gene expression. *Hum. Mol. Genet.*, **24**, 5299–5312.

378. Beccano-Kelly,D., Volta,M., Munsie,L., Paschall,S., Tatarnikov,I., Co,K., Chou,P., Cao,L., Bergeron,S., Mitchell,E., *et al.* (2014) LRRK2 overexpression alters glutamatergic presynaptic plasticity, striatal dopamine tone, postsynaptic signal transduction, motor activity and memory. *Hum. Mol. Genet.*, **24**, 1336–1349.

379. Tong,Y., Pisani,A., Martella,G., Karouani,M., Yamaguchi,H., Pothos,E.N. and Shen,J. (2009) R1441C mutation in LRRK2 impairs dopaminergic neurotransmission in mice. *Proc Natl Acad Sci USA*, **106**, 14622-14627.

380. Yue,M., Hinkle,K.M., Davies,P., Trushina,E., Fiesel,F.C., Christenson,T.A., Schroeder,A.S., Zhang,L., Bowles,E., Behrouz,B., *et al.* (2015) Progressive dopaminergic alterations and mitochondrial abnormalities in LRRK2 G2019S knock-in mice. *Neurobiol. Dis.*, **78**, 172–195.

381. Parisiadou,L., Yu,J., Sgobio,C., Xie,C., Liu,G., Sun,L., Gu,X.-L., Lin,X., Crowley,N.A., Lovinger,D.M., *et al.* (2014) LRRK2 regulates synaptogenesis and dopamine receptor activation through modulation of PKA activity. *Nat. Neurosci.*, **17**, 367–376.

382. Liu,H.-F., Lu,S., Ho,P.W.-L., Tse,H.-M., Pang,S.Y.-Y., Kung,M.H.-W., Ho,J.W.-M., Ramsden,D.B., Zhou,Z.-J. and Ho,S.-L. (2014) LRRK2 R1441G mice are more liable to dopamine depletion and locomotor inactivity. *Ann. Clin. Transl. Neurol.*, **1**, 199–208.

383. Lee,B.D., Shin,J.H., Vankampen,J., Petrucelli,L., West,A.B., Ko,H.S., Lee,Y. Il, Maguire-Zeiss,K.A., Bowers,W.J., Federoff,H.J., *et al.* (2010) Inhibitors of leucine-rich repeat kinase-2 protect against models of Parkinson's disease. *Nat. Med.*, **16**, 998–1000.

384. Kritzinger,A., Ferger,B., Gillardon,F., Stierstorfer,B., Birk,G., Kochanek,S. and Ciossek,T. (2018) Age-related pathology after adenoviral overexpression of the leucine-rich repeat kinase 2 in the mouse striatum. *Neurobiol. Aging*, **66**, 97–111.

385. Baptista,M.A.S., Dave,K.D., Frasier,M.A., Sherer,T.B., Greeley,M., Beck,M.J., Varsho,J.S., Parker,G.A., Moore,C., Churchill,M.J., *et al.* (2013) Loss of Leucine-Rich Repeat Kinase 2 (LRRK2) in Rats Leads to Progressive Abnormal Phenotypes in Peripheral Organs. *PLoS One*, **8**, e80705.

386. Ness,D., Ren,Z., Gardai,S., Sharpnack,D., Johnson,V.J., Brennan,R.J., Brigham,E.F. and Olaharski,A.J. (2013) Leucine-Rich Repeat Kinase 2 (LRRK2)-Deficient Rats Exhibit Renal Tubule Injury and Perturbations in Metabolic and Immunological Homeostasis. *PLoS One*, **8**, e66164.

387. Boddu,R., Hull,T., Bolisetty,S., Hu,X., Moehle,M., Daher,J., Kamal,A., Joseph,R., George,J., Agarwal,A., *et al.* (2015) Leucine-rich repeat kinase 2 deficiency is protective in rhabdomyolysis-induced kidney injury. *Hum. Mol. Genet.*, **24**, 4078–4093.

388. Daher,J.P.L., Volpicelli-Daley,L.A., Blackburn,J.P., Moehle,M.S. and West,A.B. (2014) Abrogation of α-synuclein–mediated dopaminergic neurodegeneration in LRRK2-deficient rats. *Proc. Natl. Acad. Sci.*, **111**, 9289-9294.

389. Zhou,H., Huang,C., Tong,J., Hong,W.C., Liu,Y.-J. and Xia,X.-G. (2011) Temporal expression of mutant LRRK2 in adult rats impairs dopamine reuptake. *Int. J. Biol. Sci.*, **7**, 753–761.

390. Lee,J.-W., Tapias,V., Di Maio,R., Greenamyre,J.T. and Cannon,J.R. (2015) Behavioral, neurochemical, and pathologic alterations in bacterial artificial chromosome transgenic G2019S leucine-rich repeated kinase 2 rats. *Neurobiol. Aging*, **36**, 505–518.

391. Shaikh,K.T., Yang,A., Youshin,E. and Schmid,S. (2015) Transgenic LRRK2R1441G rats–a model for Parkinson disease? *PeerJ*, **3**, e945.

392. Stafa,K., Trancikova,A., Webber,P.J., Glauser,L., West,A.B. and Moore,D.J. (2012) GTPase Activity and Neuronal Toxicity of Parkinson's Disease–Associated LRRK2 Is

Regulated by ArfGAP1. *PLOS Genet.*, **8**, e1002526.

393. Hatano,T., Kubo,S., Imai,S., Maeda,M., Hattori,N., Ishikawa,K., Mizuno,Y. and Hattori,N. (2007) Leucine-rich repeat kinase 2 associates with lipid rafts. *Hum. Mol. Genet.*, **16**, 678–690.

394. Deng,X., Dzamko,N., Prescott,A., Davies,P., Liu,Q., Yang,Q., Lee,J.-D., Patricelli,M.P., Nomanbhoy,T.K., Alessi,D.R., *et al.* (2011) Characterization of a selective inhibitor of the Parkinson's disease kinase LRRK2. *Nat. Chem. Biol.*, **7**, 203–205.

395. Stafa,K., Tsika,E., Moser,R., Musso,A., Glauser,L., Jones,A., Biskup,S., Xiong,Y., Bandopadhyay,R., Dawson,V.L., *et al.* (2014) Functional interaction of Parkinson's disease-associated LRRK2 with members of the dynamin GTPase superfamily. *Hum. Mol. Genet.*, **23**, 2055–2077.

396. Schüle,B., Pera,R.A.R. and Langston,J.W. (2009) Can cellular models revolutionize drug discovery in Parkinson's disease? *Biochim. Biophys. Acta - Mol. Basis Dis.*, **1792**, 1043–1051.

397. Falkenburger,B.H., Saridaki,T. and Dinter,E. (2016) Cellular models for Parkinson's disease. *J. Neurochem.*, **139**, 121–130.

398. Hockey,L.N., Kilpatrick,B.S., Eden,E.R., Lin-Moshier,Y., Brailoiu,G.C., Brailoiu,E., Futter,C.E., Schapira,A.H., Marchant,J.S. and Patel,S. (2015) Dysregulation of lysosomal morphology by pathogenic LRRK2 is corrected by TPC2 inhibition. *J. Cell Sci.*, **128**, 232–238.

399. Gómez-Suaga,P., Rivero-Ríos,P., Fdez,E., Blanca Ramírez,M., Ferrer,I., Aiastui,A., López De Munain,A. and Hilfiker,S. (2014) LRRK2 delays degradative receptor trafficking by impeding late endosomal budding through decreasing Rab7 activity. *Hum. Mol. Genet.*, **23**, 6779–6796.

400. Daniel,G. and Moore,D.J. (2015) Modeling LRRK2 Pathobiology in Parkinson's Disease: From Yeast to Rodents BT - Behavioral Neurobiology of Huntington's

Disease and Parkinson's Disease. In Nguyen,H.H.P., Cenci,M.A. (eds). Springer Berlin Heidelberg, Berlin, Heidelberg, pp. 331–368.

401. Weykopf,B., Haupt,S., Jungverdorben,J., Flitsch,L.J., Hebisch,M., Liu,G.-H., Suzuki,K., Belmonte,J.C.I., Peitz,M., Blaess,S., *et al.* (2019) Induced pluripotent stem cell-based modeling of mutant LRRK2-associated Parkinson's disease. *Eur. J. Neurosci.*, **49**, 561–589.

402. Manzoni,C., Mamais,A., Dihanich,S., McGoldrick,P., Devine,M.J., Zerle,J., Kara,E., Taanman,J.-W., Healy,D.G., Marti-Masso,J.-F., *et al.* (2013) Pathogenic Parkinson's disease mutations across the functional domains of LRRK2 alter the autophagic/lysosomal response to starvation. *Biochem. Biophys. Res. Commun.*, **441**, 862–866.

403. Choi,I., Kim,B., Byun,J.-W., Baik,S.H., Huh,Y.H., Kim,J.-H., Mook-Jung,I., Song,W.K., Shin,J.-H., Seo,H., *et al.* (2015) LRRK2 G2019S mutation attenuates microglial motility by inhibiting focal adhesion kinase. *Nat. Commun.*, **6**, 8255.

404. Greggio,E., Civiero,L., Bisaglia,M. and Bubacco,L. (2012) Parkinson's disease and immune system: is the culprit LRRKing in the periphery? *J. Neuroinflammation*, **9**, 94.

405. Choi,H.G., Buhrlage,S.J. and Gray,N.S. (2012) Leucine-rich repeat kinase 2 inhibitors: a patent review (2006 – 2011) AU - Deng, Xianming. *Expert Opin. Ther. Pat.*, **22**, 1415–1426.

406. Lee,H., James,W.S. and Cowley,S.A. (2017) LRRK2 in peripheral and central nervous system innate immunity: its link to Parkinson's disease. *Biochem. Soc. Trans.*, **45**, 131–139.

407. Moehle,M.S., Webber,P.J., Tse,T., Sukar,N., Standaert,D.G., DeSilva,T.M., Cowell,R.M. and West,A.B. (2012) LRRK2 inhibition attenuates microglial inflammatory responses. *J. Neurosci.*, **32**, 1602–1611.

408. Dzamko,N. and Halliday,G.M. (2012) An emerging role for LRRK2 in the immune system. *Biochem. Soc. Trans.*, **40**, 1134-1139.

409. Barrett,J.C., Hansoul,S., Nicolae,D.L., Cho,J.H., Duerr,R.H., Rioux,J.D., Brant,S.R., Silverberg,M.S., Taylor,K.D., Barmada,M.M., *et al.* (2008) Genome-wide association defines more than 30 distinct susceptibility loci for Crohn's disease. *Nat. Genet.*, **40**, 955.

410. Fava,V.M., Manry,J., Cobat,A., Orlova,M., Van Thuc,N., Ba,N.N., Thai,V.H., Abel,L., Alcaïs,A., Schurr,E., *et al.* (2016) A Missense LRRK2 Variant Is a Risk Factor for Excessive Inflammatory Responses in Leprosy. *PLoS Negl. Trop. Dis.*, **10**, e0004412–e0004412.

411. Gardet,A., Benita,Y., Li,C., Sands,B.E., Ballester,I., Stevens,C., Korzenik,J.R., Rioux,J.D., Daly,M.J., Xavier,R.J., *et al.* (2010) LRRK2 is involved in the IFN-gamma response and host response to pathogens. *J. Immunol.*, **185**, 5577–5585.

412. Cook,D.A., Kannarkat,G.T., Cintron,A.F., Butkovich,L.M., Fraser,K.B., Chang,J., Grigoryan,N., Factor,S.A., West,A.B., Boss,J.M., *et al.* (2017) LRRK2 levels in immune cells are increased in Parkinson's disease. *npj Park. Dis.*, **3**, 11.

413. MacLeod,D., Dowman,J., Hammond,R., Leete,T., Inoue,K. and Abeliovich,A. (2006) The Familial Parkinsonism Gene LRRK2 Regulates Neurite Process Morphology. *Neuron*, **52**, 587–593.

414. Blanca Ramírez,M., Lara Ordóñez,A.J., Fdez,E., Madero-Pérez,J., Gonnelli,A., Drouyer,M., Chartier-Harlin,M.-C., Taymans,J.-M., Bubacco,L., Greggio,E., *et al.* (2017) GTP binding regulates cellular localization of Parkinson's disease-associated LRRK2. *Hum. Mol. Genet.*, **26**, 2747–2767.

415. Fletcher,D.A. and Mullins,R.D. (2010) Cell mechanics and the cytoskeleton. *Nature*, **463**, 485–492.

416. Godena,V.K., Brookes-Hocking,N., Moller,A., Shaw,G., Oswald,M., Sancho,R.M., Miller,C.C.J., Whitworth,A.J. and De Vos,K.J. (2014) Increasing microtubule acetylation rescues axonal transport and locomotor deficits caused by LRRK2 Roc-COR domain mutations. *Nat. Commun.*, **5**, 5245.

417. Madero-Pérez,J., Fdez,E., Fernández,B., Lara Ordóñez,A.J., Blanca Ramírez,M., Gómez-Suaga,P., Waschbüsch,D., Lobbestael,E., Baekelandt,V., Nairn,A.C., *et al.* (2018) Parkinson disease-associated mutations in LRRK2 cause centrosomal defects via Rab8a phosphorylation. *Mol. Neurodegener.*, **13**, 1–22.

418. Vertii,A., Hehnly,H. and Doxsey,S. The Centrosome, a Multitalented Renaissance Organelle. *Cold Spring Harb. Perspect. Biol.*, **8**, a025049.

419. Dhekne,H.S., Yanatori,I., Gomez,R.C., Tonelli,F., Diez,F., Schüle,B., Steger,M., Alessi,D.R. and Pfeffer,S.R. (2018) A pathway for Parkinson's Disease LRRK2 kinase to block primary cilia and Sonic hedgehog signaling in the brain. *Elife*, **7**, 1–26.

420. Manzoni,C. (2017) The LRRK2–macroautophagy axis and its relevance to Parkinson's disease. *Biochem. Soc. Trans.*, **45**, 155–162.

421. Plowey,E.D., Cherra,S.J., Liu,Y.J. and Chu,C.T. (2008) Role of autophagy in G2019S-LRRK2-associated neurite shortening in differentiated SH-SY5Y cells. *J. Neurochem.*, **105**, 1048–1056.

422. Manzoni,C., Mamais,A., Dihanich,S., Abeti,R., Soutar,M.P.M., Plun-Favreau,H., Giunti,P., Tooze,S.A., Bandopadhyay,R. and Lewis,P.A. (2013) Inhibition of LRRK2 kinase activity stimulates macroautophagy. *Biochim. Biophys. Acta*, **1833**, 2900–2910.

423. Schapansky,J., Nardozzi,J.D., Felizia,F. and LaVoie,M.J. (2014) Membrane recruitment of endogenous LRRK2 precedes its potent regulation of autophagy. *Hum. Mol. Genet.*, **23**, 4201–4214.

424. Bravo-San Pedro,J.M., Niso-Santano,M., Gómez-Sánchez,R., Pizarro-Estrella,E., Aiastui-Pujana,A., Gorostidi,A., Climent,V., López de Maturana,R., Sanchez-Pernaute,R., López de Munain,A., *et al.* (2013) The LRRK2 G2019S mutant exacerbates basal autophagy through activation of the MEK/ERK pathway. *Cell. Mol. Life Sci.*, **70**, 121–136.

425. Sánchez-Danés,A., Richaud-Patin,Y., Carballo-Carbajal,I., Jiménez-Delgado,S., Caig,C., Mora,S., Di Guglielmo,C., Ezquerra,M., Patel,B., Giralt,A., *et al.* (2012)

Disease-specific phenotypes in dopamine neurons from human iPS-based models of genetic and sporadic Parkinson's disease. *EMBO Mol. Med.*, **4**, 380–395.

426. Gómez-Suaga,P., Luzón-Toro,B., Churamani,D., Zhang,L., Bloor-Young,D., Patel,S., Woodman,P.G., Churchill,G.C. and Hilfiker,S. (2012) Leucine-rich repeat kinase 2 regulates autophagy through a calcium-dependent pathway involving NAADP. *Hum. Mol. Genet.*, **21**, 511–525.

427. Henry,A.G., Aghamohammadzadeh,S., Samaroo,H., Chen,Y., Mou,K., Needle,E. and Hirst,W.D. (2015) Pathogenic LRRK2 mutations, through increased kinase activity, produce enlarged lysosomes with reduced degradative capacity and increase ATP13A2 expression. *Hum. Mol. Genet.*, **24**, 6013–6028.

428. Schapansky,J., Khasnavis,S., DeAndrade,M.P., Nardozzi,J.D., Falkson,S.R., Boyd,J.D., Sanderson,J.B., Bartels,T., Melrose,H.L. and LaVoie,M.J. (2018) Familial knockin mutation of LRRK2 causes lysosomal dysfunction and accumulation of endogenous insoluble α-synuclein in neurons. *Neurobiol. Dis.*, **111**, 26–35.

429. Orenstein,S.J., Kuo,S.-H., Tasset,I., Arias,E., Koga,H., Fernandez-Carasa,I., Cortes,E., Honig,L.S., Dauer,W., Consiglio,A., *et al.* (2013) Interplay of LRRK2 with chaperone-mediated autophagy. *Nat. Neurosci.*, **16**, 394–406.

430. Kalogeropulou,A.F., Zhao,J., Bolliger,M.F., Memou,A., Narasimha,S., Molitor,T.P., Wilson,W.H., Rideout,H.J. and Nichols,R.J. (2018) P62/SQSTM1 is a novel leucine-rich repeat kinase 2 (LRRK2) substrate that enhances neuronal toxicity. *Biochem. J.*, **475**, 1271-1293.

431. Mir,R., Tonelli,F., Lis,P., Macartney,T., Polinski,N.K., Martinez,T.N., Chou,M.-Y., Howden,A.J.M., König,T., Hotzy,C., *et al.* (2018) The Parkinson's disease VPS35[D620N] mutation enhances LRRK2-mediated Rab protein phosphorylation in mouse and human. *Biochem. J.*, **475**, 1861–1883.

432. Dodson,M.W., Leung,L.K., Lone,M., Lizzio,M.A. and Guo,M. (2014) Novel ethyl methanesulfonate (EMS)-induced null alleles of the Drosophila homolog of LRRK2 reveal a crucial role in endolysosomal

functions and autophagy in vivo *Dis. Model. & Mech.*, **7**, 1351-1363.

433. Feng,M., Hu,X., Li,N., Hu,F., Chang,F., Xu,H.-F. and Liu,Y.-J. (2018) Distinctive roles of Rac1 and Rab29 in LRRK2 mediated membrane trafficking and neurite outgrowth. *J. Biomed. Res.*, **32**, 145–156.

434. Cho,H.J., Yu,J., Xie,C., Rudrabhatla,P., Chen,X., Wu,J., Parisiadou,L., Liu,G., Sun,L., Ma,B., *et al.* (2014) Leucine-rich repeat kinase 2 regulates Sec16A at ER exit sites to allow ER-Golgi export. *EMBO J.*, **33**, 2314–2331.

435. Miklavc,P., Ehinger,K., Thompson,K.E., Hobi,N., Shimshek,D.R. and Frick,M. (2014) Surfactant secretion in LRRK2 knock-out rats: changes in lamellar body morphology and rate of exocytosis. *PLoS One*, **9**, e84926–e84926.

436. Yun,H.J., Park,J., Ho,D.H., Kim,H., Kim,C.-H., Oh,H., Ga,I., Seo,H., Chang,S., Son,I., *et al.* (2013) LRRK2 phosphorylates Snapin and inhibits interaction of Snapin with SNAP-25. *Exp. Mol. Med.*, **45**, e36–e36.

437. Belluzzi,E., Gonnelli,A., Cirnaru,M.-D., Marte,A., Plotegher,N., Russo,I., Civiero,L., Cogo,S., Carrion,M.P., Franchin,C., *et al.* (2016) LRRK2 phosphorylates pre-synaptic N-ethylmaleimide sensitive fusion (NSF) protein enhancing its ATPase activity and SNARE complex disassembling rate. *Mol. Neurodegener.*, **11**, 1.

438. Maas,J.W.J., Yang,J. and Edwards,R.H. (2017) Endogenous Leucine-Rich Repeat Kinase 2 Slows Synaptic Vesicle Recycling in Striatal Neurons . *Front. Synaptic Neurosci.* , **9**, 5.

439. Pan,P.-Y., Li,X., Wang,J., Powell,J., Wang,Q., Zhang,Y., Chen,Z., Wicinski,B., Hof,P., Ryan,T.A., *et al.* (2017) Parkinson's Disease-Associated LRRK2 Hyperactive Kinase Mutant Disrupts Synaptic Vesicle Trafficking in Ventral Midbrain Neurons. *J. Neurosci.*, **37**, 11366–11376.

440. Nguyen,M., Wong,Y.C., Ysselstein,D., Severino,A. and Krainc,D. (2019) Synaptic, Mitochondrial, and Lysosomal Dysfunction in Parkinson’s Disease. *Trends*

Neurosci., **42**, 140–149.

441. Nguyen,M. and Krainc,D. (2018) LRRK2 phosphorylation of auxilin mediates synaptic defects in dopaminergic neurons from patients with Parkinson's disease. *Proc. Natl. Acad. Sci.*, **115**, 5576 LP-5581.

442. Civiero,L., Vancraenenbroeck,R., Belluzzi,E., Beilina,A., Lobbestael,E., Reyniers,L., Gao,F., Micetic,I., de Maeyer,M., Bubacco,L., *et al.* (2012) Biochemical Characterization of Highly Purified Leucine-Rich Repeat Kinases 1 and 2 Demonstrates Formation of Homodimers. *PLoS One*, **7**.

443. Choudhury,A., Dominguez,M., Puri,V., Sharma,D.K., Narita,K., Wheatley,C.L., Marks,D.L. and Pagano,R.E. (2002) Rab proteins mediate Golgi transport of caveola-internalized glycosphingolipids and correct lipid trafficking in Niemann-Pick C cells. *J. Clin. Invest.*, **109**, 1541–1550.

444. Rzomp,K.A., Scholtes,L.D., Briggs,B.J., Whittaker,G.R. and Scidmore,M.A. (2003) Rab GTPases are recruited to chlamydial inclusions in both a species-dependent and species-independent manner. *Infect. Immun.*, **71**, 5855–5870.

445. Chamberland,J.P., Antonow,L.T., Dias Santos,M. and Ritter,B. (2016) NECAP2 controls clathrin coat recruitment to early endosomes for fast endocytic recycling. *J. Cell Sci.*, **129**, 2625–2637.

446. Ritter,B., Murphy,S., Dokainish,H., Girard,M., Gudheti,M. V., Kozlov,G., Halin,M., Philie,J., Jorgensen,E.M., Gehring,K., *et al.* (2013) NECAP 1 Regulates AP-2 Interactions to Control Vesicle Size, Number, and Cargo During Clathrin-Mediated Endocytosis. *PLoS Biol.*, **11**.

447. Chi,S., Cao,H., Wang,Y. and McNiven,M.A. (2011) Recycling of the epidermal growth factor receptor is mediated by a novel form of the clathrin adaptor protein Eps15. *J. Biol. Chem.*, **286**, 35196–35208.

448. Peralta,E.R., Martin,B.C. and Edinger,A.L. (2010) Differential effects of TBC1D15 and mammalian Vps39 on Rab7 activation state, lysosomal morphology, and growth factor

dependence. *J. Biol. Chem.*, **285**, 16814–16821.

449. Toyofuku,T., Morimoto,K., Sasawatari,S. and Kumanogoh,A. (2015) Leucine-Rich Repeat Kinase 1 Regulates Autophagy through Turning On TBC1D2-Dependent Rab7 Inactivation. *Mol. Cell. Biol.*, **35**, 3044–3058.

450. Katzmann,D.J., Odorizzi,G. and Emr,S.D. (2002) Receptor downregulation and multivesicular-body sorting. *Nat. Rev. Mol. Cell Biol.*, **3**, 893–905.

451. Vetter,M., Stehle,R., Basquin,C. and Lorentzen,E. (2015) Structure of Rab11-FIP3-Rabin8 reveals simultaneous binding of FIP3 and Rabin8 effectors to Rab11. *Nat. Struct. Mol. Biol.*, **22**, 695–702.

452. Dejgaard,S.Y., Murshid,A., Erman,A., Kizilay,O., Verbich,D., Lodge,R., Dejgaard,K., Ly-Hartig,T.B.N., Pepperkok,R., Simpson,J.C., *et al.* (2008) Rab18 and Rab43 have key roles in ER-Golgi trafficking. *J. Cell Sci.*, **121**, 2768–2781.

453. Braun,A.C., Hendrick,J., Eisler,S.A., Schmid,S., Hausser,A. and Olayioye,M.A. (2015) The Rho-specific GAP protein DLC3 coordinates endocytic membrane trafficking. *J. Cell Sci.*, **128**, 1386–1399.

454. Shinde,S.R. and Maddika,S. (2016) PTEN modulates EGFR late endocytic trafficking and degradation by dephosphorylating Rab7. *Nat. Commun.*, **7**, 1–11.

455. Hunter,T. (2012) Why nature chose phosphate to modify proteins. *Philos. Trans. R. Soc. B Biol. Sci.*, **367**, 2513–2516.

456. Burton,J.L., Burns,M.E., Gatti,E., Augustine,G.J. and De Camilli,P. (1994) Specific interactions of Mss4 with members of the Rab GTPase subfamily. *EMBO J.*, **13**, 5547–5558.

457. Devergne,O., Sun,G.H. and Schüpbach,T. (2017) Stratum, a Homolog of the Human GEF Mss4, Partnered with Rab8, Controls the Basal Restriction of Basement Membrane Proteins in Epithelial Cells. *Cell Rep.*, **18**, 1831–1839.

458. Nordmann,M., Cabrera,M., Perz,A., Bröcker,C., Ostrowicz,C., Engelbrecht-Vandré,S.

and Ungermann,C. (2010) The Mon1-Ccz1 complex is the GEF of the late endosomal Rab7 homolog Ypt7. *Curr. Biol.*, **20**, 1654–1659.

459. Yasuda,S., Morishita,S., Fujita,A., Nanao,T., Wada,N., Waguri,S., Schiavo,G., Fukuda,M. and Nakamura,T. (2016) Mon1-Ccz1 activates Rab7 only on late endosomes and dissociates from the lysosome in mammalian cells. *J. Cell Sci.*, **129**, 329–340.

460. Sun,Y., Bilan,P.J., Liu,Z. and Klip,A. (2010) Rab8A and Rab13 are activated by insulin and regulate GLUT4 translocation in muscle cells. *Proc. Natl. Acad. Sci. U. S. A.*, **107**, 19909–19914.

461. Hokanson,D.E. and Bretscher,A.P. (2012) EPI64 interacts with Slp1/JFC1 to coordinate Rab8a and Arf6 membrane trafficking. *Mol. Biol. Cell*, **23**, 701–715.

462. Frasa,M.A.M., Maximiano,F.C., Smolarczyk,K., Francis,R.E., Betson,M.E., Lozano,E., Goldenring,J., Seabra,M.C., Rak,A., Ahmadian,M.R., *et al.* (2010) Armus Is a Rac1 Effector that Inactivates Rab7 and Regulates E-Cadherin Degradation. *Curr. Biol.*, **20**, 198–208.

463. Jia,D., Zhang,J.-S., Li,F., Wang,J., Deng,Z., White,M.A., Osborne,D.G., Phillips-Krawczak,C., Gomez,T.S., Li,H., *et al.* (2016) Structural and mechanistic insights into regulation of the retromer coat by TBC1d5. *Nat. Commun.*, **7**, 13305.

464. Zhang,X.M., Walsh,B., Mitchell,C.A. and Rowe,T. (2005) TBC domain family, member 15 is a novel mammalian Rab GTPase-activating protein with substrate preference for Rab7. *Biochem. Biophys. Res. Commun.*, **335**, 154–161.

465. Itoh,T., Satoh,M., Kanno,E. and Fukuda,M. (2006) Screening for target Rabs of TBC (Tre-2/Bub2/Cdc16) domain-containing proteins based on their Rab-binding activity. *Genes to Cells*, **11**, 1023–1037.

466. Fukuda,M. (2011) TBC proteins: GAPs for mammalian small GTPase Rab? *Biosci. Rep.*, **31**, 159–168.

467. Jimenez-Orgaz,A., Kvainickas,A., Nägele,H., Denner,J., Eimer,S., Dengjel,J. and Steinberg,F. (2017) Control of RAB7 activity and localization through the

retromer-TBC1D5 complex enables RAB7-dependent mitophagy. *EMBO J.*, **37**, e201797128.

468. Yamano,K., Fogel,A.I., Wang,C., van der Bliek,A.M. and Youle,R.J. (2014) Mitochondrial Rab GAPs govern autophagosome biogenesis during mitophagy. *Elife*, **3**, e01612–e01612.

469. Saxena,S.K. and Kaur,S. (2006) Regulation of epithelial ion channels by Rab GTPases. *Biochem. Biophys. Res. Commun.*, **351**, 582–587.

470. Parkinson,K., Baines,A.E., Keller,T., Gruenheit,N., Bragg,L., North,R.A. and Thompson,C.R.L. (2014) Calcium-dependent regulation of Rab activation and vesicle fusion by an intracellular P2X ion channel. *Nat. Cell Biol.*, **16**, 87–98.

471. Lin-Moshier,Y., Keebler,M. V., Hooper,R., Boulware,M.J., Liu,X., Churamani,D., Abood,M.E., Walseth,T.F., Brailoiu,E., Patel,S., *et al.* (2014) The Two-pore channel (TPC) interactome unmasks isoform-specific roles for TPCs in endolysosomal morphology and cell pigmentation. *Proc. Natl. Acad. Sci.*, **111**, 13087–13092.

472. Agola,J.O., Hong,L., Surviladze,Z., Ursu,O., Waller,A., Strouse,J.J., Simpson,D.S., Schroeder,C.E., Oprea,T.I., Golden,J.E., *et al.* (2012) A competitive nucleotide binding inhibitor: in vitro characterization of Rab7 GTPase inhibition. *ACS Chem. Biol.*, **7**, 1095–1108.

473. Nakajo,A., Yoshimura,S., Togawa,H., Kunii,M., Iwano,T., Izumi,A., Noguchi,Y., Watanabe,A., Goto,A., Sato,T., *et al.* (2016) EHBP1L1 coordinates Rab8 and Bin1 to regulate apical-directed transport in polarized epithelial cells. *J. Cell Biol.*, **212**, 297–306.

474. Rapiteanu,R., Davis,L.J., Williamson,J.C., Timms,R.T., Paul Luzio,J. and Lehner,P.J. (2016) A Genetic Screen Identifies a Critical Role for the WDR81-WDR91 Complex in the Trafficking and Degradation of Tetherin. *Traffic*, **17**, 940–958.

475. Mehta,Z.B., Pietka,G. and Lowe,M. (2014) The cellular and physiological functions of the Lowe syndrome protein OCRL1. *Traffic*, **15**, 471–487.

476. Goueli,B.S., Powell,M.B., Finger,E.C. and Pfeffer,S.R. (2012) TBC1D16 is a Rab4A GTPase activating protein that regulates receptor recycling and EGF receptor signaling. *Proc. Natl. Acad. Sci.*, **109**, 15787–15792.

477. Nag,S., Rani,S., Mahanty,S., Bissig,C., Arora,P., Azevedo,C., Saiardi,A., van der Sluijs,P., Delevoye,C., van Niel,G., *et al.* (2018) Rab4A organizes endosomal domains for sorting cargo to lysosome-related organelles. *J. Cell Sci.*, **131**, jcs216226.

478. Sulzer,D. (2007) Multiple hit hypotheses for dopamine neuron loss in Parkinson's disease. *Trends Neurosci.*, **30**, 244–250.

479. Schreij,A.M.A., Fon,E.A. and Mcpherson,P.S. (2015) Endocytic membrane trafficking and neurodegenerative disease. *Cell. Mol. Life Sci.*, **73**, 1529-1545.

480. Dehay,B., Martinez-Vicente,M., Caldwell,G.A., Caldwell,K.A., Yue,Z., Cookson,M.R., Klein,C., Vila,M. and Bezard,E. (2013) Lysosomal Impairment in Parkinson's Disease. *Mov. Disord.*, **28**, 725–732.

481. Migheli,R., Grazia,M., Giudice,D., Spissu,Y., Sanna,G., Xiong,Y., Dawson,T.M., Dawson,V.L., Galioto,M., Rocchitta,G., *et al.* (2013) LRRK2 Affects Vesicle Trafficking , Neurotransmitter Extracellular Level and Membrane Receptor Localization. PLoS One, **8**.

482. Rassu,M., Grazia,M., Giudice,D., Sanna,S., Taymans,J.M., Morari,M., Brugnoli,A., Frassineti,M., Masala,A., Esposito,S., *et al.* (2017) Role of LRRK2 in the regulation of dopamine receptor trafficking. PLoS One, **12**.

483. Gardoni,F. and Bellone,C. (2015) Modulation of the glutamatergic transmission by Dopamine: a focus on Parkinson, Huntington and Addiction diseases. *Front. Cell. Neurosci.*, **9**, 25.

484. Surmeier,D.J., Ding,J., Day,M., Wang,Z. and Shen,W. (2007) D1 and D2 dopamine-receptor modulation of striatal glutamatergic signaling in striatal medium spiny neurons. *Trends Neurosci.*, **30**, 228–235.

485. Janvier,K. and Bonifacino,J.S. (2005) Role of the Endocytic Machinery in the Sorting of

Lysosome-associated Membrane Proteins. *Mol. Biol. Cell*, **16**, 4231–4242.

486. Tofaris,G.K., Goedert,M. and Spillantini,M.G. (2016) The Transcellular Propagation and Intracellular Trafficking of a -Synuclein. Cold Spring Harb Perspect Med.,**7**.

487. Tsunemi,T. and Krainc,D. (2013) Zn2+ dyshomeostasis caused by loss of ATP13A2/PARK9 leads to lysosomal dysfunction and alpha-synuclein accumulation. *Hum. Mol. Genet.*, **23**, 2791–2801.

488. Mazzulli,J.R., Xu,Y.-H., Sun,Y., Knight,A.L., McLean,P.J., Caldwell,G.A., Sidransky,E., Grabowski,G.A. and Krainc,D. (2011) Gaucher disease glucocerebrosidase and α-synuclein form a bidirectional pathogenic loop in synucleinopathies. *Cell*, **146**, 37–52.

489. Cookson,M.R. (2017) Mechanisms of Mutant LRRK2 Neurodegeneration. In Rideout,H. (ed), *Leucine-Rich Repeat Kinase 2 (LRRK2). Advances in Neurobiology*.pp. 227–239.

490. Lindström,V., Gustafsson,G., Sanders,L.H., Howlett,E.H., Sigvardson,J., Kasrayan,A., Ingelsson,M., Bergström,J. and Erlandsson,A. (2017) Extensive uptake of α-synuclein oligomers in astrocytes results in sustained intracellular deposits and mitochondrial damage. *Mol. Cell. Neurosci.*, **82**, 143–156.

491. Loria,F., Vargas,J.Y., Bousset,L., Syan,S., Salles,A., Melki,R. and Zurzolo,C. (2017) α -Synuclein transfer between neurons and astrocytes indicates that astrocytes play a role in degradation rather than in spreading. *Acta Neuropathol.*, **134**, 789-808.

492. Sacino,A.N., Brooks,M.M., Chakrabarty,P., Saha,K., Khoshbouei,H., Golde,T.E. and Giasson,B.I. (2017) Proteolysis of α-synuclein fibrils in the lysosomal pathway limits induction of inclusion pathology. *J. Neurochem.*, **140**, 662–678.

493. di Domenico,A., Carola,G., Calatayud,C., Pons-Espinal,M., Muñoz,J.P., Richaud-Patin,Y., Fernandez-Carasa,I., Gut,M., Faella,A., Parameswaran,J., *et al.* (2019) Patient-Specific iPSC-Derived Astrocytes Contribute to Non-Cell-Autonomous Neurodegeneration in Parkinson's Disease. *Stem Cell Reports*, **12**, 213-229.

494. Liu,B. and Neufeld,A.H. (2007) Activation of epidermal growth factor receptors in astrocytes: From development to neural injury. *J. Neurosci. Res.*, **85**, 3523–3529.

495. Kim,M.J., Deng,H.X., Wong,Y.C., Siddique,T. and Krainc,D. (2017) The Parkinson's disease-linked protein TMEM230 is required for Rab8a-mediated secretory vesicle trafficking and retromer trafficking. *Hum. Mol. Genet.*, **26**, 729–741.

496. Ying,H. and Yue,B.Y.J.T. (2016) Optineurin: The autophagy connection. *Exp. Eye Res.*, **144**, 73–80.

497. Corbier,C. and Sellier,C. (2016) C9ORF72 is a GDP/GTP exchange factor for Rab8 and Rab39 and regulates autophagy. *Small GTPases*, **8**, 181–186.

498. Pilli,M., Arko-Mensah,J., Ponpuak,M., Roberts,E., Master,S., Mandell,M.A., Dupont,N., Ornatowski,W., Jiang,S., Bradfute,S.B., *et al.* (2012) TBK-1 promotes autophagy-mediated antimicrobial defense by controlling autophagosome maturation. *Immunity*, **37**, 223–234.

499. De Leo,M.G., Staiano,L., Vicinanza,M., Luciani,A., Carissimo,A., Mutarelli,M., Di Campli,A., Polishchuk,E., Di Tullio,G., Morra,V., *et al.* (2016) Autophagosome-lysosome fusion triggers a lysosomal response mediated by TLR9 and controlled by OCRL. *Nat. Cell Biol.*, **18**, 839–850.

500. Wall,A.A., Luo,L., Hung,Y., Tong,S.J., Condon,N.D., Blumenthal,A., Sweet,M.J. and Stow,J.L. (2017) Small GTPase Rab8a-recruited Phosphatidylinositol 3-Kinase γ Regulates Signaling and Cytokine Outputs from Endosomal Toll-like Receptors. *J. Biol. Chem.*, **292**, 4411–4422.

501. Luo,L., Wall,A.A., Tong,S.J., Hung,Y., Xiao,Z., Tarique,A.A., Sly,P.D., Fantino,E., Marzolo,M.-P. and Stow,J.L. (2018) TLR Crosstalk Activates LRP1 to Recruit Rab8a and PI3Kγ for Suppression of Inflammatory Responses. *Cell Rep.*, **24**, 3033–3044.

502. Finetti,F., Patrussi,L., Galgano,D., Cassioli,C., Perinetti,G., Pazour,G.J. and Baldari,C.T. (2015) The small GTPase Rab8 interacts with VAMP-3 to regulate the delivery of recycling T-cell receptors to the immune synapse. *J. Cell Sci.*, **128**, 2541–

2552.

503. Yin,G., Lopes da Fonseca,T., Eisbach,S.E., Anduaga,A.M., Breda,C., Orcellet,M.L., Szegő,É.M., Guerreiro,P., Lázaro,D.F., Braus,G.H., *et al.* (2014) α-Synuclein interacts with the switch region of Rab8a in a Ser129 phosphorylation-dependent manner. *Neurobiol. Dis.*, **70**, 149–161.

504. Bae,E.-J., Kim,D.-K., Kim,C., Mante,M., Adame,A., Rockenstein,E., Ulusoy,A., Klinkenberg,M., Jeong,G.R., Bae,J.R., *et al.* (2018) LRRK2 kinase regulates α-synuclein propagation via RAB35 phosphorylation. *Nat. Commun.*, **9**, 3465.

505. Chua,C.E.L. and Tang,B.L. (2018) Rab 10—a traffic controller in multiple cellular pathways and locations. *J. Cell. Physiol.*, **233**, 6483–6494.

506. Sano,H., Eguez,L., Teruel,M.N., Fukuda,M., Chuang,T.D., Chavez,J.A., Lienhard,G.E. and McGraw,T.E. (2007) Rab10, a Target of the AS160 Rab GAP, Is Required for Insulin-Stimulated Translocation of GLUT4 to the Adipocyte Plasma Membrane. *Cell Metab.*, **5**, 293–303.

507. Di Maio,R., Hoffman,E.K., Rocha,E.M., Keeney,M.T., Sanders,L.H., De Miranda,B.R., Zharikov,A., Van Laar,A., Stepan,A.F., Lanz,T.A., *et al.* (2018) LRRK2 activation in idiopathic Parkinson's disease. *Sci. Transl. Med.*, **10**, eaar5429.

X. LIST OF PUBLICATIONS

I. **Rivero-Ríos, P**., Romo-Lozano, M., Madero-Pérez, J., Thomas, A.P., Biosa, A., Greggio, E., Hilfiker, S. (2019). G2019S-mutant LRRK2 alters endolysosomal trafficking through impairing RAB8A function (accepted for publication in *J. Biol. Chem*.).

II. **Rivero-Ríos, P**., Fernández, B., Madero-Pérez, J., Lozano, M.R., Hilfiker, S. (2017). "Two-Pore Channels and Parkinson's Disease: Where's the Link?" *Messenger (Los Angel)* 5(1-2):67-75.

III. Madero-Pérez, J., Fdez, E., Fernández, B., Lara Ordóñez, A.J., Blanca Ramírez, M., Romo Lozano, M., **Rivero-Ríos, P**., Hilfiker, S. (2017). "Cellular effects mediated by pathogenic LRRK: homing in on Rab-mediated processes". *Biochem. Soc. Trans.* 45(1): 147-154.

IV. Blanca Ramírez, M., Madero-Pérez, J., **Rivero-Ríos, P**., Martínez-Salvador, M., Lara Ordóñez, A.J., Fernández, B., Fdez, E., Hilfiker, S. (2016). "LRRK2 and Parkinson´s disease: from lack of structure to gain of function". *Curr Protein Pept Sci.* [Epub ahead of print].

V. **Rivero-Ríos, P**., Madero-Pérez, J., Fernández, B., Hilfiker, S. (2016). "Targeting the Autophagy/LysosomalDegradation Pathway in Parkinson´s Disease". *Curr Neuropharmacol.* 14(3):238-49.

VI. **Rivero-Ríos, P**., Gómez-Suaga, P., Fernández, B., Madero-Pérez, J., Schwab, A.J., Ebert, A.D., Hilfiker, S. (2015). "Alterations in late endocytic trafficking related to the pathobiology of LRRK2-linked Parkinson's disease". *Biochem Soc Trans*. 43(3):390-5.

VII. Gómez-Suaga, P., Fdez, E., Fernández, B., Martínez-Salvador, M., Blanca Ramírez, M., Madero-Pérez, J., **Rivero-Ríos, P**., Fuentes, J.M. and Hilfiker, S. (2014) "Novel insights into the neurobiology underlying LRRK2-linked Parkinson's disease". *Neuropharmacol*. 85C: 45-56.

VIII. **Rivero-Ríos, P**., Gómez-Suaga, P., Fdez, E. and Hilfiker, S. (2014) "Upstream deregulation of calcium signalling in Parkinson's disease". *Frontiers Mol. Neurosci.* 53: 1-10.

IX. Gómez-Suaga, P., **Rivero-Ríos, P**., Fdez, E., Blanca-Ramírez, M., Ferrer, I., López de Munain, A. and Hilfiker, S. (2014) "LRRK2 delays degradative receptor trafficking by impeding late endosomal budding through decreasing Rab7 activity". *Hum. Mol. Genet*. 23: 6779-6796.